POLSKIE TOWARZYSTWO MIKROBIOLOGÓW
POLISH SOCIETY OF MICROBIOLOGISTS

Polish Journal of Microbiology

2022

Polish Journal of Microbiology
formerly Acta Microbiologica Polonica
2022, Vol. 71, No 1

CONTENTS

INSTRUCTIONS FOR AUTHORS
Instructions for authors: https://www.sciendo.com/journal/PJM

MINIREVIEW
Polish Journal of Microbiology
2022, Vol. 71, No 1, 3–9
https://doi.org/10.33073/pjm-2022-005

Should Bacteriophages Be Classified as Parasites or Predators?

GRZEGORZ WĘGRZYN

Department of Molecular Biology, Faculty of Biology, University of Gdańsk, Gdańsk, Poland

Submitted 28 November 2021, accepted 8 January 2022, published online 23 February 2022

Abstract

Bacteriophages are viruses infecting bacteria and propagating in bacterial cells. They were discovered over 100 years ago, and for decades they played crucial roles as models in genetics and molecular biology and as tools in genetic engineering and biotechnology. Now we also recognize their huge role in natural environment and their importance in human health and disease. Despite our understanding of bacteriophage mechanisms of development, these viruses are described as parasites or predators in the literature. From the biological point of view, there are fundamental differences between parasites and predators. Therefore, in this article, I asked whether bacteriophages should be classified as former or latter biological entities. Analysis of the literature and biological definitions led me to conclude that bacteriophages are parasites rather than predators and should be classified and described as such. If even more precise ecological classification is needed, bacteriophages can perhaps be included in the group of parasitoids. It might be the most appropriate formal classification of these viruses, especially if strictly virulent phages are considered, contrary to phages which lysogenize host cells and those which develop according to the permanent infection mode (or chronic cycle, like filamentous phages) revealing features of classical parasites.

K e y w o r d s: bacteriophages, parasitism, predation, parasitoids

Introduction

Bacteriophages (or shortly, phages) – viruses infecting bacterial cells – have been known for over 100 years, and currently they are recognized as the most abundant biological entities on Earth (Salmond and Fineran 2015; Batinovic et al. 2019). Their biological significance in the natural environment is irrefutable (Correa et al. 2021), and examples of their use in medicine (Zalewska-Piątek and Piątek 2021) and biotechnology (Jaroszewicz et al. 2021) are very numerous.

Examples of tremendous roles of bacteriophages in the control of microbial communities in natural habitats include their action on water and soil bacteria to keep ecological equilibrium (Srinivasiah et al. 2008), their ability to mediate lateral transfer of bacterial genetic material, to modify bacterial cell metabolism, and – due to host cell lysis – to reallocate biochemical compounds originally present inside bacterial cells, thus contributing significantly to the circulation of matter in ecosystems (Naureen et al. 2020). They even participate in multi-organismal interactions in specific microbial trophic networks (Turnau et al. 2021). Properties of bacteriophages that make them able to affect bacterial communities have been employed to control and monitor wastewaters (Barrios et al. 2021; Liu et al. 2021).

Medical use of bacteriophages is focused on phage therapy, i.e., the use of these viruses to combat bacterial infections (Kortright et al. 2019). This approach receives more and more attention due to the appearance of numerous bacterial strains resistant to most or even all antibiotics used in clinical practice (Górski et al. 2020; Bhargava et al. 2021; Fathima and Archer 2021; Iszatt et al. 2021). Apart from the direct use of phages infecting pathogenic bacteria to patients, it is also essential to consider their application to control single- or mixed-species biofilms in therapy and protection of medical devices or food (Mgomi et al. 2021; Tian et al. 2021; Topka-Bielecka et al. 2021). Importantly, bacteriophages efficiently modulate the human microbiome, which has considerable effects on the physiology of the whole human organism (Pessione 2020; Duan et al. 2021; Hsu et al. 2021; Zhang et al. 2021). On the other hand, some bacteriophages encode toxins and other virulence

* Corresponding author: G. Węgrzyn, Department of Molecular Biology, Faculty of Biology, University of Gdańsk, Gdańsk, Poland; **e-mail: grzegorz.wegrzyn@ug.edu.pl**

factors, which if produced by bacterial cells after prophage induction, can cause severe human diseases (Casas and Maloy 2011; Łoś et al. 2011; Boyd 2012). Moreover, phages were also suggested as human pathogens (Tetz et al. 2017; Tetz and Tetz 2018). Therefore, interactions of bacteriophages with human and animal organisms must be carefully analyzed when considering the clinical use of these viruses (Podlacha et al. 2021).

There are numerous applications of bacteriophages or their genetic elements in genetic engineering and biotechnology. Bacteriophages can be used as cloning vectors, and regulatory elements of phage genomes serve as modules in sophisticated expression vectors (Harada et al. 2018). Phage display, based on exposing of foreign peptides on surfaces of bacteriophage virions, plays a significant role in the development of novel and very specific antibodies or antibody-like peptides, as well as in discovering new peptides with various functions useful is many fields of biotechnology and nanotechnology (Jaroszewicz et al. 2021). On the other hand, bacteriophages can be dangerous for the biotechnological processes when infecting bacteria used for large-scale synthesis of various bio-products in bioreactors (Łoś et al. 2004).

In the light of over 100 years of studies on these viruses, one scientific aspect appears surprising. Namely, in the literature, bacteriophages are presented either as parasites or predators. This ambiguity in the classification of phages is even more unexpected as they are described mostly in biological literature while biological definitions of parasitism and predation appear clear and straightforward. Therefore, I aimed to analyze this ambiguity and propose an unambiguous biological and ecological classification of bacteriophages.

Calling bacteriophages parasites and predators

When searching the PubMed database (https://pubmed.ncbi.nlm.nih.gov), on January 2, 2022, the combination of terms "bacteriophage" and "parasite" gave 814 records, while the combination of terms "bacteriophage" and "predator" gave 345 records. When looking at various publications, bacteriophages are defined by researchers as either parasites or predators. The examples of the former classification are as follows: "Bacteriophages, the viral parasites of bacteria" (Betts et al. 2016), "host bacterium (...) and its viral parasite bacteriophage" (Gorter et al. 2015), "Phages are obligate intracellular parasites" (Orzechowska and Mohammed 2019). The examples of the latter classification are as follows: "Using phage-bacterial model systems, dynamics of the coexistence of predators and preys have been the subject of theoretical and experimental studies" (Lourenço et al. 2020), "As natural predators of bacteria, phages can" (Hsu et al. 2021), "Bacteriophage ICP1: a persistent predator" (Boyd et al. 2021). Indeed, hundreds of other examples indicate bacteriophages as parasites or predators (see PubMed database https://pubmed.ncbi.nlm.nih.gov for more examples).

Biological definitions of parasites and predators

When asking whether phages are parasites or predators, first, it is necessary to provide definitions of these terms. According to Dictionary.com (https://www.dictionary.com), a parasite is "an organism that lives on or in an organism of another species, known as the host, from the body of which it obtains nutriment" (https://www.dictionary.com/browse/parasite), while a predator is "any organism that exists by preying upon other organisms" (https://www.dictionary.com/browse/predator). The Merriam-Webster dictionary (https://www.merriam-webster.com) provides the following definition of a parasite: "an animal or plant that lives in or on another animal or plant and gets food or protection from it" (https://www.merriam-webster.com/dictionary/parasite), and the following definition of a predator "an animal that lives by killing and eating other animals: an animal that preys on other animals" (https://www.merriam-webster.com/dictionary/predator). As evident, various sources' definitions are similar, though they differ slightly in wording.

When considering a more specialistic source of definitions of parasitism and predation, one can use those provided by the New England Complex Systems Institute (Cambridge, MA, USA) (https://necsi.edu). According to this institute: "A parasitic relationship is one in which one organism, the parasite, lives off another organism, the host, harming it and possibly causing death. The parasite lives on or in the body of the host" (https://necsi.edu/parasitic-relationships); and "A predator is an organism that eats another organism. The prey is the organism which the predator eats" (https://necsi.edu/predator-prey-relationships). Finally, precise biological and ecological definitions are provided by Nature Education (Cambridge, MA, USA). On their web pages, the following definitions of parasitism and predation are found: "In parasitism, an individual organism, the parasite, consumes nutrients from another organism, its host, resulting in a decrease in fitness to the host" and "In predation, one organism kills and consumes another. Predation provides energy to prolong the life and promote the reproduction of the organism that does the killing, the predator, to the detriment of the organism being consumed, the prey", respectively (Stevens 2010). Although classical definitions of parasites and predators concern animals, it is evident that some plants can also be clearly included in one of these groups. Dodder

(genus *Cuscuta*) (Noureen et al. 2019) and Venus flytrap (genus *Dionaea*) (Hedrich and Neher 2018) are examples of parasite and predatory plants, respectively.

Considering all the definitions provided above, to make a general statement, one may indicate that a parasite exploits its host to get nutriment and propagate either inside or on this organism when it is still living. On the other hand, a predator kills its prey and uses the death entity to get nutriment. Hence, one should note that there are drastic differences between biological/ecological definitions of parasites and predators. The most important one is that a parasite exists in or on a living host, whereas a predator kills its prey and uses the resources of a dead creature. Sometimes, a predator can start to consume fragments of the prey even if it is not yet killed, but this event of consumption of a living prey is always short and strictly connected to the killing process. In other words, by definition, a predator does not feed on a still-living organism but kills it before or in the relatively short process of consumption.

Lifestyles of bacteriophages

Knowing the definitions of parasites and predators, let us analyze lifestyles of bacteriophages. There are generally three major developmental schemes of bacteriophages, lytic cycle, lysogenic cycle, and permanent infection (chronic cycle), as summarized and depicted recently (Grabowski et al. 2021). See also Fig. 1 for a simple scheme. These developmental possibilities are presented briefly below, while for more details, a reader is referred to a recent book on bacteriophage biology (Harper et al. 2021).

In the lytic cycle, a bacteriophage infects a bacterial host by injecting its genome (either DNA or RNA) into the cell, followed by the phage genome replication and expression of its genes, leading to the formation of progeny phages. All these processes occur inside a living cell, and in fact, there are no lytic bacteriophages able to propagate in dead cells or even in non-growing cells. This is because phages use resources, both chemical compounds (including functional molecules, like enzymes and tRNAs, higher-order functional structures, like ribosomes, and low-molecular-mass compounds, likes nucleotides, amino acids, and ions) and energy (in the form of ATP and GTP), from a metabolically active host. Suppose the metabolism of a bacteriophage-infected bacterial cell is halted. In that case, some phages may enter a specific stage called 'pseudolysogeny', during which phage development is stopped, and its genome neither replicates nor is degraded inside the host cell, and no insertion into the host DNA is observed (Łoś and Węgrzyn 2012). A bacteriophage can

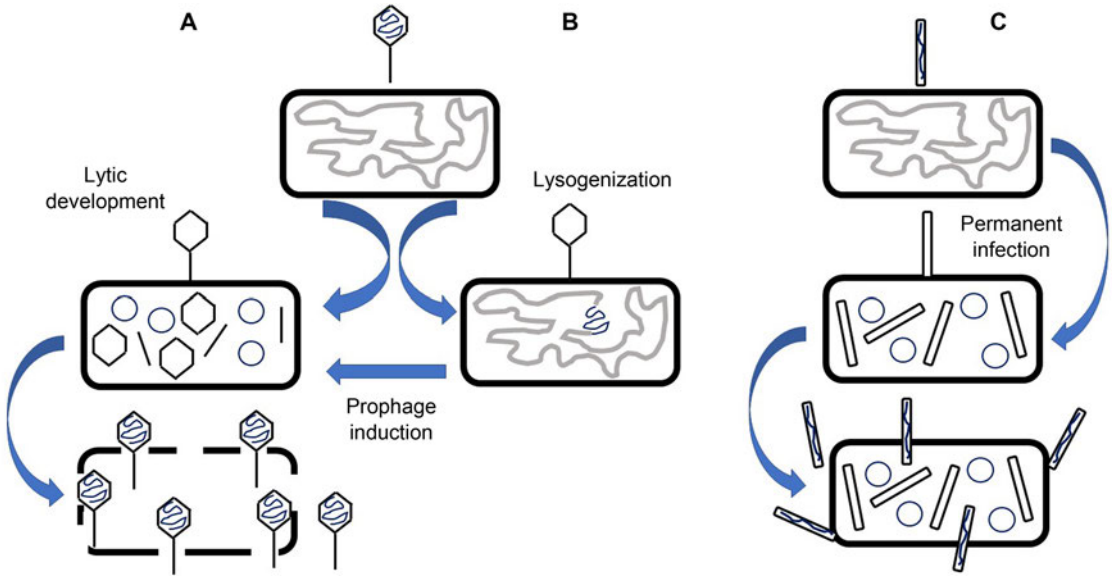

Fig. 1. Three developmental pathways of bacteriophages: lytic development (or lytic cycle) (panel A), lysogenization (or lysogenic cycle) (panel B), and permanent infection (or chronic cycle) (panel C). Phage virion (exemplified by a caudate phage in panels A and B, and a filamentous phage in panel C) adsorbs on the host cell and introduces its genome into this cell while the protein capsid remains outside the host. During the lytic development (A), the phage genome replicates intensively, and due to the expression of phage genes, structural proteins, forming capsids, are produced. After assembling progeny virions, the host cell is lysed due to the action of phage-encoded lytic proteins, and newly formed bacteriophages are liberated to the environment. During the lysogenic cycle (B), the phage genome integrates into the host chromosome by the site-specific recombination mechanism, forming a prophage, and it is passively replicated together with the bacterial nucleoid. In some cases, the phage genome can replicate as an extrachromosomal genetic element in the form of a plasmid. Under stress conditions, prophage is induced, phage DNA is excised from the host chromosome, and the development switches to the lytic mode. During the permanent infection (C), the development proceeds similarly to that during the lytic cycle; however, the host cell is not lysed when progeny phages leave the bacterium; thus, production of newly formed bacteriophages and their release into the environment proceed continuously.

restart its development only after re-establishing the cellular metabolism. The lytic development ends with host cell lysis and liberation of progeny phages. However, although the lysis means the death of the bacterial cells, one should note that bacteriophages no longer use the host resources after this event.

During the lysogenic cycle, the dependence of a bacteriophage on its living host is even more pronounced. In this case, after injection of the phage genome into the host cell, bacteriophage DNA is integrated into the bacterial chromosome, and then it is passively replicated as a part of the nucleoid (such a form of bacteriophage is called a prophage). In some cases, the phage genome can behave as a plasmid that replicates independently from the host chromosome (Rybchin and Svarchevsky 1999; Li and Austin 2002). Nevertheless, irrespective of the form of lysogenization, a prophage which is an episome or a plasmid, always requires a living bacterial host to survive. Importantly, under conditions endangering bacterial cell life, a prophage can be induced and the developmental cycle is switched to the lytic one.

The permanent infection, also called the chronic cycle (Pessione 2020), generally resembles the lytic cycle; however, in this case, propagating bacteriophage does not kill its bacterial host (at least not immediately and directly) but progeny virions of the bacteriophage continuously formed are released through a cell envelope without killing the bacterium. Interestingly, this cycle causes a lower growth rate of the host bacterial cell because part of the cell energy is directed to phage functions (Munson-McGee et al. 2018).

The analysis: parasites versus predators

In the light of various bacteriophage life cycles, let us analyze whether these viruses fulfill the definition of a parasite, a predator, or both. In the beginning, it is worth noting that definitions of parasites and predators and a distinguishment between a parasite and a predator were elaborated primarily based on observations of relationships between multicellular eukaryotic organisms. Therefore, one should consider whether such definitions can reflect any virus-host interactions. For example, in the classical definitions, the way of acquiring nutrients is crucial, while viruses (including bacteriophages) do not need to acquire nutrients the way that, for example, a helminth in an animal gut or a lion hunting for a zebra do. On the other hand, a good biological or ecological definition should reflect all forms of life or biological entities; therefore, it should also be extended to microorganisms and viruses. In fact, although viruses do not acquire nutrients in an animal-like manner, and they do not digest food, they still need nucleotides for the synthesis of their nucleic acids, and they still require amino acids to produce their proteins, and those low-molecular-weight compounds must be obtained from their host cells. Hence, definitions of parasites and predators can also be used when considering bacteriophages if remembering the specificity of development and 'nutrition' of these viruses. Considering this, I will discuss bacteriophages as biological entities being either parasites or predators, showing whether they correspond more closely to the former or the latter group of organisms.

The crucial point is that in all kinds of bacteriophage development, all types of bacteriophages require living hosts to propagate. No stage of bacteriophage lytic development can proceed inside a bacterial cell that is dead. The same rule applies to the permanent infection when the living host is necessary to provide resources for continuously developing phages. The living cell is also indispensable for the existence of a prophage; thus, the lysogenic development is fully dependent on the life of the host. Therefore, it appears clear that all bacteriophages meet the conditions of being parasites. They live inside the living host from which they get nutrients and energy for their propagation.

The question remains whether bacteriophages meet the conditions of being predators. Phages kill other organisms (bacteria in this case), as all predators do. However, the vital difference is that bacteriophages cannot use resources of killed organisms to eat them or to propagate. No phage can exploit a dead bacterial cell to perform its biological functions. Therefore, the host's death is an effect of bacteriophage propagation as a parasite rather than a way to obtain nutrients, as in the case of predation. After cell lysis, bacteriophages cannot use any compounds of such a 'prey'; thus, a killed organism is entirely useless for these viruses, indicating a great contrast to typical features of predators that first kill their prey and then eat them.

One more argument for classifying bacteriophages as parasites rather than predators comes from the concept of the general shifts from parasitism to mutualism, demonstrated in various biological systems. Namely, some primary parasites can evolve together with their hosts to form couples of mutualistically cooperating organisms (Paszkowski 2006; Leung and Poulin 2008; Mandyam and Jumpponen 2015; Drew et al. 2021). Importantly, a shift from parasitism to mutualism does not exist when predation is involved, as a predator could never become a symbiont. In this light, it is crucial to indicate that many bacteriophages can provide advantages to their host bacteria, primarily when occurring in the lysogenic state. They include the production of compounds that help the bacterial host to survive in the human or animal gut (Wandro et al. 2019; Dragoš et al. 2021), promotion of

the fitness of bacterial biofilms (Thingstad et al. 2015), transduction mechanisms allowing DNA exchanges among bacteria (Harrison and Brockhurst 2017), facilitation of bacterial membrane vesicles' formation and release (Turnbull et al. 2016; Toyofuku et al. 2017), and protection of the bacterial population against protist predators (Łoś et al. 2013).

On the other hand, according to Nature Education, "In most situations, parasites do not kill their hosts" (Stevens 2010). Therefore, one might doubt if bacteriophages developing by the lytic cycle can really be called 'parasites'. This dilemma can be solved by introducing the definition of parasitoids – a kind of parasites that exploit their hosts intensively and eventually kill them. The Nature Education indicates that contrary to classical parasites, parasitoids kill their hosts "which blur the line between parasitism and predation", and then, which is crucial: "The major distinguishing difference between parasitoids and predators is that parasitoids feed on living tissue, whereas the predator kills its prey before, or in the process of, consuming it" (Stevens 2010). In this light, prophages (during the lysogenic cycle) and phages developing according to the permanent infection model appear to fulfill the definition of parasites. However, it would be hard to indicate that phages kill their prey before consumption (this is not the case) or even in the process of consumption of bacterial cells, as these viruses use resources of the host for their multiplication rather than 'eat' the bacterium. Therefore, bacteriophages do not meet the requirements indicated in the precise definition of predators and should not be classified as such.

Conclusions

In summary, all known bacteriophages exploit only living host cells to get nutriment and energy for their propagation which is a characteristic of parasites. On the contrary, although bacteriophages can kill bacterial cells, they cannot use any resources of a dead entity, in contrast to predators that kill the prey and then use them as a source of nutrients. Thus, I conclude that according to biological definitions and ecological relationships between different forms of life, bacteriophages should be classified as parasites rather than predators. This applies especially to phages occurring in host cells as prophages during the lysogenic cycle and those which propagate according to the permanent infection mode. Strictly virulent bacteriophages, which multiply solely by lytic development, can be classified as particular parasites, called parasitoids. They ultimately kill their hosts after exploiting them as sources of chemical compounds and energy required to produce phage progeny.

ORCID
Grzegorz Węgrzyn https://orcid.org/0000-0003-4042-7466

Acknowledgments
I thank members of the team I lead for many inspirating discussions. This work was supported by the University of Gdansk (task grant No. 531-D020-D242-21).

Conflict of interest
The author does not report any financial or personal connections with other persons or organizations, which might negatively affect the contents of this publication and/or claim authorship rights to this publication.

Literature

Barrios ME, Blanco Fernández MD, Cammarata RV, Torres C, Power P, Mbayed VA. Diversity of beta-lactamase-encoding genes in wastewater: bacteriophages as reporters. Arch Virol. 2021 May; 166(5):1337–1344. https://doi.org/10.1007/s00705-021-05024-y

Batinovic S, Wassef F, Knowler SA, Rice DTF, Stanton CR, Rose J, Tucci J, Nittami T, Vinh A, Drummond GR, et al. Bacteriophages in natural and artificial environments. Pathogens. 2019 Jul 12; 8(3):100. https://doi.org/10.3390/pathogens8030100

Betts A, Gifford DR, MacLean RC, King KC. Parasite diversity drives rapid host dynamics and evolution of resistance in a bacteriaphage system. Evolution. 2016 May;70(5):969–978. https://doi.org/10.1111/evo.12909

Bhargava K, Nath G, Bhargava A, Aseri GK, Jain N. Phage therapeutics: from promises to practices and prospectives. Appl Microbiol Biotechnol. 2021 Dec;105(24):9047–9067. https://doi.org/10.1007/s00253-021-11695-z

Boyd CM, Angermeyer A, Hays SG, Barth ZK, Patel KM, Seed KD. Bacteriophage ICP1: A persistent predator of *Vibrio cholerae*. Annu Rev Virol. 2021 Sep 29;8(1):285–304. https://doi.org/10.1146/annurev-virology-091919-072020

Boyd EF. Bacteriophage-encoded bacterial virulence factors and phage-pathogenicity island interactions. Adv Virus Res. 2012; 82:91–118. https://doi.org/10.1016/B978-0-12-394621-8.00014-5

Casas V, Maloy S. Role of bacteriophage-encoded exotoxins in the evolution of bacterial pathogens. Future Microbiol. 2011 Dec;6(12): 1461–1473. https://doi.org/10.2217/fmb.11.124

Correa AMS, Howard-Varona C, Coy SR, Buchan A, Sullivan MB, Weitz JS. Revisiting the rules of life for viruses of microorganisms. Nat Rev Microbiol. 2021 Aug;19(8):501–513. https://doi.org/10.1038/s41579-021-00530-x

Dragoš A, Andersen AJC, Lozano-Andrade CN, Kempen PJ, Kovács ÁT, Strube ML. Phages carry interbacterial weapons encoded by biosynthetic gene clusters. Curr Biol. 2021 Aug 23;31(16):3479–3489.e5. https://doi.org/10.1016/j.cub.2021.05.046

Drew GC, Stevens EJ, King KC. Microbial evolution and transitions along the parasite-mutualist continuum. Nat Rev Microbiol. 2021 Oct;19(10):623–638. https://doi.org/10.1038/s41579-021-00550-7

Duan Y, Young R, Schnabl B. Bacteriophages and their potential for treatment of gastrointestinal diseases. Nat Rev Gastroenterol Hepatol. 2021 Nov 15. https://doi.org/10.1038/s41575-021-00536-z

Fathima B, Archer AC. Bacteriophage therapy: recent developments and applications of a renaissant weapon. Res Microbiol. 2021 Sep-Oct;172(6):103863. https://doi.org/10.1016/j.resmic.2021.103863

Górski A, Międzybrodzki R, Węgrzyn G, Jończyk-Matysiak E, Borysowski J, Weber-Dąbrowska B. Phage therapy: Current status and perspectives. Med Res Rev. 2020 Jan;40(1):459–463. https://doi.org/10.1002/med.21593

Gorter FA, Hall AR, Buckling A, Scanlan PD. Parasite host range and the evolution of host resistance. J Evol Biol. 2015 May;28(5): 1119–1130. https://doi.org/10.1111/jeb.12639

Grabowski Ł, Łepek K, Stasiłojć M, Kosznik-Kwaśnicka K, Zdrojewska K, Maciąg-Dorszyńska M, Węgrzyn G, Węgrzyn A. Bacteriophage-encoded enzymes destroying bacterial cell membranes and walls, and their potential use as antimicrobial agents. Microbiol Res. 2021 Jul;248:126746. https://doi.org/10.1016/j.micres.2021.126746

Harada LK, Silva EC, Campos WF, Del Fiol FS, Vila M, Dąbrowska K, Krylov VN, Balcão VM. Biotechnological applications of bacteriophages: State of the art. Microbiol Res. 2018 Jul-Aug;212–213: 38–58. https://doi.org/10.1016/j.micres.2018.04.007

Harper DR, Abedon ST, Burrowes BH, McConville ML. Bacteriophages. Biology, technology, therapy. Cham (Switzerland): Springer, Cham; 2021. https://doi.org/10.1007/978-3-319-41986-2

Harrison E, Brockhurst MA. Ecological and evolutionary benefits of temperate phage: What does or doesn't kill you makes you stronger. Bioessays. 2017 Dec;39(12):1700112. https://doi.org/10.1002/bies.201700112

Hedrich R, Neher E. Venus flytrap: How an excitable, carnivorous plant works. Trends Plant Sci. 2018 Mar;23(3):220–234. https://doi.org/10.1016/j.tplants.2017.12.004

Hsu CL, Duan Y, Fouts DE, Schnabl B. Intestinal virome and therapeutic potential of bacteriophages in liver disease. J Hepatol. 2021 Dec;75(6):1465–1475. https://doi.org/10.1016/j.jhep.2021.08.003

Iszatt JJ, Larcombe AN, Chan HK, Stick SM, Garratt LW, Kicic A. Phage therapy for multi-drug resistant respiratory tract infections. Viruses. 2021 Sep 11;13(9):1809. https://doi.org/10.3390/v13091809

Jaroszewicz W, Morcinek-Orłowska J, Pierzynowska K, Gaffke L, Węgrzyn G. Phage display and other peptide display technologies. FEMS Microbiol Rev. 2021 Oct 21:fuab052. https://doi.org/10.1093/femsre/fuab052

Kortright KE, Chan BK, Koff JL, Turner PE. Phage therapy: A renewed approach to combat antibiotic-resistant bacteria. Cell Host Microbe. 2019 Feb 13;25(2):219–232. https://doi.org/10.1016/j.chom.2019.01.014

Leung TLF, Poulin R. Parasitism, commensalism, and mutualism: Exploring the many shades of symbioses. Vie et Milieu – Life Environ. 2008;58(2):107–115.

Li Y, Austin S. The P1 plasmid in action: time-lapse photomicroscopy reveals some unexpected aspects of plasmid partition. Plasmid. 2002 Nov;48(3):174–178. https://doi.org/10.1016/s0147-619x(02)00104-x

Liu R, Li Z, Han G, Cun S, Yang M, Liu X. Bacteriophage ecology in biological wastewater treatment systems. Appl Microbiol Biotechnol. 2021 Jul;105(13):5299–5307. https://doi.org/10.1007/s00253-021-11414-8

Łoś JM, Łoś M, Węgrzyn A, Węgrzyn G. Altruism of Shiga toxin-producing *Escherichia coli*: recent hypothesis versus experimental results. Front Cell Infect Microbiol. 2013 Jan 4;2:166. https://doi.org/10.3389/fcimb.2012.00166

Łoś JM, Łoś M, Węgrzyn G. Bacteriophages carrying Shiga toxin genes: genomic variations, detection and potential treatment of pathogenic bacteria. Future Microbiol. 2011 Aug;6(8):909–924. https://doi.org/10.2217/fmb.11.70

Łoś M, Czyz A, Sell E, Wegrzyn A, Neubauer P, Wegrzyn G. Bacteriophage contamination: is there a simple method to reduce its deleterious effects in laboratory cultures and biotechnological factories? J Appl Genet. 2004;45(1):111–120.

Łoś M, Węgrzyn G. Pseudolysogeny. Adv Virus Res. 2012;82: 339–349. https://doi.org/10.1016/B978-0-12-394621-8.00019-4

Lourenço M, Chaffringeon L, Lamy-Besnier Q, Pédron T, Campagne P, Eberl C, Bérard M, Stecher B, Debarbieux L, De Sordi L. The spatial heterogeneity of the gut limits predation and fosters coexistence of bacteria and bacteriophages. Cell Host Microbe. 2020 Sep 9;28(3):390–401.e5. https://doi.org/10.1016/j.chom.2020.06.002

Mandyam KG, Jumpponen A. Mutualism-parasitism paradigm synthesized from results of root-endophyte models. Front Microbiol. 2015 Jan 12;5:776. https://doi.org/10.3389/fmicb.2014.00776

Mgomi FC, Yuan L, Chen CW, Zhang YS, Yang ZQ. Bacteriophages: A weapon against mixed-species biofilms in the food processing environment. J Appl Microbiol. 2021 Dec 21;00:1–15. https://doi.org/10.1111/jam.15421

Munson-McGee JH, Snyder JC, Young MJ. Archaeal viruses from high-temperature environments. Genes (Basel). 2018 Feb 27;9(3):128. https://doi.org/10.3390/genes9030128

Naureen Z, Dautaj A, Anpilogov K, Camilleri G, Dhuli K, Tanzi B, Maltese PE, Cristofoli F, De Antoni L, Beccari T, et al. Bacteriophages presence in nature and their role in the natural selection of bacterial populations. Acta Biomed. 2020 Nov 9;91(13-S):e2020024. https://doi.org/10.23750/abm.v91i13-S.10819

Noureen S, Noreen S, Ghumman SA, Batool F, Bukhari SNA. The genus *Cuscuta* (Convolvolaceae): An updated review on indigenous uses, phytochemistry, and pharmacology. Iran J Basic Med Sci. 2019 Nov;22(11):1225–1252. https://doi.org/10.22038/ijbms.2019.35296.8407

Orzechowska B, Mohammed M. The war between bacteria and bacteriophages. In: Mishra M, editor. Growing and handling of bacterial cultures. London (UK): IntechOpen; 2019. https://doi.org/10.5772/intechopen.87247

Paszkowski U. Mutualism and parasitism: the yin and yang of plant symbioses. Curr Opin Plant Biol. 2006 Aug;9(4):364–370. https://doi.org/10.1016/j.pbi.2006.05.008

Pessione E. The Russian doll model: How bacteria shape successful and sustainable inter-kingdom relationships. Front Microbiol 2020 Oct 20;11:573759. https://doi.org/10.3389/fmicb.2020.573759

Podlacha M, Grabowski Ł, Kosznik-Kawśnicka K, Zdrojewska K, Stasiłojć M, Węgrzyn G, Węgrzyn A. Interactions of bacteriophages with animal and human organisms-safety issues in the light of phage therapy. Int J Mol Sci. 2021 Aug 19;22(16):8937. https://doi.org/10.3390/ijms22168937

Rybchin VN, Svarchevsky AN. The plasmid prophage N15: a linear DNA with covalently closed ends. Mol Microbiol. 1999 Sep;33(5): 895–903. https://doi.org/10.1046/j.1365-2958.1999.01533.x

Salmond GP, Fineran PC. A century of the phage: past, present and future. Nat Rev Microbiol. 2015 Dec;13(12):777–786. https://doi.org/10.1038/nrmicro3564

Srinivasiah S, Bhavsar J, Thapar K, Liles M, Schoenfeld T, Wommack KE. Phages across the biosphere: contrasts of viruses in soil and aquatic environments. Res Microbiol. 2008 Jun;159(5):349–357. https://doi.org/10.1016/j.resmic.2008.04.010

Stevens A. Predation, herbivory, and parasitism [Internet]. Nature Education Knowledge. 2010;3(10):36 [cited 2021 Nov 10]. Available from https://www.nature.com/scitable/knowledge/library/predation-herbivory-and-parasitism-13261134/

Tetz G, Tetz V. Bacteriophages as new human viral pathogens. Microorganisms. 2018 Jun 16;6(2):54. https://doi.org/10.3390/microorganisms6020054

Tetz GV, Ruggles KV, Zhou H, Heguy A, Tsirigos A, Tetz V. Bacteriophages as potential new mammalian pathogens. Sci Rep. 2017 Aug 1;7(1):7043. https://doi.org/10.1038/s41598-017-07278-6

Thingstad TF, Pree B, Giske J, Våge S. What difference does it make if viruses are strain-, rather than species-specific? Front Microbiol. 2015 Apr 20;6:320. https://doi.org/10.3389/fmicb.2015.00320

Tian F, Li J, Nazir A, Tong Y. Bacteriophage – A promising alternative measure for bacterial biofilm control. Infect Drug Resist. 2021 Jan 20;14:205–217. https://doi.org/10.2147/IDR.S290093

Topka-Bielecka G, Dydecka A, Necel A, Bloch S, Nejman-Faleńczyk B, Węgrzyn G, Węgrzyn A. Bacteriophage-derived depolymerases against bacterial biofilm. Antibiotics (Basel). 2021 Feb 10;10(2):175. https://doi.org/10.3390/antibiotics10020175

Toyofuku M, Cárcamo-Oyarce G, Yamamoto T, Eisenstein F, Hsiao C-C, Kurosawa M, Gademann K, Pilhofer M, Nomura N, Eberl L. Prophage-triggered membrane vesicle formation through peptidoglycan damage in *Bacillus subtilis*. Nat Commun. 2017 Sep 7;8(1):481. https://doi.org/10.1038/s41467-017-00492-w

Turnau K, Fiałkowska E, Ważny R, Rozpądek P, Tylko G, Bloch S, Nejman-Faleńczyk B, Grabski M, Węgrzyn A, Węgrzyn G. Extraordinary multi-organismal interactions involving bacteriophages, bacteria, fungi, and rotifers: Quadruple microbial trophic network in water droplets. Int J Mol Sci. 2021 Feb 22;22(4):2178. https://doi.org/10.3390/ijms22042178

Turnbull L, Toyofuku M, Hynen AL, Kurosawa M, Pessi G, Petty NK, Osvath SR, Cárcamo-Oyarce G, Gloag ES, Shimoni R, et al. Explosive cell lysis as a mechanism for the biogenesis of bacterial membrane vesicles and biofilms. Nat Commun. 2016 Apr 14;7:11220. https://doi.org/10.1038/ncomms11220

Wandro S, Oliver A, Gallagher T, Weihe C, England W, Martiny JBH, Whiteson K. Predictable molecular adaptation of coevolving *Enterococcus faecium* and lytic phage EfV12-phi1. Front Microbiol. 2019 Jan 31;9:3192. https://doi.org/10.3389/fmicb.2018.03192

Zalewska-Piątek B, Piątek R. Bacteriophages as potential tools for use in antimicrobial therapy and vaccine development. Pharmaceuticals (Basel). 2021 Apr 5;14(4):331. https://doi.org/10.3390/ph14040331

Zhang Y, Li CX, Zhang XZ. Bacteriophage-mediated modulation of microbiota for diseases treatment. Adv Drug Deliv Rev. 2021 Sep;176:113856. https://doi.org/10.1016/j.addr.2021.113856

MINIREVIEW

Polish Journal of Microbiology
2022, Vol. 71, No 1, 11–18
https://doi.org/10.33073/pjm-2022-007

Impact of Primary and Secondary Bile Acids on *Clostridioides difficile* Infection

AGATA ŁUKAWSKA* and AGATA MULAK

Department of Gastroenterology and Hepatology, Wroclaw Medical University, Wroclaw, Poland

Submitted 10 November 2021, accepted 31 January 2022, published online 14 March 2022

Abstract

Primary bile acids (BAs), synthesized from cholesterol in the liver, after their secretion with bile into the intestinal lumen, are transformed by gut microbiota to secondary BAs. As natural detergents, BAs play a key role in the digestion and absorption of lipids and liposoluble vitamins. However, they have also been recognized as important signaling molecules involved in numerous metabolic processes. The close bidirectional interactions between BAs and gut microbiota occur since BAs influence microbiota composition, whereas microbiota determines BA metabolism. In particular, it is well established that BAs modulate *Clostridioides difficile* life cycle *in vivo*. *C. difficile* is a cause of common nosocomial infections that have become a growing concern. The aim of this review is to summarize the current knowledge regarding the impact of BAs on the pathogenesis, prevention, and treatment of *C. difficile* infection.

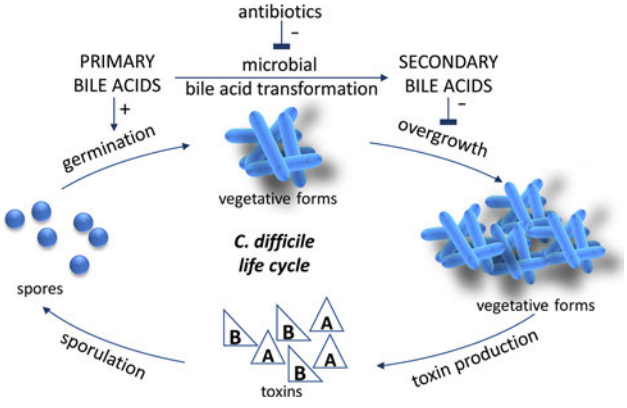

K e y w o r d s: bile acids, *Clostridioides difficile* infection, ursodeoxycholic acid, obeticholic acid

Introduction

Bile acids (BAs) are cholesterol-derived products with amphipathic properties due to several hydrophilic hydroxyl groups, a polar carboxyl group, and a steroid nucleus (Fiorucci and Distrutti 2019). There are two types of BAs: primary and secondary. Cholic acid (CA) and chenodeoxycholic acid (CDCA) are the main primary BAs produced by humans, while in mice, the predominant primary BAs are CA and muricholic acid (MCA) (Chiang and Ferrell 2019). Primary BAs are synthesized in the liver, and after conjugation with taurine or glycine, they are secreted into the biliary tracts. BAs constitute a main component of bile, which is accumulated in the gallbladder and, following the food intake, is secreted into the intestinal lumen (Ridlon et al. 2006). As natural detergents, BAs play a key role in lipid emulsification and absorption of lipids and liposoluble vitamins (Dawson and Karpen 2015).

Besides the participation in digestion, BAs are characterized by many other functions since they act as signaling molecules involved in regulating various metabolic processes (Fiorucci and Distrutti 2019). BAs are well-known ligands of widespread nuclear and membrane receptors. The nuclear receptors activated by BAs include farnesoid X receptor (FXR), pregnane X receptor (PXR), vitamin D receptor, liver X receptor (LXR), and glucocorticoid receptor (GR). Whereas G protein-coupled receptors (GPCR) on cell surface activated by BAs are Takeda G-protein receptor 5 (TGR5), sphingosine-1-phosphate receptor 2 (S1PR2), muscarinic receptors (M2 and M3), and formyl-peptide receptor (FPR) (Ticho et al. 2019).

The FXR activation modulates glucose, lipid, and protein metabolism, and energy expenditure. It also regulates various metabolic pathways in the liver, including hepatic fibrosis (Ferrebee and Dawson 2015). The FXR stimulation via BAs results in fibroblast

* Corresponding author: A. Łukawska, Department of Gastroenterology and Hepatology, Wroclaw Medical University, Wroclaw, Poland; **e-mail: agata.lukawska55@gmail.com**

growth factor 19 (FGF19) production in humans (FGF15 is the mouse ortholog). FGF19 regulates BA synthesis in the negative feedback loop by repressing cholesterol-7α-hydroxylase activity in hepatocytes, consequently leading to decreased hydroxylation of BAs and the reduction of BA synthesis (Babaknejad et al. 2018). Moreover, BA-mediated FXR stimulation regulates microbiota composition due to the enhanced expression of genes, the products of which, like nitric oxide, arrest bacterial overgrowth (Di Gregorio et al. 2021). Furthermore, FXR is involved in modulating intestinal innate inflammatory reactions through nuclear factor-kappa B (NF-κB) signaling. The BA binding to FXR also enhances mucosal integrity contributing to the protection against intestinal infections (Matsubara et al. 2013).

BA-mediated TGR5 activation influences glucose metabolism through enhanced secretion of incretins: glucose like peptide-1 and glucose like peptide-2 into the portal vein (Dawson and Karpen 2015). Moreover, it stimulates intestinal motility (Xie et al. 2021), induces gallbladder relaxation, reduces intrahepatic biliary pressure, and modulates BA pool composition (Bidault-Jourdainne et al. 2021). Additionally, the TGR5 activation restrains hepatic macrophage activity (Xie et al. 2021) and diminishes proinflammatory cytokines in monocytes, hence modulating inflammatory processes (Duboc et al. 2014). A summary of the main BA functions is presented in Fig. 1.

Due to the direct relationship between BAs and gut microbiota, and the impact of BAs on the regulation of various metabolic processes, especially modulation of the immune response, there is a growing attention directed toward the relationship between BAs and gastrointestinal infections, in particular *Clostridioides difficile*. It has already been well established that BAs modulate *C. difficile* life cycle (Abt et al. 2016). Moreover, several studies report BA alterations in the course of *C. difficile* infection (CDI) and during its treatment. The aim of this review is to summarize the current knowledge concerning the impact of BAs on the pathogenesis of CDI and the role of BAs in its prevention and treatment.

Two publication databases have been searched: PubMed and Scopus. Combinations of the following keywords were used ("bile acid" or "bile acids" or "ursodeoxycholic acid" or "ursodiol" or "obeticholic acid") and ("*Clostridioides difficile*" or "*Clostridioides difficile* infection" or "*Clostridium difficile*" or "*C. difficile*"). The search was limited to papers published between January 2005 and August 2021. Exclusion criteria were as follows: CDI only mentioned and non-English language.

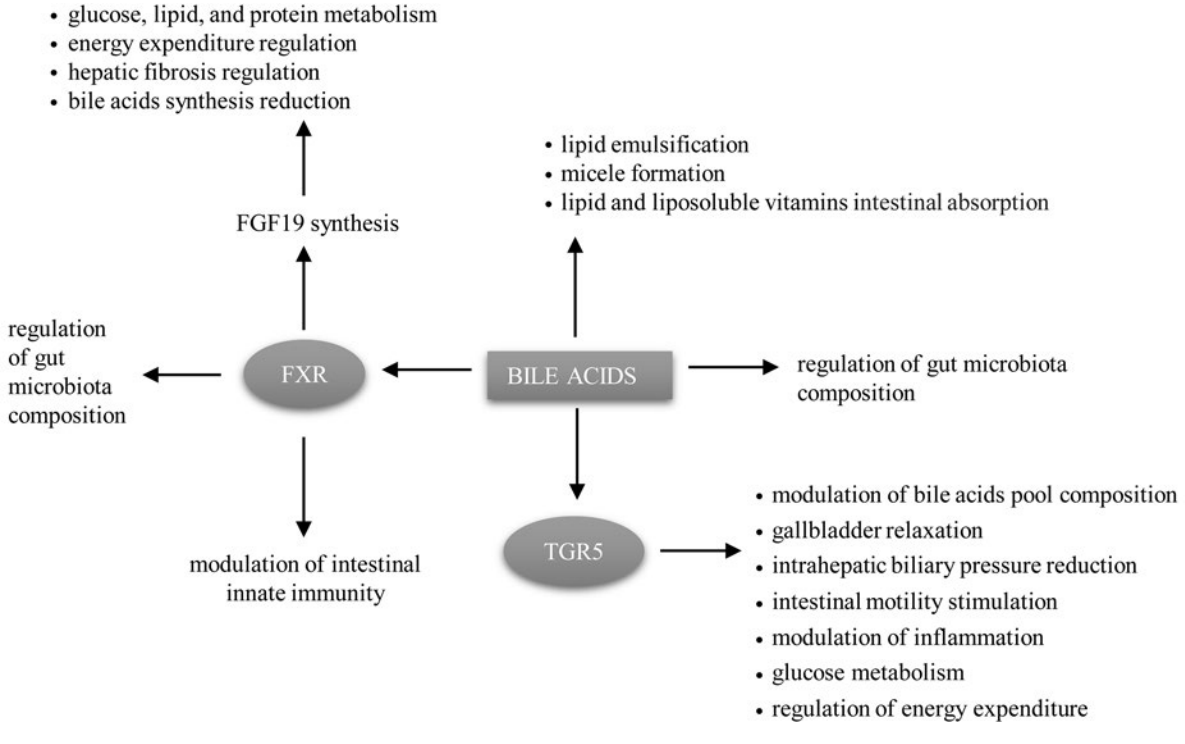

Fig. 1. Main functions of bile acids. Bile acids (BAs), as the main bile component, are responsible for lipid emulsification, micelle formation, and participation in the absorption of lipids and liposoluble vitamins. BAs also have an important impact on gut microbiota composition. BAs are farnesoid X receptor (FXR) ligands leading to fibroblast growth factor 19 (FGF19) synthesis. Moreover, FXR stimulation influences gut microbiota composition and intestinal innate immune response. BAs also activate Takeda G-protein receptor 5 (TGR5), stimulating intestinal motility, inducing gallbladder relaxation, reducing intrahepatic biliary pressure, modulating the composition of the BA pool, and affecting glucose metabolism. Additionally, the TGR5 activation regulates inflammatory processes and energy expenditure. Based on Dawson and Karpen (2015).

Crosstalk between bile acids and gut microbiota

In the small intestine, the gut bacteria metabolize BAs. The main transformation processes include deconjugation and oxidation of hydroxyl groups (Marin et al. 2015). Bile salt hydrolases (BSHs), the only enzymes responsible for the pivotal deconjugation reaction, allow BAs to become less toxic to the microbiota. BSHs cleave the conjugated glycine or taurine from BAs. The activity of BSHs serves as a gatekeeper to subsequent BA transformations (Foley et al. 2019). Approximately 95% of BAs are actively reabsorbed in the terminal ileum by the apical sodium-dependent bile acid transporter (ASBAT) to the portal vein from where they reach the liver and return into bile. It is called enterohepatic circulation (Ticho et al. 2019). The remaining 5% of unabsorbed BAs pass to the large intestine, where they undergo further microbial transformation (Marin et al. 2015). Only a narrow group of commensal bacteria can perform 7α-dehydroxylation, which is the crucial reaction in secondary BA origination. The *Lachnospiraceae* and *Ruminococcaceae* family members, including *Clostridium scindens*, *Clostridium hiranonis, Clostridium hylemonae*, and *Clostridium sordellii*, exert 7α-dehydroxylation activity (Wells and Hylemon 2000). 7α-Dehydratase releases hydroxyl group from BAs. As a result, primary BAs – CA, and CDCA are transformed into DCA and LCA, respectively. This reaction is possible due to prior deconjugation. Dihydroxylation and oxidation/epimerization of hydroxyl groups also occur in the large intestine. Epimerization of CDCA 7α-hydroxyl group to 7β-hydroxyl group provides the origination of ursodeoxycholic acid (UDCA) (Marin et al. 2015).

BA biotransformation results in modifying their properties, allowing for passive absorption of some BAs in the colon. Secondary BAs constitute an essential part of the BA metabolome. Partially BAs are also eliminated in the feces (Marin et al. 2015). Fig. 2 presents an overview of the BA circulation and biotransformation.

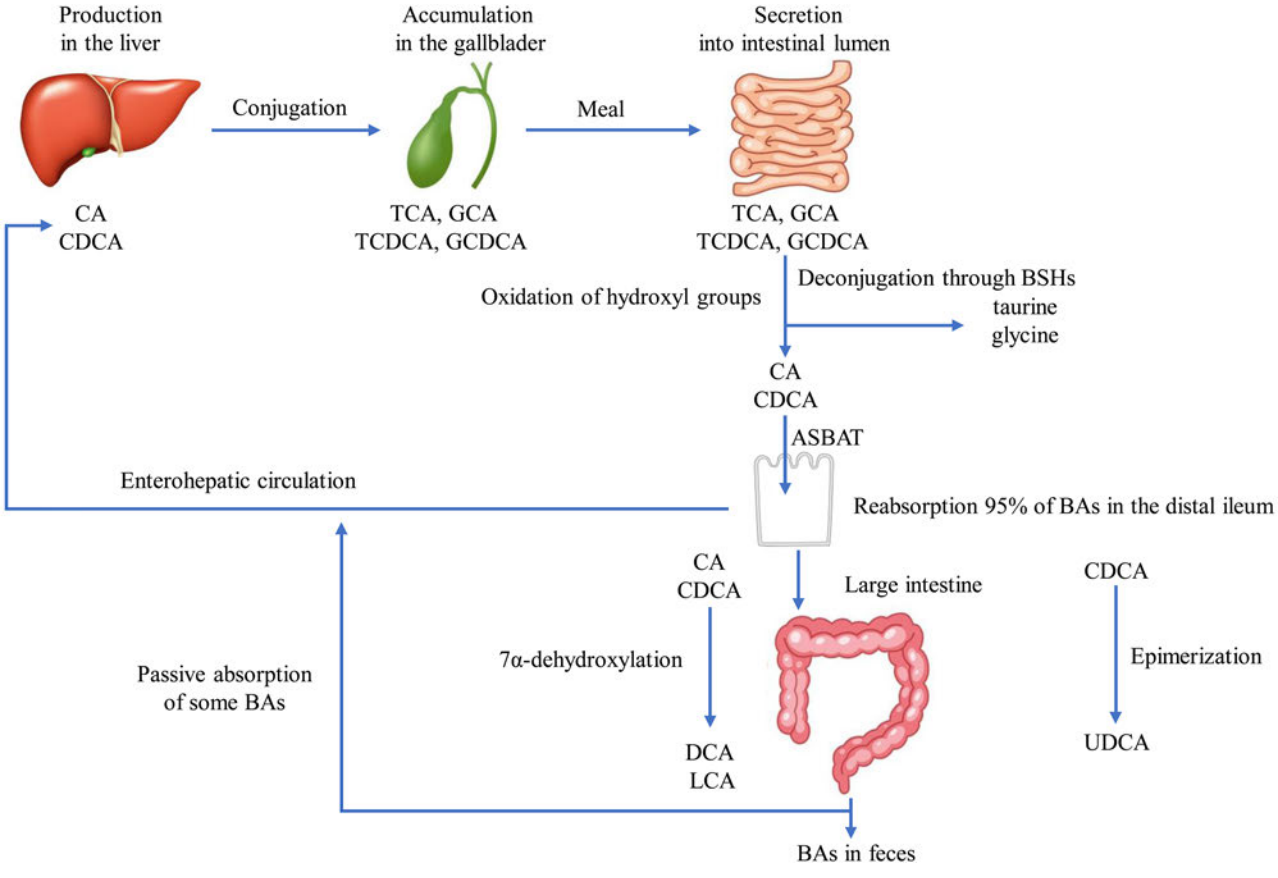

Fig. 2. Enterohepatic circulation and bile acid biotransformation. Primary bile acids (BAs) are produced in the liver and after conjugation with taurine or glycine are secreted into bile ducts. As a component of bile, they are accumulated in the gallbladder. After every meal, they are secreted into the intestinal lumen. In the small intestine, microbiota biotransformation starts. The deconjugation is performed by bile salt hydrolases (BSH), which constitute the key reaction enabling further transformations. Most BAs are absorbed in the distal ileum by the apical sodium-dependent bile acid transporter (ASBAT) to the portal vein from where they reach the liver and return into bile. The unabsorbed BAs pass to the large intestine, undergoing further microbial transformation. 7α-dehydroxylation is the crucial reaction in secondary BA origination. Some BAs are passively absorbed in the colon, and some are also eliminated in the feces. CA – cholic acid, CDCA – chenodeoxycholic acid, TCA – taurocholic acid, GCA – glycocholic acid, TCDCA – taurochenodeoxycholic acid, GCDCA – glycochenodeoxycholic acid, UDCA – ursodeoxycholic acid. Based on Fiorucci and Distrutti (2019).

Clostridioides difficile infection

CDI is the most common cause of antibiotic-associated diarrhea (Abt et al. 2016). It is related to a significant morbidity, mortality, and a substantial global burden to the healthcare system (Guh et al. 2020).

C. difficile is a Gram-positive bacillus with an ability to produce endospores, which are commonly found in the environment as well as in the intestinal tract of humans and animals (Czepiel et al. 2019). In the gastrointestinal tract, the spores may germinate and outgrow to pathogenetic vegetative forms, producing toxins A and B that evoke symptoms of CDI (Mahida 2019). Toxins A and B bind to specific surface receptors in the colon leading to intestinal epithelium necrosis and exfoliation, resulting in mucosal integrity disturbances. In consequence, immune cells and intoxicated epithelial cells release proinflammatory cytokines and chemokines such as interferon-gamma (IFN-γ), tumor necrosis factor-alpha (TNF-α), interleukin 6 (IL-6), and IL-1β. Subsequently, an acute inflammatory reaction in the intestinal wall develops (Winston et al. 2020).

CDI may be manifested by an asymptomatic carriage, mild to moderate diarrhea, colitis, pseudomembranous colitis, or even fulminant colitis. Antibiotic therapy, abdominal surgery, hospitalization, age over 65, and severe concomitant diseases are the major risk factors of CDI (Napolitano and Edmiston 2017).

The gut microbiota composition has an ability to protect against invasion by pathogenic microorganisms. The mechanism is not fully known; however, it is proposed that microbiota-derived secondary BAs take an important part in this process (Winston and Theriot 2016).

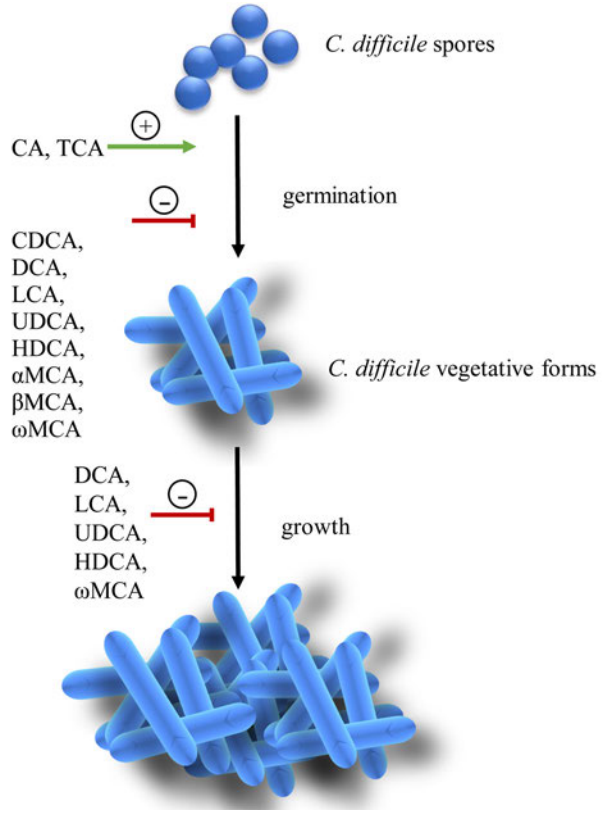

Fig. 3. Impact of bile acids on the life cycle of *Clostridioides difficile*. *C. difficile* is a Gram-positive bacillus, with an ability to produce endospores. Spores may germinate and outgrow in the gastrointestinal tract to produce pathogenic vegetative forms secreting toxins. Primary BAs such as cholic acid (CA) and taurocholic acid (TCA) are endogenous triggers to *C. difficile* spore germination. However, other primary BAs, including chenodeoxycholic acid (CDCA), α and β stereoisomers of muricholic acid (MCA), arrest *C. difficile* spore germination. Secondary BAs such as DCA, LCA, ursodeoxycholic acid (UDCA), hyodeoxycholic acid (HDCA), and ω-MCA inhibit *C. difficile* spore germination and the growth of *C. difficile* vegetative forms. Based on Studer et al. (2016).

Bile acid pool composition and *Clostridioides difficile* life cycle

Primary BAs such as CA and taurocholic acid (TCA), which are present in significant concentrations in the small intestine, promote *C. difficile* spore germination (Theriot et al. 2016). However, other primary BAs, including CDCA as well as α and β stereoisomers of MCA, prevent this process. Secondary BAs such as DCA, LCA, UDCA, hyodeoxycholate acid, and ω-MCA inhibit *C. difficile* spore germination as well as inhibit the growth of *C. difficile* vegetative forms (Studer et al. 2016) (Fig. 3). In the large intestine, secondary BAs are present in much higher concentrations than primary BAs. Therefore, *C. difficile* spores germinate to some extent in the small intestine, but the proper ratio of secondary BAs in the colon is pivotal for CDI prevention (Theriot et al. 2016). BAs influences *C. difficile* germination through the recently identified germinant receptor CspC (Weingarden et al. 2016b). They are capable of binding and inhibiting *C. difficile* toxin B as well. Secondary BAs are more potent in toxin inhibition than primary BAs (Mullish and Allegretti 2021). Interestingly, *C. scindens* and *C. sordellii* also produce tryptophan-derived antibiotics, which can inhibit the growth of *C. difficile*. DCA and LCA intensify the inhibitory activity of these antibiotics (Kang et al. 2019).

The healthy microbiota inhibits *C. difficile* spore germination and vegetative form growth through secondary BA production (Britton and Young 2014). Antibiotic therapy can lead to dysbiosis, disturbing secondary BA production and the BA pool composition (Studer et al. 2016). Consequently, increased primary BA level and decreased secondary BA level in the colon are observed (Theriot et al. 2016). It has been demonstrated that rats treated with antibiotics have higher primary BA concentration in stool than untreated rats (Hashimoto et al. 1996). In physiological conditions, secondary BAs constitute the majority of fecal BAs.

Disproportion in primary to secondary BA ratio after antibiotic therapy can be associated with loss of resistance to CDI (Keith et al. 2020).

Noteworthy, obesity constitutes CDI risk factor (Mulki et al. 2017). One potential mechanism underlying greater susceptibility of obese subjects to a more severe CDI course might be an obesity-related dysbiosis resulting in BA disturbances. In a study conducted by Jose et al. (2021), mice with diet-induced obesity had a significantly higher ratio of primary to secondary BAs in cecal content compared to mice on a regular chow diet. Primary BA production in the liver was enhanced in these obese mice, and consequently, *C. difficile* spore germination was promoted by cecal content contrary to non-obese mice. Obese mice developed severe and prolonged CDI (Jose et al. 2021).

In the study conducted by Wei et al. (2020), the number of *C. scindens* and *C. hylemonae* in feces was remarkably decreased in mice with diet-induced obesity contrary to non-obese mice (Wei et al. 2020). As aforementioned, *C. scindens* and *C. hylemonae* belong to a narrow group of bacteria, which can perform 7α-dehydroxylation, the crucial reaction in secondary BA origination (Wells and Hylemon 2000).

BA dysregulation has been reported in patients with CDI. Allegretti et al. (2016) have observed the shift in BA concentration in human stool with the primary BA predominance during CDI. Moreover, higher primary BA content in feces was noted during recurrent CDI compared to the first episode of CDI (Allegretti et al. 2016). On the other hand, *C. difficile* multiplication is associated with microbiota dysregulation contributing to the disturbances in BA metabolism. The perturbations of intestinal bacteria lead to *C. difficile* predominance and colonization (Czepiel et al. 2019). The presence of vegetative forms of *C. difficile* restrains from the colonization of other microorganisms. Numerous studies have shown a reduction in gut microbiota richness in patients with CDI compared to healthy controls, and in the first CDI episode compared to recurrent CDI (Theriot et al. 2011; 2014; Buffie et al. 2015). Lack of bacteria with 7α-dehydroxylation activity leads to decreased secondary BA production (Sehgal and Khanna 2021). It results in a a cause-and-effect relationship in which dysbiosis and BA pool alterations intensify and aggravate each other, leading inexorably to worsening of the situation, which could be described as a "vicious circle".

Therapeutic role of bile acids in *Clostridioides difficile* infection

Fecal microbiota transplantation. Antibiotics are the mainstay of CDI therapy. Vancomycin and fidaxomicin are recommended in the first CDI episode (Guh et al. 2020). However, these drugs can also lead to microbiota dysregulation. Even after successful treatment, 5–20% of patients with CDI may develop recurrent infection (Napolitano and Edmiston 2017). Relapses are treated with vancomycin for an extended time. However, while vancomycin eliminates *C. difficile* vegetative forms, it does not influence endospores (McDonald et al. 2018). Fecal microbiota transplantation (FMT) is the last choice option recommended in recurrent and refractory infections after the unsuccessful antibiotic treatment (Guh et al. 2020).

FMT is based on administering bacteria present in donor fecal filtrate to reestablish the resident microbiota. Apart from living bacteria, the products of their metabolism also significantly contribute to the FMT effectiveness. The microbial species with 7α-dehydroxylase activity present in the transplanted microbiota play a pivotal role in restoring resistance to *C. difficile* colonization, since 7α-dehydroxylase is responsible for the metabolism of primary BAs to secondary BAs in the colon (Mahida 2019).

Buffie et al. (2015) demonstrated that administration of *C. scindens*, a bacterial species with 7α-dehydroxylase activity, was associated with resistance to CDI in antibiotic-treated susceptible mice. Weingarden et al. (2016b) confirmed significant alterations in BA profile before and after FMT in patients with recurrent CDI. They have also demonstrated that the content of primary BAs in pre-FMT stool samples induces *C. difficile* spores germination and vegetative form growth, while post-FMT stool samples abounding in secondary BAs inhibit the life cycle of *C. difficile* (Weingarden et al. 2016b). Therefore, FMT contributes to the inversion of fecal BA profile from the predominance of primary BAs to the predominance of secondary BAs (Seekatz et al. 2018).

Ursodeoxycholic acid (UDCA). Given the relevant impact of BAs on the *C. difficile* life cycle, it has been proposed that secondary BAs can be possible therapeutic targets in preventing and treating CDI. UDCA, also known as ursodiol, is one of the human secondary BAs. UDCA has hydrophilic properties and is profusely reabsorbed in the distal ileum. Oral administration of UDCA results in its increased concentration in bile that leads to decreased hepatotoxic effects of bile (Cabrera et al. 2019). Therefore, UDCA is used in liver diseases such as primary biliary cholangitis and nonalcoholic steatohepatitis (Floreani 2020; Sodum et al. 2021). UDCA directly arrests germination and vegetative overgrowth of *C. difficile in vitro* (Thanissery et al. 2017). However, the direct impact of UDCA on microbiota *in vivo* is not fully understood.

The study conducted by Winston et al. (2020) demonstrated that no significant difference in microbiome after UDCA application could be seen in a mouse model.

However, another study showed that the UDCA administration results in reducing the abundance of *Bifidobacterium*, *Lactobacillus*, and *Lactobacillaceae* in the human gut microbiota composition (Kim et al. 2018).

As mentioned above, CDI is associated with decreased secondary BA and increased primary BA levels in the stool. Importantly, UCDA treatment of mice with CDI is associated with the BA pool alteration leading to the enhanced concentration of β-MCA, tauro-β-MCA, TCA, tauroursodeoxycholic acid (TUDCA), and UDCA in feces (Palmieri et al. 2018; Winston et al. 2020). However, differences in BA profiles and metabolism among species may constitute major limitations in BA research, making it challenging to translate animal models into clinic (Winston and Theriot 2020).

Palmieri et al. (2018) revealed that UDCA administration failed in CDI prevention in a rodent model. Similar results were obtained by Winston et al. (2020). They demonstrated in a murine model that UDCA treatment did not prevent CDI; however, it was associated with a retardation of the onset of symptoms. Therefore, UDCA may impact on the early stages of CDI pathogenesis (Winston et al. 2020). The retrospective analysis showed that the UDCA treatment of primary sclerosing cholangitis in patients with inflammatory bowel disease did not protect from CDI development (Palmieri et al. 2018). In another study, UDCA was prescribed off-label to patients with recurrent CDI and risk factors of relapses. In those cases, UDCA treatment was associated with 87.5% effectiveness in CDI prevention at a median follow-up of 264 days (Webb et al. 2019). Weingarden et al. (2016a) presented a single case report on a patient with recurrent *C. difficile* ileal pouchitis. They showed that oral UDCA treatment influenced *C. difficile* elimination and long-term prevention from CDI recurrence (Weingarden et al. 2016a). Currently, ursodiol is in phase IV clinical trials to prevent *C. difficile* recurrence (Winston et al. 2020).

Noteworthy, UDCA can modulate the immune response through NF-κB signaling. In the study by Winston et al. (2020) in a mouse model, UDCA application was associated with decreased expression of genes encoding products mediating the inflammatory response to CDI, including IFN-γ, IL-6, TNF-α, and IL-1β. Therefore, it may be concluded that UDCA treatment could reduce the excessive inflammatory response during CDI, subsequently alleviating severe forms of CDI. Moreover, the immune response modulation was associated with the UDCA-induced activation of TGR5 and FXR. Pretreatment with UDCA resulted in a significantly enhanced expression of TGR5, FXR, and FGF15 during CDI compared to the no-UDCA treatment (Winston et al. 2020). However, this effect of UDCA on the FXR signaling was not confirmed in prior studies. It has been reported that UDCA administration might also lead to the suppression of FGF19 transcription and increment of CYP7A1 expression, thus suggesting that UDCA is an FXR antagonist (Gonzalez et al. 2015).

Moreover, studies performed on primary human hepatocyte cultures have demonstrated that UDCA has no effect on hepatic FXR (Liu et al. 2014; Zhang et al. 2017). However, the administration of UDCA at supratherapeutic concentrations results in the FGF19 enhancement and subsequent CYP7A1 suppression. It has been suggested that the UDCA effect in higher doses is most likely exerted through the PXR signaling pathway and not mediated by FXR mechanisms (Zhang et al. 2017). The PXR activation also downregulates the NF-κB signaling (Mohandas and Vairappan 2017).

Obeticholic acid. Obeticholic acid (OCA) is a synthetically modified BA, which was approved in 2016 for the treatment of primary biliary cholangitis (Fiorucci et al. 2019). Currently, OCA is under investigation to treat primary sclerosing cholangitis and non-alcoholic steatohepatitis (Novotny et al. 2021). Similarly to UDCA, OCA administration leads to its absorption in the distal ileum and occurrence in bile. OCA as a potent FXR ligand contributes to the diminished synthesis of primary BAs in the liver. Consequently, OCA administration leads to a decrease in hepatotoxic properties of bile and lower primary BA content in the cecum (Novotny et al. 2021). Due to the affinity to FXR, OCA promotes NF-κB signaling and afterward takes part in the modulation of the intestinal immune response (Matsubara et al. 2013).

Given that obesity is a risk factor for a severe CDI, Jose et al. (2021) conducted a study administering OCA to obese mice after exposition to *C. difficile*. The result of the treatment was associated with a reduction in severity and duration of CDI symptoms. OCA contributed to the alleviation of CDI later phases by decreasing the number of *C. difficile* bacteria in stool and the cecal contents, and diminishing the concentrations of the toxins. Consequently, treatment with OCA resulted in a significant reduction of intestinal damage (Jose et al. 2021).

Conclusions and perspectives

It is well known that gut microbiota plays a pivotal role in CDI prevention. The CDI risk factors contribute to dysbiosis leading to dysregulation of the BA metabolome. Since BAs regulate *C. difficile* life cycle, they become promising therapeutic targets. FMT is also associated with a shift in fecal BA profile, which proves their important role in CDI. The role of UDCA, OCA, and other FXR and TGR5 agonists in CDI treatment, requires further investigation because the exact mechanism of BA-mediated FXR and TGR5 activation remains to be elucidated. The modulation

of the inflammatory response through NF-κB signaling and inhibition of BA synthesis seem particularly important. Therefore, BAs constitute an encouraging treatment option in CDI. Nonetheless, further studies concerning the definite relationship between BAs and the pathogenesis of CDI and the BA impact on the course of CDI are required.

ORCID

Agata Łukawska https://orcid.org/0000-0002-3766-3073
Agata Mulak https://orcid.org/0000-0003-4678-8393

Conflict of interest

The authors do not report any financial or personal connections with other persons or organizations, which might negatively affect the contents of this publication and/or claim authorship rights to this publication.

Literature

Abt MC, McKenney PT, Pamer EG. *Clostridium difficile* colitis: pathogenesis and host defence. Nat Rev Microbiol. 2016 Oct; 14(10): 609–620. https://doi.org/10.1038/nrmicro.2016.108

Allegretti JR, Kearney S, Li N, Bogart E, Bullock K, Gerber GK, Bry L, Clish CB, Alm E, Korzenik JR. Recurrent *Clostridium difficile* infection associates with distinct bile acid and microbiome profiles. Aliment Pharmacol Ther. 2016 Jun;43(11):1142–1153. https://doi.org/10.1111/apt.13616

Babaknejad N, Nayeri H, Hemmati R, Bahrami S, Esmaillzadeh A. An overview of FGF19 and FGF21: the therapeutic role in the treatment of the metabolic disorders and obesity FGF19. Horm Metab Res. 2018 Jun;50(6):441–452. https://doi.org/10.1055/a-0623-2909

Bidault-Jourdainne V, Merlen G, Glénisson M, Doignon I, Garcin I, Péan N, Boisgard R, Ursic-Bedoya J, Serino M, Ullmer C, et al. TGR5 controls bile acid composition and gallbladder function to protect the liver from bile acid overload. JHEP Reports. 2021 Nov; 3(2):100214. https://doi.org/10.1016/j.jhepr.2020.100214

Britton RA, Young VB. Role of the intestinal microbiota in resistance to colonization by *Clostridium difficile*. Gastroenterology. 2014 May; 146(6):1547–1553. https://doi.org/10.1053/j.gastro.2014.01.059

Buffie CG, Bucci V, Stein RR, McKenney PT, Ling L, Gobourne A, No D, Liu H, Kinnebrew M, Viale A, et al. Precision microbiome reconstitution restores bile acid mediated resistance to *Clostridium difficile*. Nature. 2015 Jan;517:205–208. https://doi.org/10.1038/nature13828

Cabrera D, Arab JP, Arrese M. UDCA, NorUDCA, and TUDCA in liver diseases: a review of their mechanisms of action and clinical applications. In: Fiorucci S, Distrutti E, editors. Bile acids and their receptors. Handbook of experimental pharmacology. Cham (Switzerland): Springer; 2019(256). p. 237–264. https://doi.org/10.1007/164_2019_241

Chiang JYL, Ferrell JM. Bile acids as metabolic regulators and nutrient sensors. Annu Rev Nutr. 2019 Aug;39:175–200. https://doi.org/10.1146/annurev-nutr-082018-124344

Czepiel J, Dróżdż M, Pituch H, Kuijper EJ, Perucki W, Mielimonka A, Goldman S, Wultańska D, Garlicki A, Biesiada G. *Clostridium difficile* infection: review. Eur J Clin Microbiol Infect Dis. 2019 Jul;38(7):1211–1221. https://doi.org/10.1007/s10096-019-03539-6

Dawson PA, Karpen SJ. Intestinal transport and metabolism of bile acids. J Lipid Res. 2015 Jun;56(6):1085–1099. https://doi.org/10.1194/jlr.R054114

Di Gregorio MC, Cautela J, Galantini L. Physiology and physical chemistry of bile acids. Int J Mol Sci. 2021 Feb;22(4):1780. https://doi.org/10.3390/ijms22041780

Duboc H, Taché Y, Hofmann AF. The bile acid TGR5 membrane receptor: from basic research to clinical application. Dig Liver Dis. 2014 Apr;46(4):302–312. https://doi.org/10.1016/j.dld.2013.10.021

Ferrebee CB, Dawson PA. Metabolic effects of intestinal absorption and enterohepatic cycling of bile acids. Acta Pharm Sin B. 2015 Mar;5(2):129–134. https://doi.org/10.1016/j.apsb.2015.01.001

Fiorucci S, Di Giorgio C, Distrutti E. Obeticholic acid: an update of its pharmacological activities in liver disorders. In: Fiorucci S, Distrutti E, editors. Bile acids and their receptors. Handbook of experimental pharmacology. Cham (Switzerland): Springer; 2019 (256). p. 283–295. https://doi.org/10.1007/164_2019_227

Fiorucci S, Distrutti E. The pharmacology of bile acids and their receptors. In: Fiorucci S, Distrutti E, editors. Bile acids and their receptors. Handbook of experimental pharmacology. Cham (Switzerland): Springer; 2019(256). p. 3–18. https://doi.org/10.1007/164_2019_238

Floreani A. Experimental pharmacological agents for the treatment of primary biliary cholangitis. J Exp Pharmacol. 2020 Dec;12: 643–652. https://doi.org/10.2147/JEP.S267375

Foley MH, O'Flaherty S, Barrangou R, Theriot CM. Bile salt hydrolases: gatekeepers of bile acid metabolism and host-microbiome crosstalk in the gastrointestinal tract. PLoS Pathog. 2019 Mar;15(3):e1007581. https://doi.org/10.1371/journal.ppat.1007581

Gonzalez FJ, Jiang C, Bisson WH, Patterson AD. Inhibition of farnesoid X receptor signaling shows beneficial effects in human obesity. J Hepatol. 2015 Jun;62(6):1234–1236. https://doi.org/10.1016/j.jhep.2015.02.043

Guh AY, Mu Y, Winston LG, Johnston H, Olson D, Farley MM, Wilson LE, Holzbauer SM, Phipps EC, Dumyati GK, et al. Trends in U.S. Burden of *Clostridioides difficile* infection and outcomes. N Eng J Med. 2020 Apr;382(14):1320–1330. https://doi.org/10.1056/NEJMoa1910215

Hashimoto S, Igimi H, Uchida K, Satoh T, Benno Y, Takeuchi N. Effects of β-lactam antibiotics on intestinal microflora and bile acid metabolism in rats. Lipids. 1996 Jun;31(6):601–609. https://doi.org/10.1007/BF02523830

Jose S, Mukherjee A, Horrigan O, Setchell KDR, Zhang W, Moreno-Fernandez ME, Andersen H, Sharma D, Haslam DB, Divanovic S, et al. Obeticholic acid ameliorates severity of *Clostridioides difficile* infection in high fat diet-induced obese mice. Mucosal Immunol. 2021 Mar;14(2):500–510. https://doi.org/10.1038/s41385-020-00338-7

Kang JD, Myers CJ, Harris SC, Kakiyama G, Lee IK, Yun BS, Matsuzaki K, Furukawa M, Min HK, Bajaj JS, et al. Bile acid 7α-dehydroxylating gut gacteria secrete antibiotics that inhibit *Clostridium difficile*: role of secondary bile acids. Cell Chem Biol. 2019 Jan; 26(1):27–34.e4. https://doi.org/10.1016/j.chembiol.2018.10.003

Keith JW, Dong Q, Sorbara MT, Becattini S, Sia JK, Gjonbalaj M, Seok R, Leiner IM, Littmann ER, Pamer EG. Impact of antibiotic-resistant bacteria on immune activation and *Clostridioides difficile* infection in the mouse intestine. Infect Immun. 2020;88(4):e00362-19. https://doi.org/10.1128/IAI.00362-19

Kim DJ, Yoon S, Ji SC, Yang J, Kim YK, Lee S, Yu KS, Jang IJ, Chung JY, Cho JY. Ursodeoxycholic acid improves liver function via phenylalanine/tyrosine pathway and microbiome remodelling in patients with liver dysfunction. Sci Rep. 2018 Aug;8(1):11874. https://doi.org/10.1038/s41598-018-30349-1

Liu J, Lu H, Lu YF, Lei X, Cui JY, Ellis E, Strom SC, Klaassen CD. Potency of individual bile acids to regulate bile acid synthesis and transport genes in primary human hepatocyte cultures. Toxicol Sci. 2014 Oct;141(2):538–546. https://doi.org/10.1093/toxsci/kfu151

Mahida YR. New concepts in *C. difficile* management. Br Med Bull. 2019 Sep;131(1):109–118. https://doi.org/10.1093/bmb/ldz029

Marin JJG, Macias RIR, Briz O, Banales JM, Monte MJ. Bile acids in physiology, pathology and pharmacology. Curr Drug Metab. 2015; 17(1):4–29. https://doi.org/10.2174/1389200216666151103115454

Matsubara T, Li F, Gonzalez FJ. FXR signaling in the enterohepatic system. Mol Cell Endocrinol. 2013 Apr;368(1–2):17–29. https://doi.org/10.1016/j.mce.2012.05.004

McDonald LC, Gerding DN, Johnson S, Bakken JS, Carroll KC, Coffin SE, Dubberke ER, Garey KW, Gould CV, Kelly C, et al. Clinical practice guidelines for *Clostridium difficile* infection in adults and children: 2017 update by the Infectious Diseases Society of America (IDSA) and Society for Healthcare Epidemiology of America (SHEA). Clin Infect Dis. 2018 Mar;66(7):e1–e48. https://doi.org/10.1093/cid/cix1085

Mohandas S, Vairappan B. Role of pregnane X-receptor in regulating bacterial translocation in chronic liver diseases. World J Hepatol. 2017 Nov;9(32):1210–1226. https://doi.org/10.4254/wjh.v9.i32.1210

Mulki R, Baumann AJ, Alnabelsi T, Sandhu N, Alhamshari Y, Wheeler DS, Perloff S, Katz PO. Body mass index greater than 35 is associated with severe *Clostridium difficile* infection. Aliment Pharmacol Ther. 2017 Jan;45(1):75–81. https://doi.org/10.1111/apt.13832

Mullish BH, Allegretti JR. The contribution of bile acid metabolism to the pathogenesis of *Clostridioides difficile* infection. Therap Adv Gastroenterol. 2021 May;14:17562848211017724. https://doi.org/10.1177/17562848211017725

Napolitano LM, Edmiston CE. *Clostridium difficile* disease: diagnosis, pathogenesis, and treatment update. Surgery. 2017 Aug; 162(2): 325–348. https://doi.org/10.1016/j.surg.2017.01.018

Novotny K, Hapshy V, Nguyen H, Parmar M. Obeticholic Acid. [Internet]. Treasure Island (USA): StatPearls Publishing; 2021 [cited 2021 Oct 11]. Available from https://www.ncbi.nlm.nih.gov/books/NBK567735/

Palmieri LJ, Rainteau D, Sokol H, Beaugerie L, Dior M, Coffin B, Humbert L, Eguether T, Bado A, Hoys S, et al. Inhibitory effect of ursodeoxycholic acid on *Clostridium difficile* germination is insufficient to prevent colitis: a study in hamsters and humans. Front Microbiol. 2018 Nov;9:2849. https://doi.org/10.3389/fmicb.2018.02849

Ridlon JM, Kang DJ, Hylemon PB. Bile salt biotransformations by human intestinal bacteria. J Lipid Res. 2006 Feb;47(2):241–259. https://doi.org/10.1194/jlr.R500013-JLR200

Seekatz AM, Theriot CM, Rao K, Chang YM, Freeman AE, Kao JY, Young VB. Restoration of short chain fatty acid and bile acid metabolism following fecal microbiota transplantation in patients with recurrent *Clostridium difficile* infection. Anaerobe. 2018 Feb; 53:64–73. https://doi.org/10.1016/j.anaerobe.2018.04.001

Sehgal K, and Khanna S. Gut microbiome and *Clostridioides difficile* infection: a closer look at the microscopic interface. Therap Adv Gastroenterol. 2021 Feb;14:1–9. https://doi.org/10.1177/1756284821994736

Sodum N, Kumar G, Bojja SL, Kumar N, Rao CM. Epigenetics in NAFLD/NASH: Targets and therapy. Pharmacol Res. 2021 May; 167:105484. https://doi.org/10.1016/j.phrs.2021.105484

Studer N, Desharnais L, Beutler M, Brugiroux S, Terrazos MA, Menin L, Schürch CM, McCoy KD, Kuehne SA, Minton NP, et al. Functional intestinal bile acid 7α-dehydroxylation by *Clostridium scindens* associated with protection from *Clostridium difficile* infection in a gnotobiotic mouse model. Front Cell Infect Microbiol. 2016 Dec;6:191. https://doi.org/10.3389/fcimb.2016.00191

Thanissery R, Winston JA, Theriot CM. Inhibition of spore germination, growth, and toxin activity of clinically relevant *C. difficile* strains by gut microbiota derived secondary bile acids. Anaerobe. 2017 Jun;45:86–100. https://doi.org/10.1016/j.anaerobe.2017.03.004

Theriot CM, Bowman AA, Young VB. Antibiotic-induced alterations of the gut microbiota alter secondary bile acid production and allow for *Clostridium difficile* spore germination and outgrowth in the large intestine. MSphere. 2016 Jan;1(1):e00045-15. https://doi.org/10.1128/msphere.00045-15

Theriot CM, Koenigsknecht MJ, Carlson PE, Hatton GE, Nelson AM, Li B, Huffnagle GB, Li JZ, Young VB. Antibiotic-induced shifts in the mouse gut microbiome and metabolome increase susceptibility to *Clostridium difficile* infection. Nat Commun. 2014 Jan;5:3114. https://doi.org/10.1038/ncomms4114

Theriot CM, Koumpouras C, Carlson PE, Bergin II, Aronoff DM, Young VB. Cefoperazone-treated mice as an experimental platform to assess differential virulence of *Clostridium difficile* strains. Gut Microbes. 2011 Nov-Dec;2(6):326–234. https://doi.org/10.4161/GMIC.19142

Ticho AL, Malhotra P, Dudeja PK, Gill RK, Alrefai WA. Intestinal absorption of bile acids in health and disease. Compr Physiol. 2019 Dec;10(1):21–56. https://doi.org/10.1002/cphy.c190007

Webb BJ, Brunner A, Lewis J, Ford CD, Lopansri BK. Repurposing an old drug for a new epidemic: ursodeoxycholic acid to prevent recurrent *Clostridioides difficile* infection. Clin Infect Dis. 2019 Jan;68(3):498–500. https://doi.org/10.1093/cid/ciy568

Wei M, Huang F, Zhao L, Zhang Y, Yang W, Wang S, Li M, Han X, Ge K, Qu C, et al. A dysregulated bile acid-gut microbiota axis contributes to obesity susceptibility. EBioMedicine. 2020 May; 55: 102766. https://doi.org/10.1016/j.ebiom.2020.102766

Weingarden AR, Chen C, Zhang N, Graiziger CT, Dosa PI, Steer CJ, Shaughnessy MK, Johnson JR, Sadowsky MJ, Khoruts A. Ursodeoxycholic acid inhibits *Clostridium difficile* spore germination and vegetative growth, and prevents the recurrence of ileal pouchitis associated with the infection. J Clin Gastroenterol. 2016a Sep;50(8):624–630. https://doi.org/10.1097/MCG.0000000000000427

Weingarden AR, Dosa PI, DeWinter E, Steer CJ, Shaughnessy MK, Johnson JR, Khoruts A, Sadowsky MJ. Changes in colonic bile acid composition following fecal microbiota transplantation are sufficient to control *Clostridium difficile* germination and growth. PLoS One. 2016b Jan;11(1):e0147210. https://doi.org/10.1371/journal.pone.0147210

Wells JE, Hylemon PB. Identification and characterization of a bile acid 7α-dehydroxylation operon in *Clostridium* sp. strain TO-931, a highly active 7α-dehydroxylating strain isolated from human feces. Appl Environ Microbiol. 2000 Mar;66(3):1107–1113. https://doi.org/10.1128/AEM.66.3.1107-1113.2000

Winston JA, Rivera AJ, Cai J, Thanissery R, Montgomery SA, Patterson AD, Theriot CM. Ursodeoxycholic acid (UDCA) mitigates the host inflammatory response during *Clostridioides difficile* infection by altering gut bile acids. Infect Immun. 2020 May; 88(6): e00045-20. https://doi.org/10.1128/IAI.00045-20

Winston JA, Theriot CM. Diversification of host bile acids by members of the gut microbiota. Gut Microbes. 2020 Oct;11(2):158–171. https://doi.org/10.1080/19490976.2019.1674124

Winston JA, Theriot CM. Impact of microbial derived secondary bile acids on colonization resistance against *Clostridium difficile* in the gastrointestinal tract. Anaerobe. 2016 Oct;41:44–50. https://doi.org/10.1016/j.anaerobe.2016.05.003

Xie C, Huang W, Young RL, Jones KL, Horowitz M, Rayner CK, Wu T. Role of bile acids in the regulation of food intake, and their dysregulation in metabolic disease. Nutrients. 2021 Mar;13(4):1104. https://doi.org/10.3390/nu13041104

Zhang Y, LaCerte C, Kansra S, Jackson JP, Brouwer KR, Edwards JE. Comparative potency of obeticholic acid and natural bile acids on FXR in hepatic and intestinal in vitro cell models. Pharmacol Res Perspect. 2017 Dec;5(6):e00368. https://doi.org/10.1002/prp2.368

ORIGINAL PAPER

Polish Journal of Microbiology
2022, Vol. 71, No 1, 19–26
https://doi.org/10.33073/pjm-2022-001

Vaginal Secretion Epithelium Count as a Prognostic Indicator of High Abundance of Ureaplasmas in Women with a Normal Nugent Score

MAŁGORZATA BIERNAT-SUDOLSKA[1], KATARZYNA TALAGA-ĆWIERTNIA[1*] and PAULINA GAJDA[2]

[1] Jagiellonian University Medical College, Faculty of Medicine, Chair of Microbiology, Department of Molecular Medical Microbiology, Cracow, Poland
[2] Jagiellonian University Medical College, Faculty of Medicine, Chair of Epidemiology and Preventive Medicine, Department of Epidemiology, Cracow, Poland

Submitted 1 July 2021, accepted 7 December 2021, published online 27 February 2022

Abstract

Genital tract ureaplasma infections are associated with numerous complications, ranging from inflammation, through infertility, to problematic pregnancy. In the course of ureaplasma infection, the risk of human papillomavirus infection increases. Diagnostic tests for ureaplasma infections are not always carried out, especially in women with the normal Nugent test results. The study attempts to check whether it is possible to find a prognostic indicator that could suggest a high abundance of ureaplasmas ($\geq 10^4$ CFU/ml) at the stage of the initial examination of vaginal discharge. Such a prognostic factor could qualify women for further tests to detect infections with these atypical bacteria. Six hundred twenty-seven white women with a score of 0–3 on the Nugent scale were tested, including 322 patients with a high abundance of ureaplasmas ($\geq 10^4$ CFU/ml) and 305 who tested negative for these bacteria. Ureaplasma infections were detected statistically significant in women who had few or no epithelial cells in the genital swab specimens compared to the results obtained for women with numerous or very numerous epithelial cells ($p < 0.001$). The risk of the high density of ureaplasmas was 38.7% higher with fewer or no epithelial cells than with high numbers. In patients aged 18–40 years with few or no epithelial cells, a high density of ureaplasmas ($\geq 10^4$ CFU/ml) was observed significantly more frequently ($p = 0.003$). Determining the number of epithelial cells in Gram-stained slides may be the prognostic indicator of ureaplasma infection. Testing for genital ureaplasma infection should be considered, especially in women of childbearing age (18–40 years), even if the Nugent test value is normal and pH ≤ 4.6.

K e y w o r d s: *Ureaplasma*, epithelial cells, Nugent scale, *Lactobacillus*, leukocytes, pH

Introduction

The primary method for studying the microorganisms of the lower genital tract in women is the Nugent method. It was considered the gold standard worldwide due to its low cost and ease of implementation (Schwebke et al. 1996). It was a routine test performed for every woman in Poland to initially assess the possible etiological factors of the observed genital tract symptoms. This method is based on the evaluation of Gram-stained preparations, so it only shows typical bacteria classified as Gram-positive or Gram-negative (Nugent et al. 1991). In its current form, the Nugent method does not show the presence of atypical bacteria lacking a cell wall, such as ureaplasmas. Ureaplasmas belong to the family *Mycoplasmataceae* and are the smallest and the simplest self-reproducing bacteria (Razin 1992). They are most commonly sexually transmitted and have been detected in both healthy and symptomatic people. These bacteria are believed to have low virulence and are part of the normal vaginal microbiota. Their pathogenicity has not been confirmed, and the research results on this problem are inconclusive. However, it is believed that their excessive multiplication ($\geq 10^4$ CFU/ml – considered an infection) may cause complications. Most often, ureaplasma infections are assigned a role in NGU (non-gonococcal urethritis) and male infertility (negative influence on sperm metabolism, mobility, and penetration into the ovum) (Taylor-Robinson 1986; Núñez-Calonge et al. 1998). Ascending

* Corresponding author: K. Talaga-Ćwiertnia, Jagiellonian University Medical College, Faculty of Medicine, Chair of Microbiology, Department of Molecular Medical Microbiology, Cracow, Poland; **e-mail: katarzyna.talaga@uj.edu.pl**

infection with urinary tract ureaplasma may lead to cystitis and glomerulonephritis and nephritis with plaque deposition (McDonald et al. 1982; Dewan et al. 1997). Infection of the cervix may result in premature birth (Kundsin et al. 1996) and infections in neonates in whom respiratory symptoms are mainly observed. There are suggestions that chronic ureaplasma-induced cervicitis could damage the mucosal barrier and immune protection (Lv et al. 2019). Ureaplasmas causing inflammation of the cervix increase the production of free radicals, which damages the cervical epithelial barrier and reduces the immune clearance facilitating the penetration of other pathogens (Bıyık et al. 2020).

The aim of the study was to find potential prognostic factors indicating high number of ureaplasmas in women without clinical symptoms and with normal Nugent score. The analysis included indicators such as the number of epithelial cells, leukocytes, and lactobacilli, as well as pH measurement, which can be simultaneously assessed using the criteria of the Nugent method as it has an established place in the diagnosis of female genital dysfunction (Nugent et al. 1991; Taj et al. 2014). Such preliminary assessment could qualify patients for further research, including more expensive molecular diagnostics.

Experimental

Materials and Methods

Our analysis (No. KBET/1072.6120.191.2020; approved by the Bioethics Committee of the Jagiellonian University) had a retrospective character and covered 627 women who were examined in 2007–2014.

The authors decided not to use the term 'ureaplasma infection' in this study because the patients included in the analysis did not show clinical symptoms.

Cervical and vaginal swabs were taken from each woman using sterile polystyrene shafts with viscose swabs and placed in sterile transport tubes without a medium (Deltalab, Poland). Material from the genital tract was not collected during menstrual bleeding, from women undergoing antibiotic therapy, or within two weeks after the antibiotic therapy. Vaginal swabs were seeded for *Trichonema vaginalis*, yeast-like fungi of the genus *Candida*, *Neisseria,* streptococci, enterococci, Enterobacterales, and *Gardnerella vaginalis.* Only women with a high number of ureaplasmas ($\geq 10^4$ CFU/ml) were included. We excluded women with mycoplasma-ureaplasma co-infections and ureaplasma with all of the above. The presence of *T. vaginalis* was confirmed from direct preparations of the collected vaginal discharge. Aerobic bacteria were cultured on Columbia Agar with 5% sheep blood (Biocorp) incubated in aerobic conditions at 37°C for 24 hours. The same conditions were applied to Enterobacterales cultured on MacConkey agar (Biocorp) and enterococci cultured on Bile Esculin Azide LAB-agar (Biocorp). The presence of *G. vaginalis* was confirmed by the BD Gardnerella Selective Agar with 5% Human Blood (BD), whereas MRS Agar (Oxoid) was used for lactobacilli. *Neisseria gonorrhoeae* was detected on the Roiron agar incubated in 5% CO_2 atmospheric conditions for 24–48 hours. Schaedler medium (BD) with vitamin K and 5% sheep blood was used for strictly anaerobic bacteria. Anaerobic bacteria were cultured under strictly anaerobic conditions at 37°C for 48 hours. Clinical materials were incubated on Sabouraud agar (Biocorp) under aerobic conditions at 37°C for 24 hours to detect the genus *Candida* yeast-like fungi.

Specimens collected from the cervix wall were examined for the presence of atypical bacteria (*Mycoplasma hominis*, *Ureaplasma* spp., and *Chlamydia trachomatis*). The presence of *C. trachomatis* was confirmed by demonstrating intracytoplasmic inclusions in the bacteria grown in McCoy cells. Intracytoplasmic inclusions were detected after 48 hours by iodine staining. A Mycoplasma IST 2 kit was used for detection of mycoplasma and ureaplasma infections (BioMérieux). This test allows identification of genital mycoplasma within 48 hours and quantitative estimation of the number of bacteria ($\geq 10^4$ CFU/ml). The cervical secretions were transferred to the BioMérieux transport medium, which was then transferred to BioMérieux culture media, and liquid and solid PPLO medium according to the procedures described earlier by Hayflick (Hayflick 1965; Biernat-Sudolska et al. 2006).

The collected vaginal discharge allowed to concurrently prepare a smear on a slide and stain it with the Gram method for the Nugent method (Nugent et al. 1991). Then, the smears were evaluated by the Nugent scoring system and assigned scores of 0–10. The Nugent score for bacterial vaginosis (BV) is based on the total number of large Gram-positive rods (*Lactobacillus* morphotypes), the number of small Gram-variable and Gram-negative rods (*G. vaginalis*, *Bacteroides*, and *Prevotella* morphotypes), and curved Gram-negative rods (*Mobiluncus* morphotypes). Each morphotype was quantified per field, and a summed score was given. A score of 0–3 is representative of a normal microbiota, a score of 4–6 coresponds to disturbed or altered microbiota, and a score of 7–10 is consistent with BV microbiota. The Nugent score was evaluated by only one experienced microbiologist to prevent the inter-observer variation, using a magnification of 1,000× (an oil immersion). Two categories were adopted when assessing the number of leukocytes and epithelial cells: I – no/few (0–2), and II – numerous/very numerous ($3 \geq 4$) per slide field. When assessing the number of *Lactobacillus* morphotypes, the categories as presented

Table I
Control and study group patient characteristics considering patient age and pH value.

	Control group n = 305						Study group n = 322					
	Med	IQR	M	SD	Min	Max	Med	IQR	M	SD	Min	Max
Age	30.0	(27.0; 34.0)	30.8	6.1	18.0	63.0	31.0	(26.0; 35.0)	31.4	6.5	19.0	56.0
pH	4.6	(4.6; 4.9)	4.7	0.3	3.8	5.5	4.6	(4.6; 4.9)	4.7	0.3	4.0	5.6

Med – median, M – mean, SD – standard deviation, IQR – interquartile range, Min – minimum, Max – maximum

previously in the Nugent scoring were adopted, and there were: I – no (0), II – few (1–5), III – numerous (6–30), IV – very numerous (> 30) per field.

The pH of the vaginal discharge was assessed immediately after collection. It was measured with the PEHANON colored indicator strips (Macherey-Nagel GmbH & Co. KG) and ranged from 3.8 to 5.5. The values of ≤ 4.6 were considered correct.

The analysis covered adult white women who visited the Microbiological Diagnostics Laboratory of the Department of Microbiology of the Jagiellonian University Medical College. The women came for a prophylactic examination of the vaginal microbiota before a planned pregnancy (without subjective symptoms of infection in the genital tract) or due to symptoms such as vaginal discharge, irritation, and itching.

Specimens with a score of 0–3 on the Nugent scale were selected for our analysis. The control group (n = 305) included women who did not demonstrate the presence of infection with ureaplasma. The study group (n = 322) included women with the high number of ureaplasmas (≥ 10^4 CFU/ml). In both the control group and the study group to determine the influence of age on the assessed prognostic indicators, the subjects were divided into four age groups: I: 18–30 years; II: 31–40; III: 41–50; IV: over 50. In the study group, the number of patients in the 1st group was n = 160; II: n = 137; III: n = 20; IV: n = 5, and in the control group, respectively, I: n = 173; II: n = 110; III: n = 20; IV: n = 2.

Control and study group patient characteristics are presented in Table I. The age and pH values were expressed as the median and interquartile range (IQR). Intergroup differences were analyzed using Fisher's exact and Pearson's chi-square test. A one-way logistic regression model was used to estimate the risk of the high density of ureaplasmas (≥ 10^4 CFU/ml). Statistical analysis was performed using IBM SPSS Statistics 26. The significance level for all statistical tests was set at $p < 0.05$.

Results

To determine the risk of high abundance of ureaplasmas (≥ 10^4 CFU/ml) based on the presence of the prognostic indicators studied by us, we conducted analyses covering both a single indicator and several indicators in various combinations with one another.

The high density of ureaplasmas versus the pH value. A high number of ureaplasmas (≥ 10^4 CFU/ml) were observed in 53.6% of women with pH ≤ 4.6 and in 48.6% of women with pH > 4.6. These differences were not statistically significant ($p = 0.242$, Pearson's chi-square test).

The high abundance of ureaplasmas and the number of bacteria of the genus *Lactobacillus*. A high number of ureaplasmas (≥ 10^4 CFU/ml) occurred in 52% of women in whom *Lactobacillus* bacteria were numerous and very numerous. In contrast, those infections were found in 44% of women with few or any bacteria. These differences were not statistically significant ($p = 0.349$; Pearson's chi-square test).

The high density of ureaplasmas and the number of epithelial cells. In our studies, the high number of ureaplasmas (≥ 10^4 CFU/ml) was confirmed more often in women who had few or no epithelial cells in the specimens from the genital swabs. Compared to the results obtained for women with numerous or very numerous epithelial cells, these results were statistically significant (58.1% vs. 36.4%, $p < 0.001$, Pearson's chi-square test).

Using a one-way logistic regression model, it was shown that in women with the Nugent score 0–3 (n = 627), the risk of a high abundance of ureaplasmas (≥ 10^4 CFU/ml) is 38.7% higher with few / no epithelial cells than with numerous/very numerous epithelial cells (OR 1.38, CI 1.14–1.68, $p = 0.001$).

The high density of ureaplasmas versus the presence and number of leukocytes. In our study, the high number of ureaplasmas (≥ 10^4 CFU/ml) were observed in 52.8% of patients with low or no leukocytes in the vaginal smear and in 44.0% of women with numerous or very numerous leukocytes. There were no statistically significant differences between these groups ($p = 0.135$, Pearson's chi-square test). The comparison of the control group and the study group, taking into account individual prognostic indicators, is shown in Fig. 1.

Incidence of high abundance of ureaplasmas versus different combinations of prognostic indicators. The statistically significant results were obtained only in three cases when assessing the frequency of the high

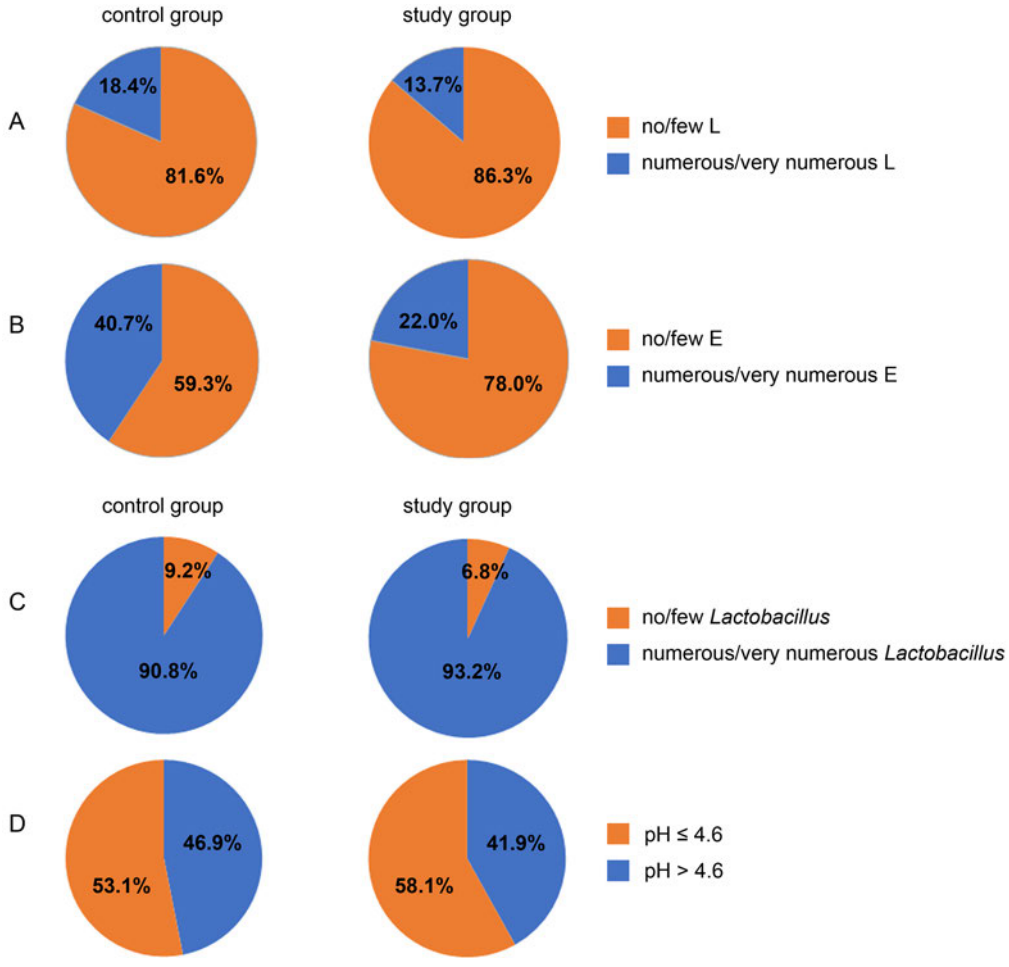

Fig. 1. Comparison between the control group and the study group, taking into account individual diagnostic indicator tested in the study: A) leukocytes – L, B) epithelial cells – E

number of ureaplasmas ($\geq 10^4$ CFU/ml), with various combinations of the analyzed indicators. Our analysis showed that high density of these atypical bacteria occurs significantly more often when i) leukocytes and epithelia were few or absent (57.8% vs. 32.2%, $p < 0.001$, Pearson's chi-square test); ii) in the presence of few/no epithelia and pH ≤ 4.6 (60.6% vs. 39.0%, $p < 0.001$, Pearson's chi-square test); iii) when there were no leukocytes and epithelial cells, or there were few of these cells, and the pH value was below 4.6 (60.6% vs. 39.5%, $p = 0.022$, Pearson's chi-square test). A comparison of the percentage of women in the control and study groups, taking into account the combined prognostic indicators for which statistical significance was determined, is presented in Fig. 2. Using a one-way logistic regression model, it was shown that the risk of high abundance of ureaplasmas ($\geq 10^4$ CFU/ml) is 37.0% higher in the case when, simultaneously, leukocytes and epithelia were almost absent or absent (n = 450; OR 1.37, CI 1.12–1.67, $p = 0.002$). Our analysis also showed that the risk of the high number of ureaplasmas is 53.9% higher in women with a pH value below 4.6 who have few or no epithelial cells (n = 364 OR 1.54, CI 1.20–1.97, $p = 0.001$). With the simultaneous presence of three indicators: scarce or absent leukocytes and epithelial cells and a pH ≤ 4.6, the risk of the high density of ureaplasmas ($\geq 10^4$ CFU/ml) is 54.1% higher (n = 287; OR 1.54, CI 1.19–1.98, $p = 0.001$), compared to when the pH value is above 4.6, and the epithelial cells and leukocytes are abundant.

Incidence of the high density of ureaplasmas versus age. In the age groups I and II, the high number of ureaplasmas were significantly more frequent in patients with few or no epithelial cells (respectively, 55.5% vs. 33.6%, $p < 0.001$ and 61.6% vs. 40.0%, $p = 0.003$, Pearson's chi-square test). In the case of other indicators, analyzed separately or in various combinations, no statistically significant differences were found in individual age groups.

The age-standardized logistic regression model showed that the risk of the high density of ureaplasmas was 121.3% higher (OR 2.21, CI 1.58–3.10, $p < 0.001$) in the presence of only a few or absence of epithelial cells. The risk of high abundance of ureaplasmas decreases with the patient's age, by 1.5% with each subsequent year (OR 0.98, CI 0.97–0.99, $p = 0.001$).

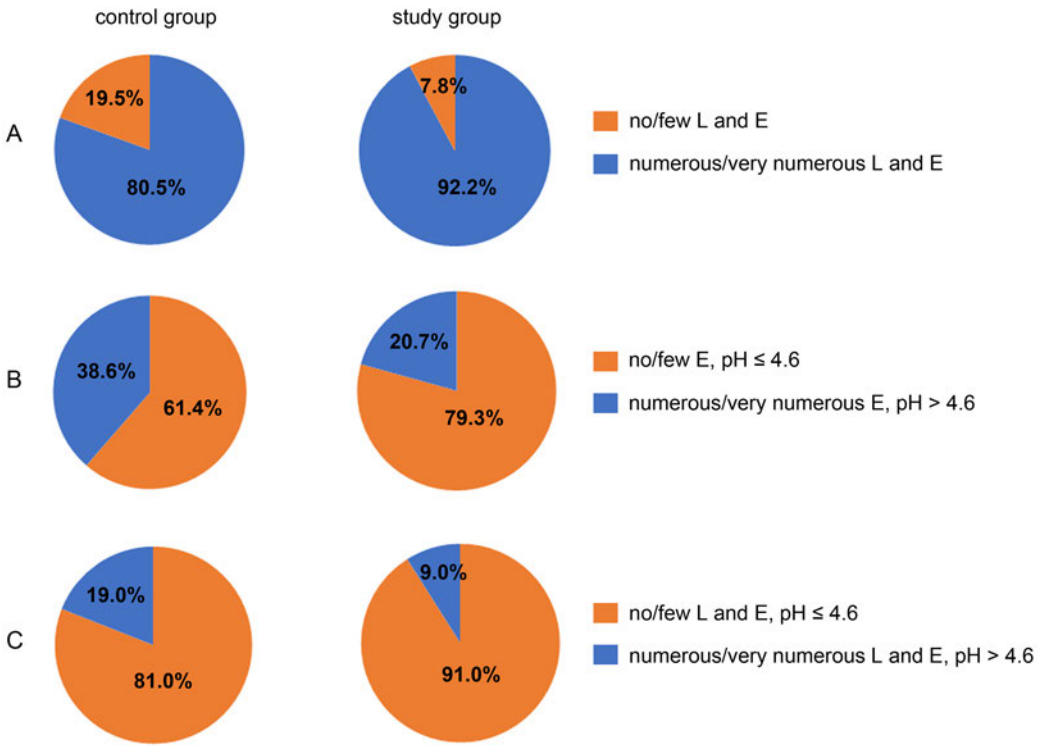

Fig. 2. Comparison of the control and study groups, taking into account the combination of the diagnostic indicators tested: A) leukocytes – L and epithelial cells – E, $p < 0.001$; B) epithelial

Discussion

Our many years of experience in the diagnosis of genital tract infections were the starting point for the initial assessment of the dependence of ureaplasma infections on the results of the Nugent scale. The results not presented in this study showed that ureaplasma infections were significantly more common in women with a score of 0–3 on the Nugent scale (n = 768, $p < 0.001$, Pearson's chi-square test). Our observations suggested that the results obtained with this method do not correlate with the high density of ureaplasmas. Therefore, our present research attempted to find prognostic indicators assessed in parallel with the commonly used Nugent method, which could indirectly indicate infection with these bacteria. The indicators selected for our analysis included the number of *Lactobacillus*, the number of epithelia and leukocytes, and the pH value in determining the risk of ureaplasma infection. Epithelial cells and leukocytes are visible on microbiological slides after Gram staining but are not assessed in the Nugent method. The diagnostic value of leukocytes as a prognostic indicator indirectly suggestive of ureaplasma infection was demonstrated by Okodo et al. (2017). These researchers, analyzing preparations made with the Papanicolaou technique, showed a statistically significant relationship between the *Ureaplasma urealyticum* infection and the presence of secondary changes in the cells of the cervical squamous epithelium called cannonballs. Out of the morphotypes assessed by the Nugent method, we chose the number of *Lactobacillus*, noting the considerable impact of this type of bacteria on the vaginal microbiota, which is clearly emphasized in the literature (Tachedjian et al. 2017; Witkin and Linhares 2017).

It has long been known that numerous antibacterial agents produced by lactobacilli, including bacteriocins, H_2O_2, or lactic acid, can inhibit the excessive multiplication of various pathogens. In our study, however, no dependence of the high number of ureaplasmas on the number of lactobacilli was observed. Some *Lactobacillus* species, regardless of their abundance, may be more active than others in keeping *Ureaplasma* spp. below the level considered being an infection. This, however, requires further research (Daniele et al. 2011).

Lactic acid, produced by *Lactobacillus*, plays a unique role in the vagina, favoring the domination of microorganisms with low pathogenic potential. Some *Lactobacillus* species produce only the D-isomer of lactic acid, which has a weaker protective effect (Amabebe and Anumba 2018). For example, *Lactobacillus iners* that dominate the vaginal microbiota is usually associated with dysbiosis. It appears to be less stable and more susceptible to alteration (since this species does not produce lactic acid). Similarly, *Lactobacillus jensenii* has weaker protective properties (it only produces D-lactic acid). On the other hand, *Lactobacillus crispatus* is beneficial as this species produces both D- and

L-lactic acid, associated with increased stability of the vaginal microbiota (developing dysbiosis is less probable), thus producing lower risk of BV. Perhaps routine determination of the number and species of *Lactobacillus* would be beneficial as it could indicate the risk of BV (Virtanen et al. 2019) and the possibility of various infections, including genital mycoplasmas.

Another indicator selected here was the number of epithelia. It is known that ureaplasmas strongly adhere to various cells, including epithelial cells (Razin 1992; 1999). *G. vaginalis* is a microorganism with strong adhesive properties. Its adherence to the epithelium is observed in Gram-stained preparations as characteristics indicator cells. To clearly assess the impact of high number of ureaplasmas ($\geq 10^4$ CFU/ml) on vaginal epithelial cells, the analysis did not include women infected with *G. vaginalis*. By adhering to the epithelium, ureaplasmas can damage the cells, and the irritating ammonia produced by them can influence the development of the inflammation. We expected that such actions could affect the number of exfoliated epithelial cells and leukocytes found in Gram-stained slides. The abundance of these cells could be a possible marker of an ongoing ureaplasma infection. In our analysis, a higher incidence of ureaplasma infections was observed only in the absence or with low numbers of epithelia. This relationship is also visible when the pH value is within the normal range. The beneficial effects of lactic acid on the cervix and vaginal epithelial cells (increased survival of vaginal epithelial cells, facilitated repair of damaged DNA) were demonstrated (Wagner et al. 2015; Amabebe and Anumba 2019). As a result, vaginal epithelial cells protected with lactic acid probably peel to a lesser extent, hence perhaps in Gram-stained preparations, their small number was observed with a large number of *Lactobacillus* bacteria.

Our analysis showed no dependence of high density of ureaplasmas ($\geq 10^4$ CFU/ml) on the number of leukocytes. Our observations regarding the number of leukocytes are in line with the previous literature reports. Lactic acid produced by lactobacilli supports antimicrobial defense through multiple mechanisms without causing immune-mediated inflammation. The vaginal microbiome dominated by *L. crispatus*, *L. gasseri*, and *L. jensenii* is potentially associated with a lower pro-inflammatory response (Smith and Ravel 2017; Witkin and Linhares 2017). This anti-inflammatory effect was previously observed in the presence of a large number of lactobacilli, especially at low pH, which enhances lactic acid activity (Hearps et al. 2017; Tachedjia et al. 2017; Amabebe and Anumba 2018). In a study of urinary tract infections, Moi et al. (2017) observed a weaker inflammatory response with ureaplasma than *C. trachomatis* and *M. genitalium*. Other researchers, such as Geisler et al. (2003), indicated that assessing the number of leukocytes in vaginal and cervical infections has a low positive and negative predictive value and moderate sensitivity and specificity. We also included pH measurements in our analysis, as it is known from the literature that the low pH of the vaginal discharge is most often associated with normal vaginal microbiota. Nevertheless, reports indicate that vaginal acidity may be more critical for the proper functioning of the vaginal mucosa than for inhibiting potential pathogens or regulating the normal microbiota. Measuring the pH alone in the screening of vaginal microbiota seems insufficient as it is known that *Candida* infections can occur at low pH values (Linhares et al. 2011). Different species of *Lactobacillus* lower the pH of the vaginal discharge to a varying extent, and in women with a score of 0–3 on the Nugent scale, a differentiation in pH was found, with an upward trend closer to the limit of the range (O'Hanlon et al. 2019). The products of ureaplasma metabolism alkalize the environment, which may neutralize the acidity resulting from the presence of *Lactobacillus*. With a huge population of *Lactobacillus* spp., the acidity of vaginal secretions is not always disturbed. There is no apparent shift of the measurement results towards alkaline values. As a result, this may have resulted in the pH values being within the normal range despite the ureaplasma infection. In our research, only the pH value combined with the determination of the number of epithelia and leukocytes gained a significant diagnostic significance.

The results obtained here turned out to be statistically significant in women of reproductive age, who are usually the most sexually active. Due to the prospect of motherhood, women from this group most often report for vaginal microbiota tests. Therefore, the assessment of epithelial cells would be particularly important for this group of women due to the consequences of ureaplasma vertical infection in their children. It would also be valuable due to the relationship between ureaplasma ($\geq 10^4$/ml) and possible damage to the epithelium in the genital system, which creates good conditions for the penetration of other sexually transmitted pathogens which have a negative impact on women health (Lv et al. 2019; Ye et al. 2018).

In our study, statistically significant results were obtained when the number of epithelia was analyzed as a single prognostic indicator as well as together with other analyzed indicators. Therefore, it seems to us that vaginal secretion epithelial cell count has the greatest importance and can be considered a prognostic indicator of the presence of high density of ureaplasmas.

The use of molecular methods that are currently widely available might have some impact on the results presented. However, in the years 2007–2014 in which the studies covered by our analysis were performed, the methods of bacterial cultivation on microbiological

media were routinely used in Poland. In those years, culture methods were considered the gold standard in microbiological diagnostics and, in many countries, they have been the most important until now. Our study only involved women from the white ethnic group, which of course, limits the possibility of extending the conclusions to the entire female population. A weakness of our work, resulting from its retrospective nature, was also the lack of data that could be obtained from the patients included in the analysis, concerning e.g., hygienic behavior, number of sexual partners, the possibility of using lubricants, hormonal contraception, or the day of the menstrual cycle on which the vaginal discharge was collected. Such data could have influenced the results of our analysis.

Conclusions

Our analysis showed that even the introduction of additional prognostic indicators expanding the Nugent scale did not allow the presence of the high number of ureaplasmas to be clearly demonstrated. The relatively best prognostic indicator of the ongoing high density of ureaplasmas ($\geq 10^4$ CFU/ml) in women with normal Nugent scores was the determination of the number of epithelial cells. Our analysis also shows that testing for genital ureaplasma should be considered, especially in women of childbearing age (18–40 years), even if the Nugent test value is normal and the pH is ≤ 4.6.

ORCID
Małgorzata Biernat-Sudolska https://orcid.org/0000-0002-5943-6007
Katarzyna Talaga-Ćwiertnia https://orcid.org/0000-0003-0811-9295
Paulina Gajda https://orcid.org/0000-0001-7687-7536

Ethical statement

This study was approved by the Bioethics Committee of the Jagiellonian University (No. KBET/1072.6120.191.2020).

Acknowledgments

The authors would like to thank prof. Małgorzata Bulanda for providing the database.

Author contributions

Conceptualization, M. B-S.; Methodology, M. B-S. and K. T-Ć.; Formal Analysis, M. B-S., K. T-Ć. and P.G.; Investigation, P.G.; Resources, M. B-S.; Data Curation, M. B-S.; Writing – Original Draft Preparation, M. B-S. and K. T-Ć.; Writing – Review & Editing, M. B-S. and K. T-Ć.; Visualization, M. B-S. and K. T-Ć.; Supervision, M. B-S. and K. T-Ć.; Project Administration, K. T-Ć.

Conflict of interest

The authors do not report any financial or personal connections with other persons or organizations, which might negatively affect the contents of this publication and/or claim authorship rights to this publication.

Literature

Amabebe E, Anumba, DOC. The vaginal microenvironment: the physiologic role of *Lactobacilli*. Front Med (Lausanne). 2018 Jun; 5:181. https://doi.org/10.3389/fmed.2018.00181

Biernat-Sudolska M, Rojek-Zakrzewska D, Lauterbach, R. Assessment of various diagnostic methods of ureaplasma respiratory tract infections in newborns. Acta Biochim Pol. 2006 Oct;53(3):609–611.

Bıyık İ, Keskin N, Gülcan A, İnce O, Erten Ö, Şişman Hİ. Coinfection of *Ureaplasma urealyticum*/*Mycoplasma hominis* in HPV positive women: frequency, risk factors and multidrug resistance. J Clin Obstet Gynecol. 2020;30(3):92–99. https://doi.org/10.5336/jcog.2020-76299

Daniele M, Ruiz F, Pascual L, Barberis L. *Ureaplasma urealyticum* and *Mycoplasma hominis* sensitivity to bacteriocins produced by two lactobacilli strains. Curr Microbiol. 2011 Oct;63(4):360–365. https://doi.org/10.1007/s00284-011-9989-y

Dewan B, Sharma M, Nayak N, Sharma SK. Upper urinary tract stones and *Ureaplasma urealyticum*. Indian J Med Res. 1997 Jan; 105:15–21.

Geisler WM, Yu S, Venglarik M, Schwebke, JR. Vaginal leucocyte counts in women with bacterial vaginosis: relation to vaginal and cervical infections. Sex Transm Infect. 2004 Oct;80:401–405. https://doi.org/10.1136/sti.2003.009134

Hayflick L. The Mycoplasmatales and the L-phase of bacteria. New York (USA): Meredith Corporation; 1965.

Hearps AC, Tyssen D, Srbinovski D, Bayigga L, Diaz DJD, Aldunate M, Cone RA, Gugasyan R, Anderson DJ, Tachedjian G. Vaginal lactic acid elicits an anti-inflammatory response from human cervicovaginal epithelial cells and inhibits production of pro-inflammatory mediators associated with HIV acquisition. Mucosal Immunol. 2017 Nov;10(6):1480–1490. https://doi.org/10.1038/mi.2017.27

Kundsin RB, Leviton A, Allred EN, Poulin SA. *Ureaplasma urealyticum* infection of the placenta in pregnancies that ended prematurely. Obstet Gynecol. 1996 Jan;87(1):122–127. https://doi.org/10.1016/0029-7844(95)00376-2

Linhares IM, Summers PR, Larsen B, Giraldo PC, Witkin SS. Contemporary perspectives on vaginal pH and lactobacilli. Am J Obstet Gynecol. 2011 Feb;204(2):120.e1–120.e1205. https://doi.org/10.1016/j.ajog.2010.07.010

Lv P, Zhao F, Xu X, Xu J, Wang Q, Zhao Z. Correlation between common lower genital tract microbes and high-risk human papillomavirus infection. Can J Infect Dis Med Microbiol. 2019 Nov;2019: 9678104. https://doi.org/10.1155/2019/9678104

McDonald MI, Lam MH, Birch DF, D'Arcy AF, Fairley KF, Pavillard ER. *Ureaplasma urealyticum* in patients with acute symptoms of urinary tract infection. J Urol. 1982 Sep;128(3):517–519. https://doi.org/10.1016/s0022-5347(17)53025-6

Moi H, Reinton N, Randjelovic I, Reponen EJ, Syvertsen L, Moghaddam A. Urethral inflammatory response to ureaplasma is significantly lower than to *Mycoplasma genitalium* and *Chlamydia trachomatis*. Int J STD AIDS. 2017 Jul;28(8):773–780. https://doi.org/10.1177/0956462416666482

Nugent RP, Krohn MA, Hillier SL. Reliability of diagnosing bacterial vaginosis is improved by a standardized method of gram stain interpretation. J Clin Microbiol. 1991 Feb;29(2):297–301. https://doi.org/10.1128/JCM.29.2.297-301.1991

Núñez-Calonge R, Caballero P, Redondo C, Baquero F, Martínez-Ferrer M, Meseguer MA. *Ureaplasma urealyticum* reduces motility and induces membrane alterations in human spermatozoa. Hum Reprod. 1998 Oct;13(10):2756–2761. https://doi.org/10.1093/humrep/13.10.2756

O'Hanlon DE, Come RA, Moench TR. Vaginal pH measured *in vivo*: lactobacilli determine pH and lactic acid concentration. BMC Microbiol. 2019 Jan;19(1):13. https://doi.org/10.1186/s12866-019-1388-8

Okodo M, Kawamura J, Okayama K, Kawai K, Fukui T, Shiina N, Caniz T, Yabusaki H, Fujii M. Cytological features associated with *Ureaplasma urealyticum* in pap cervical smear. Asian Pac J Cancer Prev. 2017 Aug;18(8):2239–2242. https://doi.org/10.22034/APJCP.2017.18.8.2239

Razin S. Adherence of pathogenic mycoplasmas to host cells. Biosci Rep. 1999 Oct;19(5):367–372. https://doi.org/10.1023/a:1020204020545

Razin S. Peculiar properties of mycoplasmas: the smallest self-replicating prokaryotes. FEMS Microbiol Lett. 1992 Dec;100(1–3):423–431. https://doi.org/10.1111/j.1574-6968.1992.tb14072.x

Schwebke JR, Hillier SL, Sobel JD, McGregor JA, Sweet RL. Validity of the vaginal Gram stain for the diagnosis of bacterial vaginosis. Obstet Gynecol. 1996 Oct;88(4 Pt 1):573–576. https://doi.org/10.1016/0029-7844(96)00233-5

Smith SB, Ravel J. The vaginal microbiota, host defence and reproductive physiology. J Physiol. 2017 Jan;595(2):451–463. https://doi.org/10.1113/JP271694

Tachedjian G, Aldunate M, Bradshaw CS, Cone RA. The role of lactic acid production by probiotic *Lactobacillus* species in vaginal health. Res Microbiol. 2017 (Nov–Dec);168(9–10):782–792. https://doi.org/10.1016/j.resmic.2017.04.001

Taj N, Ul Alam MS, Bajwa Z, Waheed A, Ullah E. Bacterial vaginosis in pregnant women and its diagnosis using Amsel's Clinical Criteria and Nugent's Method. Pak J Med Health Sci. 2014; 8: 133–135.

Taylor-Robinson D. Evaluation of the role of *Ureaplasma urealyticum* in infertility. Pediatr Jnfect Dis. 1986(Nov–Dec);5(6 Suppl): S262–S265.

Virtanen S, Rantsi T, Virtanen A, Kervinen K, Nieminen P, Kalliala I, Salonen A. Vaginal microbiota composition correlates between pap smear microscopy and next generation sequencing and associates to socioeconomic status. Sci Rep. 2019 May;9(1):7750. https://doi.org/10.1038/s41598-019-44157-8

Wagner W, Ciszewski WM, Kania KD. L- and D-lactate enhance DNA repair and modulate the resistance of cervical carcinoma cells to anticancer drugs via histone deacetylase inhibition and hydroxycarboxylic acid receptor 1 activation. Cell Commun Signal. 2015 Jul; 13:36. https://doi.org/10.1186/s12964-015-0114-x

Witkin SS, Linhares IM. Why do lactobacilli dominate the human vaginal microbiota? BJOG. 2017 Mar;124(4):606–611. https://doi.org/10.1111/1471-0528.14390

Ye H, Song T, Zeng X, Li L, Hou M, Xi M. Association between genital mycoplasmas infection and human papillomavirus infection, abnormal cervical cytopathology, and cervical cancer: a systematic review and meta-analysis. Arch Gynecol Obstet. 2018 Jun;297(6): 1377–1387. https://doi.org/10.1007/s00404-018-4733-5

ORIGINAL PAPER
Polish Journal of Microbiology
2022, Vol. 71, No 1, 27–34
https://doi.org/10.33073/pjm-2022-002

Genetic Polymorphisms of *Pneumocystis jirovecii* in HIV-Positive and HIV-Negative Patients in Northern China

TING XUE[1]*, WEI-QIN DU[2], WEN-JUAN DAI[1], YI-SHAN LI[1], SHU-FENG WANG[3], JUN-LING WANG[4] and XIN-RI ZHANG[1]

[1] NHC Key Laboratory of Pneumoconiosis, Key Laboratory of Prophylaxis and Treatment and Basic Research of Respiratory Diseases of Shanxi Province, Department of Respiratory and Critical Care Medicine, First Affiliated Hospital of Shanxi Medical University, Taiyuan, P.R. China
[2] Department of clinical inspection, Eleventh Affiliated Hospital of Shanxi Medical University, Lvliang, P.R. China
[3] Department of Clinical Inspection, First Affiliated Hospital of Shanxi Medical University, Taiyuan, P.R. China
[4] Department of Translation Medicine, Jinzhou Medical University, Jinzhou, P.R. China

Submitted 18 September 2021, accepted 15 December 2021, published online 23 Febrary 2022

Abstract

Pneumocystis jirovecii is an opportunistic fungus that can cause severe and potentially fatal *Pneumocystis* pneumonia (PCP) in immunodeficient patients. In this study, we investigated the genetic polymorphisms of *P. jirovecii* at eight different loci, including six nuclear genes (ITS, 26S rRNA, *sod*, *dhps*, *dhfr* and β-Tub) and two mitochondrial genes (mtLSU-rRNA and *cyb*) in three PCP cases, including two patients with HIV infection and one without HIV infection in Shanxi Province, P.R. China. The gene targets were amplified by PCR followed by sequencing of plasmid clones. The HIV-negative patient showed a coinfection with two genotypes of *P. jirovecii* at six of the eight loci sequenced. Of the two HIV-positive patients, one showed a coinfection with two genotypes of *P. jirovecii* at the same two of the six loci as in the HIV-negative patient, while the other showed a single infection at all eight loci sequenced. None of the three drug target genes (*dhfr, dhps* and *cyb*) showed mutations known to be potentially associated with drug resistance. This is the first report of genetic polymorphisms of *P. jirovecii* in PCP patients in Shanxi Province, China. Our findings expand our understanding of the genetic diversity of *P. jirovecii* in China.

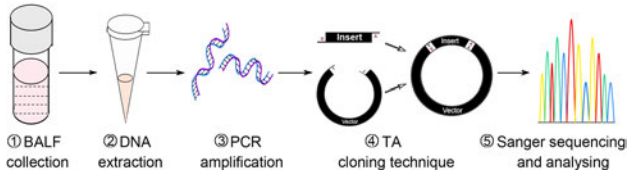

Keywords: *Pneumocystis jirovecii*, genetic polymorphisms, genotypes, multilocus, epidemiology

Introduction

Pneumocystis is a genus of atypical fungi demonstrating different degrees of genetic diversity between and within different species that infect mammals with high host specificity. The human-specific species, *Pneumocystis jirovecii,* causes life-threatening *Pneumocystis* pneumonia (PCP) in immunodeficient individuals, especially those with human immunodeficiency virus (HIV) infection (Ma et al. 2018). Recent studies have indicated a high prevalence of *P. jirovecii* colonization and infection in individuals with chronic obstructive pulmonary disease (COPD) (Wang et al. 2015; Cañas-Arboleda et al. 2019; Xue et al. 2020). However, the epidemiology and genetic diversity of *P. jirovecii* in different patient populations remain poorly understood.

Although genetic diversity of *P. jirovecii* has been reported in multiple studies from different regions in China (Li et al. 2013; Deng et al. 2014; Sun et al. 2015; Wang et al. 2019), all these studies are limited to only a few loci, and there is no such report from Shanxi Province in Northern China. In this study, we retrospectively investigated three confirmed cases of PCP, including two in HIV-positive patients and one in the HIV-negative patient from our hospital in Shanxi Province. Genetic polymorphisms of *P. jirovecii* in these patients were determined at eight different loci.

* Corresponding author: T. Xue, NHC Key Laboratory of Pneumoconiosis, Key Laboratory of Prophylaxis and Treatment and Basic Research of Respiratory Diseases of Shanxi Province, Department of Respiratory and Critical Care Medicine, First Affiliated Hospital of Shanxi Medical University, Taiyuan, P.R. China; **e-mail: beyondtinger@126.com.**

Experimental

Materials and Methods

Patients and samples. Three patients with PCP were included in this study, including two positive and one negative for HIV-1. Patients were admitted to the Department of Respiratory and Critical Care Medicine of First Affiliated Hospital of Shanxi Medical University between August 2019 and June 2020. The diagnosis of PCP was confirmed based on clinical manifestations and laboratory tests, including hematology, high-resolution computed tomography (HRCT), modified Gomori methenamine silver nitrate staining (GMS) of bronchoalveolar lavage fluid (BALF) samples. The two HIV-positive patients had a confirmed diagnosis of the acquired immune deficiency syndrome (AIDS) but did not receive highly active antiretroviral therapy. Based on the ELISA results, the HIV-negative patient was seronegative for HIV-1 and HIV-2 antibodies.

The Medical Ethics Committee approved this retrospective study of our hospital (2019-K051). In addition, written informed consent was obtained from all three patients.

DNA extraction. The BALF specimens were centrifuged at 350 g for 15 min, followed by washing the cell pellets with saline solution three times. DNA was extracted from washed cell pellets using the conventional phenol-chloroform extraction method. DNA extracts were quantified using a NanoDrop-UV-Vis spectrophotometer (Thermo Fisher Scientific, USA) and stored at –80°C until use.

DNA amplification, cloning, and sequencing. We amplified eight different loci of the *P. jirovecii* genome using nested PCR with the Premix-Taq PCR kit (TaKaRa Biotechnology Co., Ltd., Dalian, China) following the manufacturer's instructions. The loci included mitochondrial large-subunit rRNA (mtLSU-rRNA), cytochrome b (*cyb*), nuclear large rRNA subunit (26S), and the complete internal transcribed spacers 1 and 2 (ITS1 and ITS2) along with the 5.8S rRNA of the nuclear rRNA operon (referred to as ITS hereafter), superoxide dismutase (*sod*), dihydropteroate synthase (*dhps*), dihydrofolate reductase (*dhfr*), and β-tubulin (β-Tub). The primers used in this study are listed in Table I. The PCR amplification conditions for β-Tub and 26S were the same as those previously reported

Table I
PCR primers used in this study.

Genes (reference)	Primer names and sequences (5'-3')	Size of nested PCR products (bp)
ITS (Lee et al. 1998)	1724F 5'-AAGTTGATCAAATTTGGTC-3' ITS2R 5'-CTCGGACGAGGATCCTCGCC-3' ITS1F 5'-CGTAGGTGAACCTGCGGAAGGATC-3' ITS2R1 5'-GTTCAGCGGGTGATCCTGCCTG-3'	578
sod (Esteves et al. 2010b)	MnSOD_Fw 5'-GGGTTTAATTAGTCTTTTTAGGCAC-3' MnSOD_Rw 5'-CATGTTCCCACGCATCCTAT-3' SODF3 5'-AGTCTTTTTAGGCACTTGAACCT-3' SODR4 5'-TCCAAGAATAACTTTGCCTTGAGT-3'	560
dhfr (Lane et al. 1997)	FR208 5'-GCAGAAAGTAGGTACATTATTACGAGA-3' FR1018 5'-AAGCTTGCTTCAAACCTTGTGTAACGCG-3' FR242 5'-GTTTGGAATAGATTATGTTCATGGTGTACG-3' FR1038 5'-GCTTCAAACCTTGTGTAACGCG-3'	798
dhps (Ma et al. 1999)	DHPS1 5'-CAAATTAGCGTATCGAATGACC-3' DHPS2 5'-GCAAAATTACAATCAACCAAAGTA-3' DHPS3 5'-AGCGCCTACACATATTATGG-3' DHPS4 5'-GTTCTGCAACCTCAGAACG-3'	278
cyb (Esteves et al. 2010a)	CytbFw 5'-CCCAGAATTCTCGTTTGGTCTATT-3' CytbRw 5'-AAGAGGTCTAAAAGCAGAACCTCAA-3' CytbF3 5'-TCTCGTTTGGTCTATTGGTG-3' CytbR4 5'-AAGCAGAACCTCAAATTCAAGATA-3'	590
mtLSU rRNA (Wakefield 1996)	pAZ102_E 5'-GATGGCTGTTTCCAAGCCCA-3' pAZ102_H 5'-GTGTACGTTGCAAAGTACTC-3' pAZ102_X 5'-GTGAAATACAAATCGGACTAGG-3' pAZ102_Y 5'-TCACTTAATATTAATTGGGGACC-3'	252
β-Tub (Pasic et al. 2020)	Pneumo Tub_F 5'-TCATTAGGTGGTGGAACGGG-3' Pneumo Tub_R 5'-ATCACCATATCCTGGATCCG-3'	303
26S rRNA (Pasic et al. 2020)	PneumoLSU_F 5'-TCAGGTCGAACTGGTGTACG-3' PneumoLSU_R 5'-TGTTCCAAGCCCACTTCTT-3'	297

(Pasic et al. 2020), and the conditions for other genes were the same as described in previous studies (Lee et al. 1998; Wang et al. 2019; Xue et al. 2019). DNA from *P. jirovecii*-positive specimens stored in our laboratory was used as the positive control. A non-template control with ultrapure-distilled water was included in each PCR run. To prevent cross-contamination of the samples, separate rooms were used, and the PCR mixture from each step of nested PCR was covered with 40 μl of sterile liquid paraffin. All PCR products were separated by electrophoresis on 2% agarose gels, stained with 4S Green Plus Nucleic Acid Stain (Sangon Biotech Co., Ltd. Shanghai, China), and visualized under UV irradiation. The amplified DNA bands of the expected sizes were excised from the gel and extracted using an agarose gel DNA extraction kit (Tiangen Biotech Co., Ltd., Beijing, China). Following the manufacturer's instructions, the extracted DNA fragment was cloned into the TA cloning vector pMD18-T (TaKaRa Biotechnology Co., Ltd., Dalian, China). Recombinant plasmid clones were selected by blue-white screening on agar plates containing ampicillin. For each PCR product, 8 to 13 plasmid clones were randomly selected for Sanger sequencing in the ABI 3730xl DNA analyzer (Thermo Fisher Scientific, USA).

Sequence analysis and genotyping. The nucleotide sequences obtained in this study were analyzed and aligned using ClustalW software (https://www.genome.jp/tools-bin/clustalw). At least two plasmid clones are required to define a nucleotide polymorphism. The genotypes were named based on previously published nomenclature (Table II). The reference sequence for each gene was obtained from GenBank, with its accession number listed as follows: *ITS*, MK300654; *mtLSU-rRNA,* M58605; *cyb*, AF320344; *sod*, AF146753; *dhfr*, AF090368; *dhps*, AF139132; β-Tub, MG208106 and 26S KT272445. Known *P. jirovecii* multi-locus sequence type (MLST) profiles at β-Tub, *cyb*, *26S*, and *sod* genes were retrieved from the Fungal MLST Database at http://mlst.mycologylab.org.

Table II
Nucleotide polymorphic sites and number of plasmid clones sequenced at eight distinct loci of *Pneumocystis jirovecii*.

Locus	Genotypes[a]	Location[b]	No. of plasmid clones sequenced		
			SX_0001	SX_0002	SX_0003
ITS	ITS 4	KC470776	0	12	0
	ITS 10	JQ365725	0	0	4
	ITS 16	AB469817	0	0	8
	ITS 22	KC470795	6	0	0
	ITS 59	MK300661	10	0	0
sod	*sod 1*	110C/215T	11	13	8
	sod 2	110T/215C	0	0	2
dhps	*dhps WT*	165A (55Thr) / 171C (57Pro)	12	12	12
dhps	*dhfr312*	312C (117Gly)	12	11	11
cyb	*cyb 1*	279C/348A/516C/547C/566C/838C	0	0	6
	cyb 2	279C/348A/516C/547C/566C/838T	0	8	0
	cyb 7	279C/348A/516C/547C/566T/838C	9	0	0
	cyb 8	279T/348A/516C/547C/566C/838C	0	0	3
mt LSU rRNA	mt1	85C/248C	0	0	2
	mt2	85A/248C	0	0	8
	mt3	85T/248C	10	10	0
β-Tub	β-Tub 1	86G/281A	8	0	6
	β-Tub 2	86G/281G	4	12	5
26S rRNA	26S 2	86T/290A	12	11	0
	26S 3	86C/290A	0	0	5
	26S 4	86A/290A	0	0	6

ITS – internal transcribed spacer regions of rRNA operon, *sod* – superoxide dismutase, *dhfr* – dihydrofolate reductase, *dhp* – dihydropteroate synthase, WT – wild-type, *cyb* – cytochrome b, mt – mitochondrial large rRNA subunit, β-Tub – β-tubulin, 26S rRNA – 26S ribosomal RNA gene

[a] – the genotype nomenclature based on previously published studies and [b] – the genotype locations according to the studies previously reported (Walker et al. 1998; Ma et al. 1999; Beard et al. 2000; Denis et al. 2000; Takahashi et al. 2002; Esteves et al. 2010b; Maitte et al. 2013; Xue et al. 2019; Pasic et al. 2020)

Results

General information on PCP patients. Clinical information of the patients involved in this study is summarized in Table III. The presence of *P. jirovecii* in all patients was confirmed by microscopic observation of *P. jirovecii* cysts in BALF samples stained with GMS (Fig. 1).

Multilocus sequence genotyping. All eight genetic loci *P. jirovecii* were successfully amplified and sequenced in the BALF specimen from all three patients. Table II shows the polymorphic nucleotide sites, and the number of plasmid clones sequenced for each PCR product from 8 loci. Genotype profiles are summarized in Table IV.

The HIV-negative patient (SX_0003) showed a co-infection with two genotypes of *P. jirovecii* at six of the eight loci sequenced. Of the two HIV-positive patients, one (SX_0001) showed a co-infection with two genotypes of *P. jirovecii* at two loci, while the other (SX_0002) showed a single infection at all eight loci sequenced.

Of note, the *dhps* gene (the target of sulfa drugs) in all three *P. jirovecii* specimens was present as a wild-type sequence. The *dhfr* gene (the target of trimethoprim) in all three *P. jirovecii* specimens showed a single synonymous change in the same position (from

Table III
Clinical characteristics of patients with *Pneumocystis jirovecii* pneumonia.

Clinical information	Patient No.		
	SX_0001	SX_0002	SX_0003
Age (years)	65	51	65
Sex	Male	Male	Male
Underlying conditions	NA[a]	Hepatic cysts	ILD
Thoracic HRCT findings	GGO[d] +	GGO +	GGO +
HIV 1/2 antibody	+/–	+/–	–/–
CD_4 T-lymphocyte count (cells/μl)	232	176	NA
Serum parameters			
1,3-β-D-glucan, normal < 10 pg/ml	> 600	NA	> 600
Lactate dehydrogenase, normal 120–250 U/l	432	699	9,734
C-reactive protein, normal 0–6 mg/l	73.63	129.17	340.00
Procalcitonin, normal 0–0.05 ng/ml	0.975	0.161	11.26
Partial pressure of oxygen, normal 80–110 mmHg	80	65	59.70
Erythrocyte sedimentation rate, normal 0–15 mm/h	61.10	60.80	47.30
Concurrent infection	–	–	*C.n.* and *B.c.*[b]
Anti-PCP therapy[a]	–	–	–
HAART before PCP	–	–	–
Clinical outcomes	survived	survived	died

NA – not available; ILD – interstitial lung disease; HRCT – high-resolution computed tomography;
GGO – ground-glass opacity; HIV – human immunodeficiency virus;
HAART – highly active antiretroviral therapy
+– positive, – – negative
[a] – Anti-PCP therapy, TMP-SMZ prophylaxis for *P. jirovecii* pneumonia
[b] – *Candida norvegensis* and *Burkholderia cepacia*

Table IV
Genotypes of *Pneumocystis jirovecii* detected at eight genetic loci.

Patient No.	HIV1/2 antibody	Genotypes at 8 loci							
		ITS	*sod*	*dhfr*	*dhps*	*cyb*	mtLSU rRNA	β-Tub	26S rRNA
SX_0001	+/–	ITS2 + ITS59	*sod1*	*dhfr312*	*WT*	*cyb7*	mt3	β-Tub1 + β-Tub2	26S2
SX_0002	+/–	ITS4	*sod1*	*dhfr312*	*WT*	*cyb2*	mt3	β-Tub2	26S2
SX_0003	–/–	ITS10 + ITS16	*sod1* + *sod2*	*dhfr312*	*WT*	*cyb1* + *cyb8*	mt1 + mt 2	β-Tub1 + β-Tub2	26S3 + 26S4

ITS – internal transcribed spacer regions of rRNA operon, *sod* – superoxide dismutase, *dhfr* – dihydrofolate reductase, *dhps* – dihydropteroate synthase, WT – wild-type, *cyb* – cytochrome b, mt – mitochondrial large rRNA subunit, β-Tub – β-tubulin, 26S rRNA – 26S rRNA gene

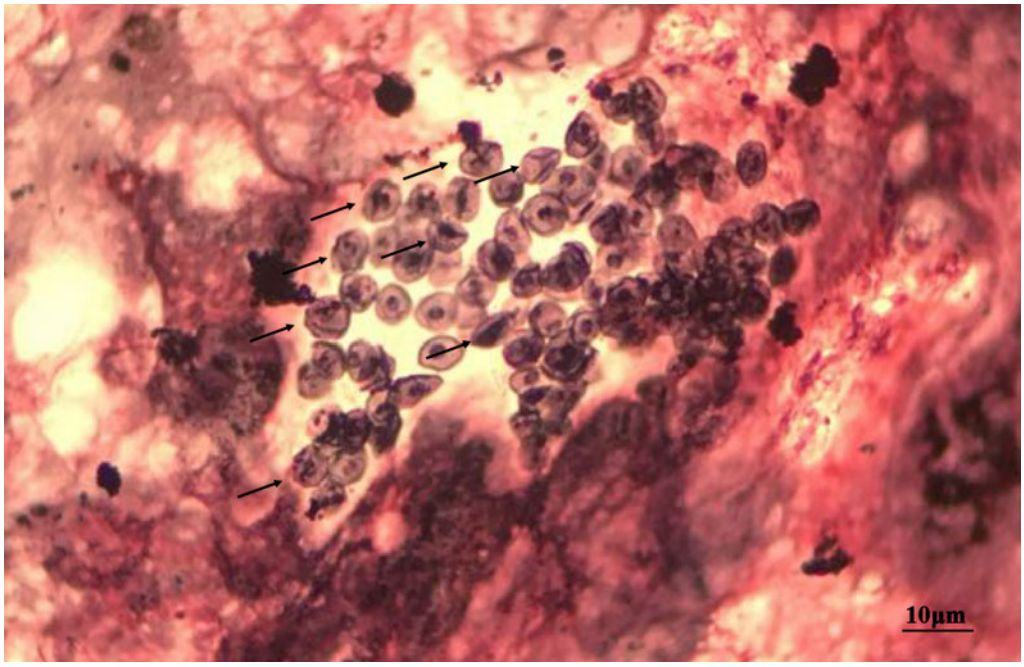

Fig. 1. Identification of *Pneumocystis jirovecii* using GMS staining methods. Cysts appear as brown or puce spheres or ovoids with a small black stick inside (arrows). The reddish background instead of the typical greenish background is most likely due to periodic acid treatment and without light green counterstaining in our staining method.

T to C at nucleotide 312). The *cyb* gene (the target of atovaquone) in the three *P. jirovecii* specimens showed polymorphisms in three nucleotide positions (at 279, 566 and 838), resulting in 4 genotypes including *cyb 1, cyb 2, cyb 7* and *cyb 8* based on the nomenclature system described by Esteves and Maitte (Esteves et al. 2010b; Maitte et al. 2013). Genotypes *cyb 2* and *cyb 7* were presented only in patients SX_0002 and SX_0001, respectively, while genotypes *cyb 1* and *cyb 8* were present as a mixture in the patient SX_003. Of the three polymorphisms, one is synonymous (at 279 in genotype *cyb 8*) and the other two are nonsynonymous (at 566 in genotype *cyb 7* and 838 in genotype *cyb 2*).

Due to the presence of coinfection with two genotypes at 2 or 6 loci in two of the three patients (SX_0001 and SX_0003), we could not determine the exact MLST types in either patient (Table V).

Table V
Multi-locus sequence type (MLST) profiles of *P. jirovecii* from PCP patients in this study in comparison with known *P. jirovecii* MLST profiles in Fungal MLST Database.

MLST types*	β-Tub	*cyb*	26S rRNA	*sod*	Patient no.
3	1	1	4	2	SX_0003
8	2	8	4	1	SX_0003
13	1	1	4	1	SX_0003
15	1	8	4	1	SX_0003
19	1	8	3	2	SX_0003
21	2	1	3	1	SX_0003
22	2	1	3	2	SX_0003
23	2	1	4	1	SX_0003
35	2	7	2	1	SX_0001
51	1	7	2	1	SX_0001
52	2	2	2	1	SX_0002
NA	1	1	3	2	SX_0003
NA	2	8	3	1	SX_0003
NA	2	8	3	2	SX_0003
NA	2	1	4	2	SX_0003
NA	2	8	4	2	SX_0003
NA	1	1	3	1	SX_0003
NA	1	8	3	1	SX_0003
NA	1	8	4	2	SX_0003

* – The first 11 MLST types (numbered 3 to 52) identified in this study correspond to those in the Fungal MLST Database at http://mlst.mycologylab.org

NA – types identified in this study and not available from the Fungal MLST Database

In both patients SX_0001 and SX_0003 (with co-infection of two genotypes at 2 or 6 loci, respectively), there were a total of four and 64 potential MLST profiles, respectively. Only two and 16 of those profiles are listed in this table while the true profiles could not be determined in this study.

Discussion

Despite having been recognized as an important human pathogen for many years, strain variation of *P. jirovecii* remains poorly understood due largely to the absence of a reliable in vitro culture system. To date, *P. jirovecii* strain typing has relied primarily on analyzing genetic markers after PCR amplification. While there have been about a dozen genetic markers reported (Ma et al. 2018), most studies have used only a small number of genetic markers in epidemiological investigations, potentially limiting the discriminatory power for strain differentiation. In this study, we performed strain typing of *P. jirovecii* using a total of eight genetic markers, including six nuclear genes (ITS, 26S rRNA,

sod, *dhps*, *dhfr* and β-Tub) and two mitochondrial genes (mtLSU-rRNA and *cyb*).

While only three clinical specimens were examined including two from HIV-infected patients and one from a non-HIV patient, we identified complex genotype profiles (Table II). Multiple unique genotypes (from 2 to 5) were identified at all these eight loci except for two (*dhps* and *dhfr*), which showed a single genotype. Two of three clinical specimens showed a mixture of multiple genotypes at two or six loci, suggesting a coinfection with multiple *P. jirovecii* strains, without any strains shared between the three patients. This represents the first report of genetic polymorphisms in PCP patients in Shanxi Province, China. Our findings expand our understanding of the genetic diversity of *P. jirovecii* in China.

The ITS locus involved in this study includes ITS1 and ITS2, and 5.8S rRNA of the nuclear rRNA operon was amplified in one fragment of approximately 490 bp and is also known as ITS1-5.8S-ITS2 (Xue et al. 2019). Sequence analysis of this locus in this study identified five unique genotypes (nos. 4, 10, 16, 22, and 59) based on the genotype nomenclature system in our earlier report (Xue et al. 2019), which is more than genotypes identified from all other seven loci examined. This is consistent with many previous studies showing this locus to be the most polymorphic genetic marker for *P. jirovecii* genotyping (Ma et al. 2018). All ITS genotypes identified in this study have also been reported from previous studies conducted by our group (Xue et al. 2019) and others in China (Li et al. 2013; Sun et al. 2015) as well as studies from other countries (Atzori et al. 1998; Miller and Wakefield 1999; Matsumura et al. 2011).

In this study, we examined genetic polymorphisms of three drug target genes, including *dhfr*, *dhps* and *cyb*, which are the targets of trimethoprim, sulfa, and atovaquone drugs, respectively. No nonsynonymous mutation was found at *dhfr* or *dhps* in any specimens in this study, while a single synonymous change in the same position at *dhfr* (from T to C at nucleotide 312) was present in all three specimens. This change has been reported in previous studies from China (Deng et al. 2014; Wang et al. 2019) and other countries (Esteves et al. 2010b; Muñoz et al. 2012; Suárez et al. 2017; Singh et al. 2019). As for the *cyb* gene, we identified nucleotide changes at three positions (at 279, 566 and 838), which gave rise to 4 unique genotypes (*cyb 1*, *cyb 2*, *cyb 7* and *cyb 8*). All these genotypes have also been reported from China (Deng et al. 2016; Wang et al. 2019) and other countries (Esteves et al. 2010b; Maitte et al. 2013; Sokulska et al. 2018; Szydlowicz et al. 2019; Le Gal et al. 2020; Goterris et al. 2022). The nucleotide changes at two positions (566 and 838) are synonymous (S189L and L180F) but do not correspond to any of the seven mutations that are suggested to be associated with atovaquone resistance in previous studies (Kessl et al. 2004). The absence of mutations in all these three drug targets potentially associated with resistance is consistent with no known use of the respective drugs in the history of the patients.

The major limitation of this study is the small sample size, which precludes the generalization of the results to a larger population and the assessment of correlation of genotypes with clinical characteristics and treatment outcomes. Further studies are required using more samples from different patient populations.

Conclusions

In conclusion, we assessed and analyzed the genetic polymorphisms of *P. jirovecii* genotypes at eight loci and identified complex genotype profiles, including the presence of coinfection with up to 5 genotypes at six loci. This is the first report of genetic polymorphisms in PCP patients in Shanxi Province, China. Our findings expand our understanding of the genetic diversity of *P. jirovecii* in China. However, a large-scale collection of clinical isolates of *P. jirovecii* from different patient populations is required for more detailed studies and the correlation of genotypes with clinical characteristics and outcomes.

Acknowledgments

This work was supported by the Basic Research Projects of Natural Sciences in Shanxi Province (No. 20210302124039), the Scientific and Technological Innovation Programs of Higher Education Institutions in Shanxi (STIP: No. 2020L0201), the Start-up Foundation for Doctoral Scientific Research of Shanxi Medical University (No. XD1905), the Start-up Foundation for Doctoral Scientific Research of Shanxi province (No. SD1905), and Natural Science Foundation of LiaoningProvince (No. LJKZ0796). We thank the staff members at the Shanxi Key Laboratory of Carcinogenesis and Translational Research on Esophageal Cancer for their assistance.

Conflict of interest

The authors do not report any financial or personal connections with other persons or organizations, which might negatively affect the contents of this publication and/or claim authorship rights to this publication.

Literature

Atzori C, Angeli E, Agostoni F, Mainini A, Micheli V, Cargnel A. Biomolecular techniques to detect *Pneumocystis carinii* f. sp. *hominis* pneumonia in patients with acquired immunodeficiency syndrome. Int J Infect Dis. 1998;3(2):76–81. https://doi.org/10.1016/s1201-9712(99)90013-9

Beard CB, Carter JL, Keely SP, Huang L, Pieniazek NJ, Moura IN, Roberts JM, Hightower AW, Bens MS, Freeman AR, et al. Genetic

variation in *Pneumocystis carinii* isolates from different geographic regions: implications for transmission. Emerg Infect Dis. 2000;6(3): 265–272. https://doi.org/10.3201/eid0603.000306

Cañas-Arboleda A, Hernández-Flórez C, Garzón J, Parra-Giraldo CM, Burbano JF, Cita-Pardo JE. Colonization by *Pneumocystis jirovecii* in patients with chronic obstructive pulmonary disease: association with exacerbations and lung function status. Braz J Infect Dis. 2019;23(5):352–357. https://doi.org/10.1016/j.bjid.2019.08.008

Deng X, Xiong M, Lan Y, Zhuo L, Chen W, Tang X. [The gene polymorphisms of drug targets in *Pneumocystis jirovecii* isolates] (in Chinese). Chin J Infect Dis. 2016;34(7):395–399. https://doi.org/10.3760/cma.j.issn.1000-6680.2016.07.002

Deng X, Zhuo L, Lan Y, Dai Z, Chen WS, Cai W, Kovacs JA, Ma L, Tang X. Mutational analysis of *Pneumocystis jirovecii* dihydropteroate synthase and dihydrofolate reductase genes in HIV-infected patients in China. J Clin Microbiol. 2014;52(11):4017–4019. https://doi.org/10.1128/JCM.01848-14

Denis CM, Mazars E, Guyot K, Odberg-Ferragut C, Viscogliosi E, Dei-Cas E, Wakefield AE. Genetic divergence at the SODA locus of six different formae speciales of *Pneumocystis carinii*. Med Mycol. 2000;38(4):289–300. https://doi.org/10.1080/mmy.38.4.289.300

Esteves F, Gaspar J, Marques T, Leite R, Antunes F, Mansinho K, Matos O. Identification of relevant single-nucleotide polymorphisms in *Pneumocystis jirovecii:* relationship with clinical data. Clin Microbiol Infect. 2010a;16(7):878–884. https://doi.org/10.1111/j.1469-0691.2009.03030.x

Esteves F, Gaspar J, Tavares A, Moser I, Antunes F, Mansinho K, Matos O. Population structure of *Pneumocystis jirovecii* isolated from immunodeficiency virus-positive patients. Infect Genet Evol. 2010b;10(2):192–199. https://doi.org/10.1016/j.meegid.2009.12.007

Goterris L, Pasic L, Murillo MG, Kan A, Anton A, Company JA, Ruiz-Camps I, Meyer W, Martin-Gomez MT. *Pneumocystis jirovecii* genetic diversity in a Spanish tertiary hospital. Med Mycol. 2022; 60(1):myab065. https://doi.org/10.1093/mmy/myab065

Kessl JJ, Hill P, Lange BB, Meshnick SR, Meunier B, Trumpower BL. Molecular basis for atovaquone resistance in *Pneumocystis jirovecii* modeled in the cytochrome bc(1) complex of *Saccharomyces cerevisiae*. J Biol Chem. 2004;279(4):2817–2824. https://doi.org/10.1074/jbc.M309984200

Lane BR, Ast JC, Hossler PA, Mindell DP, Bartlett MS, Smith JW, Meshnick SR. Dihydropteroate synthase polymorphisms in *Pneumocystis carinii*. J Infect Dis. 1997;175(2):482–485. https://doi.org/10.1093/infdis/175.2.482

Le Gal S, Hoarau G, Bertolotti A, Negri S, Le Nan N, Bouchara JP, Papon N, Blanchet D, Demar M, Nevez G. *Pneumocystis jirovecii* diversity in Réunion, an overseas French Island in Indian Ocean. Front Microbiol. 2020;11:127. https://doi.org/10.3389/fmicb.2020.00127

Lee CH, Helweg-Larsen J, Tang X, Jin S, Li B, Bartlett MS, Lu JJ, Lundgren B, Lundgren JD, Olsson M, et al. Update on *Pneumocystis carinii* f. sp. *hominis* typing based on nucleotide sequence variations in internal transcribed spacer regions of rRNA genes. J Clin Microbiol. 1998;36(3):734–741. https://doi.org/10.1128/JCM.36.3.734-741.1998

Li K, He A, Cai WP, Tang XP, Zheng XY, Li ZY, Zhan XM. Genotyping of *Pneumocystis jirovecii* isolates from Chinese HIV-infected patients based on nucleotide sequence variations in the internal transcribed spacer regions of rRNA genes. Med Mycol. 2013; 51(1):108–112. https://doi.org/10.3109/13693786.2012.695458

Ma L, Borio L, Masur H, Kovacs JA. *Pneumocystis carinii* dihydropteroate synthase but not dihydrofolate reductase gene mutations correlate with prior trimethoprim-sulfamethoxazole or dapsone use. J Infect Dis. 1999;180(6):1969–1978. https://doi.org/10.1086/315148

Ma L, Cisse OH, Kovacs JA. A molecular window into the biology and epidemiology of *Pneumocystis* spp. Clin Microbiol Rev. 201813;31(3):e00009-18. https://doi.org/10.1128/CMR.00009-18

Maitte C, Leterrier M, Le Pape P, Miegeville M, Morio F. Multilocus sequence typing of *Pneumocystis jirovecii* from clinical samples: how many and which loci should be used? J Clin Microbiol. 2013;51(9):2843–2849. https://doi.org/10.1128/JCM.01073-13

Matsumura Y, Shindo Y, Iinuma Y, Yamamoto M, Shirano M, Matsushima A, Nagao M, Ito Y, Takakura S, Hasegawa Y, et al. Clinical characteristics of *Pneumocystis* pneumonia in non-HIV patients and prognostic factors including microbiological genotypes. BMC Infect Dis. 2011;11:76. https://doi.org/10.1186/1471-2334-11-76

Miller RF, Wakefield AE. *Pneumocystis carinii* genotypes and severity of pneumonia. Lancet. 1999;353(9169):2039–2040. https://doi.org/10.1016/S0140-6736(99)01690-6

Muñoz C, Zuluaga A, Restrepo A, Tobon A, Cano LE, Gonzalez A. Molecular diagnosis and detection of *Pneumocystis jirovecii* DHPS and DHFR genotypes in respiratory specimens from Colombian patients. Diagn Microbiol Infect Dis. 2012;72(3):204–213. https://doi.org/10.1016/j.diagmicrobio.2011.11.015

Pasic L, Goterris L, Guerrero-Murillo M, Irinyi L, Kan A, Ponce CA, Vargas SL, Martin-Gomez MT, Meyer W. Consensus multilocus sequence typing scheme for *Pneumocystis jirovecii*. J Fungi (Basel). 2020;6(4):259. https://doi.org/10.3390/jof6040259

Singh Y, Mirdha BR, Guleria R, Kabra SK, Mohan A, Chaudhry R, Kumar L, Dwivedi SN, Agarwal SK. Genetic polymorphisms associated with treatment failure and mortality in pediatric *Pneumocystosis*. Sci Rep. 2019;9(1):1192. https://doi.org/10.1038/s41598-018-38052-x

Sokulska M, Kicia M, Wesolowska M, Piesiak P, Kowal A, Lobo ML, Kopacz Z, Hendrich AB, Matos O. Genotyping of *Pneumocystis jirovecii* in colonized patients with various pulmonary diseases. Med Mycol. 2018;56(7):809–815. https://doi.org/10.1093/mmy/myx121

Suárez I, Roderus L, van Gumpel E, Jung N, Lehmann C, Fätkenheuer G, Hartmann P, Plum G, Rybniker J. Low prevalence of DHFR and DHPS mutations in *Pneumocystis jirovecii* strains obtained from a German cohort. Infection. 2017;45(3):341–347. https://doi.org/10.1007/s15010-017-1005-4

Sun L, Huang M, Wang J, Xue F, Hong C, Guo Z, Gu J. Genotyping of *Pneumocystis jirovecii* isolates from human immunodeficiency virus-negative patients in China. Infect Genet Evol. 2015;31:209–215. https://doi.org/10.1016/j.meegid.2015.01.021

Szydlowicz M, Jakuszko K, Szymczak A, Piesiak P, Kowal A, Kopacz Z, Wesolowska M, Lobo ML, Matos O, Hendrich AB, et al. Prevalence and genotyping of *Pneumocystis jirovecii* in renal transplant recipients-preliminary report. Parasitol Res. 2019;118(1):181–189. https://doi.org/10.1007/s00436-018-6131-0

Takahashi T, Endo T, Nakamura T, Sakashita H, Kimura K, Ohnishi K, Kitamura Y, Iwamoto A. Dihydrofolate reductase gene polymorphisms in *Pneumocystis carinii* f. sp. *hominis* in Japan. J Med Microbiol. 2002;51(6):510–515. https://doi.org/10.1099/0022-1317-51-6-510

Wakefield AE. DNA sequences identical to *Pneumocystis carinii* f. sp. *carinii* and *Pneumocystis carinii* f. sp. *hominis* in samples of air spora. J Clin Microbiol. 1996;34(7):1754–1759. https://doi.org/10.1128/JCM.34.7.1754-1759.1996

Walker DJ, Wakefield AE, Dohn MN, Miller RF, Baughman RP, Hossler PA, Bartlett MS, Smith JW, Kazanjian P, Meshnick SR. Sequence polymorphisms in the *Pneumocystis carinii* cytochrome b

gene and their association with atovaquone prophylaxis failure. J Infect Dis. 1998;178(6):1767–1775. https://doi.org/10.1086/314509

Wang DD, Zheng MQ, Zhang N, An CL. Investigation of *Pneumocystis jirovecii* colonization in patients with chronic pulmonary diseases in the People's Republic of China. Int J Chron Obstruct Pulmon Dis. 2015;10:2079–2085. https://doi.org/10.2147/COPD.S89666

Wang M, Xu X, Guo Y, Tao R, Hu C, Dong X, Huang Y, Zhu B. Polymorphisms involving the *Pneumocystis jirovecii*-related genes in AIDS patients in eastern China. Infect Genet Evol. 2019;75:103955. https://doi.org/10.1016/j.meegid.2019.103955

Xue T, Ma Z, Liu F, Du W, He L, Wang J, An C. *Pneumocystis jirovecii* colonization and its association with pulmonary diseases: a multicenter study based on a modified loop-mediated isothermal amplification assay. BMC Pulm Med. 2020;20(1):70. https://doi.org/10.1186/s12890-020-1111-4

Xue T, Ma Z, Liu F, Du WQ, He L, Ma L, An CL. Genotyping of *Pneumocystis jirovecii* by use of a new simplified nomenclature system based on the internal transcribed spacer regions and 5.8S rRNA gene of the rRNA operon. Clin Microbiol. 2019;57(6):e02012–18. https://doi.org/10.1128/JCM.02012-18

ORIGINAL PAPER
Polish Journal of Microbiology
2022, Vol. 71, No 1, 35–42
https://doi.org/10.33073/pjm-2022-003

The Relation Between Host TLR9 -1486T/C, rs187084 Gene Polymorphisms and *Helicobacter pylori cagA*, *sodB*, *hsp60*, and *vacA* Virulence Genes among Gastric Cancer Patients

AMIRA M. SULTAN[1]*, RAGY SHENOUDA[1], AHMAD M. SULTAN[2], AHMED SHEHTA[2] and YASMIN NABIEL[1]

[1] Medical Microbiology and Immunology Department, Faculty of Medicine, Mansoura University, Mansoura, Egypt
[2] Gastroenterology Surgical Center, Faculty of Medicine, Mansoura University, Mansoura, Egypt

Submitted 13 October 2021, accepted 19 December 2021, published online 27 February 2022

Abstract

To identify the associations between different genotypes of TLR9 -1486T/C (rs187084) with gastric cancer patients and reveal their relation to *Helicobacter pylori* virulence genes (*cagA*, *sodB*, *hsp60* and *vacA)*. Patients with gastric cancer were recruited to our study, diagnosed both endoscopically and histopathologically. *H. pylori* were isolated from gastric samples by culture and PCR amplification of the *glmM* gene. Virulence genes *cagA*, *sodB*, *hsp60*, and *vacA* were detected by multiplex PCR. Blood samples were used for genotyping of TLR9 -1486T/C (rs187084) by PCR-RFLP. Out of 132 patients with gastric cancer, 106 (80.3%) were positive for *H. pylori*. A similar number of healthy participants was recruited as controls. The prevalence of *cagA, sodB, hsp60*, and *vacA* genes among *H. pylori* was 90.6%, 70.8%, 83.0%, and 95.3%, respectively. The *vacA* gene alleles had a prevalence of 95.3% for *vacAs1*/*s2*, 52.8% for *vacAm1*, and 42.5% for *vacAm2*. The CC genotype of TLR9 -1486T/C had a significantly higher frequency in gastric cancer patients when compared to healthy participants ($p = 0.045$). Furthermore, the CC genotype demonstrated a significant association with *H. pylori* strains carrying *sodB*, *hsp60*, and *vacAm1* virulence genes ($p = 0.021$, $p = 0.049$, and $p = 0.048$ respectively). Patients with CC genotype of TLR9 -1486T/C (rs187084) might be at higher risk for the development of gastric cancer, and its co-existence with *H. pylori* strains carrying *sodB*, *hsp60*, or *vacAm1* virulence genes might have a synergistic effect in the development of gastric cancer. Further studies on a wider scale are recommended.

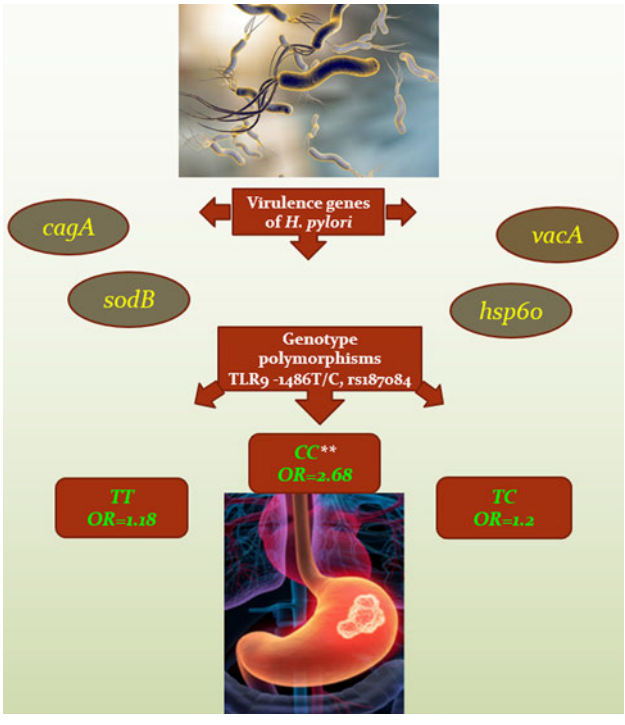

K e y w o r d s: *Helicobacter pylori*, gastric cancer, gene polymorphism, Toll-like receptor-9, virulence genes

Introduction

Helicobacter pylori, described as spiral-shaped Gram-negative bacteria, can infect gastric mucosa in more than half of the population all over the world (Trindade et al. 2017). Such infection disturbs the homeostasis of the gastric mucosa and induces the release of inflammatory cytokines (Cadamuro et al. 2014). Subsequently, the high association was described between *H. pylori* infection and several gastric pathologies as chronic gastritis and gastric cancer (Polk and Peek 2010; Kao et al. 2016). Moreover, the WHO has classified *H. pylori* as a type one carcinogen because of its high association with gastric cancer (Santos et al.

* Corresponding author: A.M. Sultan, Medical Microbiology and Immunology Department, Faculty of Medicine, Mansoura University, Mansoura, Egypt; **e-mail: amira110sultan@yahoo.com**

2012). The development of such different gastric diseases has been linked to the interaction between *H. pylori* virulence factors, host genetics, immune responses, and environmental factors (Wroblewski et al. 2010; Bagheri et al. 2018).

Alterations in the host immune components, including Toll-like receptors (TLRs), through their prominent role in activating the innate and adaptive arms following infection, may influence the progress of the disease elicited by *H. pylori* (Wang et al. 2014; Song et al. 2018). These receptors are known as pattern recognition receptors as they identify the pathogen-associated molecular patterns (PAMPs) present in most pathogens (Varga and Peek 2017; Susi et al. 2019). During *H. pylori* infection, TLRs located on immune cells and local gastric epithelium identify various PAMPs present on that pathogen.

TLR9 detects unmethylated CpG oligonucleotides present abundantly in bacterial DNA (Fukata and Abreu 2008). As TLR9 is located inside the intracellular endosomes, its activation requires intracellular transfer of unmethylated CpG oligonucleotides through endocytosis (Fűri et al. 2013). They are expressed by gastric epithelial cells and contribute considerably to immune recognition and signaling following *H. pylori* infection. Moreover, the proper TLRs activation is vital for gut protection and recovery from injury (Wang et al. 2013). Single nucleotide polymorphism (SNP) of TLR9 genes, such as TLR9 -1486 TC (rs187084), can result in altered expression along with dysregulation of TLR9 signaling leading to unbalanced production of inflammatory cytokines with subsequent chronic inflammation, which promotes the development of gastric cancer (Wang et al. 2013). Such associations between TLR9 SNPs and increased risk to develop gastric cancer were previously reported (Wang et al. 2013; Susi et al. 2019).

Different virulence agents of *H. pylori* can be used as tools to predict the clinical outcomes of the infection (Polk and Peek 2010, Yamaoka and Graham 2014). The cytotoxin-associated gene A (CagA) is considered one of the main toxins of *H. pylori* (Ayala et al. 2014) that can cause morphological alterations in the host cell triggering cell differentiation and multiplication, which can help in the development of gastric cancer (Yong et al. 2015). The C-terminal region of CagA protein contains different Glu-Pro-Ile-Tyr-Ala (EPIYA) motifs that serve as phosphorylation sites for the protein. These EPIYA segments were classified into four types according to their flanking sequences: EPIYA-A, B, C, and D (Cristancho Liévano et al. 2018). The CagA oncogenic potential has been linked to the EPIYA motifs C and D (Ofori et al. 2019). This could be related to the affinity of the SHP2 phosphatase protein to join the EPIYA C and D motifs, which affect the carcinogenic ability of *Helicobacter* strains (Cristancho Liévano et al. 2018).

The vacuolating cytotoxin (VacA) is another effective toxin produced by *H. pylori* strains and encoded by the *vacA* gene. It is a pore-inducing toxin that triggers apoptosis by inducing epithelial cellular vacuolation of the stomach (Palframan et al. 2012). The *vacA* gene has a mosaic structure with two main variation regions; the signal (s1 and s2), and the middle regions (m1 and m2), which determine the toxin vacuolating activity (Ofori et al. 2019). The s1/m1 and s1/m2 genotypes are associated with high and moderate vacuolating activity, respectively. On the other hand, the vacuolating activity is absent in the s2/m2 genotypes (Ofori et al. 2019). It was also reported that patients infected with *vacAs1m1* positive *H. pylori* strains are more likely of developing the clinical disease (Miernyk et al. 2011; Ofori et al. 2019).

The superoxide dismutase enzyme (SOD), encoded by the *sodB* gene is an important bacterial enzyme that helps *H. pylori* strains to survive (Seyler et al. 2001; Ryberg et al. 2008). Furthermore, heat shock protein 60 (Hsp60) is a protein expressed abundantly by *H. pylori* that acts as a molecular chaperone, which guards unfolded proteins against acid accumulation (Mendoza et al. 2017).

The TLR9 plays a significant role in initiating the immune response following *H. pylori* infection. Hence, genetic variability in its promoter region as TLR9 -1486T/C (rs187084) SNP may alter the expression of this receptor, modify the response to *H. pylori* infection, and increase the risk of gastric cancer. The outcome of *H. pylori* infection is considerably affected by the interactions between bacterial virulence factors and the host immune responses. Therefore, the aim of this study was to identify the associations between different genotypes of TLR9 -1486T/C (rs187084) with gastric cancer patients and reveal their relation to *H. pylori* virulence genes (*cagA*, *sodB, hsp60*, and *vacA*).

Experimental

Materials and Methods

Patients selection. This study was conducted over 15 months (from December 2019 to February 2021). We have recruited 132 patients with gastric cancer at the Gastro-Enterology Surgical Center, Mansoura University, Egypt. They initially presented with gastric symptoms confirmed endoscopically and histopathologically to be gastric cancer. The control group included healthy participants who presented with gastric symptoms and proved to be free of any gastric pathology by histopathology and negative for *H. pylori* by microbiological processing of the biopsy samples. All the participants' epidemiological and clinical data were gathered from medical records. In addition, clinicians have medically interviewed all subjects.

We have excluded any participant who fulfilled one or more of the set exclusion criteria: the previous gastric surgery and the use of anti-*H. pylori* eradication therapy, antibiotics, anti-inflammatory agents, proton pump inhibitors, chemotherapeutic drugs, or radiotherapy within one month before the endoscopy procedure.

Samples collection. A total of 238 stomach biopsies (each of size of 5 mm × 5 mm) were collected by clinicians during the performance of diagnostic gastric endoscopy procedures. The obtained biopsies were stored on ice and immediately transferred to the Medical Microbiology and Immunology Department, Mansoura University, Egypt, for further processing.

A peripheral blood sample of 10 ml was collected under complete aseptic precautions from each study participant for investigating TLR9 gene polymorphisms (TLR9 -1486T/C, rs187084 SNPs).

Isolation of *H. pylori* from gastric tissue samples. The collected biopsies were inoculated in sterile tubes with brain heart infusion (BHI) broth (Oxoid-UK), and then homogenized by a scalpel on a sterile slide. Homogenized samples were cultured on Colombia agar (Oxoid-UK) plates containing 10% of freshly defibrinated sheep's blood. Besides, plates were supplemented with amphotericin B (4 mg/l), vancomycin (10 mg/l), polymyxin B (10 mg/l), and trimethoprim (5 mg/l) antibiotics (Oxoid-UK). Cultured plates were incubated under microaerophilic circumstances (Campy pack systems, BBL, Cockeysville, Maryland, USA) at 37°C for three days (Adinortey et al. 2018).

After three days, culture plates were examined for colonies where *H. pylori* isolates were identified by having small, translucent, and round colonies. Further recognition of *H. pylori* isolates was conducted by microscopic examination by seeing curved-shaped bacteria along with Gram-stained films followed by biochemical reactions (positive catalase, urease, and oxidase). Suspensions of *H. pylori* strains were prepared using BHI broth supplemented with 20% glycerol and then kept at –20°C for further analysis (Idowu et al. 2019).

Molecular confirmation of isolated *H. pylori* strains through amplification of the *glmM* gene. Whole genomic DNA was obtained from cultured isolates using (QIAamp DNA Mini Kit; Qiagen, Hilden, Germany), in line with the provider's rules, then the resulted DNA was kept –20°C until further completing of laboratory work.

The set of primers used to amplify the targeted gene was mentioned in Table I (Santos et al. 2012). The PCR was carried out using a master mix (Fermentas, Germany) that included 4 mM $MgCl_2$, 0.4 mM of each dNTP, and 0.05 U/µl *Taq* DNA polymerase. In addition, 10 pmol of each primer and 0.5 µg of template DNA were included in the reaction mixture (25 µl) (Menoni et al. 2013).

For amplification of the *glmM* gene, the PCR program started by an initial denaturation at 94°C for five minutes, then 40 cycles of denaturation for sixty seconds at 94°C, annealing for ninety seconds at 55°C, and extension for 120 seconds at 72°C. The final extension was performed at 72°C for seven minutes (Menoni et al. 2013).

Molecular detection of *cagA*, *sodB*, *hsp60*, and *vacA* virulence genes of *H. pylori* using multiplex PCR.

Table I
Sequences of primer sets used.

Gene targeted	Sequence	Size of amplified product (bp)	Ref
glmM	F: 5'-AAGCTTTTAGGGGTGTTAGGGGTTT-3' R: 5'-AAGCTTACTTTCTAACACTAACGC-3'	294	Santos et al. 2012
cagA	F: 5'-GATAACAGGCAAGCTTTTGAGG-3' R: 5'-CTGCAAAAGATTGTTTGGCAG-3'	349	Amin et al. 2019
sodB	F: 5'-GCCCTGTGGCGTTTGATTTCC-3' R: 5'-CATGCTCCCACACATCCACC-3'	425	Ryberg et al. 2008
hsp60	F: 5'-GCTCCAAGCATCACCAAAGACG-3' R: 5'-GCGGTTTGCCCTCTTTCATGG-3'	603	Ryberg et al. 2008
vacA	F: 5'-CAATCGTGTGGGTTCTGGAGC-3' R: 5'-GCCGATATGCAAATGAGCCGC-3'	678	Ryberg et al. 2008
vacAs1/s2	F: 5'-ATGGAAATACAACAAACACAC-3' R: 5'-CTGCTTGAATGCGCCAAAC-3'	259	Harrison et al. 2017
vacAm1	F: 5'-GGTCAAAATGCGGTCATGG-3' R: 5'-CCATTGGTACCTGTAGAAAC-3'	290	Harrison et al. 2017
vacAm2	F: 5'-CATAACTAGCGCCTTGCAC-3' R: 5'-GGAGCCCC*AG*GAAACATTG-3'	352	Harrison et al. 2017
TLR9-1486T/C, rs187084	5'-TTCATTCATTCAGCCTTCACTCA-3' 5'-GAGTCAAAGCCACAGTCCACA-3'	490	Roszak et al. 2012

Multiplex PCR was undertaken following the coming steps simultaneously: beginning with incubation for 5 minutes at 95°C; then 34 cycles consisted of one minute at 94°C, then another one minute for primer annealing at 55°C, followed by extension for 60 seconds at 72°C; to be finished with the final extension step at 72°C for ten minutes (Amin et al. 2019). The reaction volume was 25 µl and consisted of a PCR master mix (Fermentas, Germany) that included 4 mM $MgCl_2$, 0.4 mM of each dNTP, and 0.05 U/µl *Taq* DNA polymerase. Besides, 0.5 µg of DNA and 10 pmol of each primer were added. PCR products were then electrophoresed (Farshad et al. 2007). The reference strain (ATCC26695) was used as a positive control (Ryberg et al. 2008). Primer sets used were supplemented in Table I.

Molecular detection of different *vacA* gene alleles in *vacA*-positive *H. pylori* isolates (*vacAs1*/*s2*, *vacAm1*, and *vacAm2*). PCR was conducted by applying the following cycling parameters – first: 95°C for 5 minutes; second: 35 cycles (95°C for 30 seconds, 54°C for 30 seconds and 72°C for 16, 18, and 21 seconds respectively according to the required allele to be amplified (*vacAs1*/*s2*, *vacAm1* and *vacAm2*)). Then final extension was at 72°C for 10 minutes (Harrison et al. 2017). Sets of primers used were listed in Table I.

Genotyping of TLR9 -1486T/C, rs187084 polymorphisms by PCR-RFLP. Genomic DNA was extracted from the obtained buffy coat (leukocyte-enriched fraction of whole blood) using Gene JET Whole Blood Genomic DNA purification Mini kit (Fermentas Life Sciences, Canada) according to provider's guidelines then exposed to PCR-RFLP. Blood samples were subjected to centrifugation at 2,500 × *g* for 10 minutes to release three layers: the upper transparent layer containing plasma, the intermediate buffy coat, and the bottom layer of concentrated erythrocytes.

PCR reaction was run with thermal cycling conditions of 4 minutes at 95°C then 35 cycles each starting with 30 seconds at 95°C followed by 20 seconds at 60°C, and 30 seconds at 72°C to be ended with final extension for 5 minutes at 72°C to produce a DNA piece of 490 bp (Paradowska et al. 2016). The primers used were illustrated in Table I (Roszak et al. 2012).

Then the DNA products were digested using AflII restriction enzyme (Thermo Scientific, EU, Lithuania) by incubation for three hours at 37°C to yield one of three variants: two fragments of 192 bp, and 327 bp that indicated TT allele, or three fragments of 192 bp, 327 bp, and 490 bp that proved the presence of TC allele or an intact PCR fragment of 490 bp indicating the presence of CC allele (Paradowska et al. 2016).

Statistical analysis. The data obtained were evaluated by the computer program SPSS (Statistical package for social science) version 22.0. Descriptive items were shown as means ± standard deviation (SD) or frequency (number-percent). *p*-Values less than 0.05 were significant. The relation between genotypes and the risk of gastric cancer was detected by calculating the odd ratios (ORs) and 95% confidence interval (CIs). We applied Hardy-Weinberg equilibrium to compare genotype frequencies we observed to the expected ones in studied healthy control. The relation between the virulence genes of *H. pylori* and TLR9 -1486T/C, rs187084 genotypes in gastric cancer patients was identified using chi-square test.

Results

This study included 106 subjects with gastric cancer and positive for *H. pylori* infection. A similar number of 106 subjects free of any gastric pathology and negative for *H. pylori* infection were recruited as a control group. No significant difference was found between both groups in both age and sex, as shown in Table II. Gastric cancer lesions were classified according to the histopathologi-

Table II
Demographic and histopathological data of the subjects included in the study.

Variable	Gastric cancer patients	Healthy study participants	*p*-value
Age			
Years (mean ± SD)	56.55 ± 8.63	53.27 ± 8.55	0.93
Sex			
Male	63 (59.4)	59 (55.7%)	0.76
Female	43 (40.6%)	47 (44.3%)	
Differentiation of the tumor			
Well differentiated tumor	16 (15.1%)	NA	–
Moderately differentiated tumor	35 (33.0%)		
Poorly differentiated tumor	55 (51.9%)		

Values are given as mean ± SD, or number (percentage)
NA – Not applicable

Table III
Distribution of *H. pylori* among gastric tissue samples in studied gastric cancer patients.

	Number	%	*p*-value
Positive	106	80.3	0.000*
Negative	26	19.7	
Total	132	100%	

* – statistically significant

Table IV
Distribution of virulence genes in *H. pylori* strains isolated from gastric cancer patients.

Virulence gene	N = 106	%	*p*-value
cagA			
Positive	96	90.6	0.000*
Negative	10	9.4	
sodB			
Positive	75	70.8	0.000*
Negative	31	29.2	
hsp60			
Positive	88	83.0	0.000*
Negative	18	17.0	
vacA			
Positive	101	95.3	0.000*
Negative	5	4.7	
vacAs1/s2			
Positive	101	95.3	0.000*
Negative	5	4.7	
vacAm1			
Positive	56	52.8	0.56
Negative	50	47.2	
vacAm2			
Positive	45	42.5	0.12
Negative	61	57.5	

* – statistically significant

cal examination into well-differentiated tumors (15.1%), moderately differentiated tumors (33.0%), and poorly differentiated tumors (51.9%) (Table II).

Of the 132 gastric cancer patients, 106 (80.3%) gave positive results for *H. pylori* by both culture and PCR, whereas 26 (19.7%) were negative. The results were statically significant (p-value = 0.000) (Table III). The multiplex PCR revealed that the prevalence of *cagA*, *sodB*, *hsp60*, and *vacA* genes among the isolated *H. pylori* strains were 90.6%, 70.8%, 83.0%, and 95.3%, respectively. Regarding the *vacA* gene alleles, they had a prevalence of 95.3% for *vacAs1*/*s2*, 52.8% for *vacAm1*, and 42.5% for *vacAm2* (Table IV).

We screened both the case and control groups for TLR9 -1486T/C, rs187084 polymorphism by PCR-RFLP. The obtained frequencies of genotypes of TLR9 -1486T/C, rs187084 in the healthy group were all on line with Hardy-Weinberg equilibrium. In gastric cancer patients, the frequencies of T and C alleles were 72 (34.0%) and 140 (66.0%), respectively, whereas in the control group, the T allele frequency was 122 (57.5%), and the C allele frequency was 90 (42.5%). We found that the frequency of the C allele in gastric cancer patients was significantly higher than in the control group ($p = 0.047$). The frequency of CC genotype in gastric cancer patients (52.8%) was significantly higher than the control group (22.6%) with a p-value of 0.045, whereas both TT and TC genotypes were not, as they recorded p-values of 0.73 and 0.68, respectively as demonstrated in Table V.

The CC genotype of TLR9 -1486T/C, rs187084, when compared to TT + TC genotypes, demonstrated a significant relation with *H. pylori* strains carrying the *sodB*, *hsp60* or *vacAm1* virulence genes ($p = 0.021$, $p = 0.049$ and $p = 0.048$ respectively). None of the *cagA*, *vacA, vacAs1*/*s2,* or *vacAm2* genes showed a significant association to CC genotype ($p = 0.075$, $p = 0.88$, $p = 0.88$ and $p = 0.81$, respectively) (Table VI).

Discussion

We have reported a prevalence of *H. pylori* of 80.3% in patients with gastric cancer that was in agreement with previous studies (Ang and Fock 2014; Park et al.

Table V
Distribution of genotypes of TLR9 -1486T/C, rs187084 polymorphism in studied groups.

Genotype frequency	Healthy study participants N = 106		Gastric cancer patients N = 106		OR	95% CI	X^2	*p*-value
	N	%	N	%				
TT	40	37.7	22	20.8	1.18	0.45–3.1	0.12	0.73
TC	42	39.6	28	26.4	1.2	0.49–2.88	0.16	0.68
CC	24	22.6	56	52.8	2.68	1.0–7.14	4.03	0.045*

Genotype frequencies are presented in the form of absolute numbers with percentages
OR – Odds ratio; CI – Confidence interval; * – statistically significant

Table VI
The relation between virulence genes of *H. pylori* and TLR9 -1486T/C, rs187084 genotypes in gastric cancer patients.

TLR9-1486T/C, rs187084 genotype	CC N = 56		TT + TC N = 50		*p*-value
Virulence gene	N	%	N	%	
cagA	55	98.2	41	82.0	0.075
sodB	53	94.6	22	44.0	0.021*
hsp60	53	94.6	35	70.0	0.049*
vacA	54	96.4	47	94.0	0.88
vacAs1/s2	54	96.4	47	94.0	0.88
vacAm1	35	62.5	21	42.0	0.048*
vacAm2	19	33.9	26	52.0	0.81

* – statistically significant

2018). A slightly lower prevalence of *H. pylori* at 74.2% has been reported by Wang and his colleagues (2013). Nevertheless, Ezzat et al. (2012) reported a 100% prevalence of *H. pylori* infection in gastric cancer patients. Such differences in *H. pylori* prevalence can be attributed to the host immune response, bacterial virulence factors, and environmental elements (Ofori et al. 2019).

In our study, the prevalence of *cagA* in *H. pylori* strains was 90.6% that was nearly similar to previous reports from Vietnam at 95% (Uchida et al. 2009), North America at 88% (Yamaoka et al. 1999), and Sweden at 82% (Ryberg et al. 2008). In our study, the *vacA* gene was detected in most of the isolated *H. pylori* strains (95.3%) consistent with other reports (Ezzat et al. 2012; Amin et al. 2019). Also, we have reported the prevalence of the *vacAm1* allele at 52.8%, which was higher than that of *vacAm2* (42.5%). In line with our results, the *vacAm1* allele is commoner in Northern Asia while the *vacAm2* allele predominates in Southeast Asia, which has a lower incidence of gastric cancer (Yamaoka and Graham 2014). Similarly, it was suggested that patients infected with the *vacAm1*-positive *H. pylori* strains are at more risk for severe outcomes as gastric cancer than *vacAm2* genotype-positive *H. pylori* strains (Yamaoka and Graham 2014; Idowu et al. 2019). We detected the *sodB* and *hsp60* genes in 70.8% and 83.0% of *H. pylori* strains, respectively, which was in line with Ryberg and his colleagues (2008).

TLR9 plays a vital role in recognizing *H. pylori* DNA and initiating immune responses (Wang et al. 2013). Rad and his colleagues (2009) reported that TLR9 recognition of *H. pylori* has resulted in proinflammatory responses. It was recently suggested that *H. pylori* could reduce the inflammatory response through TLR9, leading to persistent infection (Varga and Peek 2017). Besides, it was reported that *H. pylori* DNA triggered TLR9-dependent activation of NF-kB in human neutrophils that increased IL-8 production, which can participate in gastric cancer development (Alvarez-Arellano et al. 2014). Interestingly, some studies have reported that *H. pylori* can induce TLR9 expression, resulting in stimulating cellular mitogen-activated protein kinases, which trigger angiogenesis and cellular invasion (Chang et al. 2005). Furthermore, TLR9 has been associated with the up-regulation of cyclooxygenase-2 in *H. pylori*-infected gastric mucosa, which was linked to gastric cancer (Fukata and Abreu 2008).

For TLR9 -1486T/C gene polymorphisms, we found that the frequency of CC genotype was significantly higher in gastric cancer patients than the control group (p-value = 0.045). Also, the frequency of the C allele in gastric cancer patients was significantly higher than in the control group ($p = 0.047$). Our findings suggested that C allele might have a role in modifying the immune response to *H. pylori* infection and subsequently promoting gastric carcinogenesis. In line with our findings, Wang and his colleagues (2013) reported that CC and TC genotypes of TLR9 -1486 and the C allele carriers were associated with a higher gastric cancer risk among the Chinese population. Meanwhile, Susi et al. (2019) reported an association between CT and TT genotypes and increased risk of gastric cancer among the Brazilian population. On the other hand, Liu et al. (2015) found no association between TLR9 -1486 T/C polymorphism and gastric cancer risk. These different findings can be attributed to racial differences, environmental factors, and diverse genetic backgrounds in various populations.

In a gene assay conducted by Tao et al. (2007), the C allele of TLR9 -1486T/C down-regulates the expression of TLR9, which leads to deficient immune recognition and signaling in response to *H. pylori*. Consequently, both innate and adaptive immune responses will be reduced, which favors the development of chronic gastritis. This state of chronic gastritis can promote the development of gastric cancer, which can explain our findings. In a more recent study, Xu and his colleagues (2018) have reported a significant association between the CC genotype of TLR9 -1486T/C and increased expression of TNF-α and IL-1β cytokines, affecting the infection outcome. Therefore, such SNP can modify the TLR9 expression, affect the pathogenesis of *H. pylori* infection and increase the risk of gastric cancer (Wang et al. 2013). Still, the precise mechanism by which this SNP affects the risk of *H. pylori*-induced gastric cancer has to be clarified in future studies.

Most studies have focused on either host or bacterial risk factors for developing gastric cancer; however, we explored the relationship between the studied virulence genes of *H. pylori* and genotypes of TLR9 -1486T/C (rs187084) polymorphism in gastric cancer patients. Interestingly, our findings have shown that

the CC genotype had a significantly higher frequency in gastric cancer patients than the control group and that the CC genotype is significantly associated with *H. pylori* strains to harbor the *sodB*, *hsp60* or *vacAm1* virulence genes. Our findings can help clinicians stratify patients according to their tendency to develop gastric cancer and plan strategies for eradicating *H. pylori* infection.

Conclusions

This study suggested that patients with CC genotype of TLR9 -1486T/C (rs187084) might be at higher risk for the development of gastric cancer. In addition, our results offered some evidence that the co-existence of CC genotype of TLR9 -1486T/C and *H. pylori* strains to carry the *sodB*, *hsp60* or *vacAm1* virulence genes might have a synergistic effect promoting the development of gastric cancer. Our findings support the link between host genetics, bacterial virulence genes, and gastric cancer. However, further studies are recommended on a larger number of cases and in more diverse populations.

Abbreviations

BHI – brain heart infusion broth
CagA – cytotoxin-associated gene A
Hsp60 – heat shock protein 60
PAMPs – pathogen-associated molecular patterns
PCR-RFLP – PCR-based restriction fragment length polymorphism
TLRs – Toll-like receptors
SOD – superoxide dismutase enzyme
VacA – vacuolating cytotoxin
SNP – single nucleotide polymorphism

Ethical statement

This study was conducted in accordance with the Declaration of Helsinki, besides the national and institutional standards. Its protocol was approved by the Mansoura Faculty of Medicine Research Board (R.21.01.1165). Informed written consent was received from all participants included in the study.

Author contributions

Both Yasmin Nabiel and Amira Sultan were the creators of the research idea. They both shared in designing the protocol to be carried out, conducting the sample procedures, writing the manuscript, and analyzing the resulting data. Ragy Shenouda shared in processing the samples besides writing and revising the manuscript. Both Ahmed M. Sultan and Ahmed Shehata shared in performing surgical maneuvers and collecting required samples from included study members.

Conflict of interest

The authors do not report any financial or personal connections with other persons or organizations, which might negatively affect the contents of this publication and/or claim authorship rights to this publication.

Literature

Adinortey MB, Ansah C, Adinortey CA, Bockarie AS, Morna MT, Amewowor DH. Isolation of *Helicobacter pylori* from gastric biopsy of dyspeptic patients in Ghana and *in vitro* preliminary assessment of the effect of *Dissotis rotundifolia* Extract on Its Growth. J Trop Med. 2018 Oct 31;2018:1–6.
https://doi.org/10.1155/2018/8071081

Alvarez-Arellano L, Cortés-Reynosa P, Sánchez-Zauco N, Salazar E, Torres J, Maldonado-Bernal C. TLR9 and NF-κB are partially involved in activation of human neutrophils by *Helicobacter pylori* and its purified DNA. PLoS One. 2014 Jul 2;9(7):e101342.
https://doi.org/10.1371/journal.pone.0101342

Amin M, Shayesteh AA, Serajian A. Concurrent detection of *cagA*, *vacA*, *sodB* and *hsp60* virulence genes and their relationship with clinical outcomes of disease in *Helicobacter pylori* isolated strains of southwest of Iran. Iran J Microbiol. 2019 Aug 06;11(3):198–205.
https://doi.org/10.18502/ijm.v11i3.1315

Ang TL, Fock KM. Clinical epidemiology of gastric cancer. Singapore Med J. 2014 Dec;55(12):621–628.
https://doi.org/10.11622/smedj.2014174

Ayala G, Escobedo-Hinojosa WI, de la Cruz-Herrera CF, Romero I. Exploring alternative treatments for *Helicobacter pylori* infection. World J Gastroenterol. 2014;20(6):1450–1469.
https://doi.org/10.3748/wjg.v20.i6.1450

Bagheri N, Razavi A, Pourgheysari B, Azadegan-Dehkordi F, Rahimian G, Pirayesh A, Shafigh M, Rafieian-Kopaei M, Fereidani R, Tahmasbi K, et al. Up-regulated Th17 cell function is associated with increased peptic ulcer disease in *Helicobacter pylori* -infection. Infect Genet Evol. 2018 Jun;60:117–125.
https://doi.org/10.1016/j.meegid.2018.02.020

Cadamuro ACT, Rossi AF, Maniezzo NM, Silva AE. *Helicobacter pylori* infection: host immune response, implications on gene expression and microRNAs. World J Gastroenterol. 2014;20(6):1424–1437.
https://doi.org/10.3748/wjg.v20.i6.1424

Chang YJ, Wu MS, Lin JT, Chen CC. *Helicobacter pylori*-induced invasion and angiogenesis of gastric cells is mediated by cyclooxygenase-2 induction through TLR2/TLR9 and promoter regulation. J Immunol. 2005 Dec 15;175(12):8242–8252.
https://doi.org/10.4049/jimmunol.175.12.8242

Cristancho Liévano F, Trujillo Gama E, Bravo Hernández MM. Cag pathogenicity island of *Helicobacter pylori* and its association to preneoplastic lesion and gastric cancer. Rev Udca Actual Divulg Cient. 2018;21(2):309–318.
https://doi.org/10.31910/rudca.v21.n2.2018.972

Ezzat AHH, Ali MH, El-Seidi EA, Wali IE, Sedky NAER, Naguib SMM. Genotypic characterization of *Helicobacter pylori* isolates among Egyptian patients with upper gastrointestinal diseases. Chin-Ger J Clin Oncol. 2012 Jan;11(1):15–23.
https://doi.org/10.1007/s10330-011-0880-x

Farshad S, Japoni A, Alborzi A, Hosseini M. Restriction fragment length polymorphism of virulence genes *cagA*, *vacA* and *ureAB* of *Helicobacter pylori* strains isolated from Iranian patients with gastric ulcer and nonulcer disease. Saudi Med J. 2007 Apr;28(4):529–534.

Fukata M, Abreu MT. Role of Toll-like receptors in gastrointestinal malignancies. Oncogene. 2008 Jan;27(2):234–243.
https://doi.org/10.1038/sj.onc.1210908

Fűri I, Sipos F, Germann TM, Kalmár A, Tulassay Z, Molnár B, Műzes G. Epithelial Toll-like receptor 9 signaling in colorectal inflammation and cancer: clinico-pathogenic aspects. World J Gastroenterol. 2013;19(26):4119–4126.
https://doi.org/10.3748/wjg.v19.i26.4119

Harrison U, Fowora MA, Seriki AT, Loell E, Mueller S, Ugo-Ijeh M, Onyekwere CA, Lesi OA, Otegbayo JA, Akere A, et al. *Helicobacter pylori* strains from a Nigerian cohort show divergent

antibiotic resistance rates and a uniform pathogenicity profile. PLoS One. 2017 May 2;12(5):e0176454. https://doi.org/10.1371/journal.pone.0176454

Idowu A, Mzukwa A, Harrison U, Palamides P, Haas R, Mbao M, Mamdoo R, Bolon J, Jolaiya T, Smith S, et al. Detection of *Helicobacter pylori* and its virulence genes (*cagA*, *dupA*, and *vacA*) among patients with gastroduodenal diseases in Chris Hani Baragwanath Academic Hospital, South Africa. BMC Gastroenterol. 2019; 19(1):73. https://doi.org/10.1186/s12876-019-0986-0

Kao CY, Sheu BS, Wu JJ. *Helicobacter pylori* infection: an overview of bacterial virulence factors and pathogenesis. Biomed J. 2016 Feb;39(1):14–23. https://doi.org/10.1016/j.bj.2015.06.002

Liu S, Wang X, Shi Y, Han L, Zhao Z, Zhao C, Luo B. Toll-like receptor gene polymorphisms and susceptibility to Epstein-Barr virus-associated and -negative gastric carcinoma in Northern China. Saudi J Gastroenterol. 2015;21(2):95–103. https://doi.org/10.4103/1319-3767.153832

Mendoza JA, Weinberger KK, Swan MJ. The Hsp60 protein of *Helicobacter pylori* displays chaperone activity under acidic conditions. Biochem Biophys Rep. 2017 Mar;9:95–99. https://doi.org/10.1016/j.bbrep.2016.11.011

Menoni SMF, Bonon SHA, Zeitune JMR, Costa SCB. PCR-based detection and genotyping of *Helicobacter pylori* in endoscopic biopsy samples from Brazilian patients. Gastroenterol Res Pract. 2013;2013:1–8. https://doi.org/10.1155/2013/951034

Miernyk K, Morris J, Bruden D, McMahon B, Hurlburt D, Sacco F, Parkinson A, Hennessy T, Bruce M. Characterization *of Helicobacter pylori cagA* and *vacA* genotypes among Alaskans and their correlation with clinical disease. J Clin Microbiol. 2011 Sep; 49(9): 3114–3121. https://doi.org/10.1128/JCM.00469-11

Ofori EG, Adinortey CA, Bockarie AS, Kyei F, Tagoe EA, Adinortey MB. *Helicobacter pylori* infection, virulence genes' distribution and accompanying clinical outcomes: The West Africa situation. BioMed Res Int. 2019 Dec 10;2019:1–13. https://doi.org/10.1155/2019/7312908

Palframan SL, Kwok T, Gabriel K. Vacuolating cytotoxin A (VacA), a key toxin for *Helicobacter pylori* pathogenesis. Front Cell Infect Microbiol. 2012;2:92. https://doi.org/10.3389/fcimb.2012.00092

Paradowska E, Jabłońska A, Studzińska M, Skowrońska K, Suski P, Wiśniewska-Ligier M, Woźniakowska-Gęsicka T, Nowakowska D, Gaj Z, Wilczyński J, et al. TLR9 -1486T/C and 2848C/T SNPs are associated with human cytomegalovirus infection in infants. PLoS One. 2016 Apr 22;11(4):e0154100. https://doi.org/10.1371/journal.pone.0154100

Park J, Forman D, Waskito L, Yamaoka Y, Crabtree J. Epidemiology of *Helicobacter pylori* and CagA-positive infections and global variations in gastric cancer. Toxins (Basel). 2018 Apr 19;10(4):163. https://doi.org/10.3390/toxins10040163

Polk DB, Peek RM Jr. *Helicobacter pylori*: gastric cancer and beyond. Nat Rev Cancer. 2010 Jun;10(6):403–414. https://doi.org/10.1038/nrc2857

Rad R, Ballhorn W, Voland P, Eisenächer K, Mages J, Rad L, Ferstl R, Lang R, Wagner H, Schmid RM, et al. Extracellular and intracellular pattern recognition receptors cooperate in the recognition of *Helicobacter pylori*. Gastroenterology. 2009 Jun;136(7): 2247–2257. https://doi.org/10.1053/j.gastro.2009.02.066

Roszak A, Lianeri M, Sowińska A, Jagodziński PP. Involvement of toll-like receptor 9 polymorphism in cervical cancer development. Mol Biol Rep. 2012 Aug;39(8):8425–8430. https://doi.org/10.1007/s11033-012-1695-8

Ryberg A, Borch K, Sun YQ, Monstein HJ. Concurrent genotyping of *Helicobacter pylori* virulence genes and human cytokine SNP sites using whole genome amplified DNA derived from minute amounts of gastric biopsy specimen DNA. BMC Microbiol. 2008 Dec;8(1):175. https://doi.org/10.1186/1471-2180-8-175

Santos JC, Ladeira MSP, Pedrazzoli J Jr, Ribeiro ML. Relationship of IL-1 and TNF-α polymorphisms with *Helicobacter pylori* in gastric diseases in a Brazilian population. Braz J Med Biol Res. 2012 Sep; 45(9):811–817. https://doi.org/10.1590/S0100-879X2012007500099

Seyler RW Jr, Olson JW, Maier RJ. Superoxide dismutase-deficient mutants of *Helicobacter pylori* are hypersensitive to oxidative stress and defective in host colonization. Infect Immun. 2001 Jun; 69(6):4034–4040. https://doi.org/10.1128/IAI.69.6.4034-4040.2001

Song M, Rabkin CS, Camargo MC. Gastric cancer: an evolving disease. Curr Treat Options Gastroenterol. 2018 Dec;16(4):561–569. https://doi.org/10.1007/s11938-018-0203-1

Susi MD, Lourenço CM, Rasmussen LT, Payão SLM, Rossi AFT, Silva AE, Oliveira-Cucolo JG. Toll-like receptor 9 polymorphisms and *Helicobacter pylori* influence gene expression and risk of gastric carcinogenesis in the Brazilian population. World J Gastrointest Oncol. 2019 Nov 15;11(11):998–1010. https://doi.org/10.4251/wjgo.v11.i11.0000

Tao K, Fujii M, Tsukumo S, Maekawa Y, Kishihara K, Kimoto Y, Horiuchi T, Hisaeda H, Akira S, Kagami S, et al. Genetic variations of Toll-like receptor 9 predispose to systemic lupus erythematosus in Japanese population. Ann Rheum Dis. 2007 Feb 02;66(7):905–909. https://doi.org/10.1136/ard.2006.065961

Trindade LMDF, Menezes LBO, Souza Neta AM, Leite Rolemberg PC, Souza LD, Barreto IDC, Meurer L. Prevalence of *Helicobacter pylori* infection in samples of gastric biopsies. Gastroenterol Res. 2017;10(1):33–41. https://doi.org/10.14740/gr785w

Uchida T, Nguyen LT, Takayama A, Okimoto T, Kodama M, Murakami K, Matsuhisa T, Trinh TD, Ta L, Ho DQD, et al. Analysis of virulence factors of *Helicobacter pylori* isolated from a Vietnamese population. BMC Microbiol. 2009 Dec;9(1):175. https://doi.org/10.1186/1471-2180-9-175

Varga MG, Peek RM. DNA Transfer and Toll-like receptor modulation by *Helicobacter pylori*. Curr Top Microbiol Immunol. 2017; 400:169–193. https://doi.org/10.1007/978-3-319-50520-68

Wang TR, Peng JC, Qiao YQ, Zhu MM, Zhao D, Shen J, Ran ZH. *Helicobacter pylori* regulates TLR4 and TLR9 during gastric carcinogenesis. Int J Clin Exp Pathol. 2014 Sep 15;7(10):6950–6955.

Wang X, Xue L, Yang Y, Xu L, Zhang G. TLR9 promoter polymorphism is associated with both an increased susceptibility to gastric carcinoma and poor prognosis. PLoS One. 2013 Jun 12;8(6):e65731. https://doi.org/10.1371/journal.pone.0065731

Wroblewski LE, Peek RM Jr, Wilson KT. *Helicobacter pylori* and gastric cancer: factors that modulate disease risk. Clin Microbiol Rev. 2010 Oct;23(4):713–739. https://doi.org/10.1128/CMR.00011-10

Xu F, Mai C, Zhu Q. Association of TLR-9 polymorphisms with the development of gastroduodenal ulcer: A hospital-based study in a Chinese cohort. Eur J Inflamm. 2018;16:1–9. https://doi.org/10.1177/1721727X18757262

Yamaoka Y, Graham DY. *Helicobacter pylori* virulence and cancer pathogenesis. Future Oncol. 2014 Jun;10(8):1487–1500. https://doi.org/10.2217/fon.14.29

Yamaoka Y, Kodama T, Gutierrez O, Kim JG, Kashima K, Graham DY. Relationship between *Helicobacter pylori iceA*, *cagA*, and *vacA* status and clinical outcome: studies in four different countries. J Clin Microbiol. 1999 Jul;37(7):2274–2279. https://doi.org/10.1128/JCM.37.7.2274-2279.1999

Yong X, Tang B, Li BS, Xie R, Hu CJ, Luo G, Qin Y, Dong H, Yang SM. *Helicobacter pylori* virulence factor CagA promotes tumorigenesis of gastric cancer via multiple signaling pathways. Cell Commun Signal. 2015 Dec;13(1):30. https://doi.org/10.1186/s12964-015-0111-0

ORIGINAL PAPER

Polish Journal of Microbiology
2022, Vol. 71, No 1, 43–53
https://doi.org/10.33073/pjm-2022-006

A Salt-Tolerant *Streptomyces paradoxus* D2-8 from Rhizosphere Soil of *Phragmites communis* Augments Soybean Tolerance to Soda Saline-Alkali Stress

YAMEI GAO[1, 2, 3], YIQIANG HAN[1], XIN LI[1, 2], MINGYANG LI[1, 2], CHUNXU WANG[1, 2], ZHIWEN LI[1, 2], YANJIE WANG[1, 2*] and WEIDONG WANG[1, 2*]

[1] College of Life Science and Technology, Heilongjiang Bayi Agricultural University, Daqing, China
[2] Heilongjiang Provincial Key Laboratory of Environmental Microbiology and Recycling of Argo-Waste in Cold Region, College of Life Science and Technology, Heilongjiang Bayi Agricultural University, Daqing, China
[3] College of Agriculture, Heilongjiang Bayi Agricultural University, Daqing, China

Submitted 10 December 2021, accepted 21 January 2022, published online 14 March 2022

Abstract

Soil salinity and alkalization limit plant growth and agricultural productivity worldwide. The application of salt-tolerant plant growth-promoting rhizobacteria (PGPR) effectively improved plant tolerance to saline-alkali stress. To obtain the beneficial actinomycetes resources with salt tolerance, thirteen isolates were isolated from rhizosphere saline and alkaline soil of *Phragmites communis*. Among these isolates, D2-8 was moderately halophilic to NaCl and showed 120 mmol soda saline-alkali solution tolerance. Moreover, the plant growth-promoting test demonstrated that D2-8 produced siderophore, IAA, 1-aminocyclopropane-1-carboxylate deaminase (ACCD), and organic acids. D2-8 showed 99.4% homology with the type strain *Streptomyces paradoxus* NBRC 14887^T and shared the same branch, and, therefore, it was designated *S. paradoxus* D2-8. Its genome was sequenced to gain insight into the mechanism of growth-promoting and saline-alkali tolerance of D2-8. IAA and siderophore biosynthesis pathway, genes encoding ACC deaminase, together with six antibiotics biosynthesis gene clusters with antifungal or antibacterial activity, were identified. The compatible solute ectoine biosynthesis gene cluster, production, and uptake of choline and glycine betaine cluster in the D2-8 genome may contribute to the saline-alkali tolerance of the strain. Furthermore, D2-8 significantly promoted the seedling growth even under soda saline-alkali stress, and seed coating with D2-8 isolate increased by 5.88% of the soybean yield in the field. These results imply its significant potential to improve soybean soda saline-alkali tolerance and promote crop health in alkaline soil.

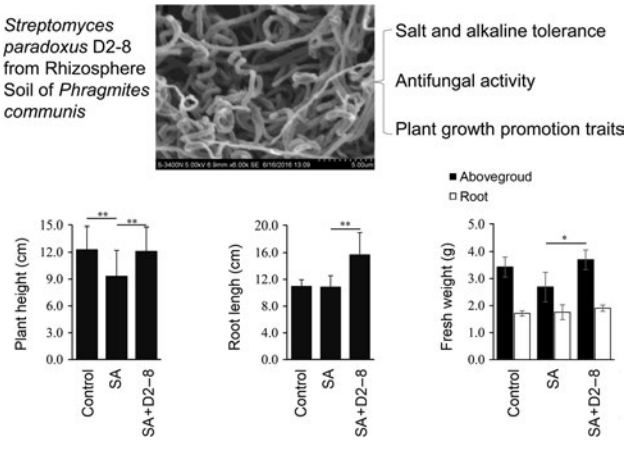

K e y w o r d s: Actinomycetes, *Phragmites communis*, rhizosphere, soda saline-alkali tolerance, plant growth promotion

Introduction

Salinization-alkalization of soil is a serious threat worldwide, and the total area of saline soils exceeds 8.3×10^8 hm^2 worldwide, including 53% alkaline soils and 47% saline soils. In China, it reaches 9.9×10^7 hm^2. The Songnen Plain, an important plantation base of soybean production, is one of China's five largest salt-affected soil regions and has 3.42×10^6 hm^2 salt soil (Huang et al. 2016). Salinity stress has detrimental effects on soybean growth and agronomy traits, such as nodulation, seed quality and quantity, and yield (Phang et al. 2008). Except for plant breeding and agricultural practices, applying a salt-tolerant bioagent may be an effective and sustainable means to enhance crop health and augment plant tolerance to salinity stress

* Corresponding authors: Y.J. Wang, College of Life Science and Technology, Heilongjiang Bayi Agricultural University, Daqing, China; **e-mail: wangyanjie1972@163.com**
W.D. Wang, College of Life Science and Technology, Heilongjiang Bayi Agricultural University, Daqing, China; **e-mail: wwdcyy@126.com**

without environmental damage. To date, only several commercial bioagent products in the market have been applied in agriculture (Zeng et al. 2012; Panda et al. 2014). Moreover, the effect of the biological agent was influenced by variable conditions in the field (Chatterton and Punja 2010). Additionally, it is estimated that 50% of annual yield losses in major crops were caused by abiotic stress worldwide (Zörb et al. 2019). So, it is urgent to isolate more microorganisms with tolerance to various abiotic stress in the field, such as salt, alkaline, drought, etc., that could be applied as bioagents. Nowadays, some salt-tolerant plant growth-promoting rhizobacteria (PGPR) have shown great potential for alleviating salinity stress of many crops, such as *Bacillus*, *Rhizobium, Pseudomonas*, and others (Han et al. 2021). For soybean, *Bacillus*, *Pseudomonas*, and *Rhizobacteria* were reported to alleviate the harmful effects of salinity stress (Khan et al. 2019; Costa-Gutierrez et al. 2020; Abulfarajand Jalal 2021). To our best of knowledge, most PGPR were investigated under salt (NaCl) stress, and few actinobacteria were studied its potential to prime the alkaline or saline-alkali tolerance of soybean in soda alkaline soils. Alkaline or soda saline-alkali soils are composed primarily of $NaHCO_3/Na_2CO_3$ with excess Na^+, HCO_3^-/CO_3^{2-}, high-pH (>8.5), and poor soil structure imposes more damages on plant growth than saline soils. Hence, more microorganism resources with saline-alkali tolerance are essential to increase crop yields under soda saline-alkali stress.

Actinomycetes produce many bioactive compounds and have a great capacity to promote plant growth (Bhatti et al. 2017; Rehan et al. 2021). Nowadays, several commercial biocontrol agents are developed from actinobacteria, such as Actinovate based on *Streptomyces lydicus*, Mycostop based on *Streptomyces griseoviridis*, and Rhizovit based on *Streptomyces* sp. DSMZ 12424 (Lahdenperä et al. 1991; Berg et al. 2001; Minuto et al. 2006; Zeng et al. 2012). Actinobacteria can survive in various environments, such as saline or alkaline soils (Vasavada et al. 2006; Sadeghi et al. 2013). They are promising microorganisms to apply in abiotic stress environments for sustainable agriculture.

Phragmites communis (common reed), a tall perennial grass, is widely distributed in alkaline and saline soils of Songnen plain. The survival threshold of salt tolerance of the reed is 1%. It can grow normally in soil with a pH value of 6.5 ~ 9 and has strong salt and alkali resistance. Actinomycetes from rhizosphere soil of *Phragmites* were supposed to be salt and alkali tolerant and beneficial plant growth-promoting rhizobacteria. To test the above hypothesis and obtain soda saline-alkali tolerant PGPR to improve crop health in alkaline soils, the actinomyces were isolated from the rhizosphere soil of *Phragmites*, and antifungal activity of salt-tolerant strain D2-8 was screened. Soda saline-alkali tolerance was focused, and the survival ability of D2-8 in 0 ~ 120 mM mixed saline-alkali solution (NaCl, Na_2CO_3, $NaHCO_3$, and Na_2SO_4) was confirmed. Meanwhile, plant growth promotion characteristic of the strain was measured. Then, the polyphasic taxonomy analysis was carried out, and the genome was sequenced to reveal the antifungal, plant growth promotion, and saline-alkali tolerant mechanisms. Furthermore, pot and field experiments evaluated its soda saline-alkali tolerance improvement and growth promotion. This study provided the multifarious PGPR *Streptomyces* strain with soda saline-alkali tolerance, which has great potential to improve soybean productivity, and it is also an important source of new secondary metabolite substances.

Experimental

Materials and Methods

Isolation of actinomycete strains from rhizosphere soil of *P. communis*. Rhizosphere soil was collected from the rhizosphere of *P. communis* grown in the saline and alkaline land (34°290' N, 113°20' E), Daqing, China. The soil sample (pH 9.9 and salinity 20.89 g/kg) was air-dried at room temperature for 14 days, then ground into powder. The sample was suspended in sterile water and incubated at 28°C and 200 rpm on a rotary shaker for 30 min. A standard serial dilution technique was used to isolate actinomyces on the Gause No. 1 culture medium. Cycloheximide (50 mg/l) and nalidixic acid (20 mg/l) were added to the medium to inhibit the growth of bacteria and fungi. After seven days of aerobic incubation at 28°C, the colonies were picked out, continually purified, and finally maintained as glycerol suspensions (20%, v/v) at –80°C refrigerator.

Screening for antagonistic actinomycetes. The phytopathogenic strains and fungi used in this study were stored by the Heilongjiang Bayi Agricultural University (Daqing, China). Those fungi included *Gibberella zeae*, *Fusarium avenaceum*, and *Fusarium solani*. Antagonistic activity of isolates was evaluated with the culture plate assay. The isolates were firstly point-inoculated at the center of potato dextrose agar (PDA) plates. After three days of culture, four fresh mycelial PDA agars plugs of the fungus were put in the corresponding plate's margin and incubated for an additional seven days at 28°C. The inhibition activity of isolates against *Phytophthora sojae* was measured on CA plates following the same method. Each experiment was repeated three times. The inhibition rates were calculated according to the formula:

$$\text{inhibition rate (\%)} = Wi/W \times 100\%$$

Wi is the width of inhibition, and W is the width between the pathogen and actinomycetes.

NaCl and soda saline-alkali tolerance. NaCl tolerance (0–10% in 1% intervals, 12%, and 15%, w/v) of strain D2-8 was measured in Glucose-Yeast extract (GY) medium at 28°C for seven days on a rotary shaker. D2-8 was also tested for their tolerance to various concentrations (0, 10, 20, 40, 80, 120 160, and 200 mmol/l) of soda saline-alkali supplemented in GY medium. Soda saline-alkali solution contained NaCl, Na_2CO_3, $NaHCO_3$, and Na_2SO_4 (molar ratio 1:1:9:9). The strains were cultured at 28°C on a rotary shaker. After seven days, the cultures were visualized for the growth of the strains.

Morphological, physiological, and biochemical characteristics of strain D2-8. Gram staining was carried out by the standard Gram stain. After growing on ISP 3 agar at 28°C for four weeks, morphological characteristics of D2-8 were observed using scanning electron microscopy (Hitachi SU8010, Hitachi Co., Tokyo, Japan) according to Jin et al. (2019). The growth at different temperatures (10, 15, 20, 25, 28, 32, 35, 40, 45, and 50°C) was examined on ISP 3 medium after incubation for 14 days. The growth in the pH range (4.0 ~ 12.0 at intervals of 1.0 pH unit) was tested in GY (Glucose-Yeast extract) medium at 28°C for 14 days on a rotary shaker. Cultural characteristics were observed on the ISP 1 agar, ISP media 2 ~ 7, Czapek's, Bennett's, and Nutrient agar after14 days at 28°C. The utilization of sole carbon and nitrogen sources, decomposition of cellulose, hydrolysis of starch and aesculin, reduction of nitrate, coagulation and peptonization of milk, liquefaction of gelatin, and production of H_2S were measured.

Phylogenetic analysis of strain D2-8. For DNA extraction, strain D2-8 was cultured in GY medium for seven days. The biomass was harvested using centrifugation and stored at –80°C until use. Genomic DNA was extracted by the method of sodium dodecyl sulfate (SDS)-based DNA extraction. The 16S rRNA gene sequence was amplified using the universal bacterial primers 27F (5'-AGAGTTTGATCCTGGCTCAG-3') and 1492R (5'-GGTTACCTTGTTACGACT-3'). The PCR product was sequenced by the HuaDa company (Beijing, China). The 16S rRNA gene sequence of strain was compared with type strains available at the EzBioCloud server (https://www.ezbiocloud.net/). Phylogenetic trees were constructed by Molecular Evolutionary Genetics Analysis (MEGA) software version 7.0. Neighbor-joining and maximum likelihood algorithms were used.

Evaluation of plant growth-promoting traits of strain D2-8. The strain D2-8 was inoculated into Gause No. 1 liquid medium supplemented with tryptophan (500 μg/ml) at 28°C, 180 rpm in the dark for seven days. Indole-3-acetic acid (IAA) content in the supernatant was measured according to the Salkowski colorimetric method (Gang et al. 2019). A standard curve of IAA solution (5, 15, 20, 30, 40, 50, and 60 μg/ml) was prepared to determine the IAA concentration of strain D2-8. To quantify siderophore production, D2-8 was placed on CAS (Chrome-Azurol S) plates and incubated at 28°C for seven days. The diameter of the orange loop around D2-8 was then measured. In 1-aminocyclopropane-1-carboxylic acid (ACC) degradation assays, D2-8 was streaked onto Dworkin and Foster (DF) minimal salts agar with 5 mmol/l ACC as a sole nitrogen source. Dworkin and Foster medium with 0.2% (wt/vol) $(NH_4)_2SO_4$ or no nitrogen source was inoculated as positive and negative controls. The plates were incubated at 28°C for 10 days before imaging. The growth of the strain was compared to that of the no-nitrogen medium. The supernatant (10 ml) of strain D2-8 was mixed with methyl red reagent (3–5 drops) to test organic acid production. The resulting color was recorded.

Draft genome sequencing and bioinformatic analysis of strain D2-8. For DNA extraction, strain D2-8 was cultured in tryptone soya broth (TSB). DNA library preparation and sequencing by Illumina MiSeq 2000 (Paired-end 2 × 250 bp) were performed at the Personalbio Genomics (Shanghai, China). The raw reads were adapter clipped, quality trimmed, and error corrected as standard procedure. All good-quality sequences were assembled into several scaffolds. The GeneMarkS was used to predict genes in the assembled genome. Genes were further annotated by BLAST in the Swiss-Prot, GO, eggNOG, and KEGG databases. The contig sequence was submitted to antibiotics and secondary metabolite analysis shell AntiSMASH, and the default options were selected (Weber et al. 2015). Genes associated with plant growth promotion and stress tolerance, such as IAA biosynthesis genes, ACC deaminase, ectoine biosynthesis gene cluster, production and uptake of choline and glycine betaine cluster genes, were analyzed.

Assessment of plant growth promotion of the strain in pot and field experiments. The pot experiment was carried out to measure the seedling growth promotion of strain D2-8 under normal condition. D2-8 spores were washed with ddH_2O from Gause No. 1 medium and diluted to the final concentration of 10^8, 10^7, and 10^6 CFU/ml. Seeds were soaked with the spores for 12 h, and seeds of control treatment were soaked with ddH_2O. Soybeans were planted in 10 cm pods. The soil: sand: vermiculite (1:1:1, pH 7.8) mixed substrate, which contained 54.19 mg/kg available nitrogen, 9.63 mg/kg available phosphorus, 128.45 mg/kg available potassium, 8.8 mg/g organic matter, was sterilized and used. The plants were cultured in the greenhouse with 16 h/8 h light and darkness for 14 d. The plant height, fresh weight of aboveground and root, dry weight of aboveground, and root were measured. Each treatment with five plants was repeated three times.

The effect of strain D2-8 on seedling growth under soda saline-alkali stress was further studied. Soybean

seeds were soaked with 10^7 CFU/ml of D2-8 spores for 12 h, and seeds of control treatment were soaked with sterile water. Soybeans were planted in 10 cm pods. The same soil composed of sand: vermiculite (1:1:1) mixed substrate was sterilized and watered with 80 mM saline-alkali solution containing NaCl, Na_2CO_3, $NaHCO_3$, and Na_2SO_4 (molar ratio 1:1:9:9) at first and 8th days, and sterile water was used in other days. The plants were cultured in greenhouse with 16 h/8 h light and darkness for 14 d. The plant height, root length, fresh weight of aboveground, and root were measured after 14 d. There were three treatments, including water soaking under normal condition (Control group), water soaking under saline-alkali stress condition (SA group), D2-8 soaking under saline-alkali stress condition (SA + D2-8 group), and each treatment was repeated five times.

The field experiment was carried out to measure the growth promotion of strain D2-8. Seeds were coated with 10^7 CFU/ml of D2-8 spores, and seeds of control treatment were coated without the strain. Soybeans were planted in the field on May 15th, 2020. The field soil contained 256.56 mg/kg available nitrogen, 65.49 mg/kg available phosphorus, 277.75 mg/kg available potassium, 52.9 mg/g organic matter. The soil pH was 7.1. There are four replicates in the field plot, and each plot has six lines with five meters. Soybeans were managed as routine. Soybeans were harvested on October 25th, 2020. The plant height, number of effective sections, pod number per plant, grain number per plant, 100 grains weight, the yield and theoretical yield were investigated.

Data analysis. Data analysis was performed using SPSS Statistics 22 software. All experiments were analyzed using unpaired *t*-tests (n = 15 plants).

Results

Isolation of salt and saline-alkali tolerant actinomyces strain D2-8 with antagonistic activity. To obtain the biocontrol actinomyces resources with soda saline-alkali tolerance, we isolated 13 strains from the rhizosphere soil of *P. communis* using the dilution plate method. The antagonistic activity of the 13 strains (D2-1 ~ D2-13) against *P. sojae* displayed significant variation (0 ~ 28 ± 0.77 mm). Specifically, strain D2-8 significantly inhibited the mycelia growth of *P. sojae* by 28 ± 0.77 mm (62%) compared to the control and other strains. In addition, it also had the antagonistic activity against *Fusarium* and *Gibberella* (Table SI). So, strain D2-8 was further identified and studied in detail. We measured the resistance of D2-8 to abiotic stresses. It could grow in the presence of 0 ~ 10% NaCl (w/v) with an optimal level of 4% (w/v) (Fig. 1a). Furthermore, it could grow well in 10 ~ 80 mmol soda saline-alkali solution (NaCl, Na_2CO_3, $NaHCO_3$, and Na_2SO_4, molar ratio 1:1:9:9) except for the weak growth in 120 mmol saline-alkali solutions (Fig. 1b).

Identification of strain D2-8. The morphological characteristics of strain D2-8 showed the typical characteristics of the genus *Streptomyces*. Strain D2-8 exhibited a white aerial spore mass and a grey substrate mycelium and formed chains of smooth spore. The spore (0.6 ~ 0.8 × 0.9 ~ 1.1 μm) was rhabditiform (Fig. 2a and 2b). The strain grew well and developed more abundant aerial mycelia on ISP 3 (oatmeal agar) and Czapek's agar (Table SII). The growth of strain D2-8 was observed at 15 ~ 40°C (optimum temperature, 28°C), and pH 5 ~ 9 (optimum pH 7). Detailed physiological characteristics are presented in Table I. Strain D2-8 could liquefy gelatin and produce H_2S and protease.

The 16S rRNA gene sequence (1,487 bp) of strain D2-8 was closely related to members of the genus *Streptomyces*. The strain shared a high 16S rRNA gene sequence similarity of 99.4% to *Streptomyces paradoxus* NBRC 14887^T and *Streptomyces hawaiiensis* NBRC 12784^T. The neighbor-joining tree showed that strain D2-8 formed a distinct phyletic line and occupied a subclade with *S. paradoxus* NBRC 14887^T (Fig. 3). Based on morphological, physiological, and phylogenetic analysis, strain D2-8 was considered a species of the genus

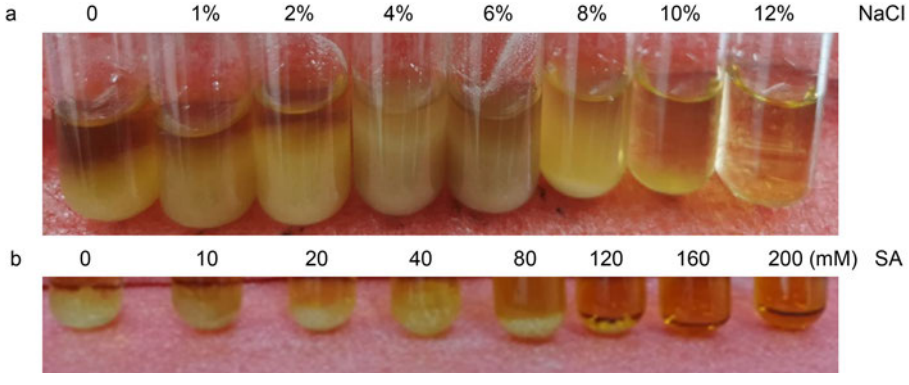

Fig. 1. a) Stress tolerance of strain D2-8 in different concentration of salt and b) saline-alkali solutions.
SA represents saline and alkaline solution, which contains NaCl, Na_2CO_3, $NaHCO_3$, and Na_2SO_4 (molar ratio 1:1:9:9).

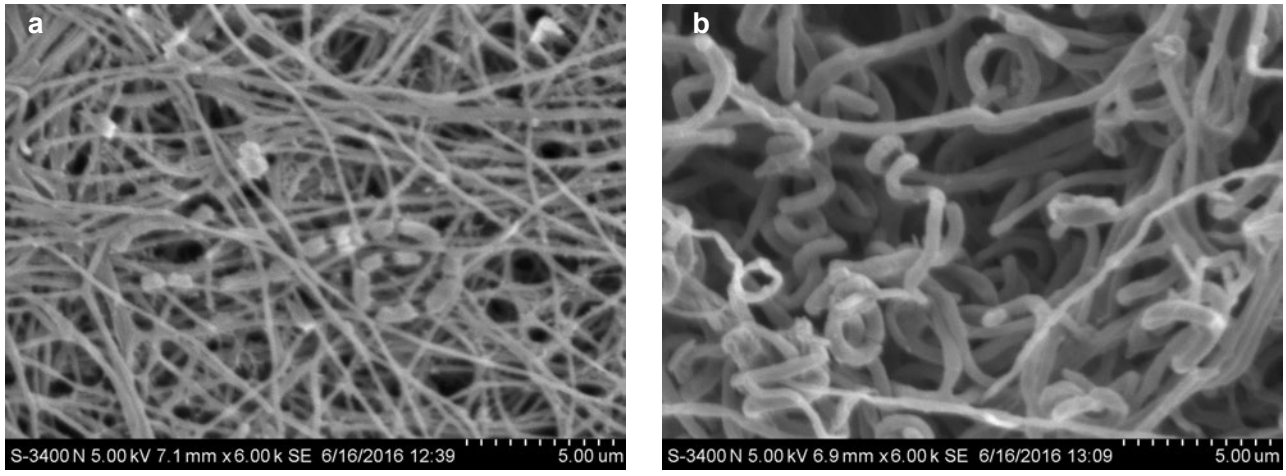

Fig. 2. Morphological characteristics of strain D2-8 observed by scanning electron microscopy.

Streptomyces. The name of *Streptomyces paradoxus* D2-8 was proposed. It was deposited in the China Center for Type Culture Collection (Wuhan) CCTCC M2019949.

Multiple plant growth promotion properties of strain D2-8. Stain D2-8 showed prominent properties for plant growth promotion. On the brilliant blue CAS plate, D2-8 could form an orange loop, which indicated the production of siderophore (Table II). It could produce major phytohormone indole acetic acid (IAA) in Gause No1 liquid medium with tryptophan (Table II), and the yield was 29.1 μg/ml. When testing for changes due to organic acids, the supernatant turned to yellow upon adding methyl red, which suggested D2-8 could produce organic acid (Table II). The ability of D2-8 to produce ACC deaminase was proved by the fact that it grew on the minimal salt medium supplemented with ACC (Table II). These results indicated that D2-8 produced IAA, organic acids, ACC deaminase, and siderophore, which likely contributed to the plant growth promotion by D2-8.

Table I
Physiological characteristics of strain D2-8.

Characteristic	D2-8	Characteristic	D2-8	Characteristic	D2-8
Carbon source utilization		Nitrogen source utilization		Melanin formation on peptone-iron agar	+
Lucose	+	L-threonine	+	Cellulose decomposition	–
Arabinose	+	L-tyrosine	+	Enzymatic activity	
Sucrose	–	L-asparagine	+	Protease	+
Xylose	+	Alanine	+	Liquefaction of gelatin	+
Inositol	+	Glycine	+	Production of H_2S	+
Mannitol	+	L-glutaminealanine	+		
Fructose	–	L-arginine	–		
Rhamnose	–	L-proline	+		
Raffinose	+				
Lactose	+				
D-ribose	+				
D-galactose	+				

+ – positive,
– – negative

Table II
Plant growth promotion properties of strain D2-8.

Characteristic of D2-8	Value or properties
IAA production	29.1 μg/ml
siderophore production	+
organic acids production	+
1-aminocyclopropane-1-carboxylate deaminase (ACCD) production	+

Identification of genes associated with plant growth promotion in the D2-8 genome. To reveal the molecular mechanism of antagonism and plant growth promotion, the D2-8 genome was sequenced. The assembled genome sequence of strain D2-8 was

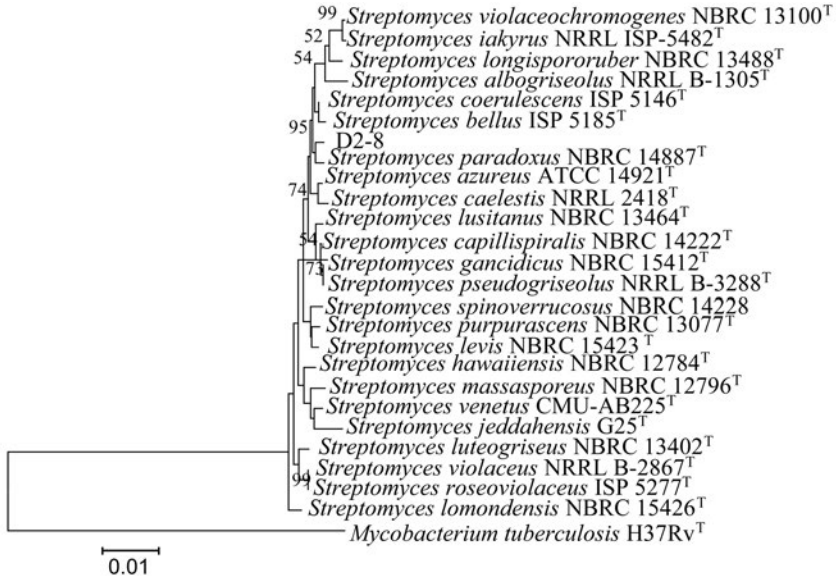

Fig. 3 Neighbor-joining tree of strain D2-8 and the related species of the genus *Streptomyces* based on the 16S rRNA gene sequences. The out-group used was *Mycobacterium tuberculosis* H37Rv^T. The stability of the topology of the phylogenetic tree was assessed by the bootstrap method with 1000 repetitions. Only bootstrap values above 50% (percentages of 1000 replications) are indicated. Scale bar represents 0.01 nucleotide substitutions per site.

8,732,707 bp long and composed of 72 contigs with N50 of 280,139 bp. The G+C content of the D2-8 genome was 71.15 mol %, and its coverage was 336×. The gene prediction resulted in 7,703 gene models. A total of 4,818 proteins were predicted (Table SIII). Annotation obtained via RAST assigned 18% sequences (1,504/8,377) to 24 subsystem categories and 82% sequences, not in subsystem. The high-ranking numbers in the subsystem categories were amino acids and derivatives, carbohydrates, protein metabolism, fatty acids, lipids, isoprenoids, respiration, nucleosides, and nucleotides (Fig. 4a). These subsystems belonged to the basic biological processes. Besides, the stress response and metabolism of aromatic compounds were relatively prominent.

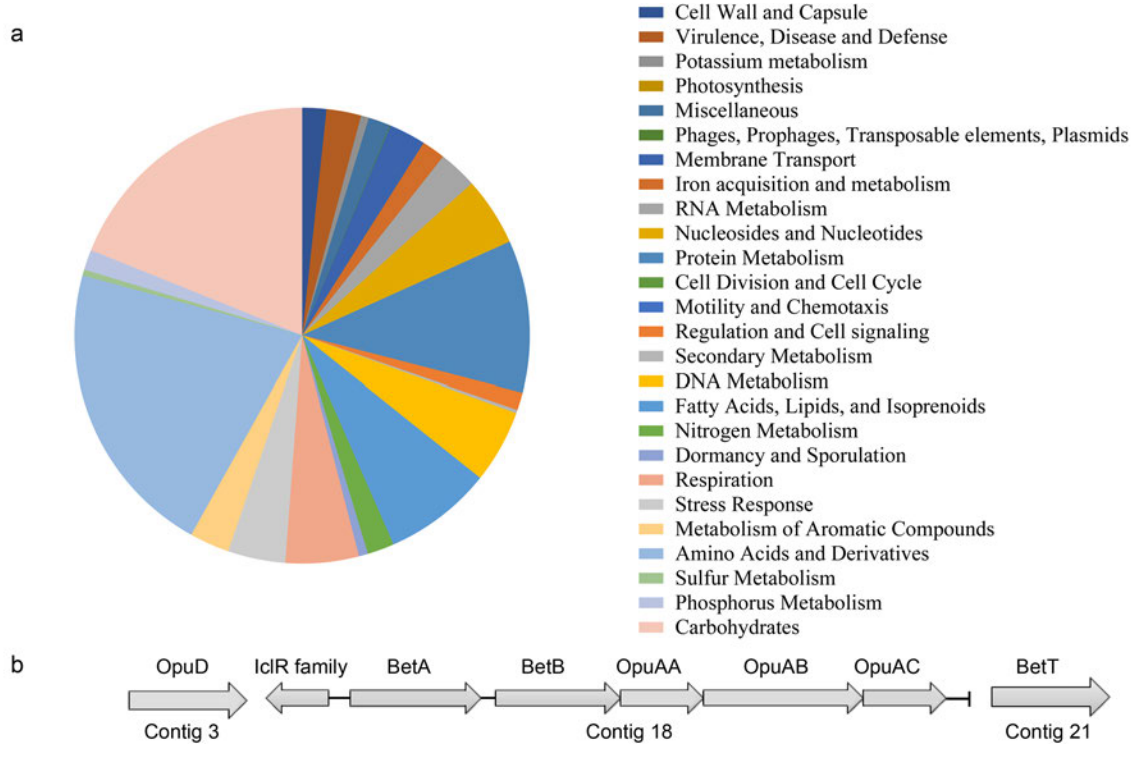

Fig. 4. a) The distribution of subsystems of the D2-8 genome annotated through the RAST webserver and b) stress response genes of D2-8 involved in the production and uptake of choline and glycine betaine.

According to the functional annotation, various genes related to plant growth-promoting traits were found in the genome. Strain D2-8 can produce IAA with a maximal yield of 29.1 μg/ml. Several genes related to IAA biosynthesis were found in the genome of D2-8, such as the genes encoding for indole-3-glycerol phosphate synthase (contig1_962), phosphoribosyl anthranilate isomerase (contig1_953), and anthranilate phosphoribosyl transferase (contig1_852). Tryptophan 2-monooxygenase (contig19_5733) and amidase (contig20_5854, contig3_1725, contig3_1776, contig13_4655, contig17_5213) in IAA biosynthesis IAM pathway were found in the genome. Aldehyde dehydrogenase (NAD^+) (contig7_3087, contig11_4153) in the IAA biosynthesis TAM pathway was also identified in the genome.

Additionally, genes of ammonia assimilation via both the GDH pathway using glutamate dehydrogenase (contig3_1507) and glutamine synthetase (GS)-glutamate synthase (GOGAT) pathway using glutamine synthetase (contig1_757, contig1_760, contig1_782, contig1_793, contig3_1528, contig3_1878) and glutamate synthase (contig1_209, contig1_975, contig1_976, contig1_1058) were identified. Furthermore, two genes encoding for 1-aminocyclopropane-1-carboxylate (ACC) deaminase (contig2_1144, contig8_3396) were found. These results were consistent with the potential ability of D2-8 to produce ACC deaminase.

Identification of genes responsible for the antifungal property in the D2-8 genome. Strain D2-8 had the potential to inhibit several plant fungi; therefore, the antiSMASH program and annotated genes sorting in the subsystem categories of RAST were performed to reveal the biologically active natural products. The antiSMASH analysis predicted that strain D2-8 contains 23 individual clusters which share homology to known gene clusters whose metabolic products are known and seven clusters that show no similarities to known clusters (Table III). These different secondary metabolite gene clusters included four siderophores, two melanins,

Table III
The secondary metabolism substances prediction results of antiSMASH.

Region	Type	From	To	Most similar known cluster	Similarity	
Region 1.1	siderophore	27,766	39,535	desferrioxamin B / desferrioxamine E	other	83%
Region 1.2	melanin, lanthipeptide	125,173	149,340	melanin	other	80%
Region 23.1	melanin	99,231	109,596	melanin	other	57%
Region 1.3	terpene, NRPS	542,592	599,827	SCO-2138	RiPP	85%
Region 8.1	terpene	65,776	90,277	isorenieratene	terpene	100%
Region 8.2	terpene	227,330	248,343	albaflavenone	terpene	100%
Region 3.1	terpene	232,223	258,904	hopene	terpene	92%
Region 9.2	terpene	221,324	243,489	geosmin	terpene	100%
Region 17.2	terpene	157,127	178,023	CC-1065	other	24%
Region 28.1	terpene	3,613	24,626	A23187 calcimycin	polyketide	10%
Region 31.1	terpene	11,837	32,925	rustmicin	polyketide: iterative type I	10%
Region 2.1	ectoine	76,359	86,757	ectoine	other	100%
Region 3.2	NRPS	364,532	415,460	coelichelin	NRP	100%
Region 36.1	NRPS	1	35,822	(2S,6R)-diamino-(5R,7)-dihydroxy-heptanoic acid	NRP	24%
Region 3.4	bacteriocin, lanthipeptide	786,397	813,467	informatipeptin	RiPP: lanthipeptide	100%
Region 5.1	PKS-like, butyrolactone	18,668	71,723	ulleungmycin	NRP	8%
Region 7.2	LAP, thiopeptide	331,828	365,008	diazepinomicin	terpene	7%
Region 3.5	T1PKS, T3PKS	874,824	939,794	alkylresorcinol	polyketide	100%
Region 9.4	T1PKS	400,230	434,396	mediomiycin A	polyketide	36%
Region 12.1	T1PKS	1	24,057	argimycin PI / argimycin PII / nigrifactin / argimycin PIV / argimycin PV / argimycin PVI / argimycin PIX	polyketide: modular type I	21%
Region 17.1	T2PKS	79,071	151,586	spore pigment	polyketide	83%
Region 39.1	T2PKS	1	25,935	collinomycin	polyketide	72%
Region 33.1	T3PKS	8,168	49,481	germicidin	other	100%

eight terpenes, one NRPS, two LAP, one ectoine, three bacteriocins, four T1PKS, two T2PKS, one T3PKS, one NRPS-like, and one PKS-like. Six clusters encoded the metabolites with antibacterial or antifungal activity, including collinomycin (72%) with antibacterial (enterococci), and no antifungal or antiviral activity, mediomiycin A (36%) with antifungal activity, calcimycin (10%) with inhibition of Gram-positive bacteria and some fungi, rustmicin (10%) with inhibition of elongation of germ tube of *Puccinia graminis*, ulleungmycin (8%) with antibacterial activity against *Staphylococcus aureus*, diazepinomicin (7%) with antibacterial, anticancer, and anti-inflammatory activity. Most such clusters displayed a low level of similarity to the known clusters. For antifungal metabolism, cluster 25 (Region 9.4) showed 36% similarity to the biosynthetic cluster of mediomiycin A in *Kitasatospora mediocidica* (Table III). It is a PKS gene cluster containing three PKS (contig 9_3944, contig 9_3945, contig 9_3946).

Cluster 15 (Region 3.2) and cluster 1 (Region 1) were predicted to produce siderophores (Table III). Cluster 15 showed 100% similarity to the biosynthetic cluster of coelichelin in *Streptomyces coelicolor* A3(2). Cluster 1 showed 83% similarity to the biosynthetic cluster of desferrioxamin B/desferrioxamine E in *S. coelicolor* A3(2). These genes further verified the ability of producing siderophores by strain D2-8.

Identification of genes responsible for salt stress adaptation of strain D2-8. For salt tolerance, several genes were found related to osmotic stress. Genes involved in production and uptake of choline and glycine betaine were found in D2-8, such as high-affinity choline uptake protein *BetT*, glycine betaine transporter *OpuD*, glycine betaine ABC transport system *OpuAA*, *OpuAB*, *OpuAC*, transcription regulator *IclR* family, choline dehydrogenase (*BetA*), and betaine aldehyde dehydrogenase (*BetB*) (Fig. 4b). These compounds could maintain membrane fluidity and enhance tolerance to salt (Guillot et al. 2000). D2-8 also contained an outer membrane protein A precursor gene. These genes were specific to D2-8, and absent from the genome of *Streptomyces avermitilis* MA-4680, *S. coelicolor* A3(2), and *Streptomyces griseus* subsp. *griseus* NBRC 13350.

Ectoine is a kind of compatible solute with protein-stabilizing properties. In addition, ectoine also stabilizes a higher-order nucleoprotein complex at the regulatory region of bacterial rRNA promoters (Pul et al. 2007). A group of microorganisms can synthesize the compatible solutes upon exposure to high salinity, including some *Streptomyces* species (Killham and Firestone 1984). In the strain D2-8 genome, there was an ectoine encoding gene cluster. Its ectoine biosynthetic gene cluster was highly like that of *Streptomyces* genus (Fig. S1). The compatible solutes ectoine and glycine betaine could influence (either as destabilizers or stabilizers) the melting temperature of the DNA helix (Rajendrakumar et al. 1997). These two substances both contributed to the salt tolerance of strain D2-8.

Plant growth-promoting activity of strain D2-8. D2-8 showed the potential to promote plant growth in the pot experiment, and the growth stage in the 10^7 CFU/ml D2-8-treatment was earlier than that of control. The height of soybean seedlings increased by 17.6% at 12 d in the 10^7 CFU-ml D2-8 treatment group compared to the control group (Fig. 5a). The treatment of strain D2-8 also affected the structure of the root. More lateral roots and longer main roots were observed. The root length increased significantly (21.3%) when the soybean seeds were soaked with 10^7 CFU/ml D2-8 spore's suspension (Fig. 5b). Fresh weight of root and aboveground were significantly improved by 65.6% and 27.4% in 10^7 CFU/ml D2-8 treatment ($p < 0.05$), respectively (Fig. 5c). These results implied that the concentration of 10^7 CFU/ml of D2-8 spores had the best effect on plant growth promotion. So, 10^7 CFU/ml of D2-8 spores were used further to investigate the plant growth under saline-alkali conditions. Compared with saline-alkali treatment (SA group), the D2-8 treatment increased the seedling's height of soybean under saline-alkali stress conditions (Fig. 5d and 5e). Additionally, the root length and fresh weight were improved by D2-8 treatment under saline-alkali stress conditions (Fig. 5f). The root length and fresh weight of aboveground increased by 44.1% and 37.5%, respectively. These results indicated D2-8 had the potential of alleviating the saline-alkali stress to promote soybean growth.

In the field experiment, seeds coating of D2-8 also showed significant plant promotion. Soybean yield increased by 5.88% (Table IV). Above all, D2-8 has not only the potential to promote soybean growth and increase its production, but also this strain can augment the soybean tolerance to saline-alkali stress.

Table IV
Effect of *Streptomyces* D2-8 on the soybean production in the field experiment.

Treatment	Density (Ten thousand/ha)	Plant height (cm)	Number of effective sections	Pod number per plant	Grain number per plant	100 grains weight (g)	Yield (kg/ha)
D2-8	33.85 ± 0.76*	92.30 ± 4.02	12.40 ± 0.37	25.45 ± 1.75	55.95 ± 1.68	19.51 ± 0.49*	2463.85 ± 56.36**
Control	31.54 ± 1.28	93.95 ± 2.42	11.90 ± 0.35	24.45 ± 0.54	57.60 ± 2.76	18.73 ± 0.29	2327.85 ± 42.46

The symbols * and ** indicate *p* values 0.05 and 0.01.

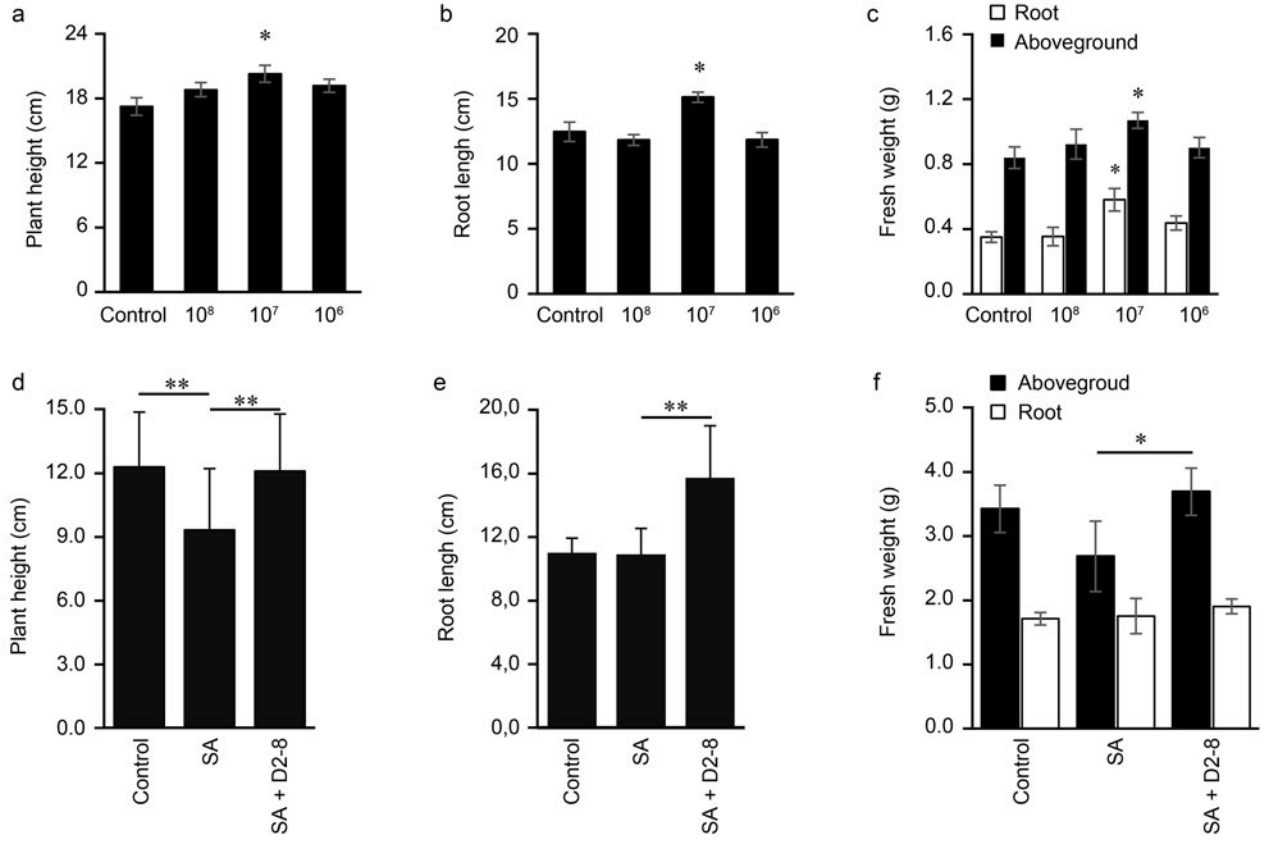

Fig. 5. The growth promotion effect of D2-8 under normal conditions (a, b, c) and saline-alkali stress (d, e, f) on soybean. For a), b), c), control group: water treatment, 10^8 D2-8: the D2-8 spore concentration of 10^8 CFU/ml; 10^7 D2-8: the D2-8 spore concentration of 10^7 CFU/ml; 10^6 D2-8: the D2-8 spore concentration of 10^6 CFU/ml. For d), e), f), control group: normal condition, SA group: saline-alkali stress treatment, SA+D2-8: D2-8 treatment under saline-alkali stress condition; Plants height, roots length, and fresh weight of roots and aboveground were analyzed using unpaired *t*-tests (n = 15 plants). The symbols * and ** indicate *p* values 0.05 and 0.01.

Discussion

A diverse range of microorganism is dispersed in the rhizosphere of plant, and rhizosphere microbial communities play a crucial role in ensuring the stability and productivity of the agricultural ecosystem, including nutrition, disease suppression, and resistance to both biotic and abiotic stresses (Newitt et al. 2019). Lots of plants growth-promoting rhizobacteria have been isolated, and some were used as microbial agents and biofertilizers in agricultural production. Many actinomyces, especially the genus *Streptomyces*, were isolated from the plant rhizosphere and were known to enhance plant growth and protect plant health (Liu et al. 2019). Three *Streptomyces* strains have been developed into commercial biocontrol agents called Actinovate, Rhizovit, and Mycostop. *P. australis* is one of the most extensively distributed plant species used for phytoremediation of different types of wastewater, soil, and sediments. As a halophyte, the rhizosphere of *P. australis* harbored some new and vital microbial groups, which are of great importance in the vegetation restoration and ecological reconstruction of salinized soil. Although the bacterial community of rhizosphere of *P. australis* was revealed and some rhizobacteria were isolated (He et al. 2019), few *Streptomyces* with alkaline tolerance from the rhizosphere of *P. australis* were isolated (Pereira et al. 2015). In this study, *Streptomyces* strain D2-8 was isolated from the rhizosphere of *Phragmites*, which grows in the saline and alkaline land. It exhibited a broad antifungal activity against the pathogen of soybean rot diseases, such as *P. sojae* and *Fusarium*. Moreover, strain D2-8 showed moderate saline and alkaline stress tolerance. It can grow in the 10% NaCl and 120 mM soda saline and alkaline solution. Some *Streptomyces* strains also showed salt tolerance, such as *Streptomyces sparsus* sp. nov. (0–15% NaCl, pH 6–10.0) (Jiang et al. 2011), and *Streptomyces clavuligerus* strain Mit-1 (up to15% NaCl, pH 11.0) (Thumar and Singh 2009). However, their tolerance to soda alkaline solution was not measured. Although D2-8 was not a halophilic bacterium, its tolerance to saline and alkaline and antifungal activity make it a promising microorganism to apply in alkaline land to protect crops against disease and improve plant production.

The beneficial microorganism can promote plant growth through nitrogen fixation, potassium solubilization, and phosphorus solubilization; meanwhile, it produces siderophores, IAA, and ACC deaminase to

enhance plant stress tolerance. In genus *Streptomyces*, two antagonistic *Streptomyces* WZS1-1 and WZS2-1 produced IAA, siderophores, solubilized phosphorus and potassium, harbored nitrogenase activity, and can promote wheat growth (Han et al. 2018). *Streptomyces* sp. NEAU-S7GS2 also produces IAA, siderophores, ACC deaminase, and inoculation of NEAU-S7GS2 showed the potential of growth promotion in soybean (Liu et al. 2019). In the current study, D2-8 was confirmed to produce IAA, siderophore, and organic acid. Its ability of growth promotion was further measured in soybean. D2-8 spores can promote the root length under normal conditions and the saline and alkaline condition in pod experiments. Moreover, seeds coated with D2-8 can increase soybean production in field experiments. The plant growth promotion of strain D2-8 under saline and alkaline condition would be valuable for agricultural production.

The genome analysis of D2-8 gave insight into its plant growth promotion mechanism. Multiple siderophores biosynthetic and uptake systems identified in this strain suggested functional duplication conferring an advantage for the bacterium as it colonizes different ecological niches. In this study, IAA biosynthesis genes were also found in D2-8, and IAA production of D2-8 consisted with the analysis results *in silico*. The plant intake of IAA released by *Streptomyces* was one of the reasons for soybean growth promotion. Streptomyces' saprotrophic and spore-forming lifestyle is beneficial to survive well under unfavorable conditions. The detailed mechanism of plant growth promotion of *Streptomyces* D2-8 under saline and alkaline stress needs further research.

Streptomyces spp. have a high performance in producing various bioactive secondary metabolism and enzymes (Zhang et al. 2017). The genomic analysis of D2-8 identified many PKS and NRPS gene clusters. Six clusters encoded the metabolites with antibacterial or antifungal activity, but the similarity of gene cluster was low, which indicate that the strain may produce some new metabolisms. Although three PKS enzymes were found, whether D2-8 produced the mediomycin or its similar antibiotics still need more experiments. Moreover, RAST analysis results revealed that production and uptake of choline and glycine betaine genes in the strain genome is uniquely present in D2-8 but absent from the related Streptomyces complete genome of *S. avermitilis* MA-4680, *S. coelicolor* A3(2), and *S. griseus* subsp. *griseus* NBRC 13350. We proposed that ectoine, choline, and glycine betaine are particularly important for adaptation to saline and alkaline stress. Altogether, the presented data demonstrate that strain D2-8 is a moderate saline and alkaline stress tolerance streptomyces with the potential of plant growth promotion and antifungal activity and streptomyces to find novel bioactive compounds.

Conclusion

Saline and alkaline tolerant actinomyces, designated as *S. paradoxus* D2-8, was isolated from rhizosphere soil of *Phragmites*, which grown in the saline and alkaline land. Except for the antifungal activity, the strain has significant saline-alkali tolerance and plant growth promotion. Moreover, genome analysis showed that IAA and siderophore biosynthesis pathway, genes encoding ACC deaminase, and secondary metabolite gene clusters were identified in the D2-8 genome. Soybean growth promotion experiments further confirmed that the strain improved plant tolerance to saline and alkaline stress and promoted host health. The yield increase of soybean after D2-8 seed's coating treatment in the field suggested that strain D2-8 could be a potential candidate for the development of bioagent with abiotic stress tolerance used in sustainable agriculture in the future.

ORCID
Yamei Gao https://orcid.org/0000-0002-1408-9646

Availability of data and materials

All data generated or analyzed in this study are presented within this manuscript. All materials used in this study, including raw data, shall be available upon reasonable request. The 16S rRNA nucleotide sequences for strain D2-8 and its genome sequence were deposited in GenBank (NCBI) under the accession numbers MT027002 and PRJNA605321.

Acknowledgments

This research was financially supported by the Natural Science Foundation of Heilongjiang Province (LH2021C065), the Post-doctor project, and Training Project of Heilongjiang Bayi Agricultural University, grant number (ZRCPY202031).

Conflict of interest

The authors do not report any financial or personal connections with other persons or organizations, which might negatively affect the contents of this publication and/or claim authorship rights to this publication.

Literature

Abulfaraj AA, Jalal RS. Use of plant growth-promoting bacteria to enhance salinity stress in soybean (*Glycine max* L.) plants. Saudi J Biol Sci. 2021 Jul;28(7):3823–3834. https://doi.org/10.1016/j.sjbs.2021.03.053

Berg G, Marten P, Minkwitz A, Brückner S. Efficient biological control of plant fungal diseases by *Streptomyces* sp. DSMZ 12424. J Plant Dis Protect. 2001 Jan;108(1):1–10.

Bhatti AA, Haq S, Bhat RA. Actinomycetes benefaction role in soil and plant health. Microb Pathog. 2017 Oct;111:458–467. https://doi.org/10.1016/j.micpath.2017.09.036

Chatterton S, Punja ZK. Factors influencing colonization of cucumber roots by *Clonostachys rosea* f. catenulata, a biological disease control agent. Biocontrol Sci Technol. 2010;20(1):37–55. https://doi.org/10.1080/09583150903350253

Costa-Gutierrez SB, Lami MJ, Santo MCC, Zenoff AM, Vincent PA, Molina-Henares MA, Espinosa-Urgel M, de Cristóbal RE. Plant growth promotion by *Pseudomonas putida* KT2440 under saline stress: role of *eptA*. Appl Microbiol Biotechnol. 2020 May;104(10): 4577–4592. https://doi.org/10.1007/s00253-020-10516-z

Gang S, Sharma S, Saraf M, Buck M, Schumacher J. Analysis of indole-3-acetic acid (IAA) production in *Klebsiella* by LC-MS/MS and the Salkowski method. Bio Protoc. 2019 May 5;9(9):e3230. https://doi.org/10.21769/BioProtoc.3230

Guillot A, Obis D, Mistou MY. Fatty acid membrane composition and activation of glycine-betaine transport in *Lactococcus lactis* subjected to osmotic stress. Int J Food Microbiol. 2000 Apr 10;55(1–3): 47–51. https://doi.org/10.1016/s0168-1605(00)00193-8

Han D, Wang L, Luo Y. Isolation, identification, and the growth promoting effects of two antagonistic actinomycete strains from the rhizosphere of *Mikania micrantha* Kunth. Microbiol Res. 2018 Mar; 208:1–11. https://doi.org/10.1016/j.micres.2018.01.003

Han L, Zhang H, Xu Y, Li Y, Zhou J. Biological characteristics and salt-tolerant plant growth-promoting effects of an ACC deaminase-producing Burkholderia pyrrocinia strain isolated from the tea rhizosphere. Arch Microbiol. 2021 Jul; 203(5): 2279-2290. http://doi.org/10.1007/s00203-021-02204-x.

He C, Zheng L, Ding J, Gao W, Chi W, Ding Y. Complete genome sequence of an *N*-acyl homoserine lactone producer, *Breoghania* sp. strain L-A4, isolated from rhizosphere of *Phragmites australis* in a coastal wetland. Microbiol Resour Announc. 2019 Jan 31;8(5): e01539-18. https://doi.org/10.1128/MRA.01539-18

Huang LH, Liang ZW, Suarez DL, Wang ZC, Wang MM, Yang HY, Liu M. Impact of cultivation year, nitrogen fertilization rate and irrigation water quality on soil salinity and soil nitrogen in saline-sodic paddy fields in Northeast China. J Agric Sci. 2016;154(04):632–646. https://doi.org/10.1017/S002185961500057X

Jiang Y, Cao YR, Wiese J, Tang SK, Xu LH, Imhoff JF, Jiang CL. *Streptomyces sparsus* sp. nov., isolated from a saline and alkaline soil. Int J Syst Evol Microbiol. 2011 Jul;61(7):1601–1605. https://doi.org/10.1099/ijs.0.020669-0

Khan MA, Asaf S, Khan AL, Jan R, Kang SM, Kim KM, Lee IJ. *Rhizobacteria* AK1 remediates the toxic effects of salinity stress via regulation of endogenous phytohormones and gene expression in soybean. Biochem J. 2019 Aug 30;476(16):2393–2409. https://doi.org/10.1042/BCJ20190435

Killham K, Firestone MK. Salt stress control of intracellular solutes in streptomycetes indigenous to saline soils. Appl Environ Microbiol. 1984 Feb;47(2):301–306. https://doi.org/10.1128/aem.47.2.301-306.1984

Lahdenperä ML, Simon E, Uoti J. Mycostop – A novel biofungicide based on *Streptomyces* bacteria. In: Beemster ABR, Bollen GJ, Gerlagh M, Ruissen MA, Schippers B, Tempel A, editors. Developments in agricultural and managed forest ecology. Amsterdam (The Netherlands): Elsevier; 1991(23), p. 258–263. https://doi.org/10.1016/B978-0-444-88728-3.50048-2

Liu D, Yan R, Fu Y, Wang X, Zhang J, Xiang W. Antifungal, plant growth-promoting, and genomic properties of an endophytic actinobacterium *Streptomyces* sp. NEAU-S7GS2. Front Microbiol. 2019 Sep 10;10:2077. https://doi.org/10.3389/fmicb.2019.02077

Minuto A, Spadaro D, Garibaldi A, Gullino ML. Control of soilborne pathogens of tomato using a commercial formulation of *Streptomyces griseoviridis* and solarization. Crop Prot. 2006;25(5):468–475. https://doi.org/10.1016/j.cropro.2005.08.001

Newitt JT, Prudence SMM, Hutchings MI, Worsley SF. Biocontrol of cereal crop diseases using *Streptomycetes*. Pathogens. 2019 Jun 13; 8(2):78. https://doi.org/10.3390/pathogens8020078

Panda AK, Bisht SS, DeMondal S, Senthil Kumar N, Gurusubramanian G, Panigrahi AK. *Brevibacillus* as a biological tool: a short review. Antonie Van Leeuwenhoek. 2014 Apr;105(4):623–639. https://doi.org/10.1007/s10482-013-0099-7

Pereira SI, Pires C, Henriques I, Correia A, Magan N, Castro PM. Assessment of rhizospheric culturable bacteria of *Phragmites australis* and *Juncus effusus* from polluted sites. J Basic Microbiol. 2015 Oct; 55(10):1179–1190. https://doi.org/10.1002/jobm.201500010

Phang TH, Shao G, Lam HM. Salt tolerance in soybean. J Integr Plant Biol. 2008 Oct;50(10):1196–1212. https://doi.org/10.1111/j.1744-7909.2008.00760.x

Pul U, Wurm R, Wagner R. The role of LRP and H-NS in transcription regulation: involvement of synergism, allostery and macromolecular crowding. J Mol Biol. 2007 Feb 23;366(3):900–915. https://doi.org/10.1016/j.jmb.2006.11.067

Rajendrakumar CS, Suryanarayana T, Reddy AR. DNA helix destabilization by proline and betaine: possible role in the salinity tolerance process. FEBS Lett. 1997 Jun 30;410(2–3):201–205. https://doi.org/10.1016/s0014-5793(97)00588-7

Rehan M, Alsohim AS, Abidou H, Rasheed Z, Al Abdulmonem W. Isolation, identification, biocontrol activity, and plant growth promoting capability of a superior *Streptomyces tricolor* strain HM10. Pol J Microbiol. 2021 Jun;70(2):245–256. https://doi.org/10.33073/pjm-2021-023

Sadeghi A, Soltani BM, Jouzani GS, Karimi E, Nekouei MK, Sadeghizadeh M. Taxonomic study of a salt tolerant *Streptomyces* sp. strain C-2012 and the effect of salt and ectoine on *lon* expression level. Microbiol Res. 2014 Feb-Mar;169(2–3):232–238. https://doi.org/10.1016/j.micres.2013.06.010

Thumar JT, Singh SP. Organic solvent tolerance of an alkaline protease from salt-tolerant alkaliphilic *Streptomyces clavuligerus* strain Mit-1. J Ind Microbiol Biotechnol. 2009 Feb;36(2):211–218. https://doi.org/10.1007/s10295-008-0487-6

Vasavada SH, Thumar, JT, Singh SP. Secretion of a potent antibiotic by salt-tolerant and alkaliphilic actinomycete *Streptomyces sannanensis* strain RIT-1. Curr Sci. 2006 Nov;91(10):1393–1397.

Weber T, Blin K, Duddela S, Krug D, Kim HU, Bruccoleri R, Lee SY, Fischbach MA, Müller R, Wohlleben W, et al. antiSMASH 3.0-a comprehensive resource for the genome mining of biosynthetic gene clusters. Nucleic Acids Res. 2015 Jul 1;43(W1):W237–W243. https://doi.org/10.1093/nar/gkv437

Zeng W, Wang D, Kirk W, Hao J. Use of *Coniothyrium minitans* and other microorganisms for reducing *Sclerotinia sclerotiorum*. Biol. Control. 2012 Feb;60(2):225–232. https://doi.org/10.1016/j.biocontrol.2011.10.009

Zhang L, Hashimoto T, Qin B, Hashimoto J, Kozone I, Kawahara T, Okada M, Awakawa T, Ito T, Asakawa Y, et al. Characterization of giant modular PKSs provides insight into genetic mechanism for structural diversification of aminopolyol polyketides. Angew Chem Int Ed Engl. 2017 Feb 6;56(7):1740–1745. https://doi.org/10.1002/anie.201611371

Zörb C, Geilfus C M, Dietz K J. Salinity and crop yield. Plant Biol J. 2019 Jan;21(Suppl 1):31–38. https://doi.org/10.1111/plb.12884

Supplementary materials are available on the journal's website.

ORIGINAL PAPER

Polish Journal of Microbiology
2022, Vol. 71, No 1, 55–62
https://doi.org/10.33073/pjm-2022-008

Cell Surface Glycosaminoglycans as Receptors for Adhesion of *Candida* spp. to Corneal Cells

HELENA ORDIALES[1, 2, 3], IGNACIO ALCALDE[1, 3], FERNANDO VÁZQUEZ[1, 2, 4], JESÚS MERAYO-LLOVES[1, 3], LUIS M. QUIRÓS[1, 2, 3*] and CARLA MARTÍN CUETO[1, 3, 5*]

[1] Instituto Universitario Fernández-Vega, Universidad de Oviedo, Oviedo, Spain
[2] Departamento de Biología functional, Universidad de Oviedo, Oviedo, Spain
[3] Fundación para la Investigación y la Innovación Biosanitaria de Asturias (FINBA), Oviedo, Spain
[4] Servicio de Microbiología, Hospital Universitario Central de Asturias, Oviedo, Spain
[5] Brill Pharma, Barcelona, Spain

Submitted 13 December 2021, accepted 10 February 2022, published online 14 March 2022

Abstract

The most common causal agents of fungal keratitis are yeasts of the *Candida* genus. Adhesion constitutes the first stage of pathogenesis. Previous studies have shown that glycosaminoglycans from the corneal cell surface play an essential role in bacterial keratitis, although little is known about their role in fungal infections. The objective of this work is to analyze the role that glycosaminoglycans (GAGs) play in the adhesion of fungi of the *Candida* genus to corneal epithelial cells. The participation of GAGs in the adhesion of fungi was studied through the specific inhibition of the synthesis of these molecules by enzymatic digestion using specific lyases and the silencing of various genes involved in heparan sulfate sulfation. The results seem to indicate that glycosaminoglycans act to some extent as receptors for this fungus, although there are differences between fungal species. Treatment with inhibitors partially reduced the adherence of fungal species. Digestion of cell surface heparan sulfate further reduced the adherence of *Candida albicans* and *Candida glabrata* compared to chondroitin sulfate, indicating that the binding is preferentially mediated by heparan sulfate. Degradation of both heparan sulfate and chondroitin sulfate produced similar effects on the adherence of *Candida parapsilosis*. However, adhesion of *C. albicans* hyphae is not dependent on GAGs, suggesting the expression of other adhesins and the recognition of other receptors present in corneal cells. Our results open the door to new strategies for stopping the adhesion of pathogenic fungi, and their subsequent invasion of the cornea; thus, reducing the probability of the keratitis development.

K e y w o r d s: fungal keratitis, cornea, glycosaminoglycan, heparan sulfate, chondroitin sulfate

Introduction

One of the most frequent ocular pathologies worldwide is corneal inflammation, or keratitis, which may be associated with infectious processes (Mellado et al. 2013). While noninfectious keratitis is generated by minor trauma, minor injury, or the use of contact lenses, infectious keratitis is the most prevalent cause of corneal blindness worldwide, and it is a consequence of infections by bacteria, viruses, fungi, or amoeba (Darren et al. 2021). Fungal keratitis, sometimes called keratomycosis, is caused by a broad spectrum of microorganisms, which differ depending on the geographical area involved. For this reason, yeasts are recognized as the most frequent causal agents in temperate climates, especially those of the *Candida* genus, with *Candida albicans* being the most common. However, in tropical climates, the main infectious agent of fungal keratitis are filamentous fungi (Mellado et al. 2013; Thomas and Kaliamurthy 2013).

The identification of the epithelial receptors which enable adherence and colonization is critical concerning fungal keratitis, as it is in any other infectious process. These receptors, which are carbohydrates, proteins, or mixed molecules, are also essential for the microbial invasion that follows and the initiation of the immune response in the host (Wilson et al. 2002). Previous studies have shown that glycosaminoglycans (GAGs)

* Corresponding authors: C. Martín Cueto, Instituto Universitario Fernández-Vega, Universidad de Oviedo, Oviedo, Spain; **e-mail: cmartincueto@gmail.com**;
L.M. Quirós, Instituto Universitario Fernández-Vega, Universidad de Oviedo, Oviedo, Spain; **e-mail: quirosluis@uniovi.es**

from corneal cell surfaces are involved in the initial adherence of pathogenic bacteria, but that the process differs depending on their Gram-type (García et al. 2016b). GAGs are polysaccharide chains that usually form part of a proteoglycan; their composition differs depending on the disaccharide of which they are composed, either N-acetylglucosamine (GlcNAc) or N-acetylgalactosamine (GalNAc), attached to glucuronic acid (GlcA) or galactose (Iozzo and Schafer 2015). Based on the structure of their disaccharides, GAGs are divided into four types: hyaluronic acid, keratan sulfate, heparan sulfate (HS), and chondroitin sulfate (CS), the last two being the most important in terms of the cell surface and the pericellular matrix. Both contain a GlcA residue, GlcNAc in the case of HS, and a GalNAc residue in that of CS. During their polymerization, the HS and CS chains undergo modifications, which provide molecules with a complex structure dependent on the tissue and the physiological or pathological state of the cells involved (Kjellén and Lindahl 1991; Iozzo and Schafer 2015). HS chain residues can suffer N-deacetylation/N-sulfation of the GlcNAc, epimerization and/or O-sulfation of C2 in GlcA, and sulfations of C3 and C6 in GlcNAc, while modifications to the CS chains are simpler: GlcA can be epimerized and sulfated at C2, while GalNAc can be sulfated at C4 and C6. As a result, HS chains have high and low sulfated domains, while CS chains do not have this domain structure, although the modifications they experience result in different types of CS chains (Rabenstein 2002; Esko et al. 2009). The fine structure of the chains allows them to participate in a great variety of biological processes, such as binding to different ligands, e.g., cytokines or growth factors (Iozzo and Schafer 2015; Gulati and Poluri 2016) or acting as receptors or coreceptors during infection (Kamhi et al. 2013; Martín et al. 2013; García et al. 2016a; Rajas et al. 2017). In many infectious processes, pathogens specifically bind to certain regions of the GAG chains present on the cell surface, which are usually highly sulfated. This phenomenon has been described in various infectious pathologies, including lung and skin conditions (Martín et al. 2019; Ordiales et al. 2021) and ocular pathologies caused by bacteria such as keratitis (García et al. 2016b). Apart from this, little is known about the role of GAGs as receptors in fungal infections.

The objective of this work is to analyze the role that GAGs play in the adhesion of pathogenic fungi of the *Candida* genus to corneal epithelial cells, and determine the role that the principal GAGs species play in these interactions. This article will thus contribute to understanding the complexity of the adhesion process and support the proposal of new strategies to prevent fungal keratitis in the adhesion or invasion stage.

Experimental

Materials and Methods

Materials. The materials were purchased from the following manufacturers: Saboureaud culture medium from Difco (BD, MD, USA); the antibiotic chloramphenicol, fluorescein isothiocyanate (FITC), rhodamine B, genistein, heparinase I and III, chondroitinase ABC, HS, chondroitin sulfate A (CS A), chondroitin sulfate B (CS B), and chondroitin sulfate C (CS C), all from Sigma-Aldrich (St. Louis, MO, USA); the yeast extract culture medium was from Conda (Spain); Dulbecco's Modified Eagle's Minimal essential medium (DMEM), fetal bovine serum (FBS), insulin, epidermal growth factor (EGF), penicillin G/streptomycin, and phosphate-buffered saline (PBS) were all from Gibco (Life Technologies, CA, USA).

Fungal strains, cell lines, and culture conditions. The fungal species used in this study were *C. albicans*, *Candida glabrata* and *Candida parapsilosis*, all clinical isolates obtained from the Central University Hospital of Asturias and identified at the species level by MALDI-TOF MS spectrometry (Bruker Daltonics, Bremen, Germany). All were grown in Saboureaud medium with chloramphenicol at a concentration of 50 μg/l at 28°C for 24 h, except *C. albicans* in its filamented form, which was grown in medium containing 0.1% glucose, 1% glycine and 0.1% yeast extract at pH 7.5 at 37°C in a 5% (v/v) CO_2 atmosphere for 48 h.

HCE-2 [50.B1] ATCC CRL-11135 corneal cell line was grown in DMEM supplemented with 10% FBS, 1.5 units/ml of insulin, 10 ng/ml of EGF and penicillin G/streptomycin (5,000 IU/ml, 5,000 μg/ml). Cultures were incubated at 37°C in a 5% (v/v) CO_2 atmosphere.

Fluorescence labeling. Overnight fungal cultures were washed four times with PBS buffer, resuspended in a 0.1 mg/ml FITC solution to an A_{600} of 0.5, and incubated in the dark at 37°C under agitation for 1 h. After that, the excess of FITC was removed by four washes with PBS. Finally, the pellet was resuspended in DMEM.

Inhibition of glycosaminoglycans biosynthesis. Cell cultures were grown in 24-well plates to 70% confluence and incubated overnight at 37°C in DMEM containing either rhodamine B at 50 μg/ml or genistein at 30 μM. Wells were then washed twice with PBS, and the cell integrity was verified under an optical microscope before being used in the adhesion assays.

Enzymatic digestion of cell surface glycosaminoglycans. The hydrolysis of the GAGs on the surface of the corneal cells was carried out by incubating for 3 h at 37°C in a 5% CO_2 atmosphere with a 500 mU/ml (final concentration) mix of heparinase I and III for

HS and 250 mU/ml (final concentration) of chondroitinase ABC for CS. Digestion of both GAG species was achieved through successive incubations of the cell cultures with the two enzymatic mixes, washing between each with PBS. The reactions were stopped through two washes with PBS. Cell integrity was verified by light microscopy before carrying out the adhesion assays.

Adhesion assays. Adhesion of the different fungi to HCE-2 monolayers was performed in 24-well plates to 70–90% confluence. The medium was removed, and the cells were washed twice with PBS and then blocked with 10% FBS in DMEM for 1 h at 37°C in a 5% CO_2 atmosphere. After that, the cells were washed with PBS, and 200 µl of FITC-labeled yeast in 300 µl of DMEM were added. The mixture was incubated for 90 min at 37°C in a 5% CO_2 atmosphere. To remove the unbound fungi, wells were rinsed four times with 500 µl of PBS. At the end of the experiment, HCE-2 cells were disaggregated with 1% SDS, and the fluorescence of the yeast attached to them was quantified in a Perkin Elmer LS55 fluorometer (Perkin Elmer, MA, USA), at 488 nm for excitation and 560 nm for emission. Values obtained for the different experiments were normalized using the adhesion value without any treatment as a reference, which was given a value of 100%.

For adherence inhibition assays, FITC-labeled yeast was co-incubated with HS, CS A, CS B, CS C, or a mixture of the four, at concentrations ranging from 0.05 to 2.5 µg/ml for 30 min. After this, adhesion assays were performed as indicated above.

Statistical analysis. All experiments were performed at least three times and with a minimum of three replications in each case. The data were analyzed with the Statistica program for Windows (Statsoft Inc., OK, USA). The mean values of two samples were compared using the Mann-Whitney U test, with $p < 0.05$ being considered as significant.

Results

GAGs are involved in the adherence of different *Candida* species to corneal epithelial cells. To analyze whether GAGs play a role during the binding of *Candida* spp. to corneal epithelial cells, the synthesis of cell surface GAGs was inhibited using either rhodamine B or genistein. The results showed a decrease in fungal binding after treatment with either inhibitor, suggesting that GAGs are involved in adherence to the corneal epithelium. The effects varied depending on the fungus and the inhibitor. Adherence of *C. albicans* was strongly reduced after treatment with both rhodamine B and genistein, decreasing by 80% and 50%, respectively (Fig. 1a). However, in the *C. glabrata* and *C. parapsilosis* experiments, rhodamine B generated

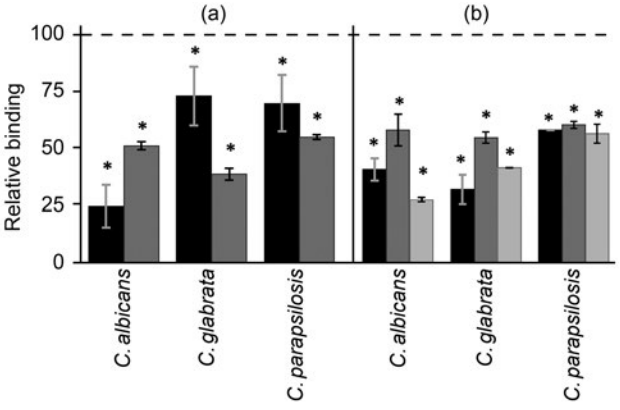

Fig. 1. Effect of reduction of cell GAGs on fungal adhesion to corneal epithelial cells.
a) Inhibition of fungal adhesion to HCE-2 cells treated with rhodamine B (black bars) and genistein (gray bars). b) Inhibition of fungal adhesion to HCE-2 cells treated with heparinases I and III (black bars), chondroitinase ABC (dark gray bars), or a mix of heparinases I and III + chondroitinase ABC (gray bars). Data were normalized using the adhesion values of fungi to non-treated cells, which were given the arbitrary value of 100. Error bars represent standard deviations. Statistically significant differences are denoted by *, which indicates $p < 0.05$.

a statistically significant decrease of 30% in the binding of both fungi, while genistein produced a reduction of 70% in *C. glabrata* and 50% in *C. parapsilosis* (Fig. 1a).

To investigate the role of GAGs on fungal adherence more deeply, the corneal cell surface GAGs were degraded using the bacterial lyases heparinase I and III and chondroitinase ABC, which degrade HS and CS, respectively. After treatment with these lyases, the adherence of all the species of *Candida* analyzed was reduced to a statistically significant degree, reinforcing the notion that both HS and CS are involved in their binding to the corneal epithelial cell surface.

Treatment with heparinase I and III similarly reduced the adherence of *C. albicans* and *C. glabrata,* by around 60%, but chondroitinase ABC produced a decrease of 45% (Fig. 1b). It appears to indicate that HS preferably mediates the binding. The degradation of both GAG species by the combined use of the lyases reduced the adherence of *C. albicans* by 70%, suggesting the existence of a cooperative effect. However, this effect was not observed in *C. glabrata* (Fig. 1b). On the other hand, degradation of HS and CS or mixture of the two molecular species produced a similar effect on the adherence of *C. parapsilosis,* reducing the binding of the fungus to corneal cells by approximately 40% (Fig. 1b).

Role of GAGs on the adherence of *C. albicans* in its two morphological forms: yeast and hyphae. To investigate whether GAGs are also involved in the binding of filamented *C. albicans*, the same tests as in the section above were carried out, and the results compared with those of their yeast morphology (Fig. 2). Unlike the inhibitory effect that rhodamine B and genistein

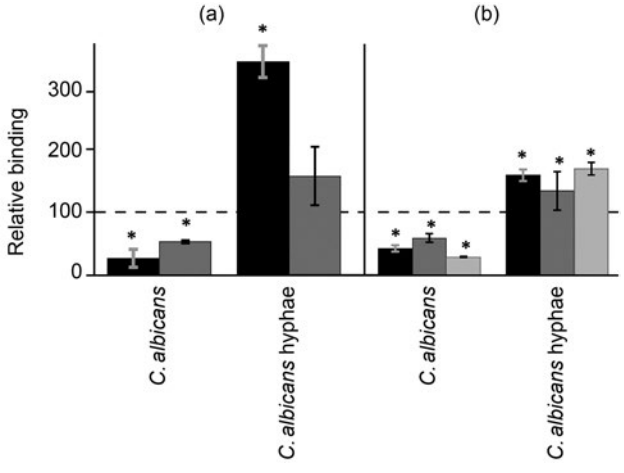

Fig. 2. Effect of reducing cell GAGs on the adhesion of *C. albicans* yeast cells and hyphal cells to corneal epithelial cells.
a) Inhibition of fungal adhesion to HCE-2 cells treated with rhodamine B (black bars) and genistein (gray bars). b) Inhibition of fungal adhesion to HCE-2 cells treated with heparinases I and III (black bars), chondroitinase ABC (dark gray bars), or a mix of heparinases I and III + chondroitinase ABC (gray bars). Data were normalized using the adhesion values of fungi adhesion to non-treated cells, given the arbitrary value of 100. Error bars represent standard deviations. Statistically significant differences are denoted by *, which indicates $p < 0.05$.

exhibited on the binding of *C. albicans* to corneal epithelial cells, the filamented form of the yeast showed the opposite behavior, its adherence increasing by about 240% after treatment with rhodamine B, and 50% after treatment with genistein (Fig. 2a).

For its part, the enzymatic degradation of GAGs by bacterial lyases also increased the level of adhesion of the filamented form, to an extent similar to that obtained by inhibition of biosynthesis and in opposition to that observed for the yeast form. The degradation of HS and CS gave rise to a statistically significant increase in the binding of the filamented form of 60% and 20%, respectively (Fig. 2b). Furthermore, the effect of mixing both lyases was similar to the response obtained after treatment with heparinases I and III, with adherence increasing by 70% (Fig. 2b).

Differential involvement of specific GAGs on the adherence of *Candida* species to corneal epithelial cells. To analyze the role of different species of GAGs on the adherence of *C. albicans*, *C. glabrata* and *C. parapsilosis* to the corneal epithelium, commercial GAGs were used (HS, CS A, CS B, CS C, and a mixture of all of them) as competing molecules. A decrease in yeast binding to corneal cells was observed in the presence of each of the GAGs, the effect being dependent on the yeast involved.

In the case of *C. albicans*, the CS molecules were most effective at lower concentrations than HS, and CS A was the most efficient, followed by CS B and CS C (Fig. 3a). In contrast, at higher concentrations, HS was the most effective interfering molecule, followed by CS B (Fig. 3a), although none of the interfering molecules was able to reduce the adherence of *C. albicans* by more than 20%. However, the mixture of GAGs showed a higher competitive capacity, which was dependent on the concentration, inhibiting binding by about 40% at a concentration of 2.5 μg/ml (Fig. 3a).

Experiments with *C. glabrata* showed that CS B and CS A were the least efficient molecules, reducing yeast binding by approximately 15% at the highest concentrations, while HS and CS C achieved inhibitions of 30% (Fig. 3b). In this case, the combined use of a mixture of GAGs did not increase the inhibitory effect concerning that caused by each species individually (Fig. 3b).

GAGs also interfered in the adhesion of *C. parapsilosis* to corneal cells. HS and CS B were less efficient as interfering molecules, with only a 15% reduction in yeast binding at the highest concentration tested (Fig. 3c). CS C was the strongest inhibitor, reaching values close to 30% (Fig. 3c), while CS A had a slightly lesser effect, although at high concentrations, it interfered with the binding of *C. parapsilosis* to the same extent as CS C (Fig. 3c). When the mix of GAGs was used, the observed effect was stronger, reaching an inhibition of nearly 60% (Fig. 3c).

The implication of specific N- and O-sulfations on the adherence of different *Candida* spp. to corneal

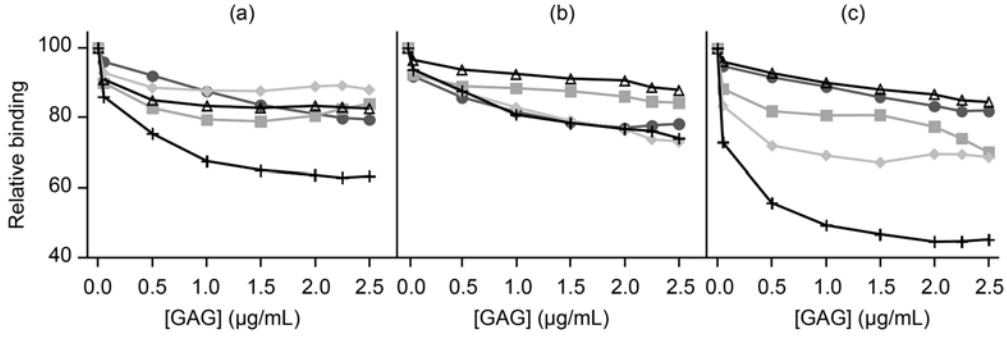

Fig. 3. Inhibition of fungal adhesion to corneal epithelial cells by the presence of different GAGs. a) adhesion of *C. albicans*, b) *C. glabrata*, c) *C. parapsilosis* in the presence of different concentrations of HS (●), CSA (■), CSB (▲), CSC (◆) and a mixture of all GAGs (+). Data were normalized using the adhesion values of fungi to non-treated cells, which was given the arbitrary value of 100.

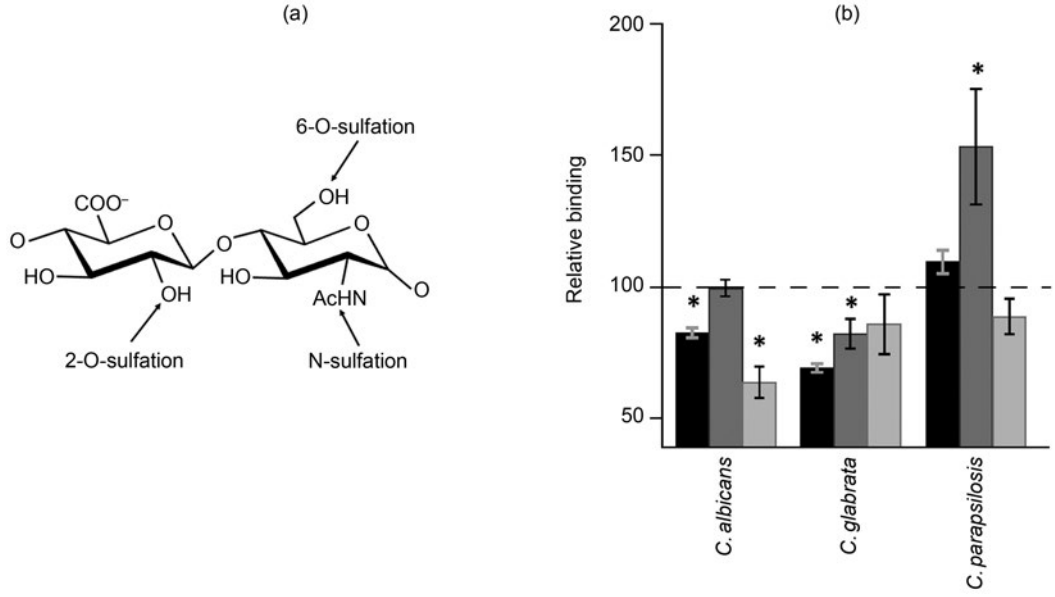

Fig. 4. Influence of specific N- and O-sulfations on pathogen adherence to corneal epithelial cells.
a) Structure of an HS disaccharide unit showing the specific positions of sulfations. b) Inhibition of fungal adhesion to corneal epithelial cells with silencing of the genes involved in N-sulfation (dark bars), 2-O-sulfation (dark gray bars), and 6-O-sulfation (gray bars). Data were normalized using the adhesion values of fungi to non-treated cells, which was given the arbitrary value of 100. Error bars represent standard deviations. Statistically significant differences are denoted by *, which indicates $p < 0.05$.

epithelial cells. To analyze how sulfations of the HS chains might influence the adherence process, we carried out experiments using HCE-2 cell lines where the specific sulfotransferases involved in these sulfations were silenced using interference RNA (García et al. 2016b). Only the adhesion of *C. albicans* and *C. glabrata* to corneal cells was reduced in these experiments (Fig. 4). A decrease in N-sulfation produced a statistically significant reduction in the binding of *C. albicans* and *C. glabrata*, of around 20% and 30%, respectively (Fig. 4). A reduction in 2-O-sulfation led to a statistically significant decrease of 20% in the adhesion of *C. glabrata*, while a statistically significant increase in the binding of *C. parapsilosis* was found (Fig. 4). On the other hand, a reduction in 6-O-sulfation only produced a statistically significant reduction, of around 40%, in the binding of *C. albicans* (Fig. 4).

Discussion

Fungal keratitis is one of the most frequent pathologies seen in ophthalmology. The corneal epithelium is the first barrier to the entrance of microorganisms as it is the first binding point in infectious processes. *Candida* spp. is the most common agent that produces eye infections, ocular trauma being the most frequent predisposing factor (Lakhundi et al. 2017). GAGs are involved in the initiation of bacterial pathogenesis, acting as receptors in, among others, lung, corneal, and epithelial tissue (García et al. 2016a; Martin et al. 2019; Rajas et al. 2017). In addition, the disaccharide composition of GAG chains and their degree of sulfation depend on the type and physiological state of the cell (García et al. 2016a). This is of great importance in analyzing GAGs as receptors in fungal keratitis.

The role of GAGs in the adhesion of *C. albicans*, *C. glabrata*, and *C. parapsilosis* to corneal epithelial cells was analyzed through the inhibition of their synthesis using either rhodamine B or genistein. The effects differed depending on the fungus involved. Both inhibitors significantly reduced the binding of the yeasts, although rhodamine B produced greater effects in *C. albicans*, as it has also been observed in other cell types such as keratinocytes of the epidermis (Ordiales et al. 2021). Genistein was more effective than rhodamine B in inhibiting the binding of *C. glabrata* and *C. parapsilosis*. The differences observed between the inhibitors may be the result of intrinsic characteristics of each yeast species, such as the expression of different adhesins, but could equally be due to the different mechanisms of action of the two inhibitors (Kaji et al. 1991; Nikitovic et al. 2003; Piotrowska et al. 2006; Roberts et al. 2006; Silva et al. 2012; Ordiales et al. 2021). Interestingly, the results were very different in the experiments using *C. albicans* hyphae, with an increase in its adherence after treatment with the inhibitors. This effect has also been observed in fibroblasts of the dermis, where *C. albicans* hyphae binding increased after treatment with both rhodamine B and genistein (Ordiales et al. 2021).

The enzymatic elimination of GAGs from the cell surface through bacterial lyases caused a significant

decrease in fungal adherence in all cases except, once again, with the filamented form of *C. albicans*. Moreover, the adherence of *C. albicans* and *C. glabrata* was more reduced when heparinases were used, indicating that HS may well be the main GAG species involved in the early stages of infection. On the contrary, the effect of the enzymatic degradation of the different GAGs reduced the adhesion of *C. parapsilosis* to a very similar degree, regardless of the lyase involved. It should be noted that the common treatment of heparinases and chondroitinases only had a combined effect in the case of *C. albicans*. What is more, the complexity of the GAGs, the possibility of them forming ternary complexes with other receptors, and the possibility that digestion was incomplete or that compensatory mechanisms were activated could explain these differences. Also, when *C. albicans* is in filament form, its interaction with corneal cells is no longer dependent on GAGs since adherence increases when GAGs are eliminated from the cell surface. This fact may point to the existence of other receptors with a high affinity for *C. albicans* hyphal adhesins, which would be more exposed to binding after the elimination of the GAGs.

Moreover, changes in morphology could also involve the expression of other adhesins necessary for colonization and perhaps display a high affinity for different receptors. The data as a whole seems to suggest that, at least in part, pathogenic yeasts use GAGs as receptors and that this phenomenon depends on the molecular species involved. As was mentioned earlier, it has been previously described that bacteria use GAGs to bind to the corneal epithelium, showing different patterns depending on their Gram nature (García et al. 2016b). It also has been shown that *C. albicans* has a preference for CS as a receptor in the keratinocytes of the epidermis. It contrasts with the findings of the present work, thus reinforcing the importance of the final structure of the GAG chains involved in the adhesion of microorganisms (Ordiales et al. 2021).

The involvement of different species of GAGs in fungal adhesion was evaluated through competition with commercial molecules. Inhibition of binding was obtained to a variable degree depending on the interfering molecule and the yeast used. HS and CS B showed the most significant inhibition in *C. albicans*, followed by CS A and CS C. However, the effect was the opposite in *C. parapsilosis*, with CS C being the most interfering molecule. CS B, unlike other species of CS, presents iduronic acid residues in variable proportions along its chain as a result of GlcA epimerization, which provides the molecule with greater flexibility (Thelin et al. 2013). The epimerization at C5 of GlcA also occurs in HS chain. Additionally, CS A and CS C are sulfated at C4 and C6 of GalNAc respectively, although CS B and HS are usually more sulfated. These characteristics may explain the results, epimerization being of paramount importance in the adhesion process of *C. albicans*, as is the sulfation of GalNAc in *C. parapsilosis*. The mix of GAGs had a combined effect, increasing the inhibition of both these yeasts, and although greater in *C. parapsilosis*, total inhibition was not achieved in either case, suggesting the existence of other receptors. One reason for the differences could be that the affinity of the yeasts for commercial GAGs may vary and could even be lower than when they interact with the GAGs of the corneal cells.

Furthermore, GAGs can frequently form complexes with other ligands or receptors. The epimerization of GlcA and the sulfation of GalNAc do not seem to be crucial for binding in *C. glabrata*. HS and CS C present a similar degree of binding inhibition, with CS A and CS B being the least interfering molecules. Furthermore, the mix of GAGs did not result in greater inhibition. Taken together, all the data point to the importance of GAGs as cell receptors in fungal adherence.

The complex and dynamic structure of GAG chains depends on the cell's type, location, and physiological state, allowing them to participate in a multitude of pathological processes, including infections. The affinity of bacteria for different species of GAGs during their pathogenesis has been widely described (Zaretzky et al. 1995; Leong et al. 1998; Tonnaer et al. 2006; Kobayashi et al. 2011; Ordiales et al. 2021).

To investigate the influence of sulfation at specific positions on adherence, we used corneal cell lines previously developed in our laboratory where the genes specifically involved in introducing sulfate groups at specific positions of the disaccharide were silenced (García et al. 2016b). The design of these cell lines took into account the inhibition of all the genes encoding isoforms responsible for the same type of sulfation ensured that the transcription of the rest of the genes involved in biosynthesis was not affected since multiple isoforms are responsible for some of these sulfations, along with the possible existence of space-time regulated enzyme complexes, both at the transcriptional and translational levels (Victor et al. 2009). The reduction of sulfation at different positions affected the attachment of the fungi differently, and no common patterns of inhibition of adherence were observed. The binding of *C. albicans* was very sensitive to 6-O sulfation of GlcNAc, although N-sulfation in this residue only affected the binding of *C. albicans* and *C. glabrata*. In addition, the 2-O sulfation of uronic acid residue only inhibited the binding of *C. glabrata*, the opposite of what happened in *C. parapsilosis* experiments. Despite the importance of GAG chain sulfation patterns in the binding of *Candida* spp. to ligands, few studies related to their influence on binding to microorganisms have been published. However, the importance of N- and 6-O sulfation of GlcNAc in corneal infections has been demonstrated, along with

the fact that 2-O sulfation of uronic acid residues has less importance (García et al. 2016b).

In conclusion, our data seems to indicate that GAGs act, at least in part, as receptors for the binding of *C. albicans*, *C. glabrata*, and *C. parapsilosis* to corneal epithelial cells although there are differences between fungal species. In the case of *C. albicans*, its morphological form is responsible for radical differences in terms of its dependence on GAGs as receptors, probably due to differences in the composition of the cell wall in the different forms (Naglik et al. 2011), which would lead to changes in the expression of adhesins. This fact might cause alterations in its affinity to GAGs and modifications in its binding to other receptors. These results approximate what can happen *in vivo*, although other factors about the cellular environment and the cell itself should be taken into account for future research. The results of this work open the door to new strategies that can inhibit the adhesion and invasion of pathogenic fungi to the cornea, thus reducing the possibility of developing keratitis.

Funding

This study was funded through the 2017 "Pierre Fabré Dermatología en Acné" award from the Academia Española de Dermatología y Venereología (AEDV), and by the Government of the Principado de Asturias (Spain) consolidated research groups grant FC-15-GRUPIN14-141. Ordiales H received a grant from Programa Severo Ochoa de Ayudas Predoctorales para la Investigación y Docencia from the Principado de Asturias (Grant BP17-057). The Instituto Universitario Fernández-Vega is supported in part by the Fundación de Investigación Oftalmológica through the Fundación Cristina Masaveu Peterson, Spain.

Conflict of interest

The authors do not report any financial or personal connections with other persons or organizations, which might negatively affect the contents of this publication and/or claim authorship rights to this publication.

Literature

Esko JD, Kimata K, Lindahl U. Proteoglycans and sulfated glycosaminoglycans. In: Varki A, Cummings RD, Esko JD, Freeze HH, Stanley P, Bertozzi CR, Hart GW, Etzler ME, editors. Essentials of glycobiology. Cold Spring Harbor (USA): Cold Spring Harbor Laboratory Press; 2009.

Aquino RS, Park PW. Glycosaminoglycans and infection. Front Biosci (Landmark Ed). 2016 Jun 1;21:1260–1277. https://doi.org/10.2741/4455

García B, Merayo-Lloves J, Martin C, Alcalde I, Quirós LM, Vazquez F. Surface proteoglycans as mediators in bacterial pathogens infections. Front Microbiol. 2016a Feb 24;7:220. https://doi.org/10.3389/fmicb.2016.00220

García B, Merayo-Lloves J, Rodríguez D, Alcalde I, García-Suárez O, Alfonso JF, Baamonde B, Fernández-Vega A, Vazquez F, Quirós LM. Different use of cell surface glycosaminoglycans as adherence receptors to corneal cells by Gram positive and Gram negative pathogens. Front Cell Infect Microbiol. 2016b Nov 30;6:173. https://doi.org/10.3389/fcimb.2016.00173

Gulati K, Poluri KM. Mechanistic and therapeutic overview of glycosaminoglycans: the unsung heroes of biomolecular signaling. Glycoconj J. 2016 Feb;33(1):1–17. https://doi.org/10.1007/s10719-015-9642-2

Iozzo R V, Schaefer L. Proteoglycan form and function: A comprehensive nomenclature of proteoglycans. Matrix Biol. 2015 Mar; 42:11–55. https://doi.org/10.1016/j.matbio.2015.02.003

Kaji T, Kawashima T, Sakamoto M. Rhodamine B inhibition of glycosaminoglycan production by cultured human lip fibroblasts. Toxicol Appl Pharmacol. 1991 Oct;111(1):82–89. https://doi.org/10.1016/0041-008x(91)90136-3

Kamhi E, Joo EJ, Dordick JS, Linhardt RJ. Glycosaminoglycans in infectious disease. Biol Rev Camb Philos Soc. 2013 Nov;88(4): 928–943. https://doi.org/10.1111/brv.12034

Kjellén L, Lindahl U. Proteoglycans: Structures and interactions. Annu Rev Biochem. 1991;60:443–475. https://doi.org/10.1146/annurev.bi.60.070191.002303

Kobayashi M, Ishida K, Matsuo J, Nakamura S, Nagasawa A, Motohashi K, Yao T, Hirai I, Yamamoto Y, Suzuki H, et al. *Chlamydophila pneumoniae* attachment and infection in low proteoglycan expressing human lymphoid Jurkat cells. Microb Pathog. 2011 Sep; 51(3):209–216. https://doi.org/10.1016/j.micpath.2011.03.010

Lakhundi S, Siddiqui R, Khan NA. Pathogenesis of microbial keratitis. Microb Pathog. 2017 Mar;104:97–109. https://doi.org/10.1016/j.micpath.2016.12.013

Leong JM, Wang H, Magoun L, Field JA, Morrissey PE, Robbins D, Tatro JB, Coburn J, Parveen N. Different classes of proteoglycans contribute to the attachment of *Borrelia burgdorferi* to cultured endothelial and brain cells. Infect Immun. 1998 Mar; 66(3): 994–999. https://doi.org/10.1128/IAI.66.3.994-999.1998

Martín C, Lozano-Iturbe V, Girón RM, Vazquez-Espinosa E, Rodriguez D, Merayo-Lloves J, Vazquez F, Quirós LM, García B. Glycosaminoglycans are differentially involved in bacterial binding to healthy and cystic fibrosis lung cells. J Cyst Fibros. 2019 May; 18(3): e19–e25. https://doi.org/10.1016/j.jcf.2018.10.017

Martín R, Martín C, Escobedo S, Suárez JE, Quirós LM. Surface glycosaminoglycans mediate adherence between HeLa cells and *Lactobacillus salivarius* Lv72. BMC Microbiol. 2013 Sep 17;13:210. https://doi.org/10.1186/1471-2180-13-210

Mellado F, Rojas T, Cumsille C. [Fungal keratitis: review of diagnosis and treatment] (in Spanish). Arq Bras Oftalmol. 2013 Jan-Feb; 76(1):52–56. https://doi.org/10.1590/s0004-27492013000100016

Naglik JR, Moyes DL, Wächtler B, Hube B. *Candida albicans* interactions with epithelial cells and mucosal immunity. Microbes Infect. 2011 Nov;13(12–13):963–976. https://doi.org/10.1016/j.micinf.2011.06.009

Nikitovic D, Tsatsakis AM, Karamanos NK, Tzanakakis GN. The effects of genistein on the synthesis and distribution of glycosaminoglycans/proteoglycans by two osteosarcoma cell lines depends on tyrosine kinase and the estrogen receptor density. Anticancer Res. 2003 Jan-Feb;23(1A):459–464.

Ordiales H, Vázquez-López F, Pevida M, Vázquez-Losada B, Vázquez F, Quirós, LM, Martín C. [Glycosaminoglycans are involved in the adhesion of *Candida albicans* and *Malassezia* species to keratinocytes but not to dermal fibroblasts] (in Spanish). Actas Dermo-Sifiliogr. 2021;112(7):619–624. https://doi.org/10.1016/j.ad.2021.02.001

Piotrowska E, Jakóbkiewicz-Banecka J, Barańska S, Tylki-Szymańska A, Czartoryska B, Wegrzyn A, Wegrzyn G. Genistein-mediated inhibition of glycosaminoglycan synthesis as a basis for gene expression-targeted isoflavone therapy for mucopolysaccharidoses. Eur J Hum Genet. 2006 Jul;14(7):846–852. https://doi.org/10.1038/sj.ejhg.5201623

Rabenstein DL. Heparin and heparan sulfate: structure and function. Nat Prod Rep. 2002 Jun;19(3):312–331. https://doi.org/10.1039/b100916h

Rajas O, Quirós LM, Ortega M, Vázquez-Espinosa E, Merayo-Lloves J, Vazquez F, García B. Glycosaminoglycans are involved in bacterial adherence to lung cells. BMC Infect Dis. 2017 May 2; 17(1):319. https://doi.org/10.1186/s12879-017-2418-5

Roberts ALK, Thomas BJ, Wilkinson AS, Fletcher JM, Byers S. Inhibition of glycosaminoglycan synthesis using rhodamine B in a mouse model of mucopolysaccharidosis type IIIA. Pediatr Res. 2006 Sep;60(3):309–314. https://doi.org/10.1203/01.pdr.0000233037.00707.da

Silva S, Negri M, Henriques M, Oliveira R, Williams DW, Azeredo J. *Candida glabrata*, *Candida parapsilosis* and *Candida tropicalis*: biology, epidemiology, pathogenicity and antifungal resistance. FEMS Microbiol Rev. 2012 Mar;36(2):288–305. https://doi.org/10.1111/j.1574-6976.2011.00278.x

Thelin MA, Bartolini B, Axelsson J, Gustafsson R, Tykesson E, Pera E, Oldberg Å, Maccarana M, Malmstrom A. Biological functions of iduronic acid in chondroitin/dermatan sulfate. FEBS J. 2013 May;280(10):2431–2446. https://doi.org/10.1111/febs.12214

Thomas PA, Kaliamurthy J. Mycotic keratitis: epidemiology, diagnosis and management. Clin Microbiol Infect. 2013 Mar; 19(3): 210–220. https://doi.org/10.1111/1469-0691.12126

Tonnaer EL, Hafmans TG, Van Kuppevelt TH, Sanders EA, Verweij PE, Curfs JH. Involvement of glycosaminoglycans in the attachment of pneumococci to nasopharyngeal epithelial cells. Microbes Infect. 2006 Feb;8(2):316–322. https://doi.org/10.1016/j.micinf.2005.06.028

Victor XV, Nguyen TK, Ethirajan M, Tran VM, Nguyen KV, Kuberan B. Investigating the elusive mechanism of glycosaminoglycan biosynthesis. J Biol Chem. 2009 Sep 18;284(38):25842–25853. https://doi.org/10.1074/jbc.M109.043208

Wilson JW, Schurr MJ, LeBlanc CL, Ramamurthy R, Buchanan KL, Nickerson CA. Mechanisms of bacterial pathogenicity. Postgrad Med J. 2002 Apr;78(918):216–224. https://doi.org/10.1136/pmj.78.918.216

Zaretzky FR, Pearce-Pratt R, Phillips DM. Sulfated polyanions block *Chlamydia trachomatis* infection of cervix-derived human epithelia. Infect Immun. 1995 Sep;63(9):3520–3526. https://doi.org/10.1128/iai.63.9.3520-3526.1995

ORIGINAL PAPER

Polish Journal of Microbiology
2022, Vol. 71, No 1, 63–71
https://doi.org/10.33073/pjm-2022-009

The Characteristics and Function of Internalin G in *Listeria monocytogenes*

HUITIAN GOU[1]*, YUANYUAN LIU[1], WENJING SHI[1], JINYU NAN[1], CHUAN WANG[1], YANAN SUN[1], QIHANG CAO[1], HUILIN WEI[1], CHEN SONG[1], CHANGQING TIAN[1], YANQUAN WEI[1] and HUIWEN XUE[1]

[1] College of Veterinary Medicine, Gansu Agricultural University, Lanzhou, China
[2] Jiuquan City Animal Control Disease Center, Jiuquan, China

Submitted 22 November 2021, accepted 10 February 2022, published online 22 March 2022

Abstract

In order to clarified characteristics and function of internalin G (inlG) in *Listeria monocytogenes* ATCC®19111 (1/2a) (LM), the immune protection of the inlG was evaluated in mice, the homologous recombination was used to construct *inlG* deletion strains, and their biological characteristics were studied by the transcriptomics analysis. As a result, the immunization of mice with the purified protein achieved a protective effect against bacterial infection. The deletion strain LM-AinlG was successfully constructed with genetic stability. The mouse infection test showed that the virulence of LM was decreased after the deletion of the *inlG* gene. The deletion strain showed enhanced adhesion to and invasion of Caco-2 cells. Compared to the wild strain, 18 genes were up-regulated, and 24 genes were down-regulated in the LM-AinlG. This study has laid a foundation for further research on the function of *inlG* and the pathogenesis of LM.

In this study, immunization of mice with the purified inlG protein achieved a protective effect against *Listeria monocytogenes* infection. The virulence of LM-ΔinlG was decreased by mouse infection. However, the adhesion and invasion ability to Caco-2 cell were enhanced. Compared to the wild strain, 18 genes were up-regulated, and 24 genes were down-regulated in the LM-ΔinlG. This study has laid a foundation for further study of the function of the inlG and the listeriosis.

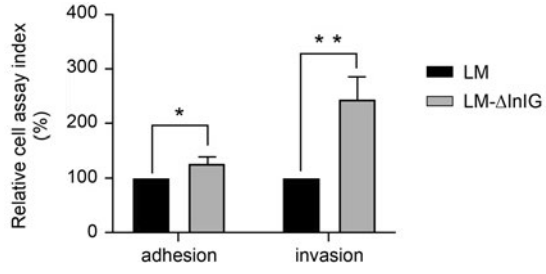

Keywords: *Listeria monocytogenes*, internalin G, immune protection, gene deletion, transcriptomics

Introduction

Listeria monocytogenes (LM) is an important zoonotic pathogen and one of the four food-borne pathogens, with a fatality rate of up to 30% (Wang et al. 2017; Radoshevich and Cossart 2018). Sixteen serotypes have been identified, and three are commonly involved in the infection, 4b and 1/2b in lineage I and 1/2a in lineage II (Datta and Burall 2018). As an intracellular bacterium, LM can stimulate the host's immune response and induce specific CD8+ and CD4+ T cell immune responses (Dowd et al. 2016). At present, LM poses a severe threat to human and animal health, primarily through frozen food, causing foremost food safety and public health concerns. Pregnant women, newborns, and the elderly are vulnerable to LM infection. Humans are mainly infected with LM through the fecal-oral route, and through eyes, mucous membranes, and damaged skin (Matle et al. 2020). The process of LM invasion into host cells is complex and involves multiple protein molecules such as pathogenic factors, adhesion molecules, and internalins (Pizarro-Cerdá and Cossart 2018).

Internalins are a protein family of LM. At present, there are 25 members, among which inlA and inlB are the earliest identified proteins related to bacterial invasion and are the main factors involved in bacterial invasion of host cells (Ireton et al. 2021). InlA mediates the internalization of LM through its interaction with the host-specific receptor E-cad, enabling LM to be endocytosed and enter the host epithelial cells (Drolia and Bhunia 2019). InlB can interact with multiple receptors

* Corresponding author: H. Gou, College of Veterinary Medicine, Gansu Agricultural University, Lanzhou, China; **e-mail: gouht@gsau.edu.cn**

on the surface of host cells to mediate LM adhesion and invasion of hepatocytes and nonphagocytes (Al-Obaidi and Desa 2018). Only some internalins play a role in mediating LM invasion (Gouin et al. 2019; Mir 2021). Balandyté et al. (2011) found that the inlG protein was mainly present in environmental isolates and rarely in strains isolated clinically from human and animal samples, suggesting that inlG is closely related to LM survival in the external environment. Jia et al. (2007) found that the *inlG* accounted for 41.1% of the 236 isolates of LM. Jiang et al. studied 133 isolates of LM and found that inlG did not exist in lineage I but was present in 74.2% of lineage II, and 30.7% of lineage III (Jianjun 2011). However, there have been few studies on the role of inlG in LM invasion of host cells.

In the present study, inlG was expressed in a prokaryotic system. After immunizing mice with the expressed product, its protection was evaluated. An *inlG* deletion strain was constructed, and the phenotype of the deletion strain was studied through growth characteristics, hemolysis test, cell adhesion, cell invasion, and mouse infection to achieve a preliminary understanding of the biological function of inlG.

Experimental

Materials and Methods

Cell and plasmid. The reference strain of LM ATCC®19111 (1/2a) and human colorectal adenocarcinoma (Caco-2) cells were purchased from the China Culture Collection Center. *Escherichia coli* competent cells BL21 (DE3), prokaryotic expression plasmid pET-28a (+), and LM shuttle plasmid pKSV7 were preserved in our laboratory. The primers used for cloning *inlG* and the construction of the deletion strain LM-AinlG are shown in Table I.

Prokaryotic expression of inlG. To grow LM ATCC®19111 strains, overnight cultures were diluted 100-fold in Brain Heart Infusion medium (BHI, China) and shaken at 37°C. The recombinant plasmid pET-28a (+)-InlG was constructed, which was transformed into the expression strain BL21 (DE3). We carried out IPTG induction to positive recombinant plasmid pET-28a (+)-InlG and optimization of the expression conditions, SDS-PAGE analysis of the expression product size, and western blotting to verify the antigenicity of the expressed protein.

Immunoprotection test of inlG in mice. Thirty-two 7-week-old male BALB/c mice were obtained from the Experimental Animal Center of the Chinese Academy Agricultural of Sciences (Lanzhou, China) and maintained in cages with food and water ad libitum. They were divided into two groups of 16 mice, respectively. Groups were immunized with 100 pg of recombinant inlG mixed with complete Freund's adjuvant (Sigma, USA) for priming and incomplete Freund's adjuvant (Sigma, USA) for boosting. Immunizations were carried out on days 1, 15, and 30. Blood was collected by tail vein bleeding before immunization. The antibody titer was measured after each immunization by indirect ELISA. When the titer increased more than 1:52,000, mice were intraperitoneally infected with LM at twice LD_{50}, and the immunoprotective effect of *inlG* on mice was evaluated by measuring the survival rate of mice.

Histopathological observation of mice. Mice in the three groups (unchallenged, unimmunized-challenged, and immunized-challenged) (n = 3, respectively) were dissected after death, and brain and liver tissues were removed and prepared in paraffin sections. After hematoxylin-eosin staining, pathological changes were observed under an optical microscope (Olympus, Japan).

Construction of the *inlG* deletion strain. The primers were designed to amplify the upstream and downstream homologous arms of the *inlG* gene. The homologous arm of AinlG was amplified with gene splicing by overlap extension PCR (SOE-PCR). After sequencing, the homologous arm of AinlG was linked to the shuttle plasmid pKSV7 to form the recombinant plasmid pKSV7-AinlG. The pKSV7-AinlG was transferred into

Table I
PCR primers used in the experiments.

Primer	Sequence	Product (bp)
ΔInlG-F1	*CG*GGATCC*G*CTTATGATACAGTAGAAGAA (*Bam*HI)	633
ΔInlG-R1	CCTCCGATGAAAAGCGTTCCTAAAATAGTAGGAATAATTCCCAAGATAGCTGTCACT	
ΔInlG-F2	ATGTTTTACTTGTAGTGACAGCTATCTTGGGAATTATTCCTACTATTTTAGGAACGC	596
ΔInlG-R2	*GCTCTAGA*AGATAATTCAAGTTCTGTTA (*Xba*I)	
D-F	TGTCCGCAACAGCTAGCCCAG	1,644/3,100
D-R	GCAAGTGGGGTTAAATCACTT	
Hly-F	GATGCATCTGCATTCAATAA	1,510
Hly-R	TTATTCGATTGGATTATCTAC	

LM competent cells by Gene Pulser MXcell™ (BioRad, USA), and the positive bacteria were screened. Homologous recombination was carried out at 41°C in the presence of chloramphenicol. After complete recombination, the pKSV7 plasmid was lost under 30°C and no-chloramphenicol conditions. The genetic stability of the gene deletion strain was tested by PCR.

Phenotypic identification of LM-inlG. The growth of wild-type LM and LM-inlG was evaluated by measuring OD_{600} at 30°C, 37°C, and 41°C and pH 5, 7, and 9. The adhesion and invasion rates of the two strains were calculated as described previously (Medeiros et al. 2021; Pereira et al. 2021). Human colon carcinoma cells (Caco-2) were cultured in Dulbecco's modified Eagle's medium (DMEM) (Gibco, China) with high glucose, supplemented with10% fetal bovine serum (FBS) (Gibco, China). They were then seeded in 12-well plates at a density of 1×10^5 cells/well and incubated at 37°C in the presence of 5% CO_2. For the adhesion assay, overnight (18 h)-grown bacterial cultures were washed thrice with PBS, adjusted to $OD_{600} = 0.12$, and suspended in DMEM to a final concentration of 1×10^8 CFU/ml. The Caco-2 cell monolayer was washed three times using DMEM, then exposed separately to the LM and LM-*inlG* and incubated for 2 h at 37°C under the atmosphere with 5% CO_2. After incubation, cells were washed three times with PBS and lysed using 500 pl of cold 0.5% Triton X-100. For the invasion assay, the monolayers were exposed to LM and LM-*inlG*, washed as performed in the adhesion assay, and treated with gentamicin (100 μg/ml, 1 h) and with 0.5% Triton X-100 (37°C, 10 min). The lysed cell suspensions from both adhesion and invasion experiments were serially diluted in PBS, and the bacterial concentration in the samples was determined by the number of colony-forming units (CFU). The adhesion/invasion efficiency (%) for each strain was calculated as the number of bacteria attached/invaded to the cells compared with the total number of CFU provided in the inoculation samples multiplied by 100. However, the LD_{50} of mice for the deletion strain was determined the same as the wild strain.

Transcriptomics analysis of LM and LM-AinlG. Total RNA was extracted from LM and LM-AinlG samples using the RNAprep Pure Kit (Tiangen, China), following the manufacturer's instructions. In total, 5 pg RNA/sample was sent to Beijing Novogene Technology Co., Ltd., China for RNA sequencing. According to the instructions, the Library Prep Kit (Tiangen, China) was used to construct the chain-specific library for RNA samples. The library was sequenced using the Illumina sequencing platform (HiSeq 4000). Raw data (raw reads) of FASTQ format were firstly processed through in-house Perl scripts. The LM reference genome (NC_003210) and associated gene annotation information were downloaded from the NCBI database. The sequence alignment software, Bowtie2 (2.3.4.3) was used for genome location analysis of clean reads.

The number of gene counts per sample was standardized using DEGSeq2 (1.20) software. We then performed hypothesis testing and set the threshold as $|\log 2 \text{ Fold Chang e}| > 1$, p_{adj} value (corrected p-value) < 0.05 to screen out DEGs between LM and LM-AinlG. To systematically analyze gene biological function and genome information, the clusterProfiler (3.8.1) software was used for Gene Ontology (GO) function enrichment and the Kyoto Encyclopedia of Genes and Genomes (KEGG) pathway analysis for DEGs. p-Values were calculated and selected p_{adj} values were set to < 0.05 to determine the significant gene enrichment (Liao et al. 2019).

Results

Prokaryotic expression of inlG. The molecular weight of the inlG protein was estimated to be 53 ku, but the size of the inlG protein was about 70 ku according to SDS-PAGE. Therefore, the expressed protein was identified by mass spectrometry. The mass spectrometry results matched the LM reference sequence to the highest degree, and the protein was confirmed to be an expression product of the *inlG* gene. LM-positive serum was used as the primary antibody, and sheep anti-rabbit IgG was used as the secondary antibody. Western blotting showed that the induced protein had potential reactogenicity (Fig. 1).

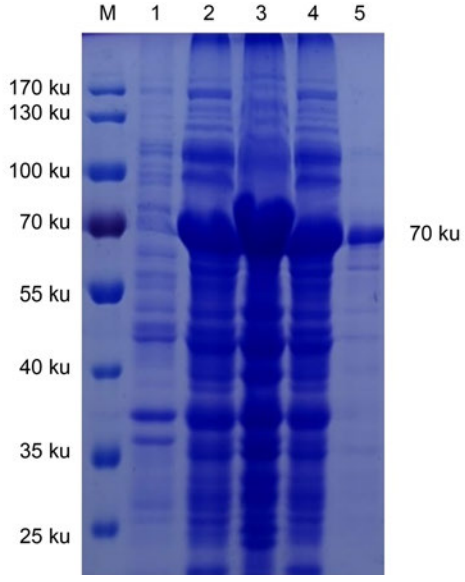

Fig. 1. Analysis of the recombinant protein. M – Protein marker, 1 – bacteria before the induction with IPTG, 2 – the induced bacteria, 3 – supernatant of lysed induced bacteria, 4 – precipitation of induced bacteria, 5 – purified *InlG* recombinant protein, 6 – uninduced bacteria reaction with positive serum, 7 – induced bacteria reaction with positive serum.

Table II
Determination of the median lethal dose of the bacteria (BACT) in mice.

BACT (CFU)	Death/Total	Mortality (%)
10^9	9/10	90
10^8	8/10	80
10^7	6/10	60
10^6	4/10	40
10^5	2/10	20
0	0/10	0

Immunoprotection test of inlG in mice. The mortality of mice infected with LM is shown in Table II and was calculated according to the formula: $\log LD_{50} = [Xm\text{-}i\ (XP\text{-}0.5)]$. Finally, the LD_{50} of LM was $1.0 \times 10^{6.6}$ CFU. The antibody titer of inlG was more than 1:52,000 in mice by indirect ELISA. After intraperitoneal infection of mice with LM, the control group had rough hair and were huddled and listless. Individual mice gradually developed tremors, increased secretion at the canthus, and accelerated respiratory rate. Fifteen mice died within 72 h, and one survived. However, eight mice in the test group developed similar symptoms and died. The remaining eight mice became normal at 48 h after the challenge (Table II).

Histopathological observation of mice. Compared with the brain tissue of the normal group (Fig. 2a), the challenge group after immunization with saline was filled with red blood cells, and a large number of lymphocytes were infiltrated in the pons (Fig. 2b). After protein immunization, the interface between the cortex and medulla in the brain tissue of mice in the challenge group was clear, and there were fissure vacuoles in the medulla (Fig. 2c). Brain tissue damage in the immunoprotein group post-challenge was milder than that in the normal saline group.

Compared with liver tissue in the normal group (Fig. 2d), mice in the challenge group after immunization with saline (Fig. 2e) suffered a severe liver injury, irregular arrangement of hepatic lobules, and dilated central veins. The hepatic cord of mice in the challenge group disappeared after protein immunization (Fig. 2f). As in the brain, liver injury in the protein challenge group was milder than in the normal saline challenge group.

Construction of LM-AinlG. The amplified upstream and downstream homologous arms of *inlG* were 633 and 596 bp, respectively. The homologous arms of the *inlG* were fused by SOE-PCR, and a fragment of 1,229 bp was obtained, which was named AinlG. The pKSV7 plasmid was ligated with AinlG by *BamHI* and *Xbal* double digestion, and the product was transformed into DH5a competent cells. The recombinant plasmid pKSV7-AinlG was transformed into LM competent cells by electric shock and cultured at 30°C

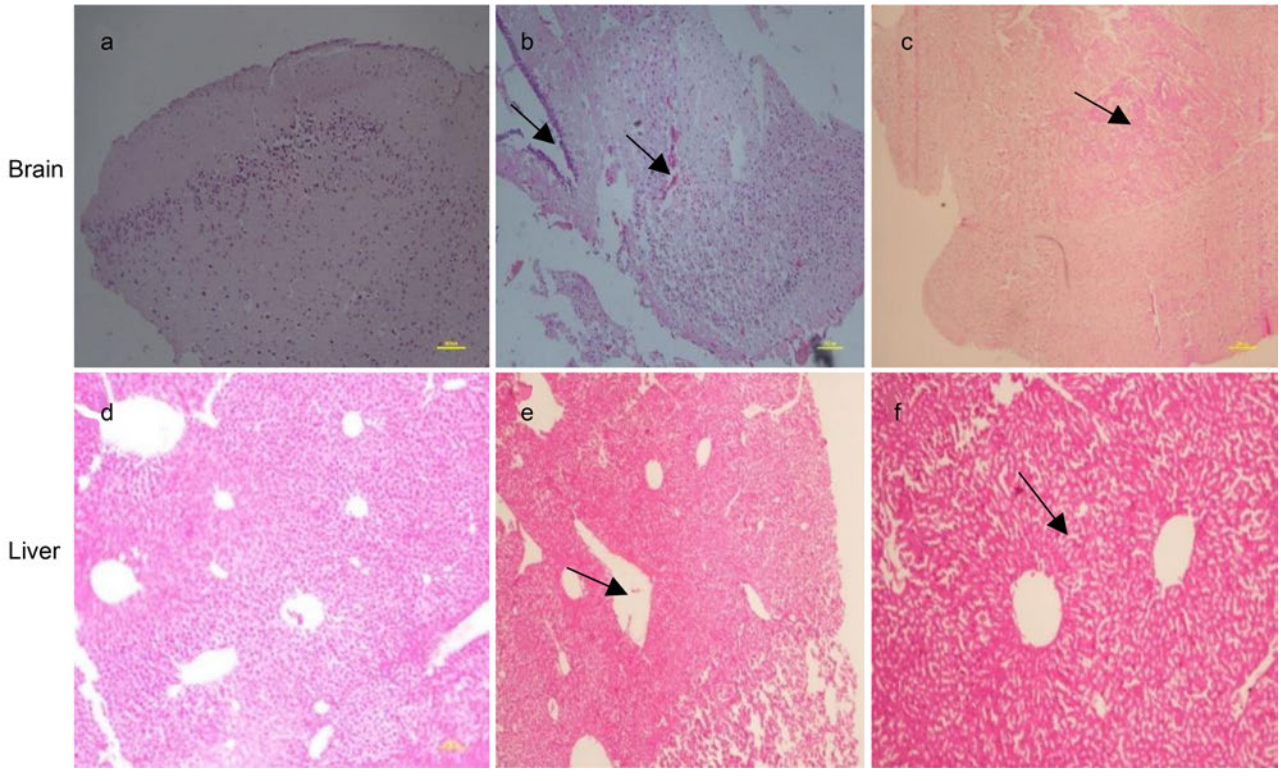

Fig. 2. Pathological changes in the tissue of infected mice stained with hematoxillin-eosin. a/d – Normal mouse, b/e – the mice immunized with normal saline, c/f – the mice immunized with protein and challenged with bacteria.

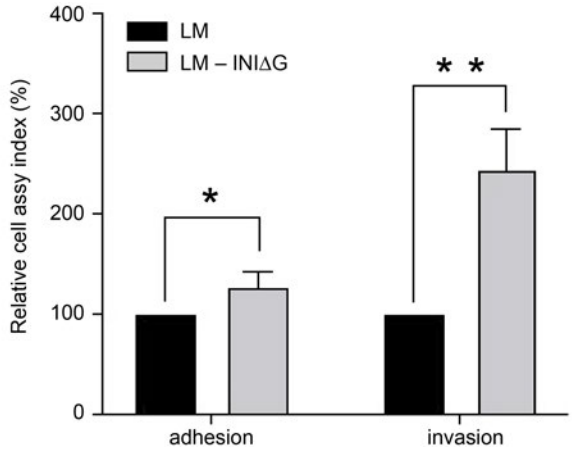

Fig. 3. Relative adhesion and invasion of LM and LM-ΔInlG in Caco-2 cells. This test was done in triplicate in each run and repeated for three times. The cell assay rates of LM19111 were set at 100%. * $p < 0.05$; ** $p < 0.01$.

with chloramphenicol. The positive transformants were screened and amplified as 1,229 bp. At the 70 th generation, the homologous recombination was completed. The shuttle plasmid was lost successfully at the 30 th generation under the condition of 30°C and no antibiotics. The recombinant strain was cultured at 37°C for 20 generations, and a genetically stable deletion strain was finally obtained.

Biological characteristics of LM-AinlG. There was no significant difference in growth characteristics and biochemical and hemolysis test results between wild-type LM and LM-AinlG. The LD_{50} of the deleted strain LM was $1.0 \times 10^{6.9}$ CFU, and the wild strain LM was $1.0 \times 10^{6.6}$ CFU. The adhesion rate of LM-AinlG to Caco-2 cells was 1.3 times higher than the wild-type strain, and the invasion rate was about 2.45 times higher than the wild-type strain (Fig. 3).

Transcriptomic results of LM and LM-AinlG. The transcribed genes were classified into gene ontology (GO) categories: 45 genes were classified into biological processes, 19 to cellular components, and 29 to molecular functions. Compared to the wild strain, 18 genes were up-regulated and 24 genes were down-regulated in the LM-AinlG (Fig. 4). The DEGs were compared

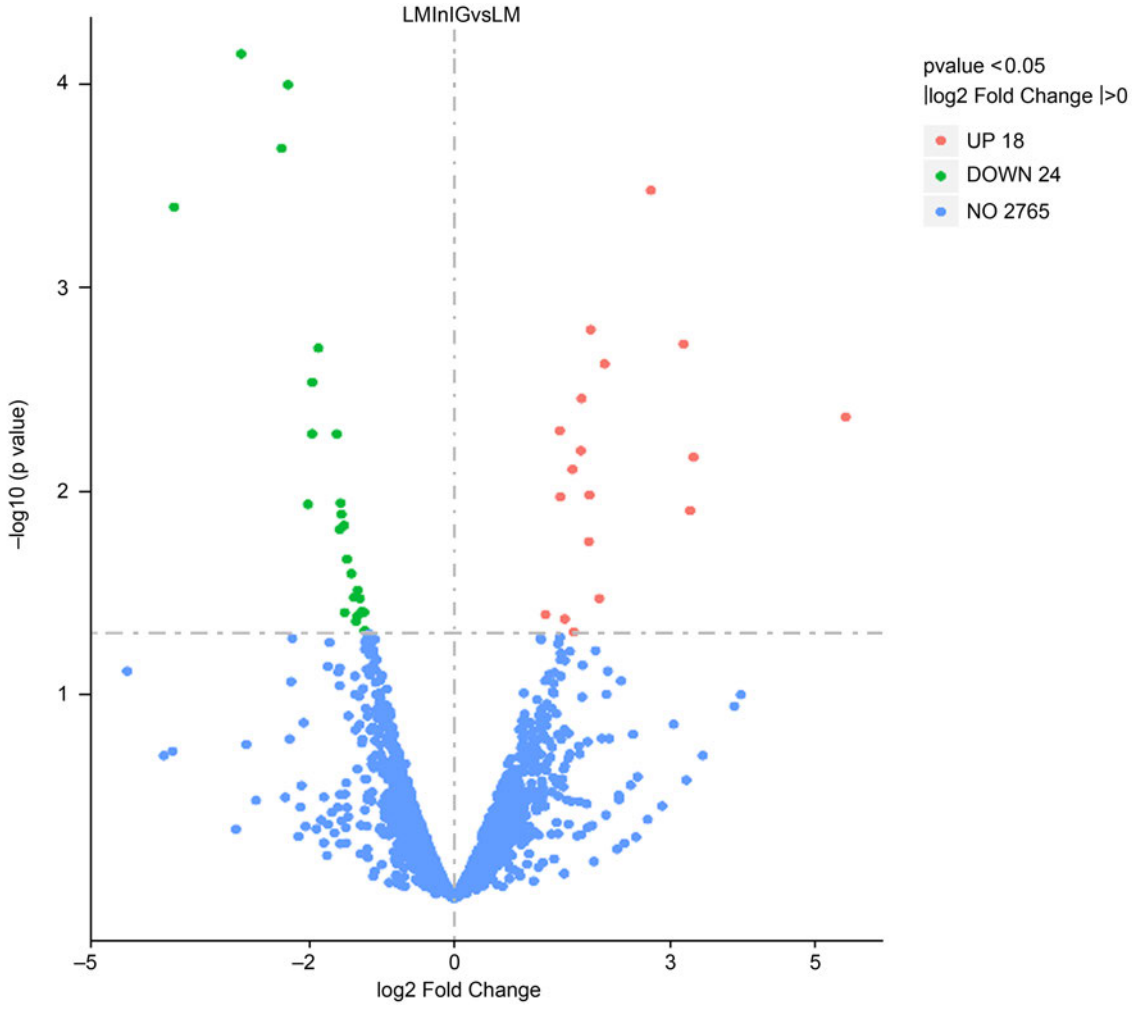

Fig. 4. Differentially expressed genes in LM-ΔInlG compared to LM. The abscissa indicates the fold change of gene expression, and the ordinate indicates the significance of the gene difference. The red dots indicate the up-regulated genes, the green dots indicate the down-regulated genes, and the blue dots indicate the genes that are not significantly different.

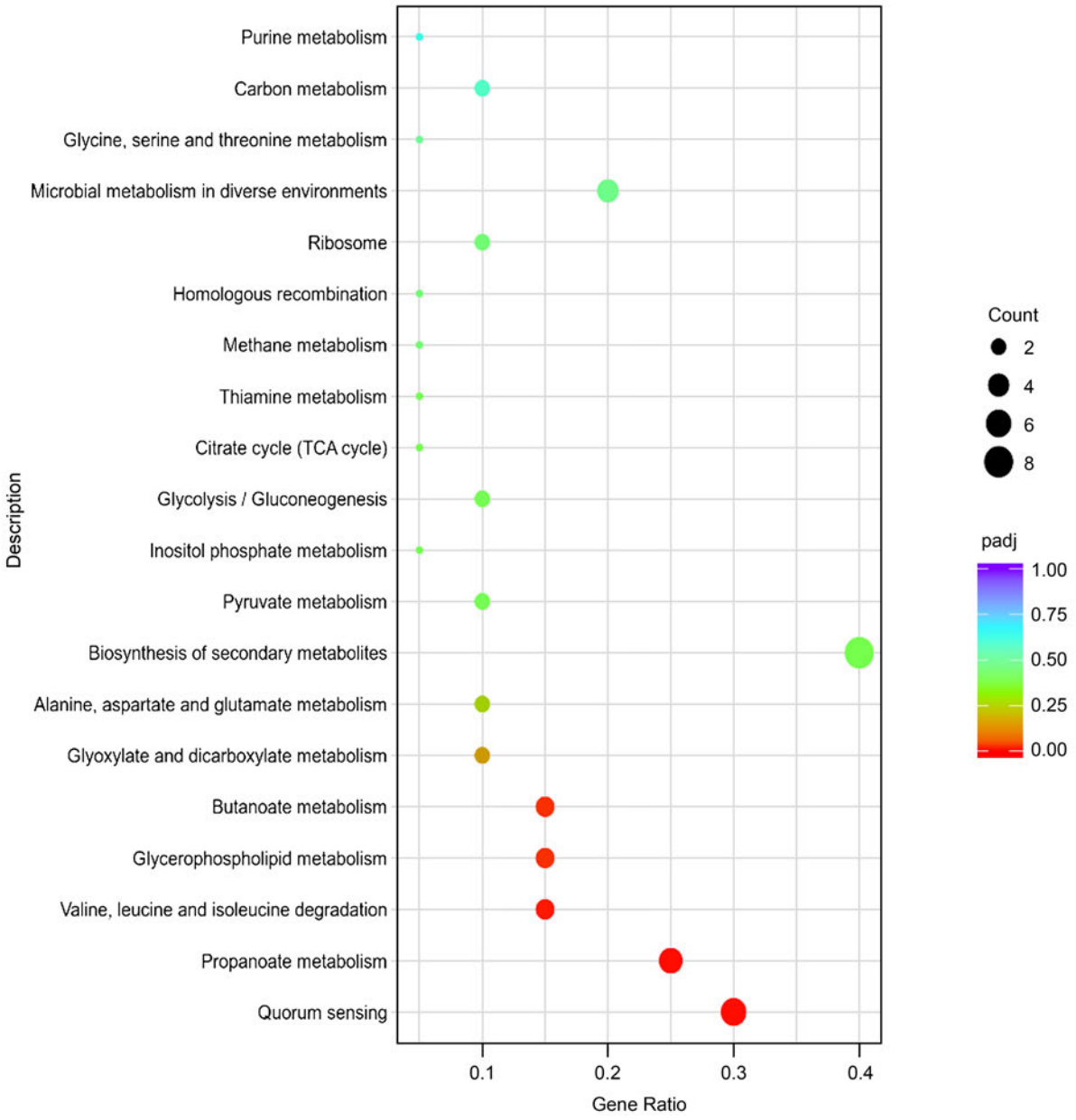

Fig. 5. KEGG pathway analysis of differentially expressed genes in LM-ΔInlG compared to LM. The enriched KEGG categories are on the vertical axis. The ratio of the enriched DEGs in the KEGG category to the total genes in that category is shown on the horizontal axis.

with the Kyoto Encyclopedia of Genes and Genomes (KEGG, http://www.genome.jp/kegg) and GO databases (http://www. geneontology. org). In Fig. 5, the abscissa represents the enrichment factor; the vertical coordinate represents the enriched function of the KEGG term. The larger the circle, the more differential genes are enriched to this function. Twenty metabolic pathways were enriched in the LM-AinlG (Fig. 5). Quorum sensing, Propanoate metabolism, Valine, leucine, and isoleucine degradation, Glycerophospholipid metabolism, Butanoate metabolism are the five significant KEGG enriched pathways from LM-AinlG compared LM (Table III).

Discussion

The *inlG* gene product consists of 490 amino acids, and the predicted molecular weight was about 53 ku. However, SDS-PAGE found the inlG protein to be about 70 ku, with a difference of 17 ku from the predicted molecular weight. After identifying inlG protein by mass spectrometry, the highest matching score was the LM reference sequence. The reason for this deviation between the experimental results and the predicted molecular weight may be the influence of the molecular weight standards of proteins at different concentrations of SDS-PAGE. After boiling, the denatured protein

Table III
Differentially expressed genes in related KEGG pathways in LM-ΔInlG compared to LM.

Term	Gene ID	Name	Log_2FC	Type	Description
Quorum sensing	lmo0205	plcB	1.89	up	phospholipase C
	lmo0202	hly	1.77	up	listeriolysin O precursor
	Novel00001	no	1.76	up	thiol-activated cytolysin
	Novel00002	no	1.64	up	thiol-activated cytolysin beta sandwich domain
	lmo2363	no	−1.35	down	glutamate decarboxylase
	lmo0447	no	1.66	up	pyridoxal-dependent decarboxylase conserved domain
Propanoate metabolism	lmo1373	no	−1.86	down	transketolase, pyrimidine binding domain
	lmo1153	no	1.88	up	propanediol dehydratase subunit alpha
	lmo2720	no	−2.02	down	AMP-binding enzyme C-terminal domain
	lmo1374	no	−1.52	down	biotin-requiring enzyme
	lmo1371	no	−1.28	down	pyridine nucleotide-disulphide oxidoreductase
Valine, leucine, nd isoleucine degradation	lmo1373	no	−1.86	down	transketolase, pyrimidine binding domain
	lmo1374	no	−1.52	down	biotin-requiring enzyme
	lmo1371	no	−1.28	down	pyridine nucleotide-disulphide oxidoreductase
Glycerophospholipid metabolism	lmo0205	plcB	1.89	up	phospholipase C
	lmo1176	eutC	3.18	up	ethanolamine ammonia-lyase small subunit
	lmo1175	eutB	1.87	up	ethanolamine ammonia-lyase large subunit
Butanoate metabolism	lmo1369	no	−2.94	down	phosphate acetyl/butaryl transferase
	lmo2363	no	−1.35	down	glutamate decarboxylase
	lmo0447	no	1.66	up	pyridoxal-dependent decarboxylase conserved domain

forms a rod-like structure, and the surface uniformly adsorbs ions. Due to amino acid composition and other reasons, different proteins do not conform to this basic assumption (Matsumoto et al. 2019).

In the mouse protective test, the mortality was 93.75% in the control group and 50% in the experimental group, indicating that inlG protein conferred some antigenic protection after immunization. The cause of death of mice in the experimental group was analyzed. The LM used in this study was the highly pathogenic 1/2a serotype. Studies have reported that >98% of listeriosis is caused by serotype 1/2b, 4b, and 1/2a strains, and serotype 1/2a is the dominant strain in China (Chen et al. 2020; Liu et al. 2020). In addition, it may be related to the weak protection of mice immunized with inlG protein. Bu et al. (2017) found that the protection of recombinant fusion antigen was better than that of a single protein in mice challenged with LM. Therefore, the genes with dominant epitopes in the internalin family can be expressed in the future to study whether they have good antigenicity.

The internalins are closely related to LM virulence and are unique to LM for adhesion and invasion of host cells. In this study, *inlG* deletion had little effect on the growth characteristics and environmental tolerance of LM. The LD_{50} of LM-AinlG was $1.0 \times 10^{6.9}$ CFU and that of LM was $1.0 \times 10^{6.6}$ CFU, indicating that the toxicity of LM-AinlG was decreased. However, after the deletion of *inlG*, the adhesion to and invasion of Caco-2 cells were enhanced, which was consistent with that after the deletion of *inlC* (Jianjun 2011). During LM intracellular infection cycle, listeriolysin O (LLO, encoded by the *hly* gene) mediates LM escape from phagosomes through lysed phagocytic vacuole and membrane perforation (Lecuit 2020). PlcB can help LM escape from host autophagy clearance by inhibiting the maturation of autophagy precursors or preventing target recognition by autophagy mechanisms (Mitchell et al. 2018). ActA recruits actin nucleated complexes in the cytoplasm to induce actin aggregation to form pseudopod-like structures termed 'listeriopods', enabling LM to escape from autophagy of the host, driving the movement of LM in the cytoplasm and between cells, and entering neighboring host cells for a new round of adhesion and invasion (de las Heras et al. 2011). InlC, as a member of the internalins family, relaxes junctional tension through interaction with a regulator of the tight junction complex (TUBA), and aids LM to invade neighboring cells (Costa et al. 2020).

From the transcriptomics result of LM-AinlG compared to LM, the expression level of LLO, PlcB, ActA, and InlC were up-regulated. So, this result explains why the adhesion to and invasion of Caco-2 cells were enhanced for LM-AinlG. KEGG annotation results indicated that quorum sensing, propanoate metabolism, valine, leucine, and isoleucine degradation, glycerophospholipid

metabolism, and butanoate metabolism are significant pathways from LM-AinlG compared to LM. The quorum sensing (QS) pathway refers to the ability of bacteria to secrete signal molecules to the outside world continuously. By detecting the concentration of signal molecules, we can sense the population density of bacteria. QS regulates many biological characteristics, such as motility, biofilm formation, colonization, adhesion, virulence factor secretion, and bioluminescence, which are necessary for the survival or virulence of many bacteria (Younis et al. 2016). Amino acid metabolism, such as valine, leucine, and isoleucine metabolism, is likely critical for protein synthesis. However, the study also demonstrated that valine, leucine, and isoleucine degradation might be related to cell adhesion (Chandrashekar et al. 2020). Enrichment of propanoate metabolism may affect energy metabolism. These KEGG pathways were also observed in other bacteria and human cells, suggesting that propanoate may control the activity or stability of enzymes involved in pathways and affect energy metabolism regulation (Yi and Xie 2021).

Conclusions

This study evaluated the potential of inlG as a vaccine candidate to protect against LM infection. In addition, by constructing the gene deleted strain, it was verified that inlG was related to the virulence of LM. We also clarified the mechanism of LM-AinlG from the transcriptomics analysis. The next step will be to explore the detailed functional mechanism of inlG by analyzing the receptor for *inlG* and whether it acts synergistically with other internalins.

Availability of data and material

All raw sequences and analyzed data for this study have been deposited in the NCBI's GEO database as the accession number PRJNA783511.

Ethical statement

All experiments were approved by the college of Veterinary Medical, Gansu Agricultural University, China.

Acknowledgments

This work was supported by Gansu Agricultural University Youth Tutor Support Fund (GAU- QDFC-2020–10), the National Nature Science Foundation of China (No. 31960726, No. 32060822, and No. 31560700), Key Research and Development Program of Gansu Province (No. 20YF8FA136), National Key Research and Development Program of China (No. 2019YFC1605705). We are indebted to international science editing for the critical correction of this manuscript.

Conflict of interest

The authors do not report any financial or personal connections with other persons or organizations, which might negatively affect the contents of this publication and/or claim authorship rights to this publication.

Literature

Al-Obaidi MMJ, Desa MNM. Mechanisms of blood brain barrier disruption by different types of bacteria, and bacterial-host interactions facilitate the bacterial pathogen invading the brain. Cell Mol Neurobiol. 2018 Oct;38(7):1349–1368. https://doi.org/10.1007/s10571-018-0609-2

Balandyté L, Brodard I, Frey J, Oevermann A, Abril C. Ruminant rhombencephalitis-associated *Listeria monocytogenes* alleles linked to a multilocus variable-number tandem-repeat analysis complex. Appl Environ Microbiol. 2011;77(23):8325–8335. https://doi.org/10.1128/AEM.06507-11

Bu RE, Wang JL, Wu JH, Xilin GW, Chen JL, Wang H. Indirect enzyme-linked immunosorbent assay method based on *Streptococcus agalactiae* rSip-Pgk-FbsA fusion protein for detection of bovine mastitis. Pol J Vet Sci. 2017 Mar 1;20(2):355–362. https://doi.org/10.1515/pjvs-2017-0043

Chandrashekar DS, Golonka RM, Yeoh BS, Gonzalez DJ, Heikenwälder M, Gerwirtz AT, Varambally S, Vijay-Kumar M. Fermentable fiber-induced hepatocellular carcinoma in mice recapitulates gene signatures found in human liver cancer. PLoS One. 2020 Jun 19;15(6):e0234726. https://doi.org/10.1371/journal.pone.0234726

Chen S, Meng F, Sun X, Yao H, Wang Y, Pan Z, Yin Y, Jiao X. Epidemiology of human listeriosis in China during 2008–2017. Foodborne Pathog Dis. 2020 Feb 01;17(2):119–125. https://doi.org/10.1089/fpd.2019.2683

Costa AC, Pinheiro J, Reis SA, Cabanes D, Sousa S. *Listeria monocytogenes* interferes with host cell mitosis through its virulence factors InlC and ActA. Toxins (Basel). 2020 Jun 20;12(6):411–415. https://doi.org/10.3390/toxins12060411

Datta AR, Burall LS. Serotype to genotype: the changing landscape of listeriosis outbreak investigations. Food Microbiol. 2018 Oct;75:18–27. https://doi.org/10.1016/j.fm.2017.06.013

de las Heras A, Cain RJ, Bielecka MK, Vázquez-Boland JA. Regulation of *Listeria* virulence: PrfA master and commander. Curr Opin Microbiol. 2011 Apr;14(2):118–127. https://doi.org/10.1016/j.mib.2011.01.005

Dowd GC, Bahey-el-din M, Casey PG, Joyce SA, Hill C, Gahan CGM. *Listeria monocytogenes* mutants defective in gallbladder replication represent safety-enhanced vaccine delivery platforms. Hum Vaccin Immunother. 2016 Aug 02;12(8):2059–2063. https://doi.org/10.1080/21645515.2016.1154248

Drolia R, Bhunia AK. Crossing the intestinal barrier via *Listeria* adhesion protein and internalin A. Trends Microbiol. 2019 May;27(5):408–425. https://doi.org/10.1016/j.tim.2018.12.007

Gouin E, Balestrino D, Rasid O, Nahori MA, Villiers V, Impens F, Volant S, Vogl T, Jacob Y, Dussurget O, et al. Ubiquitination of *Listeria* virulence factor InlC contributes to the host response to infection. MBio. 2019 Dec 24;10(6):e02778–e19. https://doi.org/10.1128/mBio.02778-19

Ireton K, Mortuza R, Gyanwali GC, Gianfelice A, Hussain M. Role of internalin proteins in the pathogenesis of *Listeria monocytogenes*. Mol Microbiol. 2021 Dec;116(6):1407–1419. https://doi.org/10.1111/mmi.14836

Jia Y, Nightingale KK, Boor KJ, Ho A, Wiedmann M, McGann P. Distribution of internalin gene profiles of *Listeria monocytogenes* isolates from different sources associated with phylogenetic lineages. Foodborne Pathog Dis. 2007 Jun;4(2):222–232. https://doi.org/10.1089/fpd.2006.0081

Jianjun J. Disruption of InlC2 enhances the internalization of *Listeria monocytogenes* by epithelial cells. [PhD Thesis]. Shihezi (China): Shihezi University; 2011.

Lecuit M. *Listeria monocytogenes*, a model in infection biology. Cell Microbiol. 2020 Apr;22(4):e13186. https://doi.org/10.1111/cmi.13186

Liao Y, Wang J, Jaehnig EJ, Shi Z, Zhang B. WebGestalt 2019: gene set analysis toolkit with revamped UIs and APIs. Nucleic Acids Res. 2019 Jul 02;47 W1:W199–W205. https://doi.org/10.1093/nar/gkz401

Liu Y, Sun W, Sun T, Gorris LGM, Wang X, Liu B, Dong Q. The prevalence of *Listeria monocytogenes* in meat products in China: A systematic literature review and novel meta-analysis approach. Int J Food Microbiol. 2020 Jan;312:108358. https://doi.org/10.1016/j.ijfoodmicro.2019.108358

Matle I, Mbatha KR, Madoroba E. A review of *Listeria monocytogenes* from meat and meat products: Epidemiology, virulence factors, antimicrobial resistance and diagnosis. Onderstepoort J Vet Res. 2020 Oct 09;87(1):e1–e20. https://doi.org/10.4102/ojvr.v87i1.1869

Matsumoto H, Haniu H, Komori N. Determination of protein molecular weights on SDS-PAGE. Methods Mol Biol. 2019; 1855: 101–105. https://doi.org/10.1007/978-1-4939-8793-1_10

Medeiros M, Castro VHL, Mota ALAA, Pereira MG, De Martinis ECP, Perecmanis S, Santana AP. Assessment of internalin A gene sequences and cell adhesion and invasion capacity of *Listeria monocytogenes* strains isolated from foods of animal and related origins. Foodborne Pathog Dis. 2021 Apr 01;18(4):243–252. https://doi.org/10.1089/fpd.2020.2855

Mir SA. Structure and function of the important internalins of *Listeria monocytogenes*. Curr Protein Pept Sci. 2021 Dec 22;22(8): 620–628. https://doi.org/10.2174/1389203722666210902163300

Mitchell G, Cheng MI, Chen C, Nguyen BN, Whiteley AT, Kianian S, Cox JS, Green DR, McDonald KL, Portnoy DA. *Listeria monocytogenes* triggers noncanonical autophagy upon phagocytosis, but avoids subsequent growth-restricting xenophagy. Proc Natl Acad Sci USA. 2018 Jan 09;115(2):E210–E217. https://doi.org/10.1073/pnas.1716055115

Pereira MG, de Almeida OGG, da Silva HRA, Ishizawa MH, De Martinis ECP. Studies on host-foodborne bacteria in intestinal three-dimensional cell culture model indicate possible mechanisms of interaction. World J Microbiol Biotechnol. 2021 Feb;37(2):31. https://doi.org/10.1007/s11274-021-02996-6

Pizarro-Cerdá J, Cossart P. *Listeria monocytogenes*: cell biology of invasion and intracellular growth. Microbiol Spectr. 2018 Nov 02;6(6):57–69. https://doi.org/10.1128/microbiolspec.GPP3-0013-2018

Radoshevich L, Cossart P. *Listeria monocytogenes*: towards a complete picture of its physiology and pathogenesis. Nat Rev Microbiol. 2018 Jan;16(1):32–46. https://doi.org/10.1038/nrmicro.2017.126

Wang Y, Lu L, Lan R, Salazar JK, Liu J, Xu J, Ye C. Isolation and characterization of *Listeria* species from rodents in natural environments in China. Emerg Microbes Infect. 2017 Jan 01;6(1):1–6. https://doi.org/10.1038/emi.2017.28

Yi Z, Xie J. Comparative proteomics reveals the spoilage-related factors of *Shewanella putrefaciens* under refrigerated condition. Front Microbiol. 2021 Dec 3;12:740482. https://doi.org/10.3389/fmicb.2021.740482

Younis KM, Usup G, Ahmad A. Secondary metabolites produced by marine streptomyces as antibiofilm and quorum-sensing inhibitor of uropathogen *Proteus mirabilis*. Environ Sci Pollut Res Int. 2016 Mar;23(5):4756–4767. https://doi.org/10.1007/s11356-015-5687-9

ORIGINAL PAPER

Polish Journal of Microbiology
2022, Vol. 71, No 1, 73–81
https://doi.org/10.33073/pjm-2022-010

Detection by Whole-Genome Sequencing of a Novel Metallo-β-Lactamase Produced by *Wautersiella falsenii* Causing Urinary Tract Infection in Tunisia

RAOUAA MAAROUFI[1, 2, 3], OLFA DZIRI[2, 3, 4], LINDA HADJADJ[1], SEYDINA M. DIENE[1], JEAN-MARC ROLAIN[1] and CHEDLY CHOUCHANI[2, 3, 4]*

[1] Aix-Marseille Université MEPHI, AP-HM, IRD, IHU Méditerranée Infection, Marseille, France
[2] Laboratoire des Microorganismes et Biomolécules Actives, Faculté des Sciences de Tunis, Université Tunis El-Manar, Tunis, Tunisie
[3] Laboratoire de Recherche Sciences et Technologies de l'Environnement, Institut Supérieur des Sciences et Technologies de l'Environnement de Borj-Cedria, Hammam-Lif Université de Carthage, Tunisie
[4] Unité de Service en Commun pour la Recherche « Plateforme Génomique », Institut Supérieur des Sciences et Technologies de l'Environnement de Borj-Cedria, Hammam-Lif, Université de Carthage, Tunisie

Submitted 20 August 2021, accepted 22 November 2021, published online 27 February 2022

Abstract

Wautersiella falsenii is a rarely non-fermenting Gram-negative bacterium and belongs to the *Flavobacteriaceae* family. This nosocomial pathogen can cause several human infections, especially among immunocompromised patients. Here, we describe the whole genome sequence of a clinical *W. falsenii* strain isolated from a urine sample of a 35-year-old woman with a urinary tract infection in Tunisia. We investigated its phenotype and genotype.

After bacterial identification by the MALDI-TOF method, the whole-genome sequencing of this strain was performed. This isolate was not susceptible to various antibiotics, including β-lactams, aminoglycosides, and quinolones. However, it remains susceptible to imipenem (MIC = 0.25 mg/l), ertapenem (MIC = 0.75 mg/l), and meropenem (MIC = 0.19 mg/l). Interestingly, the E-TEST® (MP/MPI) showed a reduced MIC of meropenem +/– EDTA (0.064 µg/ml). Besides, the color change from yellow to red in the β CARBA test only after 24 hours of incubation can be interpreted in two ways. On the one hand, as a likely low expression of the gene encoding metallo-β-lactamase. On the other hand, and more likely, it may be a false-positive result because, according to the test manufacturer's recommendations, the test should be read after 30 minutes. Perhaps, therefore, this gene is not expressed in the tested strain. Moreover, the whole-genome sequence analysis demonstrated the presence of a novel chromosomally located subclass B1 metallo-β-lactamase EBR-like enzyme, sharing 94.92% amino acid identity with a previously described carbapenemase produced by *Empedobacter brevis*, EBR-1. The results also showed the detection of other antibiotic resistance genes and the absence of plasmids. So far, this study is the first report on the detection of *W. falsenii* in Tunisia. These findings prove that *W. falsenii* could be a potential reservoir of antibiotic resistance genes, e.g., β-lactamases. Collaborative efforts and effective hygiene measures should be established to prevent the emergence of this species in our health care settings.

Keywords: MALDI-TOF, *Wautersiella falsenii*, whole-genome sequencing, metallo-β-lactamase, urinary tract infection, Tunisia

Introduction

Wautersiella falsenii, also known as *Empedobacter falsenii*, was first described in 2006 (Kämpfer et al. 2006; Zhang et al. 2014). This non-fermentative Gram-negative species belongs to the *Flavobacteriaceae* family and is characterized as a non-motile rod-shaped bacterium, positive for indole and urease production (Kämpfer et al. 2006). In addition, it grows aerobically at 37°C on standard media, such as blood agar, tryptic soy agar, or MacConkey agar (Kämpfer et al. 2006; Zhang et al. 2014). To our knowledge, this species is the only member of the *Wautersiella* genus, and it is most closely related to *Empedobacter brevis*, showing 94–95% similarity of the 16S rRNA gene sequences (Kämpfer et al. 2006). However, a previous study reported the detection of three bacterial isolates obtained from poultry, showing 97.2% of similarity with the 16S rRNA

* Corresponding author: Ch. Chouchani, Laboratoire de Recherche Sciences et Technologies de l'Environnement, Institut Supérieur des Sciences et Technologies de l'Environnement de Borj-Cedria, Hammam-Lif Université de Carthage, Tunisie;
e-mail: chedly.chouchani@gmail.com

gene of *W. falsenii*. These findings exhorted researchers to propose that these related isolates could be classified as new species of *Wautersiella* genus associated with poultry (Christensen and Bisgaard 2010). *W. falsenii* was rarely detected in clinical isolates that could be explained by the difficulty of its identification (Van der Velden et al. 2012). Indeed, the choice of the identification method for this species is very important. As previously described, the use of the Phoenix automated identification system could misidentify the isolate as *Sphingomonas paucimobilis*, unlike the MALDI-TOF MS, which identifies it correctly (Van der Velden et al. 2012).

Few data are describing the detection of *W. falsenii* species on an international scale. Even if it was rarely reported, it was recovered from various clinical specimens like blood, ear discharges, oral cavity, pleural fluid, pus, respiratory tract, vaginal swabs, wounds, urine, and cervical neck abscess samples (Kämpfer et al. 2006; Van der Velden et al. 2012; Traglia et al. 2015). It was also recovered from other origins, noting the metalworking aerosols and fluids (Perkins and Angenent 2010), the tiled carpet surface of hospitals (Harris et al. 2010), soils, polluted sediment, and rodent skin (Maleki-Ravasan et al. 2015). This species presents a potential risk to human health since it has been considered a reservoir of antibiotic resistance genes (Traglia et al. 2015). In fact, *W. falsenii* isolates are generally identified as resistant to several antibiotics, including those of the last resort, carbapenems, and colistin (Van der Velden et al. 2012; Traglia et al. 2015). It could also contribute to the spread of resistance genes to other pathogens, especially those coding for β-lactamases (Collins et al. 2018). In addition, recent studies have reported the detection of genes coding for novel subclass B1 metallo-β-lactamases among this uncommon nosocomial pathogen, named EBR-2 (Collins et al. 2018) and EBR-3 (WP_150823468.1).

A detailed analysis of the whole genome of *W. falsenii*, using the high-throughput sequencing technologies, is needed to decipher the genome of this species, explain its phenotype, and understand the different molecular mechanisms involved in antibiotic resistance. Thus, the main objectives of our study were as described above. The whole-genome sequencing seems to be a key to the detection of novel antibiotic resistance features (Collins et al. 2018). In the present study, we report for the first time the detection of a novel chromosomally located metalloenzyme in *W. falsenii* isolate recovered in 2016 from the urine sample of a Tunisian woman that suffered from a urinary tract infection. To our knowledge, this is the first case reported in Tunisia and the third in the world after the two previously reported cases in Netherlands and India (Van der Velden et al. 2012; Zaman et al. 2017).

Experimental

Materials and Methods

Clinical data and bacterial identification. In 2016, a 35-year-old woman was presented in a private medical office with symptoms of the urinary tract infection (UTIs). She had a fever, pain in the lower abdomen, and a burning sensation in the urinary tract. This non-hospitalized patient had not have a previous UTI in her medical history. Her doctor requested a cyto-bacteriological urine examination to check the causes of these symptoms.

The urine sample was submitted to a private medical analysis laboratory in El Kram, Tunisia. The sample was cultured on a nutrition agar medium and was incubated for 24 hours at 37°C in order to isolate the microorganism causing the urinary tract infection. The isolate was then identified using the matrix-assisted laser desorption ionization-time of flight mass spectrometry (MALDI-TOF MS) method. Moreover, there is no information about the antibiotic treatment taken by this infected patient.

Antimicrobial susceptibility testing. The antimicrobial susceptibility testing of the isolated bacterium was performed using the standard disk diffusion method on Mueller-Hinton E agar medium (MHE BioMérieux, Marcy-l'Etoile, France). The results were interpreted using Scan 4000® (Interscience, Saint Nom la Breteche, France), according to the Antibiogram Committee of the French Society for Microbiology (Société Française de Microbiologie 2019) and the Clinical and Laboratory Standards Institute guidelines (CLSI 2019). Thus, a total of 34 antibiotics were tested as follow: amoxicillin (AX); amoxicillin/clavulanic acid (AMC); ticarcillin (TIC); ticarcillin/clavulanic acid (TIM); cefepime (FEP); colistin (CS); amikacin (AK); tobramycin (TOB); streptomycin (S); spectinomycin (SPT); ciprofloxacin (CIP); pefloxacin (PEF); nalidixic acid (NA); furans (FF); nitrofurantoin (F); doxycycline (DO); tigecycline (TGC); piperacillin/tazobactam (TPZ); temocillin (TEL); cefoxitin (FOX); cephalothin (KF); ceftriaxone (CRO); cefotaxime (CTX); aztreonam (ATM); ertapenem (ETP); meropenem (MEM); imipenem (IPM); gentamicin (CN), kanamycin (K), ofloxacin (OFX), minocycline (MI), trimethoprim/sulfamethoxazole (SXT); rifampicin (RA) and sulfadiazine (SD).

Whole-genome sequencing and genomic analysis. Genomic DNA was extracted using the EZ1 DNA Kit (Qiagen, Courtaboeuf, France). Then, the whole-genome sequencing (WGS) was performed for *W. falsenii* isolate using Illumina MiSeq sequencer. The obtained sequences were assembled by Spades assembler and annotated using the PROKKA program. In

addition, the research of the presence of antibiotic resistance genes and plasmids was carried out using ARGANNOT and PlasmidFinder programs, respectively. Besides, for phylogenetic analysis, the conserved proteins sequences of different carbapenemases, detected among the *Flavobacteriaceae* family and other Gram-negative bacteria, were downloaded from the NCBI database and were independently aligned using MUSCLE to cluster homologous sequences.

Moreover, the screening of virulence genes was performed using the Virulence Factor Database (VFDB, http://www.mgc.ac.cn/VFs/) and the virulence Finder Database available at the Center for Genomic Epidemiology server (https://cge.cbs.dtu.dk/services/VirulenceFinder/). Besides, the bacteria's pathogenicity towards human hosts was also investigated (https://cge.cbs.dtu.dk/services/PathogenFinder/).

Phenotypic screening of carbapenemase production. The Minimal Inhibitory Concentrations (MICs) were determined for only imipenem, meropenem, and ertapenem, using the E-TEST® method (Biomérieux, Marcy l'Etoile, France). The MIC results were interpreted using the CLSI guidelines (CLSI 2019).

The detection of carbapenemase production was carried out using the β CARBA test. This colorimetric test is based on the change of color of a chromogenic substrate in the presence of carbapenemase-producing isolate. Thus, the presence of carbapenem-hydrolyzing activity is justified by the color change from yellow to orange-red, or even to purple after 30 minutes of incubation at 37°C using an NDM producing *Escherichia coli* as a positive control (Meier and Hamprecht 2019). The results were also interpreted after 1 hour and 24 hours of incubation at 37°C of *W. falsenii* isolate.

Moreover, an E-TEST® gradient strip (MP/MPI) was used to investigate the production of metallo-β-lactamases (MBLs). This reagent strip contains increasing concentrations of meropenem antibiotic (MP) on one end and meropenem supplemented with a constant level of EDTA (MPI) on the other. The EDTA inhibits MBLs' activity by chelating their active site zinc ions. Thus, a difference between the two MIC results reveals the production of a metallo-β-lactamase by the tested isolate (Girlich et al. 2013).

Results

Bacterial isolate. The cyto-bacteriological urine examination of the patient concerned showed a high number of leukocytes and epithelial cells, thus proving the urinary tract infection. The primary phenotypic tests of the urine culture showed the presence of a non-lactose fermenting Gram-negative rod, characterized as positive for oxidase production. This isolate was then identified as *W. falsenii* using MALDI-TOF MS, showing a high score value equal to 2.230.

Antimicrobial susceptibility testing. According to the antimicrobial susceptibility results, *W. falsenii* isolate showed a multi-drug resistance profile. Thus, it was resistant to several antibiotics (n = 13) that belong to different families, noting β-lactams (amoxicillin, amoxicillin/clavulanic acid, ticarcillin, and ticarcillin/clavulanic acid), aminoglycosides (amikacin, tobramycin, streptomycin, and spectinomycin), quinolones (ciprofloxacin, pefloxacin, and nalidixic acid), furans, and nitrofurantoin as shown in Table I. It was intermediate resistant to two antibiotics, doxycycline, and tigecycline. However, it was sensitive to the other 19 tested antibiotics listed above in the Material and Methods section, including carbapenems, third-generation cephalosporins, gentamicin, rifampicin, and colistin. This isolate had low minimal inhibitory concentrations (MIC) for imipenem (0.25 mg/l), ertapenem (0.75 mg/l), and meropenem (0.19 mg/l).

Genomic analysis. The whole-genome sequence of this rare bacterium was obtained using the Illumina MiSeq sequencer (Illumina, San Diego, CA, USA). The complete genome showed a total of 3,215,391-bp. Thus, it was assembled into 129 contigs with a minimum contig size of 58,696-bp and a maximum contig size of 206,832-bp. The genome annotation predicts 2,982 coding sequences (CDS). The obtained whole-genome sequence of this isolate has been submitted at the DDBJ/ENA/GenBank under the accession number JAIKTW000000000. As expected, the genome analysis of the WGS revealed the presence of three genes, bla_{EBR}, *tetX*, and *aadS*. No plasmid has been identified within the genome sequences. Besides, no virulence genes have been detected in our isolate. Also, no pathogenicity factors were found. Indeed, this isolate was predicted as a non-human pathogen, noting a very low probability of being (0.217).

Despite being susceptible to carbapenems (imipenem, meropenem, and ertapenem), this isolate exhibits a chromosomally located gene coding for a subclass-B1 metallo-β-lactamase. This enzyme presented 94.92% protein sequence similarity with a previously described carbapenemase produced by *E. brevis*, the EBR-1 enzyme (AF416700). Also, it showed 95.74% protein sequence similarity with the EBR-3 produced by *E. falsenii* (WP_150823468.1).

Furthermore, the phylogenetic tree, based on the protein sequences of the serine β-lactamases (Class A, C, and D) as well as the metallo-β-lactamases (Class B), showed that our obtained protein sequence was clustered in the group of the metallo-β-lactamases, particularly in the subclass B1 (Fig. 1). Thus, it was closely related to the three metallo-β-lactamases produced by *Flavobacteriaceae* (*E. brevis* and *E. falsenii*), noting

Table I
Comparison between all reported *Wautersiella falsenii* bacterial infections and that of the present study.

Reference	Number of isolates	Years of isolation	Country	Gender and age of infected patients	Patient suffered from	Clinical specimens	Phenotypic resistance pattern	Detected genes	Detected plasmids
Kämpfer et al. 2006	26	1980–2004	Belgium	–	–	blood, wounds, pus, respiratory tract, ear discharge, oral cavity, vaginal swab, pleural fluid, and other from an unknown origin	–	–	–
Van der Velden et al. 2012	1	2012	Netherlands	one-year-old girl	pyelonephritis	urine	nitrofurantoin, amoxicillin-clavulanic acid, piperacillin-tazobactam, ceftriaxone, ceftazidime, meropenem, tobramycin, and colistin	–	–
Traglia et al. 2015	1	2013	Argentina	18-year-old woman	acute otitis media	cervical neck abscess	ampicillin, ampicillin-sulbactam, cephalothin, meropenem, colistin	29 genes coding for efflux pumps, and tripartite multidrug resistance systems, class a β-lactamase, metallo-β-lactamase (ebr-2), three class c β-lactamases, resistance to streptogramin trimethoprim, bacitracin, and macrolide	none
Giordano et al. 2016	1	2016	Italy	32-year-old man	lymphoblastic leukemia	the respiratory tract	amikacin, amikacin-clavulanic acid, ampicillin-sulbactam, cefotaxime, ceftazidime, doripenem, gentamicin, imipenem, piperacillin-tazobactam	–	–
Zaman et al. 2017	1	2017	India	five-year-old boy	bladder cancer	urine	ampicillin, ampicillin-sulbactam, and colistin.	–	–
This study	1	2016	Tunisia	35-year-old woman	UTI	urine	amoxicillin, amoxicillin-clavulanic acid, ticarcillin, ticarcillin-clavulanic acid, amikacin, tobramycin, streptomycin, spectinomycin, ciprofloxacin, pefloxacin, nalidixic acid, furans, nitrofurantoin	$bla_{\text{EBR-like}}$, *TetX* and *aadS*	none

– – not studied

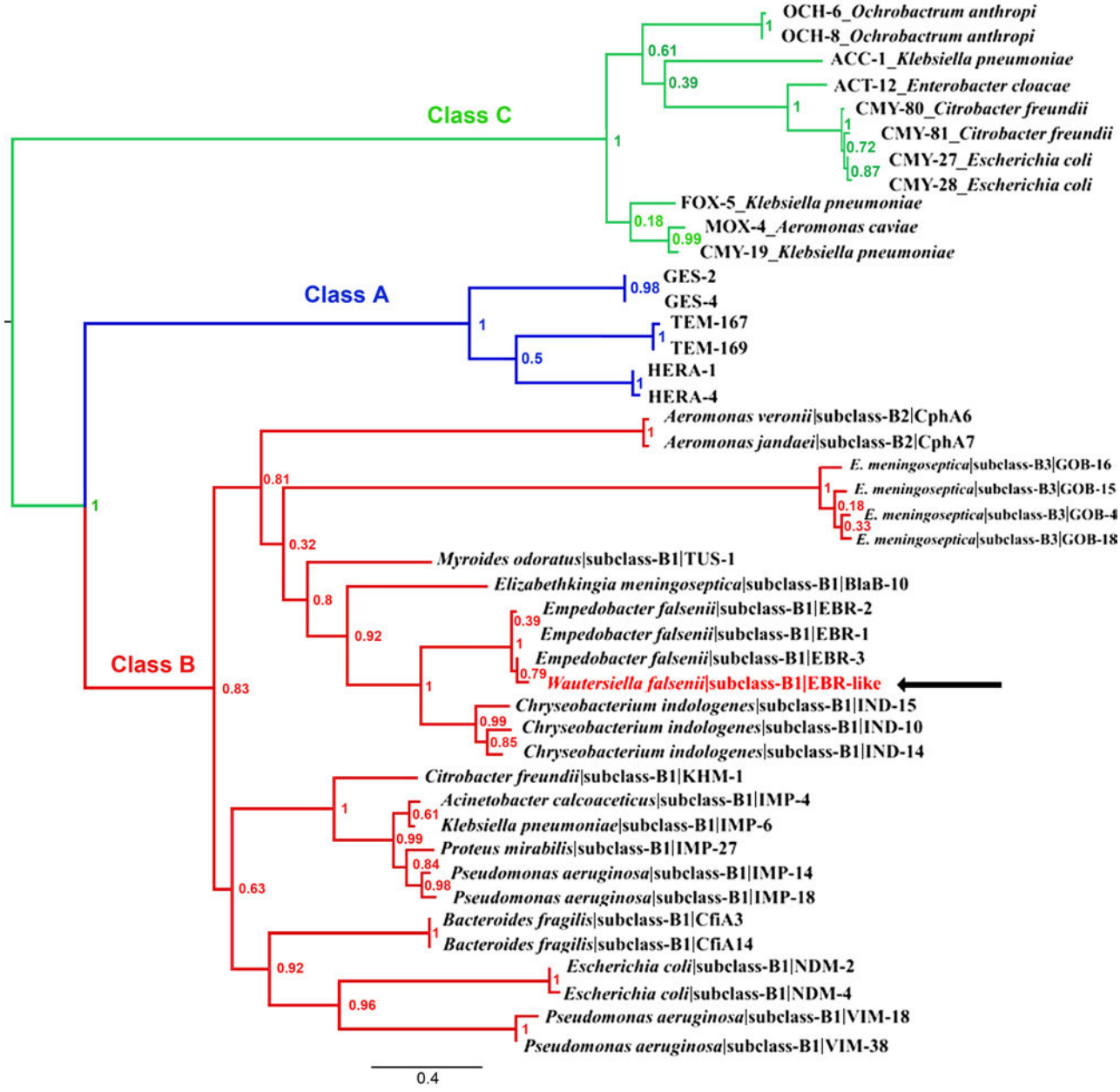

Fig. 1. Phylogenetic tree based on the protein sequences of; serine β-lactamase (Class A and Class C) and metallo-β-lactamase (Class B).

EBR-1, EBR-2, and EBR-3, showing a Bootstrap percentage greater than 70% based on maximum likelihood analyses of 1,000 replications, as presented at the node (Fig. 1).

Moreover, the alignment of our concerned protein sequence with those of other metallo-β-lactamases was presented in Fig. 2. Indeed, the conserved motif of the MBL active site (HxHxDH) and the residues of metallo-β-lactamases were highlighted by yellow color. These results confirmed that *W. falsenii* isolate produced a novel subclass-B1 metallo-β-lactamase, belonging to the EBR-like family enzyme.

Phenotypic detection of carbapenemase production. To verify the obtained WGS result, we tested the minimal inhibitory concentration (MIC) for carbapenems by E-TEST® MBL strip (Biomérieux, Marcy l'Etoile, France). This isolate had a low minimal inhibitory concentration for; imipenem (0.25 mg/l) and ertapenem (0.75 mg/l). Using the β CARBA NP test, a change of color from yellow to red was observed only after 24 hours of incubation of *W. falsenii* isolate, contrary to the positive control isolate, which showed a color shift after only thirty minutes of incubation. The color change from yellow to red in the β CARBA test only after 24 hours of incubation can be interpreted in two ways. On the one hand, as a likely low expression of the gene encoding metallo-β-lactamase. On the other hand, and more likely, it may be a false-positive result because, according to the test manufacturer's recommendations, the test should be read after 30 minutes. Perhaps,

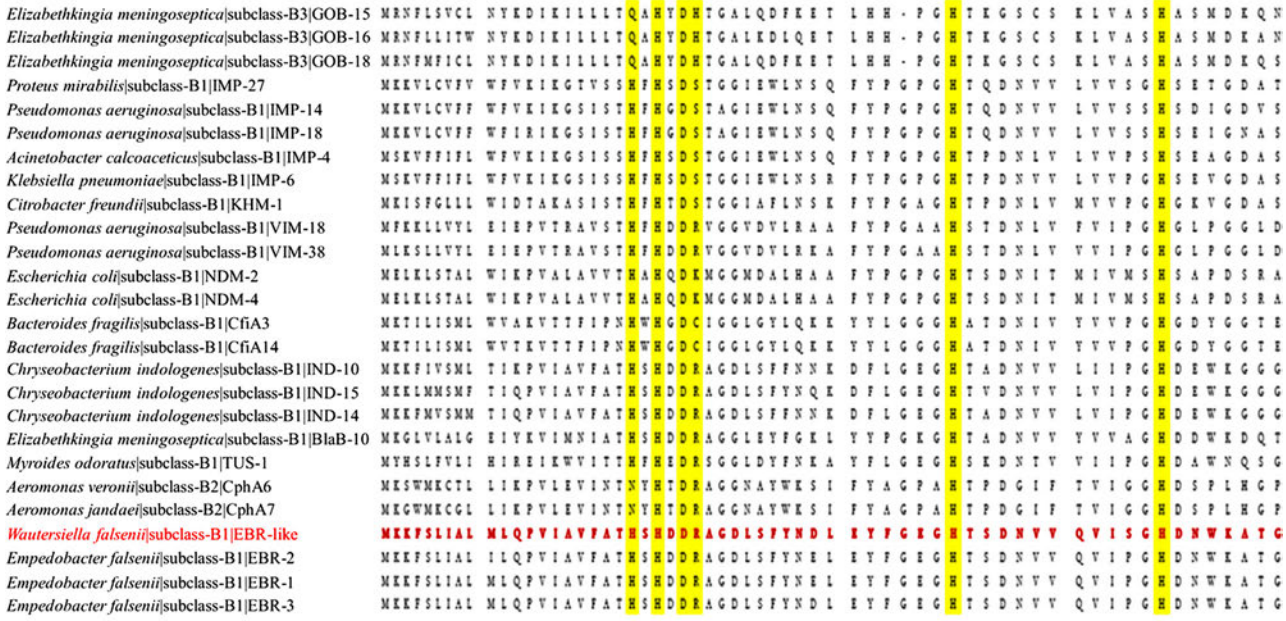

Fig. 2. Protein alignment among the metallo-β-lactamase type B genes: Our sequence was represented with red color. The conserved motif of the MBL "HxHxDH" presented in their active site, and residues of bacterial metallo-β-lactamase enzymes were represented with a yellow color.

therefore, this gene is not expressed in the tested strain. It is noteworthy that these results were confirmed using the E-TEST® strip (MP/MPI). Besides, a significant difference between the two MICs for meropenem (0.19 mg/l) and meropenem + EDTA (0.064 mg/l) was observed. Indeed, this result proved the production of a metallo-β-lactamase by our isolate.

Discussion

Since its first description in 2006, *W. falsenii* has become a real concern and a severe nosocomial pathogen, even if it has been rarely reported (Kämpfer et al. 2006). Indeed, it was isolated from various clinical origins (blood, wounds, pus, respiratory tract, ear discharge, oral cavity, vaginal swab, pleural fluid, cervical neck abscess sample, and urine), causing thus several infections types (Kämpfer et al. 2006; Van der Velden et al. 2012; Traglia et al. 2015). Few studies are describing the detection of *W. falsenii* isolates throughout the globe. Besides, all reported *W. falsenii* bacterial infections were presented in Table I and compared with the isolate detected. Moreover, we noticed the lack of information about *W. falsenii* species, including detected genes and plasmids. In-depth studies of this species are very required in order to understand its basis genomic. To date, only one study detailing the whole-genome analysis of this non-fermentative Gram-negative bacterium was reported (Collins et al. 2018). The present study is the second report deciphering the genome of *W. falsenii* in the world.

As previously reported, all *W. falsenii* isolates were detected among hospitalized patients, especially among the immunosuppressed patients of a young age (Christensen and Bisgaard 2010; Giordano et al. 2016). However, our isolate was detected among a non-hospitalized patient suffering from a urinary tract infection. To the best of our knowledge, our study is the first report describing the detection of *W. falsenii* causing UTI in Tunisia and the third in the world after the two reported cases in Netherlands and India (Van der Velden et al. 2012; Meier and Hamprecht 2019). Thus, the first case was detected among a one-year-old child with a complicated UTI in 2012 (Van der Velden et al. 2012) and the second among a five-year-old child with bladder cancer (Meier and Hamprecht 2019). The detection of such isolate has not been hitherto detected in Tunisia.

What is more, studying the whole-genome sequence of this isolate allowed us to detect a novel chromosomally located gene coding for a subclass-B1 metallo-β-lactamase. The obtained results of the β CARBA test and the E-TEST® (MP/MPI), which showed a metallo-β-lactamase at a low level, confirmed these findings. Besides, the color change from yellow to red in the β CARBA test only after 24 hours of incubation can be interpreted in two ways. On the one hand, as a likely low expression of the gene encoding metallo-β-lactamase EBR-1. On the other hand, and more likely, it may be a false-positive result because, according to the test manufacturer's recommendations, the test should be read after 30 minutes. Perhaps, therefore, this gene is not expressed in the tested strain. Thus,

the comparison of the protein sequences revealed that our detected enzyme was closely related to the three metallo-β-lactamases produced by *Flavobacteriaceae* (EBR-1, EBR-2, and EBR-3). Indeed, the analysis of this sequence by the ARGANNOT-database showed that it presented a 94.89 % protein sequence similarity with the EBR-1 enzyme produced by *E. brevis* (AF416700) (Bellais et al. 2002a). Moreover, high similarity percentages equal to 95.74% and 94.04% were recorded when compared, by the NCBI database, our obtained protein sequence with EBR-3 (WP_150823468.1), and EBR-2 produced by *E. falsenii* (Collins et al. 2018), respectively. However, it shared only 57.69% amino acid identity with the IND-1 enzyme produced by *Chryseobacterium indologenes* (Bellais et al. 1999; Bellais et al. 2000b). Besides, other bacterial species of *Flavobacteriaceae* family produced several carbapenem-hydrolyzing Ambler class B enzymes, including EBR-1 from *E. brevis* (Perkins and Angenent 2010), BlaB and GOB from *Chryseobacterium meningoseptica* (Rossolini et al. 1998; Bellais et al. 2000a), IND from *C. indologenes* (Bellais et al. 1999; Bellais et al. 2000b), CGB-1 from *Chryseobacterium gleum* (Bellais et al. 2002b), a β-lactamase from *Flavobacterium odoratum* (Sato et al. 1985).

In addition, the phylogenetic analysis, based on the comparison of the published protein sequences, revealed that our obtained protein sequence was clustered in the same group of those detected among the *Flavobacteriaceae* family. Besides, we have also identified the conserved domain of the metallo-β-lactamases. All these findings confirmed that the detected enzyme belonged to the subclass-B1 metallo-β-lactamase, especially the EBR-like family. This study is the first to report the detection of the EBR-like enzyme in Tunisia.

The whole-genome sequencing analysis also revealed the presence of several other genes associated with other antibiotic resistance. Indeed, we noted the detection of the tetracycline-inactivating monooxygenase encoding gene, *tetX*, with a 99.74 % identity. This chromosomally encoded *tetX* gene confers a low level of tigecycline resistance in *W. falsenii* isolate with a MIC value equal to 3 mg/l. The tetracycline destructase, such as Tet(X), represents a unique enzymatic tetracycline inactivation mechanism (Forsberg et al. 2015). Indeed, this mechanism has been confirmed for in vitro activity, showing the degradation of all tetracyclines, including tigecycline (Moore et al. 2005).

Additionally, we described another gene, named *aadS* and showed a 99.77% identity. This gene is associated with streptomycin-resistance in *W. falsenii* isolate, and codes for the aminoglycoside 6-adenylyltransferase. The aadS-encoded peptide demonstrated a significant homology to Gram-positive streptomycin-dependent adenyltransferases (Smith et al. 1992). It was phenotypically silent in the wild-type *Bacteroides* (Smith et al. 1992). The aminoglycosides are known as broad-spectrum antibacterial compounds and are used extensively to treat bacterial infections (Davies and Wright 1997; Ramirez and Tolmasky 2010). Thus, the genes, coding for resistance to this antibiotic family, are prevalent among Gram-positive bacteria (Vakulenko and Mobashery 2003; Tolmasky 2007), noting that enzymatic modification like streptomycin-modifying enzymes is considered as the most prevalent mechanism conferring resistance to aminoglycosides in the clinical settings (Ramirez and Tolmasky 2010).

Moreover, the *aadS* gene was identified in many organisms; *Bacteroidetes* (WP_003013318.1), *Elizabethkingia anophelis* (WP_009086755.1), *Elizabethkingia meningoseptica* (WP_016169991.1), *Flavobacteriaceae* (WP_010257826.1) and *Chryseobacterium* (WP_007842749.1): *C. indologenes* (ID: 41187294), *Chryseobacterium scophthalmum* (ID: 41008694), *Chryseobacterium vrystaatense* (ID: 35824473). Otherwise, we have noted the absence of plasmids in this isolate as previously described (Collins et al. 2018). These findings suggest that *W. falsenii* species is naturally resistant to several antibiotics, and it could be a potential reservoir of the antibiotic resistance encoding genes.

Conclusions

The emergence of infections caused by the uncommon Gram-negative bacteria such as *W. falsenii* constitutes a real concern. Although this species was rarely detected, it should not be ignored. To date, the MALDI-TOF method represents the best way to identify this species. Thus, it was very required to decipher its genomic basis using the high throughput sequencing technologies to explain its phenotype and understand its genotype. Indeed, the characterization of the different molecular mechanisms involved in antibiotic resistance could orient the therapeutic decisions. We report in this work a novel chromosomally located metallo-β-lactamase, EBR-like enzyme in *W. falsenii* isolate, causing the urinary tract infection. Interestingly, we have noted a color change from yellow to red in the β CARBA test only after 24 hours of incubation that can be interpreted in two ways. On the one hand, as a likely low expression of the gene encoding metallo-β-lactamase. On the other hand, and more likely, it may be a false-positive result because, according to the test manufacturer's recommendations, the test should be read after 30 minutes. Perhaps, therefore, this gene is not expressed in the tested strain. To the best of our knowledge, this is the first detection of *W. falsenii* isolate in Tunisia. Besides, effective hygiene measures were also required to avoid the spread of this species in healthcare settings.

ORCID
Chedly Chouchani https://orcid.org/0000-0002-8294-8289

Accession numbers

This Whole Genome Shotgun project has been deposited at DDBJ/ENA/GenBank under the accession JAIKTW000000000. The version described in this paper is version JAIKTW010000000.

Funding

This work was partly funded by IHU Méditerranée Infection, Aix-Marseille-University in France. This work was supported by the Tunisian Ministry of Higher Education and Scientific Research and Campus France Under the PHC-Utique project (Code 18G0819), which offered a scholarship to Miss Raouaa MAAROUFI to attend the IHU Méditerranée Infection, Aix-Marseille-University in France.

Conflict of interest

The authors do not report any financial or personal connections with other persons or organizations, which might negatively affect the contents of this publication and/or claim authorship rights to this publication.

Literature

Bellais S, Aubert D, Naas T, Nordmann P. Molecular and biochemical heterogeneity of class B carbapenem-hydrolyzing-lactamases in *Chryseobacterium meningosepticum*. Antimicrob Agents Chemother. 2000a Jul;44(7):1878–1886. https://doi.org/10.1128/AAC.44.7.1878-1886.2000

Bellais S, Girlich D, Karim A, Nordmann P. EBR-1, a novel Ambler subclass B1 Beta-lactamase from *Empedobacter brevis*. Antimicrob Agents Chemother. 2002a Oct;46(10):3223–3227. https://doi.org/10.1128/AAC.46.10.3223-3227.2002

Bellais S, Léotard S, Poirel L, Naas T, Nordmann P. Molecular characterization of a carbapenem-hydrolyzing-lactamase from *Chryseobacterium* (*Flavobacterium) indologenes*. FEMS Microbiol Lett. 1999 Feb 15;171(2):127–132. https://doi.org/10.1111/j.1574-6968.1999.tb13422.x

Bellais S, Naas T, Nordmann P. Genetic and biochemical characterization of CGB-1, a novel Ambler class B carbapenem-hydrolyzing Beta-lactamase from *Chryseobacterium gleum*. Antimicrob Agents Chemother. 2002b Sep;46(9):2791–2796. https://doi.org/10.1128/AAC.46.9.2791-2796.2002

Bellais S, Poirel L, Leotard S, Naas T, Nordmann P. Genetic diversity of carbapenem-hydrolyzing metallo-b-lactamases from *Chryseobacterium* (*Flavobacterium*) *indologenes*. Antimicrob Agents Chemother. 2000b Nov;44(11):3028–3034. https://doi.org/10.1128/AAC.44.11.3028-3034.2000

Christensen H, Bisgaard M. Phylogenetic relationships of *Riemerella anatipestifer* serovars and related taxa and an evaluation of specific PCR tests reported for *R. anatipestifer*. J Appl Microbiol. 2010 May;108(5):1612–1619. https://doi.org/10.1111/j.1365-2672.2009.04558.x

CLSI. Performance standards for antimicrobial susceptibility testing. 29th ed. CLSI supplement M100. Wayne (USA): Clinical and Laboratory Standards Institute; 2019.

Collins C, Almuzara M, Saigo M, Montaña S, Chiem K, Traglia G, Mussi MA, Tolmasky M, Iriarte A, Vay C, et al. Whole-Genome Analysis of an extensively drug-resistance *Empedobacter falsenii* strain reveals distinct features and the presence of a novel metallo-β-lactamase (EBR-2). Curr Microbiol. 2018 Aug;75(8):1084–1089. https://doi.org/10.1007/s00284-018-1498-9

Davies J, Wright GD. Bacterial resistance to aminoglycoside antibiotics. Trends Microbiol. 1997 Jun;5(6):234–240. https://doi.org/10.1016/S0966-842X(97)01033-0

Forsberg KJ, Patel S, Wencewicz TA, Dantas G. The tetracycline destructases: a novel family of tetracycline-inactivating enzymes. Chem Biol. 2015 Jul 23;22(7):888–897. https://doi.org/10.1016/j.chembiol.2015.05.017

Giordano C, Falleni M, Capria AL, Caracciolo F, Petrini M, Barnini S. First report of *Wautersiella falsenii* genomovar 2 isolated from the respiratory tract of an immunosuppressed man. IDCases. 2016 Mar 5;4:27–29. https://doi.org/10.1016/j.idcr.2016.02.009

Girlich D, Halimi D, Zambardi G, Nordmann P. Evaluation of Etest® strips for detection of KPC and metallo-carbapenemases in *Enterobacteriaceae*. Diagn Microbiol Infect Dis. 2013 Nov;77(3):200–201. https://doi.org/10.1016/j.diagmicrobio.2013.08.002

Harris DD, Pacheco A, Lindner AS. Detecting potential pathogens on hospital surfaces: an assessment of carpet tile flooring in the hospital patient environment. Indoor Built Environ. 2010;19(2):239–249. https://doi.org/10.1177/1420326X09347050

Kämpfer P, Avesani V, Janssens M, Charlier J, De Baere T, Vaneechoutte M. Description of *Wautersiella falsenii* gen. nov., sp. nov., to accommodate clinical isolates phenotypically resembling members of the genera *Chryseobacterium* and *Empedobacter*. Int J Syst Evol Microbiol. 2006 Oct;56(10):56:2323–2329. https://doi.org/10.1099/ijs.0.64393-0

Maleki-Ravasan N, Oshaghi MA, Afshar D, Arandian MH, Hajikhani S, Akhavan AA, Yakhchali B, Shirazi MH, Rassi Y, Jafari R, et al. Aerobic bacterial flora of biotic and abiotic compartments of a hyperendemic Zoonotic Cutaneous Leishmaniasis (ZCL) focus. Parasit Vectors. 2015 Jan 29;8:63. https://doi.org/10.1186/s13071-014-0517-3

Meier M, Hamprecht A. Systematic comparison of four methods for detection of carbapenemase-producing *Enterobacterales* directly from blood cultures. J Clin Microbiol. 2019 Oct 23;57(11):e00709-19. https://doi.org/10.1128/JCM.00709-19

Moore IF, Hughes DW, Wright GD. Tigecycline is modified by the flavin-dependent monooxygenase TetX. Biochemistry. 2005 Sep 6;44(35):11829–11835. https://doi.org/10.1021/bi0506066

Perkins SD, Angenent LT. Potential pathogenic bacteria in metalworking fluids and aerosols from a machining facility. FEMS Microbiol Ecol. 2010 Dec;74(3):643–654. https://doi.org/10.1111/j.1574-6941.2010.00976.x

Ramirez MS, Tolmasky ME. Aminoglycoside Modifying Enzymes. Drug Resist Updat. 2010 Dec;13(6):151–171. https://doi.org/10.1016/j.drup.2010.08.003

Rossolini GM, Franceschini N, Riccio ML, Mercuri PS, Perilli M, Galleni M, Frere JM, Amicosante G. Characterization and sequence of the *Chryseobacterium* (*Flavobacterium*) *meningosepticum* carbapenemase: a new molecular class B β-lactamase showing a broad substrate profile. Biochem J. 1998 May 15;332 (1):145–152. https://doi.org/10.1042/bj3320145

Sato K, Fujii T, Okamoto R, Inoue M, Mitsuhashi S. Biochemical properties of beta-lactamase produced by *Flavobacterium odoratum*. Antimicrob Agents Chemother. 1985 Apr;27(4):612–614. https://doi.org/10.1128/AAC.27.4.612

Smith CJ, Owen C, Kirby L. Activation of a cryptic streptomycin-resistance gene in the *Bacteroides erm* transposon, *Tn4551*. Mol Microbiol. 1992 Aug;6(16):2287–2297. https://doi.org/10.1111/j.1365-2958.1992.tb01404.x

Société Française de Microbiologie. CASFM/EUCAST: Société Française de Microbiologie Ed. Paris (France): Société Française de Microbiologie; 2019. [cited 2021 Jul 01]. Available from https://www.sfm-microbiologie.org/2019/01/07/casfm-eucast-2019

Tolmasky ME. Aminoglycoside-modifying enzymes: characteristics, localization, and dissemination. In: Bonomo RA, Tolmasky ME, editors. Enzyme-mediated resistance to antibiotics: mechanisms, dissemination, and prospects for inhibition. Washington (USA): ASM Press; 2007. p. 35–52.
https://doi.org/10.1128/9781555815615.ch4

Traglia GM, Dixon C, Chiem K, Almuzara M, Barberis C, Montana S, Merino C, Mussi MA, Tolmasky ME, Iriarte A, et al. Draft genome sequence of *Empedobacter* (Formerly *Wautersiella*) *falsenii* comb. nov. Wf282, a strain isolated from a cervical neck abscess. Genome Announc. 2015 Apr 2;3(2):e00235-15.
https://doi.org/10.1128/genomeA.00235-15

Vakulenko SB, Mobashery S. Versatility of aminoglycosides and prospects for their future. Clin Microbiol Rev. 2003 Jul;16(3):430–450.
https://doi.org/10.1128/CMR.16.3.430-450.2003

Van der Velden LBJ, de Jong AS, de Jong H, de Gier RPE, Rentenaar RJ. First report of a *Wautersiella falsenii* isolated from the urine of an infant with pyelonephritis. Diagn Microbiol Infect Dis. 2012 Dec;74(4):404–405.
https://doi.org/10.1016/j.diagmicrobio.2012.08.008

Zaman K, Gupta P, Kaur V, Mohan B, Taneja M. *Empedobacter falsenii*: A rare non-fermenter causing urinary tract infection in a child with bladder cancer. SOA Clin Med Cases Rep Rev. 2017; 1(1):002.

Zhang RG, Tan X, Liang Y, Meng TY, Liang HZ, Lv J. Description of *Chishuiella changwenlii* gen. nov., sp. nov., isolated from freshwater, and transfer of *Wautersiella falsenii* to the genus *Empedobacter* as *Empedobacter falsenii* comb. nov. Int J Syst Evol Microbiol. 2014 Aug;64(Pt 8):2723–2728.
https://doi.org/10.1099/ijs.0.063115-0

ORIGINAL PAPER

Polish Journal of Microbiology
2022, Vol. 71, No 1, 83–90
https://doi.org/10.33073/pjm-2022-011

Screening of *mcr-1* among Gram-Negative Bacteria from Different Clinical Samples from ICU Patients in Alexandria, Egypt: One-Year Study

AMIRA ELBARADEI[1, 2]*, MAHROUS S. SAYEDAHMED[3], GAMAL EL-SAWAF[3] and SHERINE M. SHAWKY[3]

[1] Department of Microbiology and Immunology, Faculty of Pharmacy, Pharos University in Alexandria, Alexandria, Egypt
[2] Alexandria University Hospital, Alexandria University, Alexandria, Egypt
[3] Department of Microbiology, Medical Research Institute, Alexandria University, Alexandria, Egypt

Submitted 10 November 2021, accepted 12 February 2022, published online 22 March 2022

Abstract

Antimicrobial resistance represents a global dilemma. Our present study aimed to investigate the presence of *mcr-1* among different Gram-negative bacteria including *Enterobacteriaceae* (except intrinsically resistant to colistin) and *Pseudomonas aeruginosa*. Gram-negative bacterial isolates were collected from different ICUs in several Alexandria hospitals from June 2019 to June 2020. The identification of these Gram-negative isolates was made using the VITEK-2® system (BioMérieux, France). SYBR Green-based PCR was used to screen for the presence of *mcr-1* using a positive control that we amplified and sequenced earlier in our pilot study. All isolates were screened for the presence of *mcr-1* regardless of their colistin susceptibility. Isolates that harbored *mcr-1* were tested for colistin susceptibility and for the presence of some beta-lactamase genes. *Klebsiella pneumoniae* isolates harboring *mcr-1* were capsule typed using the *wzi* sequence analysis. Four hundred eighty isolates were included in this study. Only six isolates harbored *mcr-1.1*. Of these, four were resistant to colistin, while two (*K. pneumoniae* and *P. aeruginosa*) were susceptible to colistin. Five of the six isolates were resistant to carbapenems. They harbored bla_{OXA-48}, and three of them co-harbored bla_{NDM-1}. K-58 was the most often found among our *K. pneumoniae* harboring *mcr-1.1*. To our knowledge, this is the first time to report colistin susceptible *P. aeruginosa* and *K. pneumoniae* harboring the *mcr-1.1* gene in Egypt. Further studies are needed to investigate the presence of the *mcr* genes among colistin susceptible isolates to shed more light on its significance as a potential threat.

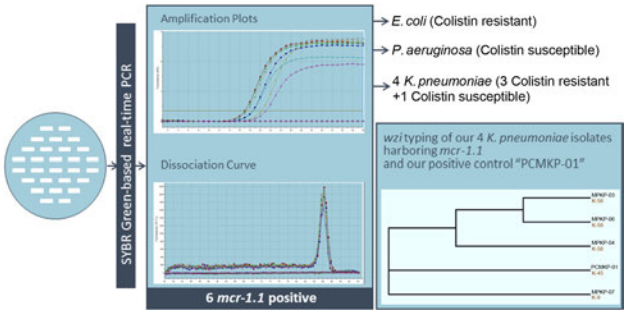

K e y w o r d s: colistin, *K. pneumoniae*, *mcr-1*, SYBR Green, *wzi* typing

Introduction

Resistance to antibacterial agents represents a global threat. Infections caused by multi-drug resistant (MDR) and extensively drug-resistant (XDR) bacteria are growing, representing a major therapeutic challenge. MDR bacteria are defined as those resistant to at least one agent in at least three distinct categories of antibacterial agents. In comparison, XDR bacteria are defined as those resistant to at least one agent in all categories except for two or fewer categories of antibacterial agents (Magiorakos et al. 2012) Currently, colistin remains one of the last resort treatments against these infections (El-Sayed Ahmed et al. 2020; Wang et al. 2020b). Colistin was first used in the 1950s to treat infections caused by Gram-negative bacteria. Then, in the 1970s, it was replaced by other newly discovered antimicrobial agents, which did not have the toxic effects caused by colistin (El-Sayed Ahmed et al. 2020). However, due to the increased resistance to all available antibacterial agents, colistin has resurfaced, in the 1990s, as the last line of defense against infections caused by MDR and XDR Gram-negative bacteria, although its safety profile has not changed and its dosing problem. There

* Corresponding author: A. ElBaradei, Department of Microbiology and Immunology, Faculty of Pharmacy, Pharos University in Alexandria, Alexandria, Egypt; **e-mail: amiraelbaradei@gmail.com**

is a lack of a universal synchronization of colistin dose units, which leads to suboptimal dosing potentially contributing to the resistance problem (Lim et al. 2010; Ahern and Schnoor 2012; Kaye et al. 2016). In addition to MDR and XDR infections, colistin can be combined with other antibacterial agents to manage pan-resistant Gram-negative bacteria (Sayyahfar et al. 2021).

Interestingly, some Gram-negative bacteria are intrinsically resistant to colistin as *Morganella* spp., *Serratia* spp., *Providencia* spp., and *Proteus* spp. Colistin resistance was thought to be only chromosomally mediated; however, in 2015, the plasmid-mediated resistance to colistin was reported for the first time. Since then, different *mcr-1* alleles have been described; furthermore, ten different *mcr* family genes (*mcr-1*-family gene to *mcr-10*-family gene) have been reported worldwide (Hussein et al. 2021). The emergence of horizontally acquired resistance hampers colistin as a last resort against MDR Gram-negative bacteria (Liu et al. 2016; Sun et al. 2018; El-Sayed Ahmed et al. 2020; Xu et al. 2021). Interestingly, colistin susceptible *Escherichia coli* isolates harboring either *mcr-1* or other *mcr* family genes have been reported (Wang et al. 2017; Chen et al. 2019). The aim of our present study was to investigate the presence of *mcr-1* among different Gram-negative bacteria including *Enterobacteriaceae* (except intrinsically resistant to colistin) and *Pseudomonas aeruginosa*.

Experimental

Materials and Methods

Sample collection. We conducted a one-year prospective study, during which Gram-negative bacterial isolates were consecutively collected over a one-year period, starting from June 2019 till June 2020. Non-duplicate isolates were collected from each patient. Isolates were collected from different ICUs in five major tertiary care hospitals in Alexandria, Egypt. Inclusion criteria included being ≥ 18 years old, minimal length of stay in ICU (five days), previous treatment with antibiotics including carbapenems, and failure of treatment denoted by the persistence of signs and symptoms of infection. We excluded *Serratia marcescens*, *Providencia* spp., and *Proteus* spp. because of their intrinsic resistance to colistin. These Gram-negative isolates were identified using the VITEK-2® system (BioMérieux, France).

Antimicrobial susceptibility testing. Susceptibility testing was performed using the disk diffusion method. Antimicrobial agents used were cefepime (FEP), ceftazidime (CAZ), imipenem (IPM), meropenem (MEM), amikacin (AK), gentamicin (GEN), tobramycin (TOB), ciprofloxacin (CIP), and trimethoprim/sulfamethoxazole (SXT), according to the CLSI guidelines (CLSI 2020). Colistin susceptibility testing was not performed at this point to ensure blind screening for the *mcr-1* gene. Antibiotic disks and culture media were purchased from Oxoid (Cambridge, UK).

Screening for the *mcr-1* gene among Gram-negative bacterial isolates. All collected Gram-negative isolates were screened for the presence of the *mcr-1* gene using SYBR Green-based real-time PCR. The primers used were CLR5-F: CGGTCAGTCCGTTTGTTC and CLR5-R: CTTGGTCGGTCTGTAGGG (Liu et al. 2016). Isolate "PCMKP-01" was used as a positive control. This isolate was found to harbor *mcr-1* (amplified and sequenced earlier in a pilot study that we conducted prior to the start of this study, and the details are shown in Supplementary materials).

Real-time PCR was performed on Stratagene Mx3000P (Agilent Technologies California, USA) using PowerUp SYBR Green Master Mix (Thermo Fischer, California, USA). The thermal profile was: activation at 95°C for 2 minutes, followed by 35 cycles of denaturation at 95°C for 20 seconds, annealing at 50°C for 30 seconds, and extension at 72°C for 1 minute, followed by melting curve analysis (95°C for 20 seconds, 50°C for 1 minute and 95°C for 20 seconds). For confirmation, any amplicon obtained using the primers mentioned above, was subsequently sequenced using an ABI 3730xl DNA sequencer (Applied Biosystems, California, USA).

Confirmation of identification and subtyping of the *mcr-1* gene. To confirm the specific subtype of the *mcr-1* gene, we amplified the whole *mcr-1* gene using the conventional PCR, and the amplicon size was 1,672 bp. The primers used were: SQmcr-1F: CTCATGATGCAGCATACTTC and SQmcr-1R: CGAATGGAGTGTGCGGTG (Elnahriry et al. 2016). The amplification scheme was: 4 minutes activation at 95°C, followed by 30 cycles of denaturation at 95°C for 30 seconds, annealing at 50°C for 30 seconds, and extension at 72°C for 90 seconds, and a final elongation step of 72°C for 7 minutes using the Veriti thermal cycler (Applied Biosystems, California, USA), and DreamTaq Green PCR Master Mix (Applied Biosystems, California, USA). Sequencing was performed using the same primers (forward and reverse) with the ABI 3730xl DNA sequencer (Applied Biosystems, California, USA).

Determination of colistin susceptibility. Isolates that were found to harbor *mcr-1* were then tested for colistin susceptibility using the broth microdilution method according to CLSI (CLSI 2020).

Capsule typing of *Klebsiella pneumoniae* isolates. *K. pneumoniae* isolates, which were found to possess *mcr-1* and our isolate "PCMKP-01" were subsequently subjected to capsule typing. The *wzi* gene was amplified and sequenced using primers wzi-F: GTGCC GCGAGCGCTTTCTATCTTGGTATTCC and wzi-R:

GAGAGCCACTGGTTCCAGAA[C or T]TT[C or G] ACCGC (Brisse et al. 2013). Sequencing was performed using the ABI 3730xl DNA sequencer (Applied Biosystems, California, USA). Typing was performed using the K-PAM platform (https://www.iith.ac.in/K-PAM/pred_sertp.php) (Patro et al. 2020).

Genotypic detection of different beta-lactamase genes. All isolates that harbored the *mcr-1* gene were further investigated for the presence of the $bla_{\text{CTX-M}}$ gene (encoding for ESBL), using conventional PCR on the Veriti thermal cycler (Applied Biosystems, California, USA), and DreamTaq Green PCR Master Mix (Applied Biosystems, California, USA). The primers used were F: CGCTTTGCGATGTGCAG, and R: ACCGCGATATCGTTGGT (Gröbner et al. 2009). Then, the isolates that harbored *mcr-1* and were carbapenem-resistant were further investigated for the presence of serine carbapenemase genes (bla_{KPC} and $bla_{\text{OXA-48}}$), and metallo-beta-lactamases genes (bla_{VIM} and $bla_{\text{NDM-1}}$). The primers used were as follows: F: TGTCACTGTATCGCCGTC, and R: CTCAGTGCTCTACAGAAAACC for bla_{KPC} (Wang et al. 2012); F: AAATCACAGGGCGTAGTTGTG, and R: GACCCACCAGCCAATCTTAG for $bla_{\text{OXA-48}}$; F: AGTGGTGAGTATCCGACAG, and R: ATGAAAGTGCGTGGAGAC for bla_{VIM} (Gröbner et al. 2009); and F: GGTTTGGCGATCTGGTTTTC, and R: CGGAATGGCTCATCACGATC) for $bla_{\text{NDM-1}}$ (Nordmann et al. 2011).

Results

A total of 480 Gram-negative isolates were collected from June 2019 to June 2020. Most of the collected isolates were *K. pneumoniae* (62.71%), followed by *E. coli* (22.71 %), *P. aeruginosa* (11.46%), *Enterobacter cloacae* complex, and *Enterobacter asburiae* represented (2.92%) and (0.20 %) of the isolates, respectively. These isolates were collected from different types of clinical samples, including blood cultures (26%), urinary tract infections (17%), aspirates and swabs from surgical site infections (fluid and tissues) (31%), sterile body fluids, including (CSF, pleural fluid and perineal fluid) (2%), and respiratory tract infections (24%). Regarding the susceptibility testing results, resistance to the third and fourth generation cephalosporins was 82.29% and 78.33%, respectively, and they were distributed as follows: *K. pneumoniae* 92.36% and 87.38%, *E. coli* 78.9% and 77.06%, *E. cloacae* complex 64.29% and 71.43%, and *P. aeruginosa* 40% and 34.5%, respectively. Moreover, 49.79% of the isolates were resistant to MEM. They were distributed as follows: *K. pneumoniae* 68.44%, *E. coli* 6.42%, *E. cloacae* complex 21.43%, and *P. aeruginosa* 41.82%. Most of the Gram-negative organisms were resistant to CAZ and FEP, and almost half of the isolates were resistant to carbapenems and gentamicin. Among 480 isolates, 338 (70.4%) were MDR Gram-negative bacteria; of these seven isolates belong to *E. cloacae* complex, 25 were *P. aeruginosa*, 60 were *E. coli*, while 246 of them were *K. pneumoniae* isolates. The susceptibility testing results are shown in (Table I).

Among 480 Gram-negative bacterial isolates, only six (1.25%) harbored the *mcr-1* gene, while 474 (98.75%) did not harbor that gene.

The *mcr-1* gene was sequenced, then the BLASTN (https://blast.ncbi.nlm.nih.gov) tool for was used for confirmation. All isolates were found to harbor *mcr-1.1*. The obtained sequences were deposited in GenBank (accession numbers: MZ820395, MZ820396, MZ820398, MZ820399, MZ820400, MZ820401).

Table I
Resistance profiles of different isolates of Gram-negative bacteria.

Antimicrobial	*Klebsiella pneumoniae* (n = 301)		*Escherichia coli* (n = 109)		*Enterobacter cloaclae* complex (n = 14)		*Enterobacter asburiae** (n = 1)		*Pseudomonas aeruginosa* (n = 55)	
	Resistant		Resistant		Resistant		Resistant		Resistant	
	No.	%	No.	%	No.	%	No.	%	No.	%
Ceftazidime	278	92.36	86	78.90	9	64.29	0	0	22	40.00
Cefepime	263	87.38	84	77.06	10	71.43	0	0	19	34.55
Imipenem	206	68.44	6	5.50	2	14.29	0	0	24	43.64
Meropenem	206	68.44	7	6.42	3	21.43	0	0	23	41.82
Amikacin	180	59.80	4	3.67	0	0	0	0	19	34.55
Gentamicin	177	58.80	36	33.03	6	42.86	0	0	24	43.64
Tobramycin	232	77.08	38	34.86	3	21.43	0	0	24	43.64
Ciprofloxacin	217	72.10	69	63.30	3	21.43	0	0	26	47.27
Trimethoprim/ Sulfamethoxazole	231	76.74	59	54.13	6	42.86	0	0	–	–

* – the isolate was susceptible to all these antibacterial agents

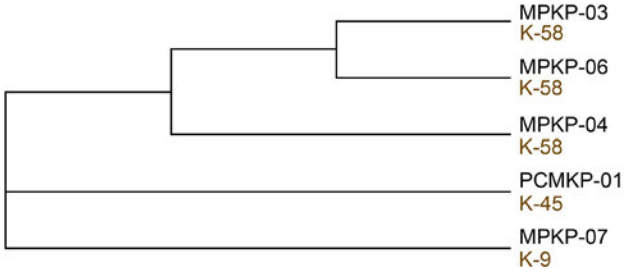

Fig. 1. Phylogenetic tree of four *Klebsiella pneumoniae* isolates and the positive control "PCMKP-01" harboring *mcr-1.1* based on the *wzi* typing.

Then, to confirm the *mcr-1* gene subtype, we amplified and sequenced the whole *mcr-1* gene of all isolates; however, it could not be amplified in one *K. pneumoniae* isolate using this pair of primers. The obtained sequences were deposited in GenBank (accession number: MZ820389, MZ820390, MZ820391, MZ820393, MZ820394).

Remarkably, two isolates out of six isolates harboring *mcr-1.1* were susceptible to colistin. Moreover, one of them could not be amplified using this pair of primers. However, it was successfully amplified and sequenced using the first primers set, and it was found to harbor *mcr-1.1*. Its sequence was submitted to GenBank, as mentioned earlier.

Then, all *K. pneumoniae* isolates harboring *mcr-1.1* and the isolate "PCMKP-01" were capsule typed using the *wzi* gene sequencing; three were K-58, one K-9, and one K-45. A phylogenetic tree was constructed, and it is shown in Fig. 1.

The characteristics of the six isolates that harbor *mcr-1.1* is shown in Table II. Three of the six isolates harbored $bla_{\text{CTX-M}}$. Five of the isolates were resistant to carbapenems. These five isolates harbored the $bla_{\text{OXA-48}}$ gene, $bla_{\text{NDM-1}}$ was present in three of them, while bla_{VIM} and bla_{KPC} were absent in these isolates. The distribution of the different beta-lactamase genes among the six isolates is shown in Table III.

Discussion

Colistin remains our last resort against MDR and XDR Gram-negative bacteria. Moreover, it has been combined with other antibacterial agents to manage

Table II
Characteristics of six bacterial isolates harboring *mcr-1*.

Organism	Isolate name	k-type	Sample Source	*mcr-1* amplified by first set of primers	*mcr-1* amplified by second set of primers	Patient gender	FEP	CAZ	IPM	MEM	AK	GN	TOB	CIP	SXT	MIC value in µg/ml*
P. aeruginosa	MPPS-05	–	BAL	*mcr-1.1*	*mcr-1.1*	F	R	R	R	I	R	R	R	R	–	≤0.5
K. pneumoniae	MPKP-07	K9	Mini BAL	*mcr-1.1*	–	F	R	R	R	R	R	R	R	R	S	≤0.5
K. pneumoniae	MPKP-03	k58	BAL	*mcr-1.1*	*mcr-1.1*	M	R	R	R	R	R	I	R	R	R	4
K. pneumoniae	MPKP-04	k58	Spinal fluid	*mcr-1.1*	*mcr-1.1*	F	R	R	R	R	R	R	R	I	R	4
K. pneumoniae	MPKP-06	k58	Sputum	*mcr-1.1*	*mcr-1.1*	M	R	R	R	R	R	S	R	R	R	4
E. coli	MPEC-02	–	Blood culture	*mcr-1.1*	*mcr-1.1*	M	R	R	S	S	S	R	R	I	R	≥4

* – colistin MIC was interpreted according to EUCAST guidelines (EUCAST 2020)

Table III
Beta-lactamase genes distribution among the *mcr-1* positive isolates.

Organism	Isolate name	*mcr-1* amplified by first set of primers	*mcr-1* amplified by second set of primers	ESBL Gene	Serine carbapenemases genes		Metallo-beta-lactamase genes	
				$bla_{\text{CTX-M}}$	bla_{KPC}	$bla_{\text{OXA-48}}$	bla_{VIM}	$bla_{\text{NDM-1}}$
P. aeruginosa	MPPS-05	*mcr-1.1*	*mcr-1.1*	–	–	+	–	+
K. pneumoniae	MPKP-07	*mcr-1.1*	–	+	–	+	–	–
K. pneumoniae	MPKP-03	*mcr-1.1*	*mcr-1.1*	+	–	+	–	+
K. pneumoniae	MPKP-04	*mcr-1.1*	*mcr-1.1*	–	–	+	–	+
K. pneumoniae	MPKP-06	*mcr-1.1*	*mcr-1.1*	–	–	+	–	–
E. coli	MPEC-02	*mcr-1.1*	*mcr-1.1*	+	NT	NT	NT	NT

NT – organism was not tested as it was sensitive to carbapenems

infections caused by pan-resistant Gram-negative bacteria (Sayyahfar et al. 2021). Different mechanisms of resistance contribute to the reduced susceptibility to colistin. However, the most worrying mechanism is plasmid-borne MCR-mediated resistance due to its ability to horizontally transfer between different species and the speed with which it is evolving. Several *mcr* family genes have been detected since they were first described in 2015 (Feng 2018; Xu et al. 2021).

Some studies reported the presence of *mcr-1* among *E. coli* isolates susceptible to colistin, which would further complicate the situation in health care settings. Patients infected with organisms harboring the *mcr-1* gene represent a potential threat for *mcr-1* transmission because these organisms could escape being detected by conventional phenotypic methods. Furthermore, other resistance genes (beta lactamases and non-beta lactamases genes) could also be transmitted along with the *mcr-1* gene. (Yuan et al. 2021) This study aimed to investigate the presence of *mcr-1* among different Gram-negative bacteria, including *Enterobacteriaceae* (except intrinsically resistant to colistin) and *P. aeruginosa*.

Using SYBR Green-based real-time PCR, we screened for *mcr-1* among the 480 Gram-negative bacterial isolates. Only 6 (1.25%) isolates harbored this gene, which was confirmed by sequencing of the amplicon obtained. Four of these six isolates were *K. pneumoniae*, one isolate was *E. coli*, and the remaining one was *P. aeruginosa*.

The first report of *mcr-1* from a clinical isolate in Egypt was provided in 2016 by Elnahriry et al. (2016). Then, different studies reported the presence of *mcr-1* among *E. coli* clinical isolates in Egypt, including Anan et al. (2021), who found only four (7.5%) *E. coli* harboring *mcr-1* among colistin-resistant isolates, and El-Mokhtar et al. (2021) who reported that all their studied *E. coli* isolates resistant to colistin carried *mcr-1*. Moreover, another study reported the presence of *mcr-1* in one *E. coli* and one *K. pneumoniae* isolate among their 450 enterobacterial isolates (Zafer et al. 2019).

Furthermore, Elmonir et al. (2021) reported that all colistin-resistant *K. pneumoniae* isolates harbored the *mcr-1* gene. Abd El-Baky et al. (2020) reported the presence of *mcr-1* among their *P. aeruginosa* isolates. Additionally, Yanat et al. (2016) reported the presence of *mcr-1* in *E. coli* clinical isolate in Algeria, Alghoribi et al. (2019) also found *mcr-1* gene in uropathogenic *E. coli* in Saudia Arabia, and *mcr-1* was also reported from *E. coli* clinical isolate in Lebanon (Al-Bayssari et al. 2021). However, some studies could not detect *mcr-1* among colistin-resistant bacterial isolates, Ramadan et al. (2020) did not find any of the eight *mcr* family genes (*mcr-1* to *mcr-8*) among 65 Gram-negative bacterial isolates (Soliman et al. 2020b). In a study in Tunisia, they could not find any of the *mcr* genes, from *mcr-1* to *mcr-5* (Jaidane et al. 2018). Sadek et al. (2020b) reported only one *E. coli* isolate harboring *mcr-1* among 128 colistin resistant *E. coli* strains isolated from meat and meat product samples in Egypt.

In this study, six isolates that harbored *mcr-1.1* were tested for colistin susceptibility; four were found to be resistant to colistin, while two isolates (one *K. pneumoniae* and one *P. aeruginosa*) were found to be susceptible to colistin (≤ 0.5 μg/ml). To confirm the *mcr-1* subtype, we attempted to amplify and sequence the whole *mcr-1* gene among the six isolates, using another set of primers. Five isolates harbored *mcr-1.1* and the remaining one (*K. pneumoniae*) could not be amplified using this set of primers. Interestingly, *mcr-1.1* was reported in Egypt before; in one uropathogenic *E. coli* (UPEC) (Zakaria et al. 2021) and five *E. coli* isolated from chicken (Soliman et al. 2021). Moreover, *mcr-1.1* was reported in *E. coli* isolate obtained from wound drainage (Eltai et al. 2020) from Qatar. Girardello et al. (2021) reported the presence of *mcr-1.1* in *E. coli* clinical isolate in Sao Paulo, and *mcr-1.1* was found in two *K. pneumoniae* clinical isolates by Rocha et al. (2020).

In this study, the *K. pneumoniae* isolate, whose *mcr-1* gene could not be amplified using the second set of primers (used to amplify the whole *mcr-1* gene), was susceptible to colistin. Another colistin susceptible isolate was *P. aeruginosa*, which was found to harbor the *mcr-1.1* gene.

Previously, some studies have reported Gram-negative isolates susceptible to colistin and harboring the *mcr-1* gene. Wang et al. (2017) described two colistin-susceptible *E. coli* isolates possessing the *mcr-1* gene. Terveer et al. (2017) also reported a colistin-susceptible *E. coli* harboring *mcr-1*, which was not functioning. Using WGS, they found that the gene was rendered not functional by a transposon (IS10R) insertion (Terveer et al. 2017). Zhou et al. (2018) also described a fluoroquinolone-resistant but colistin-susceptible *E. coli* carrying *mcr-1*, which was also non-functional by inserting a 1.7-Kb IS1294b element. Chen et al. (2019) also reported a colistin-susceptible *E. coli* harboring *mcr-1*, which was non-functional because of the insertion of another gene. Jiang et al. (2020) described a colistin susceptible *E. coli* harboring the *mcr-1* gene, which had mutations in the *mcr-1* promotor sequence.

However, to the best of our knowledge, this is the first study reporting the presence of *mcr-1* in colistin susceptible *K. pneumoniae* and *P. aeruginosa* in Egypt. The whole *mcr-1* gene in the susceptible *K. pneumoniae* could not be amplified using the second set of primers and it was found to be susceptible to colistin; it may be due to an insertion sequence that rendered the

gene non-functional. However, in our case, WGS was not feasible due to its high cost and the fact that this study was not funded. Besides the *mcr-1* gene, other *mcr* family genes have also been described in colistin-susceptible bacteria. Ragupathi et al. (2020) reported the presence of the *mcr-3.30* gene in colistin-susceptible *Aeromonas veronii*. The *mcr-3.30* gene was disrupted due to the insertion of ISAs18 (Ragupathi et al. 2020). The *mcr-9* is another *mcr* family gene that was reported in other studies, including a study conducted by Soliman et al. (2020a), who reported the presence of this gene in colistin susceptible *Enterobacter hormaechei* clinical isolate from Egypt. Other colistin susceptible *E. hormaechei* harboring *mcr-9* were also reported in Egypt in pets with respiratory diseases (Khalifa et al. 2020a) and from food of animal origin (Sadek et al. 2020a). Carroll et al. (2019) reported the presence of *mcr-9* in the MDR *Salmonella enterica* subsp. *enterica* serotype Typhimurium isolate, which was susceptible to colistin. Also, another study conducted by Kananizadeh et al. (2020) reported the presence of *mcr-9* in *E. cloacae* complex in Japan. Khalifa et al. (2020b) found *mcr-9* in colistin-susceptible foodborne *K. pneumoniae*. The *mcr-9* subtype was also reported by Marchetti et al. (2021) who reported *mcr-9.2* in a colistin susceptible *E. cloacae*. The *mcr-10* was described by Wang et al. (2020a) in *Enterobacter roggenkampii* that was susceptible to colistin.

In this study, four *K. pneumoniae* isolates that harbored the *mcr-1.1* gene and "PCMKP-01" were capsule typed using the *wzi* gene sequence analysis. The most common K-type found among these isolates was K-58. It was found in three isolates. K-58 has not been associated with virulence (Turton et al. 2010). These three isolates were MDR strains of *K. pneumoniae* resistant to colistin that harbor the *mcr-1.1* gene. The two remaining K-types were K-9 and K-45. K-45 type *K. pneumoniae* was considered the positive control isolate "PCMKP-01". It was the MDR colistin-resistant isolate, while K-45 type isolate was colistin susceptible *K. pneumoniae* that harbored *mcr-1.1*.

Three of the isolates co-harbored *mcr-1.1* and $bla_{\text{CTX-M}}$. Sadek et al. (2021) reported that nine of the isolates co-harbored the *mcr-1* gene and ESBL genes. In the present study, five isolates harbored *mcr-1.1* and were resistant to carbapenems. These five isolates had $bla_{\text{OXA-48}}$, and three of them had $bla_{\text{NDM-1}}$ (one *P. aeuruginsa* isolate and two *K. pneumoniae* isolates). bla_{VIM} and bla_{KPC} were not found among these five isolates. Singh et al. (2021) reported that all the isolates harboring *mcr-1* in their study co-harbored $bla_{\text{OXA-48}}$. Han et al. (2020) reported the identification of the XDR *E. coli* clinical isolate co-harboring *mcr-1* and $bla_{\text{NDM-1}}$. Al-Bayssari et al. (2021) reported the co-existence of $bla_{\text{NDM-4}}$ and *mcr-1* among *E. coli* clinical isolates.

Conclusion

To our knowledge, it is the first time to report colistin susceptible *P. aeruginosa* and *K. pneumoniae* harboring the *mcr-1.1* gene in Egypt. The *mcr-1.1* gene was fully sequenced in *P. aeruginosa,* while in *K. pneumoniae* it could not be fully sequenced, which indicated some abnormality in this gene. The most frequently found K-type was K-58. Five of the isolates were resistant to carbapenems and co-harbored $bla_{\text{OXA-48}}$ and *mcr-1,* and three of them co-harbored *mcr-1.1*, $bla_{\text{OXA-48}}$, and $bla_{\text{NDM-1}}$. Co-existence of these genes together is a clear therapeutic challenge. Further studies are still needed to investigate the presence of the plasmid-borne *mcr* genes among colistin susceptible isolates to shed more light on its significance as a potential threat.

ORCID
Amira ElBaradei https://orcid.org/0000-0001-6813-7896

Accession numbers

Nucleotide sequences of *mcr-1.1* genes, which were amplified using both primers, were deposited in the GenBank database under accession numbers MZ820389 – MZ820401 (the details together with the appropriate web links are shown in Supplementary materials).

Ethical statement

Ethical approval was obtained from the Ethical Committee of the Medical Research Institute, Alexandria University.

Conflict of interest

The authors do not report any financial or personal connections with other persons or organizations, which might negatively affect the contents of this publication and/or claim authorship rights to this publication.

Literature

Abd El-Baky RM, Masoud SM, Mohamed DS, Waly NGFM, Shafik EA, Mohareb DA, Elkady A, Elbadr MM, Hetta HF. Prevalence and some possible mechanisms of colistin resistance among multidrug-resistant and extensively drug-resistant *Pseudomonas aeruginosa*. Infect Drug Resist. 2020 Feb;13:323–332. https://doi.org/10.2147/IDR.S238811

Ahern JW, Schnoor JB. Colistin: potential for dosage error. Clin Infect Dis. 2012 Nov 01;55(9):1275, author reply 1275–1276. https://doi.org/10.1093/cid/cis632

Al-Bayssari C, Nawfal Dagher T, El Hamoui S, Fenianos F, Makdissy N, Rolain JM, Nasreddine N. Carbapenem and colistin-resistant bacteria in North Lebanon: coexistence of *mcr-1* and NDM-4 genes in *Escherichia coli*. J Infect Dev Ctries. 2021 Jul 31; 15(07):934–342. https://doi.org/10.3855/jidc.14176

Alghoribi MF, Doumith M, Upton M, Al Johani SM, Alzayer M, Woodford N, Ellington MJ, Balkhy HH. Complete genome sequence of a colistin-resistant uropathogenic *Escherichia coli* sequence type 131 *fimH22* strain harboring *mcr-1* on an IncHI2 plasmid, isolated in Riyadh, Saudi Arabia. Microbiol Resour Announc. 2019 May 2;8(18): e00104-19. https://doi.org/10.1128/MRA.00104-19

Anan MMG, El-Seidi EA, Mostafa MS, Rashed LA, El-Wakil DM. Detection of plasmid-mediated mobile colistin resistance gene (*mcr-1*) in *Enterobacterales* isolates from a University Hospital. Infect Drug Resist. 2021 Aug;14:3063–3070. https://doi.org/10.2147/IDR.S318787

Brisse S, Passet V, Haugaard AB, Babosan A, Kassis-Chikhani N, Struve C, Decré D. *wzi* Gene sequencing, a rapid method for determination of capsular type for *Klebsiella* strains. J Clin Microbiol. 2013 Dec 01;51(12):4073–4078. https://doi.org/10.1128/JCM.01924-13

Carroll LM, Gaballa A, Guldimann C, Sullivan G, Henderson LO, Wiedmann M. Identification of novel mobilized colistin resistance gene *mcr-9* in a multidrug-resistant, colistin-susceptible *Salmonella enterica* serotype Typhimurium isolate. MBio. 2019 Jun 25; 10(3): e00853-19. https://doi.org/10.1128/mBio.00853-19

Chen CW, Tang HJ, Chen CC, Lu YC, Chen HJ, Su BA, Weng TC, Chuang YC, Lai CC. The microbiological characteristics of carbapenem-resistant *Enterobacteriaceae* carrying the *mcr-1* gene. J Clin Med. 2019 Feb 19;8(2):261. https://doi.org/10.3390/jcm8020261

CLSI. Performance standards for antimicrobial susceptibility testing. 30th ed. CLSI supplement M100. Wayne (USA): Clinical and Laboratory Standards Institute; 2020. p. 16–38.

El-Mokhtar MA, Daef E, Mohamed Hussein AAR, Hashem MK, Hassan HM. Emergence of nosocomial pneumonia caused by colistin-resistant *Escherichia coli* in patients admitted to chest intensive care unit. Antibiotics (Basel). 2021 Feb 24;10(3):226. https://doi.org/10.3390/antibiotics10030226

Elmonir W, Abd El-Aziz NK, Tartor YH, Moustafa SM, Abo Remela EM, Eissa R, Saad HA, Tawab AA. Emergence of colistin and carbapenem resistance in extended-spectrum β-lactamase producing *Klebsiella pneumoniae* isolated from chickens and humans in Egypt. Biology (Basel). 2021 Apr 26;10(5):373. https://doi.org/10.3390/biology10050373

Elnahriry SS, Khalifa HO, Soliman AM, Ahmed AM, Hussein AM, Shimamoto T, Shimamoto T. Emergence of plasmid-mediated colistin resistance gene *mcr-1* in a clinical *Escherichia coli* isolate from Egypt. Antimicrob Agents Chemother. 2016 May;60(5):3249–3250. https://doi.org/10.1128/AAC.00269-16

El-Sayed Ahmed MAEG, Zhong LL, Shen C, Yang Y, Doi Y, Tian GB. Colistin and its role in the era of antibiotic resistance: an extended review (2000–2019). Emerg Microbes Infect. 2020 Jan 01;9(1):868–885. https://doi.org/10.1080/22221751.2020.1754133

Eltai NO, Kelly B, Al-Mana HA, Ibrahim EB, Yassine HM, Al Thani A, Al Maslmani M, Lammens C, Xavier BB, Malhotra-Kumar S. Identification of *mcr-8* in clinical isolates from Qatar and evaluation of their antimicrobial profiles. Front Microbiol. 2020 Aug 24;11:1954. https://doi.org/10.3389/fmicb.2020.01954

EUCAST. The European Committee on Antimicrobial Susceptibility Testing. Breakpoint tables for interpretation of MICs and zone diameters. Version 10.0. Basel (Switzerland): The European Committee on Antimicrobial Susceptibility Testing; 2020. Available from https://www.eucast.org/ast_of_bacteria/previous_versions_of_documents/

Feng Y. Transferability of MCR-1/2 polymyxin resistance: complex dissemination and genetic mechanism. ACS Infect Dis. 2018 Mar 09; 4(3):291–300. https://doi.org/10.1021/acsinfecdis.7b00201

Girardello R, Piroupo CM, Martins J Jr, Maffucci MH, Cury AP, Franco MRG, Malta FM, Rocha NC, Pinho JRR, Rossi F, et al. Genomic characterization of *mcr-1.1*-producing *Escherichia coli* recovered from human infections in São Paulo, Brazil. Front Microbiol. 2021 Jun 9;12:663414. https://doi.org/10.3389/fmicb.2021.663414

Gröbner S, Linke D, Schütz W, Fladerer C, Madlung J, Autenrieth IB, Witte W, Pfeifer Y. Emergence of carbapenem-non-susceptible extended-spectrum β-lactamase-producing *Klebsiella pneumoniae* isolates at the university hospital of Tübingen, Germany. J Med Microbiol. 2009 Jul 01;58(7):912–922. https://doi.org/10.1099/jmm.0.005850-0

Han S, Kim JS, Hong CK, Park SH, Kim HS, Yu JK, Park J, Kim J, Lee SM, Oh YH. Identification of an extensively drug-resistant *Escherichia coli* clinical strain harboring *mcr-1* and bla_{NDM-1} in Korea. J Antibiot (Tokyo). 2020 Dec;73(12):852–858. https://doi.org/10.1038/s41429-020-0350-1

Hussein NH, AL-Kadmy IMS, Taha BM, Hussein JD. Mobilized colistin resistance (*mcr*) genes from 1 to 10: a comprehensive review. Mol Biol Rep. 2021 Mar;48(3):2897–2907. https://doi.org/10.1007/s11033-021-06307-y

Jaidane N, Bonnin RA, Mansour W, Girlich D, Creton E, Cotellon G, Chaouch C, Boujaafar N, Bouallegue O, Naas T. Genomic insights into colistin-resistant *Klebsiella pneumoniae* from a Tunisian Teaching Hospital. Antimicrob Agents Chemother. 2018 Feb;62(2):e01601-17. https://doi.org/10.1128/AAC.01601-17

Jiang Y, Zhang Y, Lu J, Wang Q, Cui Y, Wang Y, Quan J, Zhao D, Du X, Liu H, et al. Clinical relevance and plasmid dynamics of *mcr-1*-positive *Escherichia coli* in China: a multicentre case-control and molecular epidemiological study. Lancet Microbe. 2020 May; 1(1):e24–e33. https://doi.org/10.1016/S2666-5247(20)30001-X

Kananizadeh P, Oshiro S, Watanabe S, Iwata S, Kuwahara-Arai K, Shimojima M, Ogawa M, Tada T, Kirikae T. Emergence of carbapenem-resistant and colistin-susceptible Enterobacter cloacae complex co-harboring bla_{IMP-1} and *mcr-9* in Japan. BMC Infect Dis. 2020 Dec;20(1):282. https://doi.org/10.1186/s12879-020-05021-7

Kaye KS, Pogue JM, Tran TB, Nation RL, Li J. Agents of last resort: Polymyxin resistance. Infect Dis Clin North Am. 2016 Jun; 30(2):391–414. https://doi.org/10.1016/j.idc.2016.02.005

Khalifa HO, Oreiby AF, Abd El-Hafeez AA, Okanda T, Haque A, Anwar KS, Tanaka M, Miyako K, Tsuji S, Kato Y, et al. First Report of multidrug-resistant carbapenemase-producing bacteria coharboring *mcr-9* associated with respiratory disease complex in pets: potential of animal-human transmission. Antimicrob Agents Chemother. 2020a Dec 16;65(1):e01890-20. https://doi.org/10.1128/AAC.01890-20

Khalifa HO, Soliman AM, Saito T, Kayama S, Yu L, Hisatsune J, Sugai M, Nariya H, Ahmed AM, Shimamoto T, et al. First report of foodborne *Klebsiella pneumoniae* coharboring bla_{VIM-1}, bla_{NDM-1}, and *mcr-9*. Antimicrob Agents Chemother. 2020b Aug 20;64(9):e00882-20. https://doi.org/10.1128/AAC.00882-20

Lim LM, Ly N, Anderson D, Yang JC, Macander L, Jarkowski A 3rd, Forrest A, Bulitta JB, Tsuji BT. Resurgence of colistin: a review of resistance, toxicity, pharmacodynamics, and dosing. Pharmacotherapy. 2010 Dec;30(12):1279–1291. https://doi.org/10.1592/phco.30.12.1279

Liu YY, Wang Y, Walsh TR, Yi LX, Zhang R, Spencer J, Doi Y, Tian G, Dong B, Huang X, et al. Emergence of plasmid-mediated colistin resistance mechanism MCR-1 in animals and human beings in China: a microbiological and molecular biological study. Lancet Infect Dis. 2016 Feb;16(2):161–168. https://doi.org/10.1016/S1473-3099(15)00424-7

Magiorakos AP, Srinivasan A, Carey RB, Carmeli Y, Falagas ME, Giske CG, Harbarth S, Hindler JF, Kahlmeter G, Olsson-Liljequist B, et al. Multidrug-resistant, extensively drug-resistant and pandrug-resistant bacteria: an international expert proposal for interim standard definitions for acquired resistance. Clin Microbiol Infect. 2012 Mar;18(3):268–281. https://doi.org/10.1111/j.1469-0691.2011.03570.x

Marchetti VM, Bitar I, Sarti M, Fogato E, Scaltriti E, Bracchi C, Hrabak J, Pongolini S, Migliavacca R. Genomic characterization of VIM and MCR co-producers: the first two clinical cases, in Italy. Diagnostics (Basel). 2021 Jan 06;11(1):79. https://doi.org/10.3390/diagnostics11010079

Nordmann P, Poirel L, Walsh TR, Livermore DM. The emerging NDM carbapenemases. Trends Microbiol. 2011 Dec;19(12):588–595. https://doi.org/10.1016/j.tim.2011.09.005

Patro LPP, Sudhakar KU, Rathinavelan T. K-PAM: a unified platform to distinguish *Klebsiella* species K- and O-antigen types, model antigen structures and identify hypervirulent strains. Sci Rep. 2020 Dec;10(1):16732. https://doi.org/10.1038/s41598-020-73360-1

Ragupathi NKD, Sethuvel DPM, Anandan S, Murugan D, Asokan K, Neethi Mohan RG, Vasudevan K, D TK, C GPD, Veeraraghavan B. First hybrid complete genome of *Aeromonas veronii* reveals chromosome-mediated novel structural variant *mcr-3.30* from a human clinical sample. Access Microbiol. 2020 Feb 17;2(4): acmi000103. https://doi.org/10.1099/acmi.0.000103

Ramadan H, Gupta SK, Sharma P, Ahmed M, Hiott LM, Barrett JB, Woodley TA, Frye JG, Jackson CR. Circulation of emerging NDM-5-producing *Escherichia coli* among humans and dogs in Egypt. Zoonoses Public Health. 2020 May;67(3):324–329. https://doi.org/10.1111/zph.12676

Rocha IV, dos Santos Silva N, das Neves Andrade CA, de Lacerda Vidal CF, Leal NC, Xavier DE. Diverse and emerging molecular mechanisms award polymyxins resistance to *Enterobacteriaceae* clinical isolates from a tertiary hospital of Recife, Brazil. Infect Genet Evol. 2020 Nov;85:104584. https://doi.org/10.1016/j.meegid.2020.104584

Sadek M, Nariya H, Shimamoto T, Kayama S, Yu L, Hisatsune J, Sugai M, Nordmann P, Poirel L, Shimamoto T. First genomic characterization of bla_{VIM-1} and *mcr-9*-coharbouring *Enterobacter hormaechei* isolated from food of animal origin. Pathogens. 2020a Aug 22;9(9):687. https://doi.org/10.3390/pathogens9090687

Sadek M, Ortiz de la Rosa JM, Abdelfattah Maky M, Korashe Dandrawy M, Nordmann P, Poirel L. Genomic features of MCR-1 and extended-spectrum β-lactamase-producing Enterobacterales from retail raw chicken in Egypt. Microorganisms. 2021 Jan 19; 9(1):195. https://doi.org/10.3390/microorganisms9010195

Sadek M, Poirel L, Nordmann P, Nariya H, Shimamoto T, Shimamoto T. Draft genome sequence of an *mcr-1*/IncI2-carrying multidrug-resistant *Escherichia coli* B1:ST101 isolated from meat and meat products in Egypt. J Glob Antimicrob Resist. 2020b Mar; 20:41–42. https://doi.org/10.1016/j.jgar.2019.11.015

Sayyahfar S, Choobdar FA, Mashayekhi M, Jazi FM. Successful management of pan-resistant *Acinetobacter baumannii* meningitis without intrathecal or intraventricular antibiotic therapy in a neonate. Infect Chemother. 2021;53(1):146–150. https://doi.org/10.3947/ic.2020.0202

Singh S, Pathak A, Rahman M, Singh A, Nag S, Sahu C, Prasad KN. Genetic characterisation of colistin resistant *Klebsiella pneumoniae* clinical isolates from North India. Front Cell Infect Microbiol. 2021 Jun 21;11:666030. https://doi.org/10.3389/fcimb.2021.666030

Soliman AM, Maruyama F, Zarad HO, Ota A, Nariya H, Shimamoto T, Shimamoto T. Emergence of a multidrug-resistant *Enterobacter hormaechei* clinical isolate from Egypt co-harboring *mcr-9* and bla_{VIM-4}. Microorganisms. 2020a Apr 20;8(4):595. https://doi.org/10.3390/microorganisms8040595

Soliman AM, Ramadan H, Zarad H, Sugawara Y, Yu L, Sugai M, Shimamoto T, Hiott LM, Frye JG, Jackson CR, et al. Coproduction of *tet*(X7) conferring high-level tigecycline resistance, fosfomycin fosa4, and colistin *mcr-1.1* in *Escherichia coli* strains from chickens in Egypt. Antimicrob Agents Chemother. 2021 May 18; 65(6): e02084-20. https://doi.org/10.1128/AAC.02084-20

Soliman AM, Zarad HO, Nariya H, Shimamoto T, Shimamoto T. Genetic analysis of carbapenemase-producing Gram-negative bacteria isolated from a university teaching hospital in Egypt. Infect Genet Evol. 2020b Jan;77:104065. https://doi.org/10.1016/j.meegid.2019.104065

Sun J, Zhang H, Liu YH, Feng Y. Towards understanding MCR-like colistin resistance. Trends Microbiol. 2018 Sep;26(9):794–808. https://doi.org/10.1016/j.tim.2018.02.006

Terveer EM, Nijhuis RHT, Crobach MJT, Knetsch CW, Veldkamp KE, Gooskens J, Kuijper EJ, Claas ECJ. Prevalence of colistin resistance gene (*mcr-1*) containing *Enterobacteriaceae* in feces of patients attending a tertiary care hospital and detection of a *mcr-1* containing, colistin susceptible *E. coli*. PLoS One. 2017 Jun 2;12(6): e0178598. https://doi.org/10.1371/journal.pone.0178598

Turton JF, Perry C, Elgohari S, Hampton CV. PCR characterization and typing of *Klebsiella pneumoniae* using capsular type-specific, variable number tandem repeat and virulence gene targets. J Med Microbiol. 2010 May 01;59(5):541–547. https://doi.org/10.1099/jmm.0.015198-0

Wang C, Feng Y, Liu L, Wei L, Kang M, Zong Z. Identification of novel mobile colistin resistance gene *mcr-10*. Emerg Microbes Infect. 2020a Jan 01;9(1):508–516. https://doi.org/10.1080/22221751.2020.1732231

Wang CH, Hsieh YH, Powers ZM, Kao CY. Defeating antibiotic-resistant bacteria: exploring alternative therapies for a post-antibiotic era. Int J Mol Sci. 2020b Feb 05;21(3):1061. https://doi.org/10.3390/ijms21031061

Wang L, Gu H, Lu X. A rapid low-cost real-time PCR for the detection of *Klebsiella pneumonia* carbapenemase genes. Ann Clin Microbiol Antimicrob. 2012 Jan;11(1):9. https://doi.org/10.1186/1476-0711-11-9

Wang Y, Tian GB, Zhang R, Shen Y, Tyrrell JM, Huang X, Zhou H, Lei L, Li HY, Doi Y, et al. Prevalence, risk factors, outcomes, and molecular epidemiology of *mcr-1*-positive *Enterobacteriaceae* in patients and healthy adults from China: an epidemiological and clinical study. Lancet Infect Dis. 2017 Apr;17(4):390–399. https://doi.org/10.1016/S1473-3099(16)30527-8

Xu Y, Chen H, Zhang H, Ullah S, Hou T, Feng Y. The MCR-3 inside linker appears as a facilitator of colistin resistance. Cell Rep. 2021 May;35(7):109135. https://doi.org/10.1016/j.celrep.2021.109135

Yanat B, Machuca J, Yahia RD, Touati A, Pascual Á, Rodríguez-Martínez JM. First report of the plasmid-mediated colistin resistance gene *mcr-1* in a clinical *Escherichia coli* isolate in Algeria. Int J Antimicrob Agents. 2016 Dec;48(6):760–761. https://doi.org/10.1016/j.ijantimicag.2016.09.003

Yuan J, Wang X, Shi D, Ge Q, Song X, Hu W, Wei D, Ge C, Li X, Hu C. Extensive antimicrobial resistance and plasmid-carrying resistance genes in *mcr-1*-positive *E. coli* sampled in swine, in Guangxi, South China. BMC Vet Res. 2021 Dec;17(1):86. https://doi.org/10.1186/s12917-021-02758-4

Zafer MM, El-Mahallawy HA, Abdulhak A, Amin MA, Al-Agamy MH, Radwan HH. Emergence of colistin resistance in multidrug-resistant *Klebsiella pneumoniae* and *Escherichia coli* strains isolated from cancer patients. Ann Clin Microbiol Antimicrob. 2019 Dec;18(1):40. https://doi.org/10.1186/s12941-019-0339-4

Zakaria AS, Edward EA, Mohamed NM. Genomic insights into a colistin-resistant uropathogenic *Escherichia coli* strain of O23:H4-ST641 lineage harboring *mcr-1.1* on a conjugative IncHI2 plasmid from Egypt. Microorganisms. 2021 Apr 10;9(4):799. https://doi.org/10.3390/microorganisms9040799

Zhou K, Luo Q, Wang Q, Huang C, Lu H, Rossen JWA, Xiao Y, Li L. Silent transmission of an IS*1294b*-deactivated *mcr-1* gene with inducible colistin resistance. Int J Antimicrob Agents. 2018 Jun; 51(6):822–828. https://doi.org/10.1016/j.ijantimicag.2018.01.004

Supplementary materials are available on the journal's website.

ORIGINAL PAPER

Polish Journal of Microbiology
2022, Vol. 71, No 1, 91–105
https://doi.org/10.33073/pjm-2022-012

Evaluation of the Probiotic Potential of *Lactobacillus delbrueckii* ssp. *indicus* WDS-7 Isolated from Chinese Traditional Fermented Buffalo Milk *In Vitro*

CHANGJUN WU[#], CHENWEI DAI[#], LIN TONG, HAN LV and XIUHONG ZHOU[*]

Anhui Academy of Medical Sciences, Hefei, Anhui Province, China

Submitted 10 November 2021, accepted 19 February 2022, published online 22 March 2022

Abstract

The present study aimed to evaluate the probiotic potential of lactic acid bacteria (LAB) isolated from Chinese traditional fermented buffalo milk. Out of 22 isolates, 11 were putatively identified as LAB preliminarily. A total of six LAB strains displayed strong adhesion to HT-29 cells and all these strains showed preferable tolerance to artificially simulated gastrointestinal juices. WDS-4, WDS-7, and WDS-18 exhibited excellent antioxidant capacities, including DPPH radical, $ABTS^+$ radical, and superoxide anion scavenging activities. Compared with the other two LAB strains, WDS-7 had a stronger inhibition effect on four pathogens. Based on the 16S rRNA gene sequencing and phylogenetic analysis, WDS-7 was identified as *Lactobacillus delbrueckii* ssp. *indicus* and selected to assess the potential and safety of probiotics further. The results revealed that WDS-7 strain had a strong capacity for acid production and good thermal stability. WDS-7 strain also possessed bile salt hydrolase (BSH) activity. Compared to LGG, WDS-7 was a greater biofilm producer on the plastic surface and exhibited a better EPS production ability (1.94 mg/ml as a glucose equivalent). WDS-7 was proved to be sensitive in the majority of tested antibiotics and absence of hemolytic activity. Moreover, no production of biogenic amines and β-glucuronidase was observed in WDS-7. The findings of this work indicated that *L. delbrueckii* ssp. *indicus* WDS-7 fulfilled the probiotic criteria *in vitro* and could be exploited for further evaluation *in vivo*.

K e y w o r d s: fermented buffalo milk, lactic acid bacteria, probiotic potential, *Lactobacillus delbrueckii* ssp. *indicus*, food application

Introduction

In recent years, the consumers' interest in health-promoting foods containing probiotics has risen due to probiotics' capability to promote human health (Nair and Dubhashi 2016). Probiotics are defined as living microorganisms that, when given in sufficient number, confer a health benefit to the host (Hill et al. 2014). Probiotics are generally applied in the fermentation of foods as starter cultures and are considered safe with application in the food industry. The most widely used probiotic in the food industry is lactic acid bacteria (LAB). LAB is a heterogeneous group composed of Gram-positive, non-spore-forming bacteria, including *Lactococcus* spp., *Streptococcus* spp., *Pediococcus* spp., *Enterococcus* spp., *Oenococcus* spp., and *Lactobacillus* spp., which have been traditionally used in the fermented food industry, due to their capacity to transform sugars into lactic acid (Chapot-Chartier 2014; Chapot-Chartier and Kulakauskas 2014; Mahony and van Sinderen 2014). *Lactobacillus* spp., as the LAB with probiotic potential, has received considerable attention over the past few years. In addition, *Lactobacillus* spp. is a member of the healthy microbiota of the gastrointestinal tract. Therefore, the selected strains can be used as probiotics (Ren et al. 2014). Probiotic *Lactobacillus* spp. are generally considered safe by the US Food and Drug Administration (FDA) and qualified as presumed safe by the European Food Safety Agency (EFSA). Probiotic *Lactobacillus* spp. is widely used in the food industry because of its unique characteristics and lactic acid fermentation capacity of different foods, such as vegetables, dairy products, and meat products (Pringsulaka et al. 2015; Motahari et al. 2017).

A worldwide spectrum of *Lactobacillus* spp. has been originated from different fermented foods. Based on their potential biological activities, *Lactobacillus* spp. has been applied in the food and pharmaceutical

[#] Changjun Wu and Chenwei Dai contribute equally to this work and are co-first authors.

[*] Corresponding author: X. Zhou, Anhui Academy of Medical Sciences, Hefei Anhui, Province, China; **e-mail: redshow5@163.com**

industry. Common probiotic carriers are fermented milk products at present due to the favorable conditions provided by the acid environments for the survival of probiotics. Shakibaie et al. (2017) isolated a LAB strain belonging to the species *Lactobacillus brevis* from an Iranian traditional dairy product named spar. Bao et al. (2012) found that *Lactobacillus helveticus* and *Lactobacillus casei* screened from traditional yak milk products of Gansu Province in China were considered the predominant populations in the yak milk products and may be a valuable source for further starter selection. *Lactobacillus fermentum* SJRP30 and *L. casei* SJRP145 and SJRP146 isolated from water buffalo mozzarella cheese were revealed to be safe and to possess similar or superior probiotic characteristics (Casarotti et al. 2017). Traditional fermented dairy products are rich in wild LAB as they are generally fermented with local microbiota from raw milk in the process of natural fermentation without participation with industrial starters. This microbial community plays an important part in their specific characteristics and indigenous flavor and texture (Chapot-Chartier and Kulakauskas 2014; Zuo et al. 2014). Traditional fermented milk products provide potential affordable functional products with probiotic properties. Traditional fermented dairy products, mainly manufactured in rural areas, offer potential functional products with probiotic characteristics.

Furthermore, the efficacy of probiotics has been proved to be species- or even strain-dependent, as different LAB strains can affect hosts in different ways (Cani and Van Hul 2015). Isolation and identification of such wild LAB from traditional dairy foods can be a good opportunity to develop new starter cultures and new probiotics (Bao et al. 2012). Consequently, exploration for new probiotics, especially from the relatively undeveloped rural areas, has become a hot research topic (Bajaj et al. 2014; Gupta and Bajaj 2016).

Chinese traditional buffalo milk is a kind of fermented yogurt with a unique flavor, which is made from raw milk of buffalo raised in the Changjiang river basin and fermented in clay pots by natural LAB. It is different from the yogurt products in Northwest China made from the raw milk of yak, cow, and sheep as the primary raw material. Rare reports have been available on the usage of Chinese traditional fermented buffalo milk as a potential probiotic carrier so far. A detailed study on the probiotic potential of Chinese traditional fermented buffalo milk can provide valuable information and clarify its potential use in a broader range.

Although LAB is generally considered safe to consume in the food industry, a series of *in vitro* tests have been carried out and applied to identify microorganisms with the probiotic-rich potential to establish criteria for probiotic screening (Leahy et al. 2005). Consequently, several criteria have been employed to estimate probiotic properties of a newly isolated strain, including antibacterial properties, sensitivity to antibiotics, ability to adhere to epithelial cells, and absence of hemolytic activity when used in food fermentation (Verdenelli et al. 2009; Diosma et al. 2014; Khan 2014). In addition, potential probiotics should also exhibit some specific probiotic properties, such as biofilm formation and exopolysaccharide (EPS) production. It is well known that LAB forms biofilm under specific environmental conditions, which is advantageous for intestinal colonization and probiotic potential of LAB (Elhadidy and Zahran 2014; Johansson and Rasmussen 2013; Popović et al. 2018). What is more, some studies have found that biofilms formed by LAB exhibit the ability to influence the survival and the multiplication of pathogens. In addition, the biofilms formed by LAB exhibit the ability to repress the survival and proliferation of pathogens (Guerrieri et al. 2009). EPS plays a vital role in its rheological and physicochemical properties during fermentation (Widyastuti and Febrisiantosa 2014). EPS has also been investigated as an antiviral drug (Katsuraya et al. 1995) and antitumor agent (Sun et al. 2018).

This study's objecives were to provide a more comprehensive investigation of the probiotic properties of LAB strains obtained from Chinese traditional fermented buffalo milk through various *in vitro* tests to be used in the food industry.

Experimental

Materials and Methods

Enrichment, isolation and screening of LAB. Five home-made traditional fermented buffalo milk was collected from the households of Digang Town, Fanchang County (E 118°20″, N 31°08″), Wuhu City, Anhui Province, China. The samples did not deteriorate, showed porcelain white, had milk fragrance, and no peculiar smell. To enrich LAB, the samples were added at 2% volume into 50 ml de Man, Rogosa, and Sharpe (MRS, Qingdao Hope Bio-Technology Co., Ltd.). The sample suspensions of an appropriate dilution were inoculated onto MRS plates (containing 1% $CaCO_3$), and placed in an anaerobic environment for culture at 37°C for 48 h. The separate white colonies, which showed calcium-dissolving circle by streaking on the MRS plate were selected and purified. Biochemical features were used for the identification of isolated LAB. All the experiments in this study have been carried out in triplicates. *Lactobacillus rhamnosus* GG ATCC 53103 (LGG) provided by the Institute of Microbiology, Anhui Academy of Medical Sciences, China, was used as the reference strain.

Adhesion to HT-29 cell. Adhesion to HT-29 cell was performed following the method described previously (Lee et al. 2015) with minor modifications. Human colon cancer cells HT-29 (Hunan Fenghui Biotechnology Co., Ltd.) were maintained in Dulbecco's Modified Eagle Medium F-12 (DMEM/F12, Gibco, USA), supplemented with 10% (v/v) fetal bovine serum (Zhengjiang Tianhang Biotechnology Co., Ltd.) in a carbon dioxide incubator of 5% CO_2 at 37°C for 48 h. The HT-29 cells were harvested and added into the 24-well plate (2×10^6 cells/well), and grown for 48 h. The medium was refreshed daily. A volume of 0.5 ml LAB (1×10^8 CFU/ml) was added into the wells, and the suspension was incubated at 37°C for 2 h. The wells were washed with PBS three times, then the cells were treated with Triton X-100 (BioFRoxx, Germany), and the bacteria were inoculated on the MRS agar plate. The number of the adherent bacterial cells was counted on the plates and the adhesion rate was calculated.

Tolerance to artificial simulated gastrointestinal conditions. The determination of resistance to simulated gastrointestinal juices was carried out according to the method described previously with minor modifications (Cao et al. 2018; Iraporda et al. 2019). The cultures of LAB strains incubated in MRS broth, supplemented with 0.1% (w/v) ascorbic acid at 37°C for 48 h on anaerobic condition were centrifuged at 10,000 × *g* for 10 min at 4°C, and the pellets were washed twice with PBS buffer (pH 7.4). The artificial simulated gastric juice at a volume of 4 ml (125 mM NaCl, 7 mM KCl, 45 mM $NaHCO_3$ and 3 g/l pepsin (Shanghai Lanji Technology Development Co., Ltd.), adjusted to pH 2.0 with HCl, filtrated by 0.22 μm filter membrane) was used to suspend the cell pellets. The bacterial concentration was adjusted to 10^8 CFU/ml, incubated at 37°C in a water bath for 3 h (a period, which simulated the gastric transit time for humans). After tenfold serial dilutions, the suspension of appropriate concentration was coated on MRS plates, and the number of viable bacteria was determined by colony counting. After treatment with artificial simulated gastric juice for 3 h, the LAB strains were obtained by centrifugation at 10,000 × *g* for 10 min, and the pellets were washed twice with PBS buffer. Four milliliters of artificial simulated intestinal juice (22 mM NaCl, 3.2 mM KCl, 7.6 mM $NaHCO_3$, 1.0 g/l pancreatin (Shanghai Lanji Technology Development Co., Ltd.) and 0.3 g/l bile oxgall (Beijing Solarbio Science and Technology Co., Ltd.), pH adjusted to 8.0 with NaOH, filtrated by 0.22 μm filter membrane) were used to suspend the cell pellets, incubated at 37°C in a water bath for 5 h (a period that simulated the intestinal transit time for humans). After tenfold serial dilution, the suspension of appropriate concentration was coated on the MRS plates; the number of viable bacteria was determined by colony counting. The survival rate of the LAB strains was calculated as follows:

$$Survival\ rate\ (\%) = \frac{N_1}{N_0} \times 100$$

where N_0 is the initial inoculated viable cell numbers, and N_1 is the cell numbers after treatment with artificial simulated gastric juice (3 h) or artificial simulated intestinal juice (5 h).

Antioxidant capacity. 2,2-Diphenyl-1-picrylhydrazyl (DPPH) radical scavenging activity was assessed according to the methodology used (Yu et al. 2018) with slight modifications. 0.2 ml of LAB culture (1×10^9 CFU/ml) was mixed with 1 ml DPPH solution in methanol (100 μM). After being placed against exposure to light at 37°C for 20 minutes, the mixture was centrifugated at 8,000 × *g* for 5 minutes. Finally, the absorbance value at 517 nm was measured. 2,2′-Azinobis(3-ethylbenzothiazoline-6-sulfonic acid) diammonium salt (ABTS) cation radical scavenging activity was investigated according to the methodology used (Cao et al. 2018) with simple modifications. Seven mM of $ABTS^+$ solution was prepared with 2.45 mM potassium persulfate solution and incubated in the dark at room temperature for 12 h as the $ABTS^+$ working solution. 0.1 ml of LAB culture (1×10^9 CFU/ml) was mixed with 1 ml of $ABTS^+$ working solution. After being placed against exposure to light at 37°C for 20 minutes, the mixture was centrifuged at 8,000 × *g* for 5 minutes. Finally, the absorbance value at 734 nm was measured. Superoxide anion scavenging activity was ascertained according to the previous methodology (Tang et al. 2017) with slight modifications. 0.5 ml of LAB culture (1×10^9 CFU/ml) was mixed with 1.5 ml Tris-HCl (pH = 8), and placed in water bath at 25°C for 20 min, 0.2 ml pyrogallol solution in deionized water (25 mM) was added into the suspension. A volume of 0.25 ml hydrochloric acid was used to terminate the reaction after 5 min. The mixture was centrifuged at 8,000 × *g* for 5 min. Finally, the absorbance value at 325 nm was measured. In the above three tests, PBS solution was set as blank control, and scavenging activity was calculated as the following formula:

$$Scavenging\ rate\ (\%) = (1 - \frac{A_{sample}}{A_{sample}}) \times 100$$

where A_{sample} represent the OD_{517}, OD_{734} and OD_{325} values of sample, respectively. $A_{control}$ represent the OD_{517}, OD_{734} and OD_{325} values of control, respectively.

Antibacterial activity. Antibacterial activities of LAB strains were investigated by a disc diffusion method (Piyadeatsoontorn et al. 2019) with some modifications. The pathogens were used as indicator strains in this study, including *Escherichia coli* ATCC8099,

Staphylococcus aureus ATCC6538, *Salmonella enterica* ATCC9120, and *Shigella sonnei* BNCC192105, respectively. One hundred microliters of fresh indicator bacterial culture (10^7 CFU/ml) were inoculated on the LB plate; the sterilized disc was placed on the plate after the surface of plate was left to dry. A volume of 20 µl cell-free supernatant (CFS) was carefully added onto the disc, and the plates were kept in the incubator at 37°C for 24 h, subsequently. The antibacterial activity of LAB was assessed by measuring the diameter of the inhibition circle with a vernier caliper.

16s rRNA gene sequencing for molecular identification. The LAB strain isolated was subjected to the 16S rRNA gene identification at the species level. The genomic DNA was extracted according to the manufacturer's instructions of the bacterial DNA extraction kit purchased from TIANGEN Biotech Co., Ltd., and the 16S rRNA gene was amplified with universal primers 27F (5'-AGAGTTGATCCTGGCTCAG-3') and 1492R (5'-GGTATCCTTGTTACTACTT-3') by using gradient PCR instrument (ABI, USA) (Piyadeatsoontorn et al. 2019). A total volume of 50 µl consisted of 1.0 µl template DNA, 1.0 µl Taq DNA polymer, 5.0 µl 10 × PCR buffer, 1.0 µl 10 mM dNTP, 1.5 µl 10 µM upstream and downstream primers, respectively, 39.0 µl ddH_2O. The thermal cycling parameters were as follows: initial denaturation at 95°C for 300 s, 35 denaturation cycles at 95°C for 30 s, annealing at 58°C for 30 s, elongation at 72°C for 90 s, and final elongation at 72°C for 420 s. Three microliters of PCR amplicons were visualized at 100 V for 1 h by using 1% agarose for electrophoresis. The PCR product was sent to Shanghai Personal Gene Technology Co., Ltd. for sequencing. The 16S rRNA gene sequences were compared and matched using BLAST with the available sequences in NCBI GenBank. The homology of the target gene sequence was analyzed, and the phylogenetic tree was constructed by MEGA 7.0 with bootstrap values based on 1,000 replications. The sequence identified was uploaded to the NCBI Gene Bank database.

Scanning electron microscope (SEM) observations. Observations on the morphology of isolated LAB strains exhibiting probiotic potential by SEM were conducted as described previously (Prasanna and Charalampopolous 2018). The LAB strains were placed in the incubator at 37°C for 18 h. The cultures were centrifuged at 8,000 × *g* for 10 min; the cell pellets were harvested and fixed with PBS buffer (0.1 M, pH = 7.2) containing 2.5% (w/v) glutaraldehyde at 4°C overnight. Afterward, the samples were washed twice with PBS and then dehydrated with a graded ethanol series (30%, 50%, 70%, 80%, 90%, 100%) at 4°C for 20 min, respectively. The samples were transferred into anhydrous acetone and dried in a critical point dryer (Emitech-K850, UK). The dried bacterial powders were smeared evenly using a sterile cotton swab onto the stage with electric conductive adhesive and sputter-coated with gold with a sputter-coater (Hitachi E-1010, Japan). Eventually, the samples were observed using a scanning electron microscope (Hitachi S-4800, Japan) under standard operating conditions at an accelerating voltage of 0.5–30 kV.

Determination of LAB strain's growth curve and acid production curve. The growth curve and acid production curve were drawn based on the method described (Xia et al. 2019) with modifications. The fresh culture of isolated LAB strain was subcultured twice for 24 h and added into the conical flask (250 ml) containing 150 ml MRS broth at 2% inoculation amount for static culture in an anaerobic incubator (Shanghai Longyue Biotechnology Co., Ltd.). Two milliliters of culture were taken out through the rubber gloves fixed and sealed on the operating hole left on the anaerobic incubator quickly and carefully every 2 h until 24 h, and try not to shake the conical flask to keep the static condition. The absorbance value at 600 nm and pH value were measured. The growth curve and acid production curve were drawn according to the absorbance value at 600 nm, and pH value, respectively, determined at different culture times.

Heat resistance test. According to Bacon et al. (2003), the heat resistance test was performed with modifications. The strain was cultured in MRS broth until the absorbance value at 600 nm reached 1.5 at 37°C anaerobically. A total of 1 ml culture was inoculated into 4 ml PBS solution and treated in the water bath at 40, 50, 60, 70, or 80°C for 3 minutes, respectively. As soon as the heating was over, the solution was immediately cooled on ice and diluted to 10^{-1}, 10^{-2}, 10^{-3}, 10^{-4}, and 10^{-5}, subsequently. The sample suspensions of appropriate dilution were plated onto MRS and placed in the incubator at 37°C for 18 h anaerobically.

Bile salt hydrolase (BSH) activity. BSH activity was performed as described by Shehata et al. (2016). The LAB strain was incubated in the incubator at 37°C for 18 h, and the culture was coated on the MRS plate with 0.5% (w/v) sodium taurodeoxycholic acid (TDCA) or MRS plate without TDCA, followed by incubation at 37°C for 72 h anaerobically. The appearance of precipitation indicated the BSH activity of the strain.

Biofilm formation assay. Biofilm formation on the glass and plastic surfaces was detected according to Gheziel et al. (2019). After LAB incubation the biofilm rings were collected, washed with distilled water, and stained with crystal violet (0.5%, v/v). Followed by dissolving the biofilms with acetic acid (30%, v/v), the absorbance value at 590 nm was measured. LAB was defined as strongly biofilm formation ($OD_{590} > 0.2$), weakly biofilm formation ($0.1 < OD_{590} < 0.2$), or no biofilm formation ($OD_{590} < 0.1$).

Exopolysaccharide (EPS) production capability. According to Adesulu-Dahunsi et al. (2018), the EPS production capability was detected. The strain was cultured in an MRS broth medium with 2% sucrose (w/v) at 37°C for 18 h. After the culture was centrifugated at 8,000 × *g* for 15 min, the supernatant was retained and ethanol was added into the supernatant. After an ice bath for 4 for 24 h and centrifugation at 12,000 × *g* for 15 min, the precipitate was dissolved in distilled water. The sugar equivalent of EPS (calculated as glucose) was determined.

Hemolysis test. The hemolysis test was assessed according to Menezes et al. (2020). The appearance of the hydrolytic circle (β-hemolysis) was regarded as a positive result. The appearance of the green circle (α-hemolysis) or no hydrolytic circle appearing (γ-hemolysis) was regarded as non-hemolysis.

Antibiotic susceptibility assay. Antibiotic susceptibility was assessed as Maldonado et al. (2012) with minor modifications. Under aseptic condition, 100 µl of LAB culture (1×10^7 CFU/ml) was coated on MRS plate. After 5 min, the discs containing antibiotics were placed on the plate, and the media were incubated at 37°C for 24 h. Types and dosages of antibiotics were as follows: metronidazole 5 µg, chloramphenicol 30 µg, streptomycin 10 µg, kanamycin 30 µg, ampicillin 10 µg, gentamicin 10 µg, tetracycline 30 µg, erythromycin 15 µg, rifampicin 5 µg, ciprofloxacin 5 µg, doxycycline 30 µg, vancomycin 30 µg. The diameter of the inhibition zone was measured with a vernier caliper, and the results were declared in accordance with the microbiological breakpoints for antimicrobials issued (CLSI 2012).

Biogenic amines production. Biogenic amines production was investigated following Bover-Cid and Holzapfel (1999). Pyridoxal-5-phosphate (0.005%) was added to the medium as a cofactor for decarboxylation reaction, and the pH was adjusted to 5.3. The LAB strain was streaked on MRS plate supplemented with amino acids (lysine, histidine, arginine, tyrosine, and ornithine) (Beijing Solarbio Science & Technology Co., Ltd.) at 0.5% final concentration. Bromocresol purple was used as a color indicator, and the plate was placed in the incubator at 37°C for 72 h, subsequently. The positive result was confirmed by changing the indicator from yellow to purple.

Enzyme production. Enzyme production was determined by using an API-ZYM kit (Biomerieux, France). After incubation of the strain, the culture was centrifuged at 4°C at 12,000 × *g* for 10 min, and the precipitate was resuspended with sterile saline to a concentration of 10^5 CFU/ml, and added to each cupule. The cupules were placed in the incubator at 37°C for 5 h. One drop of enzyme A and enzyme B reagents was added continuously to each cupule. According to the manufacturer's instruction, the enzyme production was declared as 0 to 5.

Statistical analysis. Experiments were conducted in triplicate in our research, and all data were expressed as means and standard deviation. SPSS version 23.0 was employed for data analysis. One-way ANOVA estimated the difference with Duncan's multiple range tests, and statistical significance was set at $p < 0.05$.

Results

Adhesion to HT-29 cell. Through preliminary screening of LAB, out of a total of 22 isolates, 11 isolated strains were putatively identified as LAB (Table I), and their adhesion to HT-29 cells was evaluated. The results

Table I
Physiological and biochemical features of 11 isolated strains.

Characteristic	WDS	WDS-7
Glucose gas production	–	–
Gelatin	3	–
Nitrate reduction	–	–
Catalase	–	–
Arginine hydrolysis	–	–
Motile	–	–
H_2S production	–	–
Indole	–	–
15°C growth test	–	–
45°C growth test	+	+
Arabinose	3	–
Cellobiose	7	–
Esculin	5	–
Fructose	+	+
Gluconate	4	–
Lactose	9	+
Mannose	6	+
Mannitol	1	–
Sorbitol	–	–
Melezitose	–	–
Melibiose	5	–
Raffinose	3	–
Rhamnose	–	–
Salicin	6	–
Glucose	+	+
Sucrose	8	+
Trehalose	6	–
Xylose	–	–
Ribose	–	–
Maltose	8	–

WDS – WDS-2, WDS-3, WDS-4, WDS-8, WDS-9, WDS-10, WDS-11, WDS-15, WDS-18, WDS-20; 10 isolates
+ – positive or weakly positive reaction
– – negative reaction
number – the number of positive reactions

are shown in Table II. The adhesion rate to HT-29 cell ranged from 2.47 ± 0.46% to 11.50 ± 1.22%. Among the 11 LAB strains, six strains displayed strong adhesion capacity to HT-29 cells, including WDS-3, WDS-4, WDS-7, WDS-9, WDS-10, and WDS-18. WDS-4 had the strongest adhesion capacity to HT-29 cells with an adhesion rate of 11.50 ± 1.22%.

Tolerance to artificial simulated gastrointestinal conditions. Tolerance to artificial simulated gastrointestinal conditions of six selected LAB strains is presented in Table III. In general, six selected strains exhibited a good tolerance to artificial simulated gastrointestinal conditions. After treatment with artificial simulated gastric juice for 3 h, the survival rate of six LAB strains decreased with the growth reduction ranging from 18.66% to 29.06%. WDS-3 showed the best tolerance to artificial simulated gastric juice with an 81.34 ± 4.41 survival rate. Subsequently, after treatment with artificial simulated intestinal juice for 5 h, the growth reduction ranged from 29.44% to 39.96%. WDS-3 also displayed the best tolerance to artificial simulated intestinal juice, showing a 70.56 ± 4.49% survival rate. Due to their high tolerance to artificial simulated gastrointestinal conditions, WDS-3, WDS-4, WDS-7, WDS-9, WDS-10, and WDS-18 were chosen for further testing.

Table II
Adhesion rate to HT-29 cells of 11 isolated LAB strains.

Strains	Adhesion capacity to HT-29 Cell (%)
WDS-2	3.79 ± 0.72^{a}
WDS-3	9.65 ± 1.50^{bcd}
WDS-4	11.50 ± 1.22^{e}
WDS-7	10.74 ± 0.99^{cde}
WDS-8	2.47 ± 0.46^{a}
WDS-9	9.43 ± 0.93^{bc}
WDS-10	8.99 ± 1.05^{b}
WDS-11	3.32 ± 0.50^{a}
WDS-15	2.92 ± 0.80^{a}
WDS-18	11.23 ± 0.71^{de}
WDS-20	4.16 ± 0.37^{a}
LGG	15.56 ± 1.31^{f}

Results are expressed as the mean ± SD.
[a-f] – different letters along the column represent statistical significance ($p < 0.05$)

Table III
Tolerance to artificial simulated gastrointestinal conditions of six isolated LAB strains.

Strains	Artificial simulated gastric juice, 3 h, survival rate (%)	Artificial simulated intestinal juice, 5 h survival rate (%)
WDS-3	81.34 ± 4.40^{b}	70.56 ± 4.49^{b}
WDS-4	77.45 ± 3.66^{ab}	62.36 ± 3.06^{ab}
WDS-7	78.99 ± 3.98^{ab}	67.81 ± 3.57^{ab}
WDS-9	76.95 ± 2.03^{ab}	66.19 ± 3.48^{ab}
WDS-10	70.94 ± 4.27^{a}	60.04 ± 1.25^{a}
WDS-18	71.29 ± 2.13^{a}	60.75 ± 5.17^{a}
LGG	84.72 ± 4.96^{b}	77.75 ± 4.25^{c}

Results are expressed as the mean ± SD.
[a-c] – different letters along the column represent statistical significance ($p < 0.05$)

Table IV
Antioxidant capacities of six isolated LAB strains.

Strains	Antioxidant capacities (%)		
	DPPH scavenging activity	$ABTS^{+}$ scavenging activity	Superoxide anion scavenging activity
WDS-3	19.32 ± 1.24^{ab}	52.35 ± 2.47^{b}	41.31 ± 2.64^{a}
WDS-4	31.04 ± 1.71^{c}	65.20 ± 2.38^{d}	49.72 ± 1.63^{b}
WDS-7	30.15 ± 2.24^{c}	68.31 ± 1.50^{d}	48.92 ± 1.36^{b}
WDS-9	18.09 ± 1.78^{a}	40.78 ± 1.43^{a}	40.77 ± 1.85^{a}
WDS-10	22.08 ± 1.61^{b}	49.01 ± 1.72^{b}	41.94 ± 1.69^{a}
WDS-18	32.00 ± 2.71^{c}	56.97 ± 1.68^{c}	48.68 ± 1.33^{b}
LGG	21.32 ± 1.13^{ab}	51.94 ± 2.04^{b}	40.12 ± 1.07^{a}

Results are expressed as the mean ± SD.
[a-d] – different letters along the column represent statistical significance ($p < 0.05$)

Antioxidant capacities. Antioxidant activities including DPPH radical scavenging, $ABTS^{+}$ radical scavenging, and superoxide anion scavenging were assayed in this study. The results are presented in Table IV. In general, WDS-4, WDS-7, and WDS-18 exhibited prominent antioxidant activities with significantly higher DPPH, $ABTS^{+}$, and superoxide anion scavenging activities than those of the reference strain LGG ($p < 0.05$). WDS-18, WDS-7, and WDS-4 showed the highest DPPH radical scavenging activity of 32.00 ± 2.71%, the highest $ABTS^{+}$ radial scavenging activity of 68.31 ± 1.50%, and the highest superoxide anion scavenging activity of 49.72 ± 1.63%, respectively.

Antibacterial activity. The inhibition activity of three isolated strains against four pathogens including *E. coli*, *S. aureus*, *S. enterica*, and *S. sonnei* is shown in Fig. 1. Overall, all isolated strains displayed certain inhibition activities against indicator pathogens, with the diameter of the clear zones ranging from 7.2 to 22.0 mm. Among the three isolates, WDS-7 exhibited the highest inhibition effect on four pathogens. It is worth noting that *S. aureus* was the most inhibited bacteria by all three isolated LAB strains compared to the other tested pathogens. Due to the remarkable antibacterial activity, WDS-7 was screened for further analysis.

Molecular identification. Due to the efficient adhesion to HT-29 cells, prominent antioxidant activity, and remarkable antimicrobial activity, the WDS-7

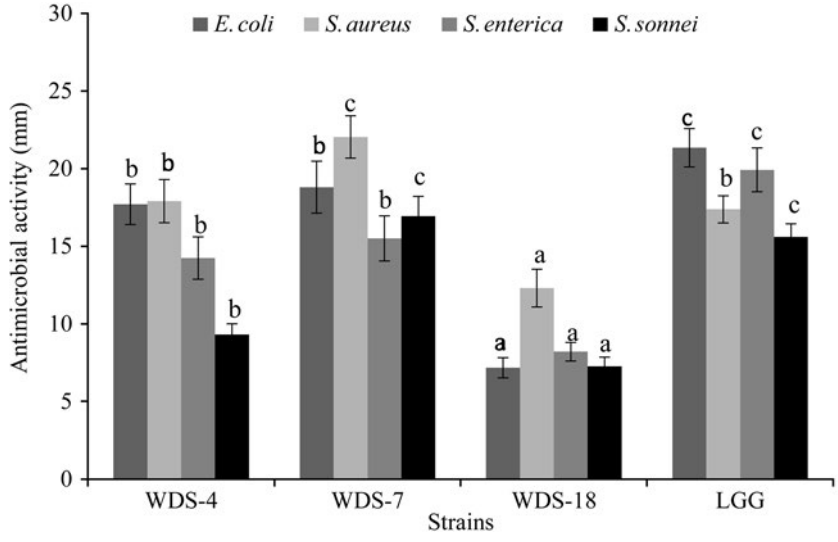

Fig. 1. Antibacterial activity of six isolated LAB strains. a–c) Different letters represent statistical significance ($p < 0.05$).

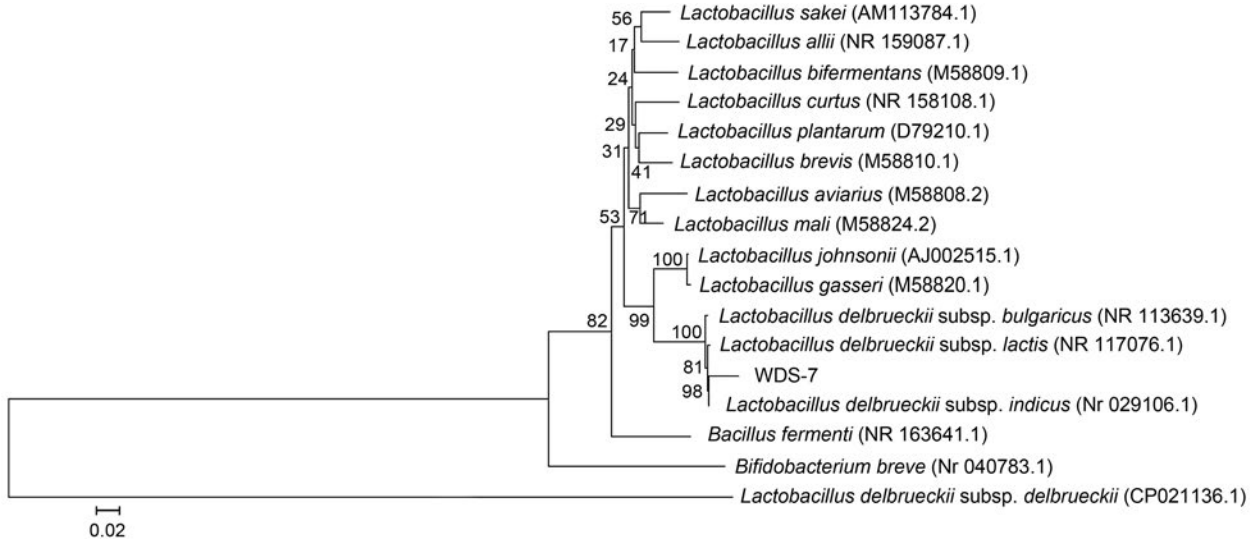

Fig. 2. Phylogenetic tree constructed based on the 16S rRNA gene sequence of *Lactobacillus delbrueckii* ssp. *indicus* WDS-7 strain.

strain was selected to be identified by the 16S rRNA gene sequencing. The 16S rRNA gene sequence of the WDS-7 strain was uploaded to NCBI (the accession No. MN 759441), and the sequence similarity comparison was performed with BLAST. The phylogenetic tree of strain is shown in Fig. 2. The homology of WDS-7 and *L. delbrueckii* ssp. *indicus* 16S rRNA gene sequence reached 98%. Therefore, based on the 16S rRNA gene sequencing and the results of colony morphology, Gram staining, physiological, and biochemical identification described above, the WDS-7 strain was identified as *L. delbrueckii* ssp. *indicus* and simply named as *L. delbrueckii* ssp. *indicus* WDS-7.

Morphological observation on WDS-7. The micrographs of *L. delbrueckii* ssp. *indicus* WDS-7 strain under SEM are shown in Fig. 3. The colonies of WDS-7 were large, rod-shaped, and smooth on the surface, neat edge, opaque, paired, or linked. The strain was Gram-positive, and it was non-motile. No flagella or polar fibers were observed under SEM imaging.

Growth curve and acid production curve. The growth curve of *L. delbrueckii* ssp. *indicus* WDS-7 strain was drawn and analyzed, as shown in Fig. 4. The strain was in the latency phase from 0 to 2 h with a low growth, but the biomass of the strain increased in the fastest rate from 2 to 12 h, when the cell growth was in the exponential phase. The biomass reached the peak value at 18 h, and the maximum absorbance value at 600 nm was about 1.71. Then the absorbance value decreased slowly; the bacterial cells entered the stable growth phase. The pH value of the initial culture of strain WDS-7 was about 6.2 (Fig. 4). However, with the increase of culture time and biomass, the pH value decreased rapidly after 2 h. After 20 h of incubation, the

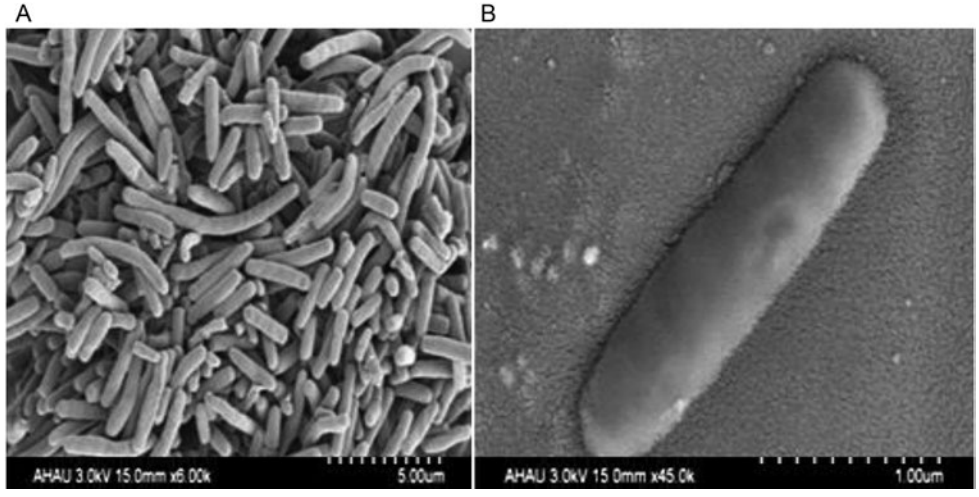

Fig. 3. SEM images of *Lactobacillus delbrueckii* ssp. *indicus* WDS-7 strain. A) SEM image of numerous bacteria located at random, B) SEM image of a single cell.

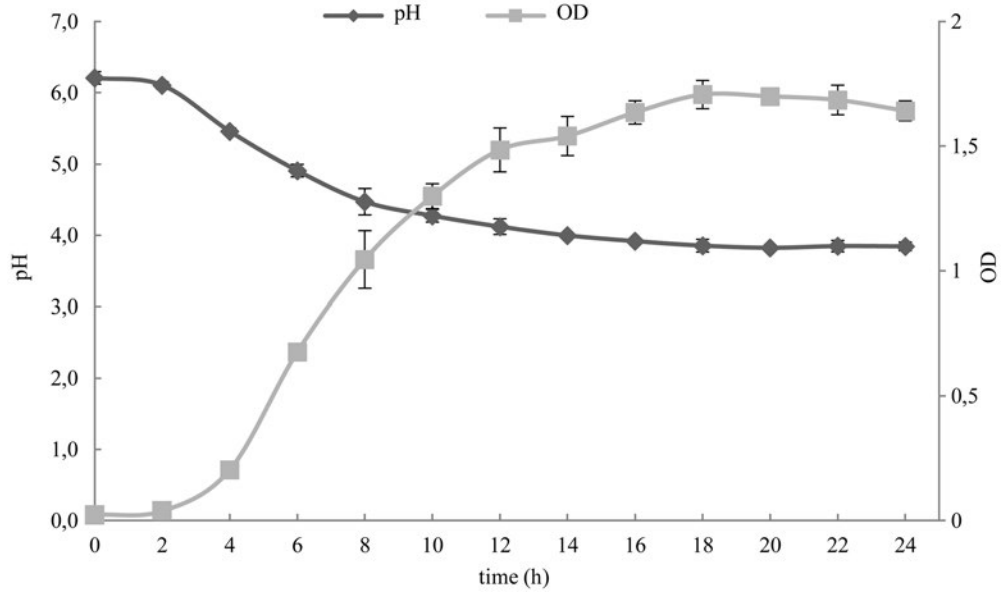

Fig. 4. Growth curve and acid production curve of *Lactobacillus delbrueckii* ssp. *indicus* WDS-7 strain.

pH value reached the lowest, i.e., 3.82, and remained under 4.0 in the stable growth phase.

Heat resistance. The heat resistance of *L. delbrueckii* ssp. *indicus* WDS-7 strain was investigated, and the results are presented in Table V. In general, WDS-7 strain was inactivated after treatment in water bath at 70°C and 80°C for 3 min, and the survival rate was about 0%. When exposed to 60°C the survival rate of the strain was 12.38 ± 2.33%. After treatment at 50°C for 3 minutes, the survival rate of the WDS-7 strain was higher than that of LGG and was 91.81 ± 7.43%.

Table V
The cell survival rates after heat treatment of *Lactobacillus delbrueckii* ssp. *indicus* WDS-7 strain.

Strains	Temperature (°C)			
	50	60	70	80
WDS-7	91.81 ± 7.43%	12.38 ± 2.33%*	≈ 0%	0%
LGG	83.38 ± 7.32%	4.79 ± 0.93%	≈ 0%	0%

Results are expressed as the mean ± SD.
* – along the column represent statistical significance ($p < 0.05$)

BSH activity. The BSH activity of *L. delbrueckii* ssp. *indicus* WDS-7 strain was assessed qualitatively in our study. In contrast to the control MRS agar plate, precipitation around the colonies on MRS agar plate with TDCA indicated that the WDS-7 strain possessed the BSH activity.

Biofilm formation. The ability of *L. delbrueckii* ssp. *indicus* WDS-7 to form biofilm on glass and plastic surfaces was evaluated with the crystal violet method. The results are illustrated in TableVI. LGG was a mild

Table VI
Biofilm formation by *Lactobacillus delbrueckii* ssp. *indicus* WDS-7 strain.

Strains	Biofilm formation	
	Glass	Plastic
WDS-7	+	++
LGG	+	+

+ and ++ represent mild biofilm producer ($0.1 < OD_{590} < 0.2$) and strong biofilm producer ($OD_{590} > 0.2$), respectively

biofilm producer ($0.1 < OD_{590} < 0.2$) due to its weak ability of biofilm formation on glass and plastic surfaces. Similarly, WDS-7 also displayed a weak biofilm formation ability on the glass surface, whereas strong on plastic surface ($OD_{590} > 0.2$). WDS-7 was the better biofilm producer on plastic surface compared to LGG.

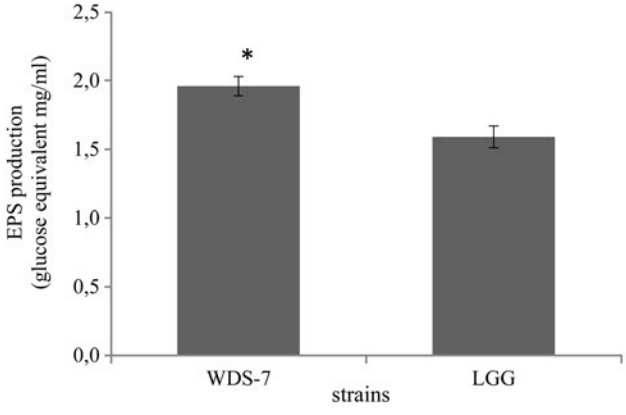

Fig. 5. EPS production activity of *Lactobacillus delbrueckii* ssp. *indicus* WDS-7 strain.
* – represents the statistical significance ($p < 0.05$).

EPS production. The EPS production by *L. delbrueckii* ssp. *indicus* WDS-7 is shown in Fig. 5. Compared to LGG, WDS-7 exhibited a significantly higher ($p < 0.05$) ability to produce EPS (1.94 mg/ml as a glucose equivalent).

Table VII
Antibiotic susceptibility of *Lactobacillus delbrueckii* ssp. *indicus* WDS-7 strain.

Strains	Antibiotic susceptibility											
	Metronidazole	Chloramphenicol	Streptomycin	Kanamycin	Ampicillin	Gentamicin	Tetracycline	Erythromycin	Rifampicin	Ciprofloxacin	Doxycycline	Vancomycin
WDS-7	R	S	R	R	S	R	I	S	S	I	S	R
LGG	R	S	R	R	S	R	S	S	S	S	S	R

R, I, and S represent resistance, intermediate susceptibility, and susceptibility to the antibiotic, respectively

Table VIII
Enzyme production by *Lactobacillus delbrueckii* ssp. *indicus* WDS-7 strain.

Enzyme	Strains	
	LGG	WDS-7
Alkaline phosphatase	1	1
Esterase	2	1
Esterase lipase	1	2
Lipase	0	0
Leucine arylamidase	2	4
Valine arylamidase	3	2
Cystine arylamidase	1	0
Trypsin	0	0
α-Chymotrypsin	0	0
Acid phosphatase	2	0
Naphthol-AS-BI-phosphohydrolase	2	2
α-Galactosidase	1	3
β-Galactosidase	2	4
β-Glucuronidase	0	0
α-Glucosidase	2	2
β-Glucosidase	1	0
N-Acetyl-b-glucosaminidase	0	0
α-Mannosidase	0	0
α-Fucosidase	1	0
Control	0	0

0: 0 nmol, 1: 5 nmol, 2: 10 nmol, 3: 20 nmol, 4: 30 nmol, 5: 40 nmol

Antibiotic susceptibility, hemolysis and production of biogenic amines. The antibiotic susceptibility of *L. delbrueckii* ssp. *indicus* WDS-7 is presented in Table VII. WDS-7 strain showed similar antibiotic resistance patterns compared to LGG, and was sensitive to most antibiotics tested, including chloramphenicol, ampicillin, tetracycline, erythromycin, rifampicin, ciprofloxacin, and doxycycline. It was resistant tometronidazole, streptomycin, kanamycin, gentamicin, and vancomycin. Moreover, any hemolytic activity and production of biogenic amines was observed for WDS-7 strain.

Enzyme production. The enzyme production by *L. delbrueckii* ssp. *indicus* WDS-7 is shown in Table VIII. Compared to LGG, the WDS-7 strain exhibited a similar enzyme production pattern. *L. delbrueckii* ssp. *indicus* WDS-7 possessed various enzyme activities, viz., alkaline phosphatase, esterase, leucine arylamidase, naphthol-AS-BI-phosphohydrolase, valine arylamidase, α-galactosidase, lipase, β-galactosidase and α-glucosidase. In contrast, the production of the α-chymotrypsin, cystine arylamidase, N-acetyl-β-glucosaminidase, β-glucuronidase, lipase, acid phosphatase, β-glucosidase, trypsin, α-fucosidase, and α-mannosidase was not observed.

Discussion

Adhesion to the intestinal mucosa is vital for cultivating probiotics, as it is a prerequisite for colonization in the gastrointestinal tract (Papadimitriou et al. 2015). Georgalaki et al. (2017) reported that the adhesion rate of *Lactobacillus plantarum* ACA-DC 805 to HT-29 cells reached up to 9.5 ± 1.3. The above results are following our results. Cao et al. (2018) found that *L. plantarum* STM6-1 showed the highest adhesion rate to HT-29 (27.2%), followed by *L. plantarum* STM6-2 (17.6%). The results obtained in our work indicated a lower adhesion rate than the reports mentioned by Cao et al. (2018). All 11 LAB strains selected in this research displayed different degrees of adhesion to HT-29 cells. The intestinal adhesion ability of probiotics varies by strain and species. The composition and structure of bacterial cell membrane and the production of secreted proteins may participate in bacterial adhesion to intestinal epithelial cells (Khan and Kang 2016).

The candidate selected as probiotic should survive under high acid conditions and maintain high cell concentration within 2–3 hours of transit in the stomach. Similarly, a potential probiotic is considered is considered to show tolerance to bile salt in the human gut (Kandylis et al. 2016). Son et al. (2017) found that *L. plantarum* Ln4 and G72 had apparent resistance to low pH after 24 h of incubation in the artificial gastric juice. The survival of *L. brevis* strain LSe isolated from an Iranian traditional dairy product was not significantly changed due to drop in pH of the simulated gastric juice from 6 to 3, and after 3 h, 6 h and 24 h of incubation (Shakibaie et al. 2017). Bao et al. (2010) reported that 11 LAB strains of *L. fermentum* originated from traditional dairy products represented survival above 80% after 3 h incubation in simulated gastric juice of pH 2.5. The result of the present study illustrated that six LAB strains showed tolerance to artificial simulated gastrointestinal conditions, which were similar to those mentioned above. It may be due to the production of organic acids by LAB in the process of fermentation, which can reduce the pH of the environment surroundings. Moreover, the traditional fermented buffalo milk is stored in a closed and cryogenic environment, resulting in the organic acid not being easy to volatilize, which maintains and reduces the pH value further. This treatment method on buffalo milk could give these LAB strains the ability to tolerate the extreme living environment, such as low pH value.

Probiotics with antioxidant activity benefit the host by destroying and neutralizing free radicals (Talebi et al. 2018). At present, DPPH and $ABTS^+$ free radical scavenging activities are important tools to evaluate the antioxidant activity of probiotics. Das et al. (2020) investigated the antioxidant activities of eight *Lactobacillus* spp. strains isolated from the traditional fermented foods of Meghalaya, India, and the $ABTS^+$ radical scavenging activity of *L. fermentum* K7 reached 80.78 ± 0.78%. Kaya Ozdgan et al. (2012) reported that the DPPH scavenging capacity of *Lactobacillus lactis* LL27 strain was 75 ± 3%. The antioxidant capacities obtained in our work were lower than in the two reports mentioned above, indicating that the antioxidant activity of *L. lactis* may be dependent on the source and strain. Cao et al. (2018) reported that DPPH radial scavenging activities of *L. plantarum* ST and STDA10 strains isolated from Yunnan De'ang Pickled Tea were almost 30%. Our findings were comparable to the above results reported by Cao et al. (2018). WDS-4, WDS-7, and WDS-18 had notable antioxidant activities in the current research.

Antimicrobial activity is an important criterion when screening potential probiotics, as antimicrobial activity prevents potentially harmful intestinal microorganisms from colonizing the host's intestinal mucosa (Gheziel et al. 2019). Edalati et al. (2019) discovered that *L. plantarum* strain CAU2522 isolated from raw camel's milk from three districts of Kerman province had antagonistic properties on *S. aureus*. Prabhurajeshwara and Chandrakanth (2019) reported that 13 *Lactobacillus* spp. strains isolated from commercial yoghurt showed antagonistic effects against seven indicator microorganisms tested, but the degree of antagonism varied among the *Lactobacillus* spp. strains. Y9, Y10 and Y13 isolates were the most effective in inhibiting pathogens. It was also reported that *L. plantarum* YS5 isolated from yogurt showed excellent antibacterial effect against *E. coli*, *S. aureus* and *Shigella flexneri*, and the inhibition zone of *S. flexneri* was the largest (31.5 ± 0.5 mm) (Nami et al. 2019). In this work, antimicrobial activity varying between strains isolated might be attributed to the differences between species and strains. Some research illustrates that antimicrobial activity is species- and strain-dependent (El-Jeni et al. 2016; Das et al. 2016).

A microbial growth curve can provide useful helpful information for understanding microbial growth trends and selecting the optimal growth stage (Yang et al. 2018). Rapid growth and low pH of the culture may constitute an important feature for the industrial production of a potential probiotic strain. Yang et al. (2021) described that eight *Lactobacillus* spp. strains isolated from soybeans showed the same growth trend, the lag period was short (0–2 h), and the logarithmic growth period was 2–8 h. Pellegrino et al. (2019) also reported three selected *Lactobacillus* spp. strains including *L. lactis* CRL1655, *Lactobacillus perolens* CRL1724, and *L. plantarum* CRL1716 that showed an incubation period of 2 h and an exponential period of growth lasting up to 8 h. In our study, the kinetic growth of

L. delbrueckii ssp. *indicus* WDS-7 strain was consistent with the above results reported. WDS-7 strain had the short latency phase and the pH value of culture reached to 3.82 after 20 h of incubation. It demonstrated that WDS-7 strain had strong capacity for acid production.

Potential probiotic must be able to withstand the harsh conditions e.g., heat, often encountered in food processing, to be successfully applied in functional foods. Ren et al. (2018) found most *Lactobacillus* spp. strains isolated from homemade fermented foods including *L. plantarum*, *Lactobacillus pentosus*, and *Lactobacillus paracasei* with antibacterial activities were highly resistant to heat (65–121°C). The above results were much better than the results of the current research. Wang et al. (2021) also reported that no strains survived incubation at 50°C, while *L. rhamnosus* ZX691 strain grew well at 45°C. The results of this study were superior to the results reported by Wang et al. (2021). In heat resistance test, WDS-7 strain had reasonable growth at 50°C and good thermal stability, making it a potential probiotic selection for food application.

The positive results showing the presence of precipitation around the colonies on MRS agar plate containing TDCA by LAB are advantageous for probiotics as it can help to detoxify bile salt by producing BSH activity (Sharma et al. 2021). It was observed that *L. plantarum* cam 15 from camel milk could combine the bile salts with BSH activity (Sharma et al. 2019). Saliba et al. (2021) reported that all *Lactobacillus* spp. strains isolated from Lebanese Baladi goat milk exhibited a partial BSH activity. The above results were in agreement with our findings. Recent works have found that intestinal probiotics, such as *Lactobacillus* spp., are resistant to the decontamination of bile salts. One of the mechanisms for the resistance is the deconjugation of bile salts through BSH (Prete et al. 2020).

The ability to form biofilm is another desirable characteristic of probiotics. Biofilms are complex multi-species communities that are closely linked to the surface. Therefore, screening of potential probiotic strains usually involves the determination of its biofilm formation capacity (Muruzović et al. 2018). Among five LAB strains isolated from Algerian infant feces, *L. plantarum* LSC3 and LSC22 were the best suited for producing biofilms on plastic and glass surfaces (Gheziel et al. 2019). The results of the present work were consistent with the above results. In this research, WDS-7 isolated from Chinese traditional fermented buffalo milk showed strong ability of biofilm formation, so it certainly has potential for further investigation as probiotics. Our results revealed some variability in biofilm formation capacity, which was consistent with previous work on *Lactobacillus reuteri* (Mackenzie et al. 2010).

Probiotics possessing the capability of EPS production are considered an advantage (Bermúdez-Humarán and Langella 2011). Comparatively with the rest of the cultures, *L. rhamnosus* K4E had the highest EPS production with 950 ± 0.256 mg/l, followed by *L. plantarum* RD7 (710 ± 0.388 mg/l) (Das et al. 2020). The result of EPS production reported above was slightly lower than that of our study. Similarly, Abouloifa et al. (2020) found all the *Lactobacillus* spp. strains isolated from traditional fermenting green olives showed an EPS production capacity. Furthermore, Sharma et al. (2019) revealed that *L. plantarum* K90, *L. fermentum* K75, and *L. fermentum* K78 strains isolated from traditionally fermented wheat flour dough known as "babroo", could be used as potential probiotic candidates with EPS production. EPS improves the colonization of probiotics on the surface of gastrointestinal mucosa by increasing the autoaggregation ability of probiotics (Kanmani et al. 2013). The capability of EPS production of these LAB strains may explain the high adhesion capacity obtained in this work.

In terms of antibiotic resistance, potential probiotic exhibiting sensitivity to antibiotics is preferable for application. Our findings were similar to the antibiotic resistance of *Lactobacillus* spp. isolates originated from traditional dairy products in East Azerbaijan Province in Iran (Faghfoori et al. 2017), and relatively better than the antibiotic resistance of *Lactobacillus curvatus* P99 isolated from fermented oat dairy beverage (Funck et al. 2019). However, LAB strains are known to be inherently sensitive to β-lactam, tetracycline, and macrolides antibiotics but resistant to aminoglycosides antibiotics (Kumar and Kumar 2015). *L. delbrueckii* ssp. *indicus* WDS-7 was resistant to metronidazole, streptomycin, kanamycin, gentamicin, and vancomycin, a cell wall synthesis inhibitor. Jatmiko et al. (2017) reported that *Lactobacilli* are naturally resistant to vancomycin, but vancomycin resistance is encoded by chromosome and cannot be transferred to other microbial species. Lack of hemolytic activity is one of the safety prerequisites for screening probiotics (FAO/WHO 2002). Our conclusion agreed with the known hemolysis of *L. fermentum* isolated from fermented dairy milks (Thirabunyanon et al. 2009).

The absence of biogenic amines production in *Lactobacillus* spp. was already expected an essential criterion of food safety for probiotic candidate strains (Casarotti et al. 2017). Colombo et al. (2020) reported 11 *Lactobacillus* spp. strains previously isolated from a dairy environment showed no *in vitro* detection of biogenic amines production. Yüceer and Özden Tuncer (2015) also described *Lactobacillus sakei* ssp. *carnosus* and *L. sakei* ssp. *sakei* strains isolated from fermented Turkish sausage did not decarboxylate histidine, lysine, or ornithine. The results obtained in this study agreed

with those mentioned above. In our study, no color change of the indicator was observed, it was proved that the WDS-7 strain did not produce biogenic amines, and *L. delbrueckii* ssp. *indicus* WDS-7 strain was safe in food application.

The lack of harmful activities, such as β-glucuronidase activity, must also be included in the safety assessment. In present study, *L. delbrueckii* ssp. *indicus* WDS-7 did not have β-glucuronidase, α-chymotrypsin, and N-acetyl-β-glucosaminidase activities, but showed higher production of β-glucosidase than LGG. *L. plantarum* SK1305 strain isolated from Korean green chili pickled pepper did not produce β-glucuronidase but produced α-and β-glucosidase, α- and β-galactosidase, naphthol-AS-BI-phosphohydrolase, acid phosphatase, and N-acetyl-β-glucosaminidase (Niu et al. 2019). *Lactobacillus* spp. strains, which had previously been isolated from traditional fermenting green olives, also produced several enzymes, such as naphthol-AS-BI-phosphohydrolase and β-galactosidase but did not produce β-glucuronidase, α-chymotrypsin, and other harmful enzymes (Abouloifa et al. 2020). The above conclusions were consistent with the results of this work. The absence of harmful enzymes and the production of valuable enzymes suggested the reliable security of the strain and the possibility of using the strain in the production of fermented milk products.

Conclusions

In this work, *L. delbrueckii* ssp. *indicus* WDS-7 strain was isolated. It fulfilled the probiotic criteria *in vitro* by exhibiting preferable adhesion capacity to HT-29 cells, good tolerance to artificial simulated gastrointestinal conditions, excellent antioxidant capacities, stronger antibacterial activity, and safety in use. Moreover, it also possessed good probiotic activities, including heat resistance, BSH activity, biofilm formation, and EPS production. This study demonstrated the probiotic potential of *L. delbrueckii* ssp. *indicus* WDS-7 strain would be a novel probiotic strain for application in fermented dairy products. For the first time, a probiotic strain isolated from Chinese traditional fermented buffalo milk displayed excellent probiotic properties, and it could be a promising candidate to produce functional probiotic food with potential health benefits.

Conflict of interest

The authors do not report any financial or personal connections with other persons or organizations, which might negatively affect the contents of this publication and/or claim authorship rights to this publication.

Literature

Abouloifa H, Rokni Y, Bellaouchi R, Ghabbour N, Karboune S, Brasca M, Salah RB, Chihib NE, Saalaoui E, Asehraou A. Characterization of probiotic properties of antifungal *Lactobacillus* strains isolated from traditional fermenting green olives. Probiotics Antimicrob Proteins. 2020 Jun;12(2):683–696. https://doi.org/10.1007/s12602-019-09543-8

Adesulu-Dahunsi AT, Sanni AI, Jeyaram K. Production, characterization and *in vitro* antioxidant activities of exopolysaccharide from *Weissella cibaria* GA44. LWT-Food Sci Technol. 2018 Jan;87:432–442. https://doi.org/10.1016/j.lwt.2017.09.013

Bacon RT, Ransom JR, Sofos JN, Kendall PA, Belk KE, Smith GC. Thermal inactivation of susceptible and multiantimicrobial-resistant *Salmonella* strains grown in the absence or presence of glucose. Appl Environ Microbiol. 2003 Jul;69(7):4123–4128. https://doi.org/10.1128/AEM.69.7.4123-4128.2003

Bajaj BK, Andrabi T, Claes IJJ, Lebeer S. Bioprospecting for functionally-proficient potential probiotics. Curr Nutr Food Sci. 2014 Dec 12;10(4):251–263. https://doi.org/10.2174/1573401311666141215212331

Bao QH, Liu WJ, Yu J, Wang WH, Qing MJ, Chen X, Wang F, Zhang JC, Zhang WY, Qiao JM, et al. Isolation and identification of cultivable lactic acid bacteria in traditional yak milk products of Gansu Province in China. J Gen Appl Microbiol. 2012 Nov 5; 58(2): 95–105. https://doi.org/10.2323/jgam.58.95

Bao Y, Zhang YC, Zhang Y, Liu Y, Wang SQ, Dong XM, Wang YY, Zhang HP. Screening of potential probiotic properties of *Lactobacillus fermentum* isolated from traditional dairy products. Food Control. 2010 May;21(5):695–701. https://doi.org/10.1016/j.foodcont.2009.10.010

Bermúdez-Humarán LG, Langella P. Importance of commensal and probiotic bacteria in human health. Curr Immunol Rev. 2011 May 20;8(3):248–253. https://doi.org/10.2174/157339512800671994

Bover-Cid S, Holzapfel WH. Improved screening procedure for biogenic amine production by lactic acid bacteria. Int J Food Microbiol. 1999 Dec 1;53(1):33–41. https://doi.org/10.1016/S0168-1605(99)00152-X

Cani PD, Van Hul M. Novel opportunities for next-generation probiotics targeting metabolic syndrome. Curr Opin Biotech. 2015 Apr; 32:21–27. https://doi.org/10.1016/j.copbio.2014.10.006

Cao ZH, Pan HB, Li SJ, Shi CY, Wang SF, Wang FY, Ye PF, Jia JJ, Ge CR, Lin QY, et al. *In vitro* evaluation of probiotic potential of lactic acid bacteria isolated from Yunnan De'ang pickled tea. Probiotics Antimicro. 2018 Feb 14;11(5):103–112. https://doi.org/10.1007/s12602-018-9395-x

Casarotti SN, Carneiro BM, Todorov SD, Nero LA, Rahal P, Penna ALB. *In vitro* assessment of safety and probiotic potential characteristics of *Lactobacillus* strains isolated from water buffalo mozzarella cheese. Ann Microbiol. 2017 Feb 28;67(4):289–301. https://doi.org/10.1007/s13213-017-1258-2

Chapot-Chartier MP, Kulakauskas S. Cell wall structure and function in lactic acid bacteria. Microb Cell Fact. 2014 Aug 29;13 (Suppl 1):S9. https://doi.org/10.1186/1475-2859-13-S1-S9

Chapot-Chartier MP. Interactions of the cell-wall glycopolymers of lactic acid bacteria with their bacteriophages. Front Microbiol. 2014 May 22;5:236. https://doi.org/10.3389/fmicb.2014.00236

CLSI. Performance standards for antimicrobial susceptibility testing; 22nd ed. CLSI supplement M100-S22. Wayne (USA): Clinical and Laboratory Standards Institute; 2012. p. 44–49.

Colombo M, Nero LA, Todorov SD. Safety profiles of beneficial lactic acid bacteria isolated from dairy systems. Braz J Microbiol. 2020 Jun;51(2):787–795. https://doi.org/10.1007/s42770-020-00227-y

Das P, Khowala S, Biswas S. *In vitro* probiotic characterization of *Lactobacillus casei* isolated from marine samples. LWT-Food Sci Technol. 2016 Nov;73:383–390. https://doi.org/10.1016/j.lwt.2016.06.029

Das S, Mishra BK, Hati S. Techno-functional characterization of indigenous *Lactobacillus* isolates from the traditional fermented foods of Meghalaya, India. Curr Res Food Sci. 2020 Nov;3:9–18. https://doi.org/10.1016/j.crfs.2020.01.002

Diosma G, Romanin DE, Rey-Burusco MF, Londero A, Garrote GL. Yeasts from kefir grains: isolation, identification, and probiotic characterization. World J Microb Biot. 2014 Jan;30(1):43–53. https://doi.org/10.1007/s11274-013-1419-9

Edalati E, Saneei B, Alizadeh M, Hosseini SS, Zahedi Bialvaei A, Taheri K. Isolation of probiotic bacteria from raw camel's milk and their antagonistic effects on two bacteria causing food poisoning. New Microbe New Infect. 2019 Jan;27:64–68. https://doi.org/10.1016/j.nmni.2018.11.008

Elhadidy M, Zahran E. Biofilm mediates *Enterococcus faecalis* adhesion, invasion and survival into bovine mammary epithelial cells. Lett Appl Microbiol. 2014 Mar;58(3):248–254. https://doi.org/10.1111/lam.12184

El-Jeni R, El-Bour M, Calo-Mata P, Böhme K, Fernández-No IC, Barros-Velázquez J, Bouhaouala-Zahar B. *In vitro* probiotic profiling of novel *Enterococcus faecium* and *Leuconostoc mesenteroides* from Tunisian freshwater fishes. Can J Microbiol. 2016 Jan;62(1):60–71. https://doi.org/10.1139/cjm-2015-0481

Faghfoori Z, Gargaria BP, Saber A, Seyyedi M, Khosroushahi AY. The investigation of the diversity of *Lactobacilli* spp. and assessment their some probiotic properties in traditional dairy products in East Azerbaijan province in Iran. Iran J Pharm Res. 2017;16(4):1538–1545. https://doi.org/10.22037/IJPR.2017.2115

FAO/WHO. Guidelines for the evaluation of probiotics in food. London (Canada): Food and Agriculture Organization of the United Nations/World Health Organization; 2002. Available from www.who.int/foodsafety/fs_management/en/probiotic_guidelines.pdf

Funck GD, De Lima Marques J, dos Santos Cruxen CE, Sehn CP, Louise Haubert L, da Silva Dannenberg G, Klajn VM, da Silva WP, Fiorentini AM. Probiotic potential of *Lactobacillus curvatus* P99 and viability in fermented oat dairy beverage. J Food Process Pres. 2019 Nov 13;43(12):e14286. https://doi.org/10.1111/jfpp.14286

Georgalaki M, Zoumpopoulou G, Mavrogonatou E, Van Driessche G, Alexandraki V, Anastasiou R, Papadelli M, Kazou M, Manolopoulou E, Kletsas D, et al. Evaluation of the antihypertensive angiotensin-converting enzyme inhibitory (ACE-I) activity and other probiotic properties of lactic acid bacteria isolated from traditional Greek dairy products. Int Dairy J. 2017 Dec;75:10–21. http://dx.doi.org/10.1016/j.idairyj.2017.07.003

Gheziel C, Russo P, Arena MP, Spano G, Ouzari HI, Kheroua O, Saidi D, Fiocco D, Kaddouri H, Capozzi V. Evaluating the probiotic potential of *Lactobacillus plantarum* strains from Algerian infant feces: towards the design of probiotic starter cultures tailored for developing countries. Probiotics Antimicrob Proteins. 2019 Mar; 11(1):113–123. https://doi.org/10.1007/s12602-018-9396-9

Guerrieri E, Niederhäusern SD, Messi P, Sabia C, Iseppi R, Anacarso I, Bondi M. Use of lactic acid bacteria (LAB) biofilms for the control of *Listeria monocytogenes* in a small-scale model. Food Control. 2009 Sep;20(9):861–865. https://doi.org/10.1016/j.foodcont.2008.11.001

Gupta M, Bajaj BK. Selection criteria for probiotics and potential of cereal based food products as novel probiotic-carriers. Curr Nutr Food Sci. 2016 Jun 9;12(3):157–174. https://doi.org/10.2174/1573401312666160610122205

Hill C, Guarner F, Reid G, Gibson GR, Merenstein DJ, Pot B, Morelli L, Canani RB, Flint HJ, Salminen S, et al. The international scientific association for probiotics and prebiotics consensus statement on the scope and appropriate use of the termprobiotic. Nat Rev Gastroenterol Hepatol. 2014 Aug;11(8):506–514. https://doi.org/10.1038/nrgastro.2014.66

Iraporda C, Rubel IA, Manrique GD, Abraham AG. Influence of inulin rich carbohydrates from Jerusalem artichoke (*Helianthus tuberosus* L.) tubers on probiotic properties of *Lactobacillus* strains. LWT-Food Sci Technol. 2019 Mar;101:738–746. https://doi.org/10.1016/j.lwt.2018.11.074

Jatmiko YD, Howarth GS, Barton MD. Assessment of probiotic properties of lactic acid bacteria isolated from Indonesian naturally fermented milk. AIP Conf Proc. 2017 Nov 29;1908(1):050008. https://doi.org/10.1063/1.5012732

Johansson D, Rasmussen M. Virulence factors in isolates of *Enterococcus faecalis* from infective endocarditis and from the normal flora. Microb Pathogenesis. 2013 Feb;55:28–31. https://doi.org/10.1016/j.micpath.2012.09.009

Kandylis P, Pissaridi K, Bekatorou A, Kanellaki M, Koutinas AA. Dairy and non-dairy probiotic beverages. Curr Opin Food Sci. 2016 Feb;7:58–63. https://doi.org/10.1016/j.cofs.2015.11.012

Kanmani P, Satish-Kumar R, Yuvaraj N, Paari KA, Pattukumar V, Arul V. Probiotics and its functionally valuable products – a review. Crit Rev Food Sci. 2013;53(6):641–658. https://doi.org/10.1080/10408398.2011.553752

Katsuraya K, Shibuya T, Inazawa K, Nakashima H, Yamamoto N, Uryu T. Synthesis of sulfated alkyl malto-oligosaccharides with potent inhibitory effects on AIDS virus infection. Macromolecules. 1995 Sep;28(20):6697–6700. https://doi.org/10.1021/ma00124a001

Kaya Ozdgan D, Akcelik N, Aslim B, Suludere Z, Akcelik M. Probiotic and antioxidative properties of *L. lactis* LL27 isolated from milk. Biotechnol Biotec Eq. 2012 Apr;26:2750–2758. https://doi.org/10.5504/BBEQ.2011.0091

Khan I, Kang SC. Probiotic potential of nutritionally improved *Lactobacillus plantarum* DGK-17 isolated from kimchi – a traditional Korean fermented food. Food Control. 2016 Feb;60:88–94. https://doi.org/10.1016/j.foodcont.2015.07.010

Khan SU. Probiotics in dairy foods: A review. Nutr Food Sci. 2014 Feb 4;44(1):71–88. https://doi.org/10.1108/NFS-04-2013-0051

Kumar A, Kumar D. Characterization of *Lactobacillus* isolated from dairy samples for probiotic properties. Anaerobe. 2015 Jun;33: 117–123. https://doi.org/10.1016/j.anaerobe.2015.03.004

Leahy SC, Higgins DG, Fitzgerald GF, Van Sinderen D. Getting better with bifidobacteria. J Appl Microbiol. 2005;98(6):1303–1315. https://doi.org/10.1111/j.1365-2672.2005.02600.x

Lee NK, Han KJ, Son SH, Eon SJ, Lee SK, Paik HD. Multifunctional effect of probiotic *Lactococcus lactis* KC24 isolated from kimchi. LWT-Food Sci Technol. 2015 Dec;64(2):1036–1041. https://doi.org/10.1016/j.lwt.2015.07.019

Mackenzie DA, Jeffers F, Parker ML, Vibert-Vallet A, Bongaerts RJ, Roos S, Walter J, Juge N. Strain-specific diversity of mucus-binding proteins in the adhesion and aggregation properties of *Lactobacillus reuteri*. Microbiology. 2010 Nov 1;156(11):3368–3378. https://doi.org/10.1099/mic.0.043265-0

Mahony J, van Sinderen D. Current taxonomy of phages infecting lactic acid bacteria. Front Microbiol. 2014 Jan 24;5:7. https://doi.org/10.3389/fmicb.2014.00007

Maldonado NC, de Ruiz CS, Otero MC, Sesma F, Nader-Macías ME. Lactic acid bacteria isolated from young calves – characterization and potential as probiotics. Res Vet Sci. 2012 Apr; 92(2): 342–349. https://doi.org/10.1016/j.rvsc.2011.03.017

Menezes AGT, Ramos CL, Cenzi G, Melo DS, Dias DR, Schwan RF. Probiotic potential, antioxidant activity, and phytase production of indigenous yeasts isolated from indigenous fermented foods. Probiotics Antimicrob Proteins. 2020 Mar;12(1):280–288. https://doi.org/10.1007/s12602-019-9518-z

Motahari P, Mirdamadi S, Kianirad M. Safety evaluation and antimicrobial properties of *Lactobacillus pentosus* 22C isolated from traditional yogurt. J Food Meas Charact. 2017 Sep;11(3):972–978. https://doi.org/10.1007/s11694-017-9471-z

Muruzović MŽ, Mladenović KG, Djilas MD, Stefanović OD, Čomić LR. *In vitro* evaluation of antimicrobial potential and ability of biofilm formation of autochthonous *Lactobacillus* spp. and *Lactococcus* spp. isolated from traditionally made cheese from Southeastern Serbia. J Food Process Preserv. 2018 Nov;42(11):e13776. https://doi.org/10.1111/jfpp.13776

Nair AS, Dubhashi AV. *In-vitro* transit tolerance of probiotic *Bacillus* species in human gastrointestinal tract. Int J Sci Res. 2016 Jun; 5(6):1899–1902. https://doi.org/10.21275/v5i6.NOV164343

Nami Y, Bakhshayesh RV, Manafi M, Hejazi MA. Hypocholesterolaemic activity of a novel autochthonous potential probiotic *Lactobacillus plantarum* YS5 isolated from yogurt. LWT-Food Sci Technol. 2019 Aug;111:876–882. https://doi.org/10.1016/j.lwt.2019.05.057

Niu KM, Kothari D, Cho SB, Han SG, Song IG, Kim SC, Kim SK. Exploring the probiotic and compound feed fermentative applications of *Lactobacillus plantarum* SK1305 isolated from Korean green chili pickled pepper. Probiotics Antimicrob Proteins. 2019 Sep; 11(3):801–812. \https://doi.org/10.1007/s12602-018-9447-2

Papadimitriou K, Zoumpopoulou G, Foligné B, Alexandraki V, Kazou M, Pot B, Tsakalidou E. Discovering probiotic microorganisms: *in vitro*, *in vivo*, genetic and omics approaches. Front Microbiol. 2015 Feb 17;6:58. https://doi.org/10.3389/fmicb.2015.00058

Pellegrino MS, Frola ID, Natanael B, Gobelli D, Nader-Macias MEF, Bogni CI. *In vitro* characterization of lactic acid bacteria isolated from bovine milk as potential probiotic strains to prevent bovine mastitis. Probiotics Antimicrob Proteins. 2019 Mar; 11(1):74–84. https://doi.org/10.1007/s12602-017-9383-6

Piyadeatsoontorn S, Taharnklaew R, Upathanpreecha T, Sornplang P. Encapsulating viability of multi-strain *Lactobacilli* as potential probiotic in pigs. Probiotics Antimicrob Proteins. 2019 Jun;11(2):438–446. https://doi.org/10.1007/s12602-018-9418-7

Popović N, Dinić M, Tolinački M, Mihajlović S, Terzić-Vidojević A, Bojić S, Djokić J, Golić N, Veljović K. New insight into biofilm formation ability, the presence of virulence genes and probiotic potential of *Enterococcus* sp. dairy isolates. Front Microbiol. 2018 Jan 30;9:78. https://doi.org/10.3389/fmicb.2018.00078

Prabhurajeshwara C, Chandrakanth K. Evaluation of antimicrobial properties and their substances against pathogenic bacteria *in-vitro* by probiotic *Lactobacilli* strains isolated from commercial yoghurt. Clin Nutr Exp. 2019 Feb;23:97–115. https://doi.org/10.1016/j.yclnex.2018.10.001

Prasanna PHP, Charalampopolous D. Encapsulation of *Bifidobacterium longum* in alginate-dairy matrices and survival in simulated gastrointestinal conditions, refrigeration, cow milk and goat milk. Food Biosci. 2018 Feb;21:72–79. https://doi.org/10.1016/j.fbio.2017.12.002

Prete R, Long SL, Gallardo AL, Gahan CG, Corsetti A, Joyce SA. Beneficial bile acid metabolism from *Lactobacillus plantarum* of food origin. Sci Rep. 2020 Jan 24;10(1):1165. https://doi.org/10.1038/s41598-020-58069-5

Pringsulaka O, Rueangyotchanthana K, Suwannasai N, Watanapokasin R, Amnueysit P, Sunthornthummas S, Sukkhum S, Sarawaneeyaruk S, Rangsiruji A. *In vitro* screening of lactic acid bacteria for multi-strain probiotics. Livest Sci. 2015 Apr;174:66–73. https://doi.org/10.1016/j.livsci.2015.01.016

Ren D, Li C, Qin Y, Yin R, Du S, Ye F, Liu C, Liu H, Wang M, Li Y, et al. *In vitro* evaluation of the probiotic and functional potential of *Lactobacillus* strains isolated from fermented food and human intestine. Anaerobe. 2014 Dec;30:1–10. https://doi.org/10.1016/j.anaerobe.2014.07.004

Ren DY, Zhu JW, Gong SJ, Liu HY, Yu HS. Antimicrobial characteristics of lactic acid bacteria isolated from homemade fermented foods. Biomed Res Int. 2018 Dec 30;2018:5416725. https://doi.org/10.1155/2018/5416725

Saliba L, Zoumpopoulou G, Anastasiou R, Hassoun G, Karayiannis Y, Sgouras D, Tsakalidoub E, Deiana P, Montanari L, Mangia NP. Probiotic and safety assessment of *Lactobacillus* strains isolated from Lebanese Baladi goat milk. Int Dairy J. 2021 Sep; 120: 105092. https://doi.org/10.1016/j.idairyj.2021.105092

Shakibaie M, Mohammadi-Khorsand T, Adeli-Sardou M, Jafari M, Amirpour-Rostami S, Ameri A, Forootanfar H. Probiotic and antioxidant properties of selenium-enriched *Lactobacillus brevis* LSe isolated from an Iranian traditional dairy product. J Trace Elem Med Bio. 2017 Mar;40:1–9. https://doi.org/10.1016/j.jtemb.2016.11.013

Sharma A, Lavania M, Singh R, Lal B. Identification and probiotic potential of lactic acid bacteria from camel milk. Saudi J Biol Sci. 2021 Mar;28(3):1622–1632. https://doi.org/10.1016/j.sjbs.2020.11.062

Sharma K, Attri S, Goel G. Selection and evaluation of probiotic and functional characteristics of autochthonous lactic acid bacteria isolated from fermented wheat flour dough babroo. Probiotics Antimicro. 2019 Sep 15;11:774–784. https://doi.org/10.1007/s12602-018-9466-z

Shehata MG, El Sohaimy SA, El-Sahn MA, Youssef MM. Screening of isolated potential probiotic lactic acid bacteria for cholesterol lowering property and bile salt hydrolase activity. Ann Agric Sci. 2016 Jun;61(1):65–75. https://doi.org/10.1016/j.aoas.2016.03.001

Son SH, Jeon HL, Jeon EB, Lee NK, Park YS, Kang DK, Paik HD. Potential probiotic *Lactobacillus plantarum* Ln4 from kimchi: Evaluation of β-galactosidase and antioxidant activities. LWT-Food Sci Technol. 2017 Nov;85(Part A):181–186. http://doi.org/10.1016/j.lwt.2017.07.018

Sun NX, Liu HP, Liu SJ, Zhang XY, Chen P, Li WH, Xu XX, Tian WT. Purification, preliminary structure and antitumor activity of exopolysaccharide produced by *Streptococcus thermophilus* CH9. Molecules. 2018 Nov 6;23(11):2898. https://doi.org/10.3390/molecules23112898

Talebi S, Makhdoumi A, Bahreini M, Matin MM, Moradi HS. Three novel *Bacillus* strains from a traditional lacto-fermented pickle as potential probiotics. J Appl Microbiol. 2018 Sep;125(3):888–896. https://doi.org/10.1111/jam.13901

Tang W, Xing Z, Li C, Wang J, Wang Y. Molecular mechanisms and *in vitro* antioxidant effects of *Lactobacillus plantarum* MA2. Food Chem. 2017 Apr 15;221:1642–1649. https://doi.org/10.1016/j.foodchem.2016.10.124

Thirabunyanon M, Boonprasom P, Niamsup P. Probiotic potential of lactic acid bacteria isolated from fermented dairy milks on antiproliferation of colon cancer cells. Biotechnol Lett. 2009 Apr;31(4):571–576. https://doi.org/10.1007/s10529-008-9902-3

Verdenelli MC, Ghelfi F, Silvi S, Orpianesi C, Cecchini C, Cresci A. Probiotic properties of *Lactobacillus rhamnosus* and *Lactobacillus paracasei* isolated from human faeces. Eur J Nutr. 2009 Sep;48(6):355–363. https://doi.org/10.1007/s00394-009-0021-2

Wang X, Wang WD, Lv HX, Zhang H, Liu Y, Zhang M, Wang YP, Tan ZF. Probiotic potential and wide-spectrum antimicrobial activity of lactic acid bacteria isolated from infant feces. Probiotics Antimicrob Proteins. 2021 Feb;13(1):90–101. https://doi.org/10.1007/s12602-020-09658-3

Widyastuti Y, Febrisiantosa A. The role of lactic acid bacteria in milk fermentation. Food Nutr Sci. 2014 Feb;5(4):435–442. https://doi.org/10.4236/fns.2014.54051

Xia Y, Qin SK, Shen YQ. Probiotic potential of *Weissella* strains isolated from horse feces. Microb Pathog. 2019 Jul;132:117–123. https://doi.org/10.1016/j.micpath.2019.04.032

Yang E, Fan LH, Yan JP, Jiang YM, Doucette C, Fillmore S, Walker B. Influence of culture media, pH and temperature on growth and bacteriocin production of bacteriocinogenic lactic acid bacteria. AMB Express. 2018 Jan 24;8(1):10. https://doi.org/10.1186/s13568-018-0536-0

Yang XY, Ke CX, Li L. Physicochemical, rheological and digestive characteristics of soy protein isolate gel induced by lactic acid bacteria. J Food Eng. 2021 Mar;292:110243. https://doi.org/10.1016/j.jfoodeng.2020.110243

Yu HS, Lee NK, Choi AJ, Choe JS, Bae CH, Paik HD. Antagonistic and antioxidant effect of probiotic *Weissella cibaria* JW15. Food Sci Biotechnol. 2018 Nov 22;28(3):851–855. https://doi.org/10.1007/s10068-018-0519-6

Yüceer Ö, Özden Tuncer B. Determination of antibiotic resistance and biogenic amine production of lactic acid bacteria isolated from fermented Turkish sausage (sucuk). J Food Saf. 2015 Jan 8;35:276–285. https://doi.org/10.1111/jfs.12177

Zuo FL, Feng XJ, Chen LL, Chen SW. Identification and partial characterization of lactic acid bacteria isolated from traditional dairy products produced by herders in the western Tianshan Mountains of China. Lett Appl Microbiol. 2014 Nov;59(5)::549–556. https://doi.org/10.1111/lam.12313

ORIGINAL PAPER

Polish Journal of Microbiology
2022, Vol. 71, No 1, 107–114
https://doi.org/10.33073/pjm-2022-013

Monitoring Multidrug-Resistant *Acinetobacter baumannii* Infections in the Neurosurgery ICU Using a Real-Time Surveillance System

YUTING ZHU[1], MINGZHU NI[1], XIAOFANG FANG[1], TONGHUA LEI[1], YAN SUN[1], RENG DING[1], XIUQIONG HU[1] and CHENGXIANG BIAN[2]*

[1] Department of Hospital Infection Management, Wuhu Second People's Hospital, Wuhu, People's Republic of China
[2] Insurance Teaching and Research Office, Wannan Medical College, Wuhu, People's Republic of China

Submitted 21 October 2021, accepted 20 February 2022, published online 22 March 2022

Abstract

Multidrug-resistant *Acinetobacter baumannii* (MDR-AB) infections are becoming increasingly common. The Real-Time Nosocomial Infection (NI) Surveillance System (RT-NISS) was used to monitor MDR-AB NI in intensive care units (ICUs) to prevent NI outbreaks. Therefore, the RT-NISS was used in the current study to monitor MDR-AB infections in a neurosurgery ICU. Clinical interventions, including recommended antibiotics, bacterial distribution in the patient analysis, and bed adjustments, were carried out based on the monitoring results. The RT-NISS was also used to monitor clinical data, implement, and provide training on NI control. The RT-NISS detected a potential cluster of XDR-AB when five patients admitted to the neurosurgery ICU were tested positive for AB between 11 and 17 June 2019. Only two infected cases originated in the hospital, and there was no NI outbreak. The hospital Infection Control Department took appropriate measures to prevent cross-infection; specifically, an epidemiologic investigation and environmental assessment were conducted, and NI prevention and outbreak management training was provided. In summary, the RT-NISS enhanced the timeliness and efficacy of NI control and surveillance in a neurosurgery ICU.

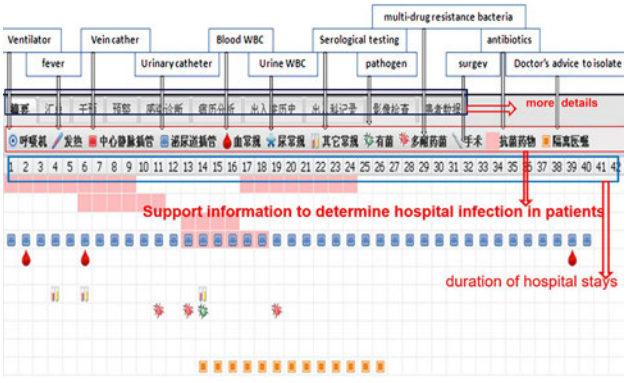

In order to prevent NI outbreaks, the Real-Time Nosocomial Infection (NI) Surveillance System (RT-NISS) was employed to monitor MDR-AB NI in critical care units (ICU). Based on the monitoring data, clinical actions such as required antibiotics, bacterial distribution in the patient analysis, and bed changes were carried out. In a neurosurgery ICU, the RT-NISS improved the timeliness and efficacy of NI control and surveillance.

Keywords: *Acinetobacter baumannii*, intervention, nosocomial infection, neurosurgery, real-time monitoring system

Introduction

Acinetobacter baumannii (AB), a non-glucose fermenting Gram-negative bacillus, is common in natural and hospital environments and can survive for a long time on table surfaces, clothing, and medical instruments (Kramer et al. 2006). In addition, AB is a nosocomial pathogen with poorly defined reservoirs outside the clinical environment (Howard et al. 2012). In recent years, advances in infection control have been achieved; however, AB infections are still globally distributed among patients in intensive care units (ICUs) (Strich and Palmore 2017). The incidence of infections with multidrug-resistant *A. baumannii* (MDR-AB) and extensively drug-resistant *A. baumannii* (XDR-AB) are on the rise (Kollef et al. 2008; Basri et al. 2015; Strich and Palmore 2017). Ineffective treatment of patients with AB infections increases the mortality rate four-fold compared with other infections (Kollef et al. 2008). AB accounts for 4% of all meningeal and shunt-related infections among neurosurgery patients, and the mortality rate of hospital-acquired meningitis in neurosurgery

* Corresponding author: Ch. Bian, Insurance Teaching and Research Office, Wannan Medical College, Wuhu, People's Republic of China; **e-mail: bianchengxiang@yeah.net**

patients is as high as 31% (Basri et al. 2015). The epidemic nature of hospital MDR-AB outbreaks is challenging to control because AB is an opportunistic pathogen mainly associated with hospital-acquired infections (Wilks et al. 2006; Landelle et al. 2013). AB is frequently related to aquatic environments and has been shown to colonize in high numbers from the respiratory and oropharynx secretions of infected individuals (Turton et al. 2006; Sebeny et al. 2008). In an epidemiologic study involving 11,546 patients with XDR-AB cultures, 88.7% of cases had antibiotic exposure, while 81% had hospital or long-term care admissions in the prior 90 days (Fitzpatrick et al. 2021). Among these patients, the 30-day and one-year mortality rates were 23.5% and 48.8%, respectively (Fitzpatrick et al. 2021). A 12-year epidemiologic study conducted in China showed that AB infection control in hospitals is difficult due to patients' complex and diverse genetic backgrounds (Jiang et al. 2021). Nevertheless, active surveillance screening can help prevent outbreaks (Wilks et al. 2006). Traditional NI surveillance includes case reporting by physicians and retrospective analyses by the hospital Infection Control Department (ICD); however, these approaches have some disadvantages, including insufficient reporting, poor early detection of infection outbreaks, and inadequate control of NIs. The Real-time Nosocomial Infection Surveillance System (RT-NISS) has been increasingly used to overcome these shortcomings (Huang et al. 2010).

We used hospital data to demonstrate RT-NISS functions. On 17 June 2019 the ICD identified suspicious NI outbreaks using the RT-NISS in a tertiary general teaching hospital with 1,900 beds and initiated an epidemiologic investigation. The significance of RT-NISS in preventing nosocomial outbreaks was assessed in the current study.

Experimental

Materials and Methods

RT-NISS. Bacterial colonization refers to the isolation of bacteria from a patient without symptoms of infection and is a prerequisite for active infection. An infection is defined as the presence of bacteria that cause pathologic changes, albeit to different degrees (Correa and Fortaleza 2019; Arzilli et al. 2022). As defined by the Chinese Ministry of Public Health in 2009, hospital outbreaks require at least three infectious cases with the same pathogenic agent in the same hospital department within seven days (The Ministry of Public Health 2009). The RT-NISS (the Xinglin Hospital Infection Real-time Monitoring System, V12.0, http://www.xinglin-tech.com) was used to extract clinical data from the hospital information system (HIS) and hospital laboratory information system (LIS), including the use of ventilators and catheters, body temperature, blood, and urine test results, procalcitonin levels, bacteria identification, number and type of surgeries, antibacterial agents, and patient isolation. Thus, data on patients who might have been diagnosed with an infection were used to provide a warning to clinicians and ICD staff, and determine the source of infection in a timely fashion.

In addition, real-time surveillance data were collected to guide clinical practice, and an interactive platform was developed to establish communication between the clinical staff and the ICD to improve case reporting, patient isolation, and intervention measures. Therefore, with basic and epidemiologic information, the ICD staff and clinicians work together to determine the source of NIs. The RT-NISS was used to extract clinical data from the HIS and LIS, including central venous catheters and antibacterial agents, pathogenic bacteria, and underreporting rates, which were analyzed by the ICD staff to confirm suspiciousness cases and guide clinical practice. A previous study showed that the specificity and sensitivity for diagnosing NIs in patients by the RT-NISS were 93.0% and 98.8%, respectively (Du et al. 2014).

Surveillance path of the RT-NISS. The surveillance path of the RT-NISS was as follows: NI-related information was achieved from the HIS, hospital LIS, and radiology information system by data access middleware, including ventilator use, fevers, central venous catheterization, urinary tract catheterization, routine blood test results, routine urine test results, other laboratory test results (e.g., procalcitonin), bacteria-positive cultures, multidrug-resistant (MDR) bacteria, surgery, antibacterial agents, and medical advice regarding isolation. In this way, the prognosis for patients with infections was generated to provide warning for the clinical medical staff and the hospital infection management staff, and detect occult hospital infection outbreaks in a timely fashion. The NI algorithm screening proceeded to send out outbreak and NI case alerts. The Chinese Ministry of Public Health defined hospital outbreaks in 2009 as at least three infection cases with the same pathogenic agent in the same hospital department within seven days (The Ministry of Public Health 2009). Algorithms were based on statistical process control (SPC). The alert threshold not only defined elementary threshold, which was according to the management standards promulgated by the Ministry of Public Health, but the alert was triggered when cases exceeded a threshold of ≥ 3 infections in two weeks on the same ward. The alert threshold was also based on past statistical variations of case frequency.

The SPC offers the possibility to monitor different types of statistical parameters, such as the incidence

count or rate, cumulative sums, or moving average. An outbreak database was set up in response to an outbreak alert, and clinical intervention was implemented to control the outbreak. In the absence of outbreak alerts, the surveillance ended. Assessments by infection control personnel (ICP) proceeded following NI case alerts. The surveillance ended if the ICP judges deemed no issues with the alerts. An NI database was set up if the ICP judges considered the alerts abnormal. Another path for NI case alerts or complicated NIs was discussing with physicians. The physician's platform differentiated the NI cases and entered the NI cases into a NI database. If the physician confirmed that the case was not an NI, the surveillance was ended. After the database was established, a hospital-wide NI analysis was performed, and NI-targeted surveillance data were collected. The details can be reviewed on the flowchart of NI cases and outbreak pre-warning and confirmation in the Du et al. (2014) study.

When it was shown that the same type of bacteria appeared in a department for a short period and >3 nosocomial infection cases were confirmed, it was suspected that NI outbreaks might occur, and clinical intervention should be arranged. The interaction platform constructed through the hospital infection real-time monitoring system was applied to realize the real-time report of infection cases, precise diagnosis, intervention, and feedback. In so doing, the special staff and clinicians involved in the diagnosis and control of infections work together and are aware of an occult hospital infection outbreak in a timely fashion.

Patient information. This study was conducted in our medical center, which is in the middle of China. Our hospital has 1,900 beds and five ICUs. The neurosurgical ICU has 17 beds with 450 patients per year. Large general hospitals must prevent infectious clusters. The current study results were intended to serve as a reference for other general hospitals. From 11–17 June 2019, a total of 42 patients were admitted to the neurosurgery ICU and included in the study. The infection rate was counted. When the outbreak alerts were sent out, 32 of the 42 patients had been discharged. The ten hospitalized patients were alerted of a suspicious outbreak. The clinical intervention was initiated to prevent the outbreak. The use of antibiotics was reviewed and adjusted. The distribution of the bacteria in patients was analyzed.

The Chinese Ministry of Public Health defined hospital outbreaks in 2009 as at least three infection cases with the same pathogenic agent in the same hospital department within seven days. After the clinical intervention, five of the ten patients with suspicious NI outbreak alerts were clinically diagnosed with a suspicious NI according to the management standards promulgated by the Ministry of Public Health. AB was detected in the sputum samples collected from these patients. According to the diagnostic criteria of nosocomial infection, the other five patients were excluded in the absence of an outbreak. These five patients did not meet the diagnostic criteria, such as admission within 48 h, and no bacterial growth occurred in the cultures (The Ministry of Public Health 2009).

The Institutional Ethical Committee approved the project of our hospital (2020-Ethics Approval-No. 12). The study was proceeded following the ethical standards of the Helsinki Declaration, as revised in 2013. The patients were informed about the study's purpose and procedures and provided written consent forms.

Clinical and environmental microbiologic method. Bacterial antibiotic susceptibility analysis was performed using the minimum inhibitory concentration (MIC) method (Andrews 2001), and the results were judged according to the CLSI (2010) standard of the American Committee for Clinical Laboratory Standardization. Strains were tested for susceptibility to ampicillin/sulbactam, ceftazidime, cefepime, imipenem, gentamicin, tobramycin, ciprofloxacin, and sulfamethoxazole.

Thirty-six environmental samples were collected from staff hands, humidified liquid, curtains, stethoscope, water bottle stopper, and water bottle shell, injection pump, faucet, bed cup and water, water feeding syringe, the railing of bed, lift the patient board. Cotton swabs were densely coated on blood plates, and the blood plates were placed in an air environment at 37°C and cultivated for 48 h, after which the strains were identified by a mass spectrometer (Repizo et al. 2017). Environmental samples were kept, collected, and tested every day within one week after the hospital infection management workers intervened in the investigation.

Statistical analyses. Statistical analyses were performed using SPSS software (version 20.0) on real-time surveillance data.

Results

Based on RT-NISS warnings, the five patients diagnosed with suspected AB infections included four males and one female, with a median age of 62 years (46–84 years). Most patients were older and had received a combination of invasive surgery and antibiotics. The baseline characteristics of the five patients are shown in Table I. A monitoring procedure (Fig. 1) was initiated to identify the source, and path of the NIs and the RT-NISS and clinical intervention were used to confirm suspected cases.

Epidemiologic information. Based on the HIS data, the number of NIs showed that the alert rate for suspicious infections or outbreaks from 11–17 June 2019 was 11.9% (5/42), which remained constant with the rates in 2018 and 2019 (Table II). The outbreak alert

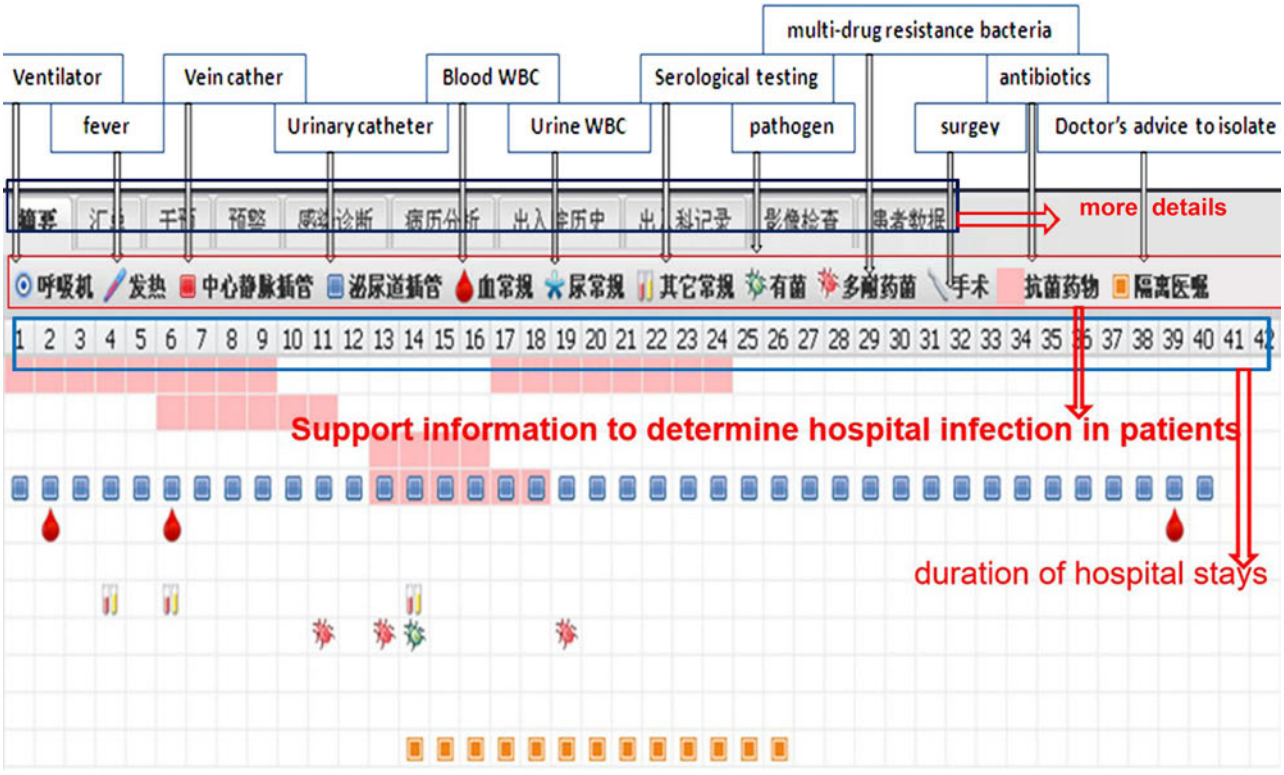

Fig. 1. This figure is a part of the visual time-series chart of inpatients shown by the software in use. Temporary clinical data shown were collected using a real-time nosocomial infection monitoring system. The data are displayed in different colors to facilitate comparison between patients. The symptoms represented in the system are displayed in Chinese and each symptom was translated into English, which was connected to the corresponding box with arrows to facilitate understanding. "More details" mean the detailed clinical data of the patients. The content of this interface only included the operation of patients with a suspected infection during hospitalization. The numbers 1–42 represent the duration of the hospitalization in days. A patient with an early warning appears as a red mark of multi-drug resistance bacteria on the warning interface. The possibility of a nosocomial infection outbreak was ruled out for multiple (≥ 3) patients, which was marked in red for multidrug resistance bacteria at any point in time. Because the warning interface contains a lot of patient information, the warning interface was not displayed completely.

rate was similar to other times throughout the year; thus, the RT-NISS could access the data quickly. Most patients with infections had severe injuries, including craniocerebral injuries and lung contusions, required intensive care, and increased the risk of cross-infections or secondary infections. Therefore, clinical examination confirmed suspicious cases to avoid underreporting and erroneous reports.

Case information. The five patients were clinically diagnosed and confirmed as below: one patient was confirmed to have a NI by the RT-NISS; one patient was suspected of having a NI by the RT-NISS and confirmed to be a NI by clinical interventions, and there were three patients with bacterial colonization originating in the hospital. The data excluded the possibility of an outbreak. The results of drug susceptibility testing are shown in Table III. The drug susceptibility test results suggested that the same pathogenic strain might be involved in the infections, potentially increasing the risk of an outbreak (Table III).

Case one. An 84-year-old man was admitted on June 9, 2019 with a craniocerebral injury and lung contusion. The patient was treated with amoxicillin and levofloxacin for four days, then cefoperazone-sulbactam from June 13 until discharge from the hospital. He had an elevated white blood cell (WBC) count on June 13, and increased interleukin-6 and procalcitonin (PCT) levels on June 14. On June 13 XDR-AB was detected in a sputum sample, and rales were present bilaterally. Invasive surgery was performed, including chest drainage, a tracheotomy, and ventilator support. On June 13 he was reported to have a hospital infection in the lower respiratory tract.

Case two. A 46-year-old man was admitted on June 3, 2019 with a spontaneous cerebral hemorrhage. He was treated with amoxicillin from 3–15 June, piperacillin-sulbactam from 15–20 June, and ceftazidime from 20–30 June. On June 8 the patient was reported to have a lower respiratory tract infection associated with *Proteus mirabilis*. The symptoms persisted under continuous inspection. XDR-AB was detected on June 17 but did not cause any clinical symptoms. Urinary catheterization, a tracheotomy, and ventilator support were carried out. The final diagnosis was bacterial coloniza-

Table I
Baseline characteristics of the study population.

	Case 1	Case 2	Case 3	Case 4	Case 5
Age (y)	84	46	62	65	57
Gender	male	male	male	female	male
Bed code	J01	23	18	22	J07
Diagnosis	traumatic brain injury	spontaneous intracerebral hemorrhage	spontaneous intracerebral hemorrhage	traumatic brain injury	thalamic hemorrhage
Date of ICU admission	9 June	3 June	1 June	31 May	14 May
Analyzed sample	sputum	sputum	sputum	sputum	sputum
Date of sample analysis	June 13	June 17	June 13	June 11	June 17
Pathogen	AB (+++)	AB (+++)	AB (+++)	AB (++)	AB (++) KP (+++)
Date of tracheostomy	June 18	June 6	no	May 31	May 17
Duration of invasive mechanical ventilation	3	30	N/A	8	23
Antibiotic combination therapy	yes	yes	yes	yes	yes
NI or colonization	NI	colonization	colonization	NI	colonization

AB – *Acinetobacter baumannii*, KP – *Klebsiella pneumoniae*
++, +++ mean semi-quantitative observation of stain under microscope according to the Health Industry Standards of the People's Republic of China (WS/T 499-2017), + means "occasionally", ++ means "a small amount", +++ means "medium amount", ++++ means "a lot"

Table II
Suspected alert rates for infections or outbreaks in different periods.

Periods	Number of suspected infections	Number of ICU patients	Rate of suspected infections	χ^2	*p*-value
11–17 June 2019	5	42	11.9%	0.267	0.875
20 May – 20 June 2018	6	38	15.8%		
20 April – 20 May 2019	6	41	14.6%		

Table III
Drug susceptibility of multidrug-resistant bacteria isolated from the patients.

Antibiotics	Case 1	Case 2	Case 3	Case 4	Case 5
Ampicillin/sulbactam	R	R	R	R	R
Ceftazidime	R	R	R	R	R
Ceftriaxone	R	R	R	R	R
Cefepime	R	R	R	R	R
Imipenem	R	R	R	R	R
Gentamicin	R	R	R	R	R
Tobramycin	S	R	R	S	S
Ciprofloxacin	R	R	R	R	R
Levofloxacin	R	R	R	R	R
Sulfamethoxazole	S	R	R	S	R

R – resistant, S – susceptible

tion because the culture results were inconsistent with the presence of sputum and symptoms of infection.

Case three. A 62-year-old man was admitted on June 1, 2019 with a spontaneous cerebral hemorrhage. He was diagnosed with a lung infection upon admission and was given piperacillin-sulbactam and combination therapy (piperacillin-sulbactam and levofloxacin) on June 6. The testing of bacterial culture upon admission

was *Pseudomonas aeruginosa*. XDR-AB was detected in sputum for the first time on June 13 and *P. aeruginosa* infection was detected in the urine on June 14. There were no related symptoms during 6–13 June. The patient was treated with amoxicillin and amikacin from 13–16 June and piperacillin-sulbactam from 17–24 June. The patient was afebrile, and the WBC count was normal. Urinary catheterization and ventilator support were performed. *P. aeruginosa* did not become the dominant bacterium in the patient and did not cause symptoms. The final diagnosis was a bacterial colonization.

Case four. A 65-year-old woman was admitted on May 31, 2019 with a severe craniocerebral injury. Ventilator support was provided upon admission, followed by combination antibiotic treatment with amoxicillin, gentamicin, and levofloxacin. *Klebsiella pneumoniae* infection was detected in a sputum sample on June 5. On June 11, XDR-AB was detected. The body temperature increased, and the WBC count was elevated. Combination antibiotic treatment included cefoperazone-sulbactam and tigecycline, followed by meropenem and fluconazole. A bacterial infection was confirmed.

Case five. A 57-year-old man was admitted on May 14, 2019 with a thalamic hemorrhage. On 17 May the patient was reported to have a lower respiratory tract infection with *K. pneumoniae*. XDR-AB was detected in urine on May 19, *K. pneumoniae* was detected in a sputum sample on May 21, a small number of AB (++) was detected in a sputum sample on 16 June, and a medium number of *K. pneumoniae* (+++) was identified in a sputum sample on June 17 and 19. The patient's body temperature was normal during this period, and minimal phlegm was aspirated during suction. The patient was treated with amoxicillin, meropenem, tigecycline, cefoperazone-sulbactam, and amikacin. The final diagnosis was AB colonization.

Environmental samples. Case analysis showed a large number of MDR-AB strains in the ICU environment. To determine the source and path of infection, the ICD screened 36 environmental samples, including surfaces, hospital staff, and ventilators, of which 20 samples (55.5%) were contaminated. MDR-AB was detected in six samples, including a stethoscope, curtains, injection pump, a water faucet, and hands from two nurse workers. No new infections were detected during the one-week environmental samples tests in the following seven days.

Discussion

The early warning data on the five cases were acquired through the RT-NISS. RT-NISS monitored the infections in real-time. Outputting data on bacterial infections, suspected cross-infections, and the prevalence of outbreaks are exported from RT-NISS. The RT-NISS captured the basic demographics about the patient and the corresponding epidemiologic information, which can lead to preliminary conclusions and save the investigation time. XDR-AB pneumonia remains a significant challenge in ICUs, and few drug treatment options are available for XDR-AB pneumonia treatment (Li et al. 2017). Ma et al. (2013) reported that mortality due to MDR and XDR-AB infections in China ICUs was 29% from 2011 to 2013. Indeed, the RT-NISS has an active role in providing accurate data to ICDs, diagnosing infections, and preventing outbreaks (Ma et al. 2013).

MDR-AB is rapidly becoming a global threat due to resistance to major classes of antibiotics (Nasr 2020). MDR-AB infections often occur in healthcare settings, especially in intensive care settings. *Acinetobacter* can survive for long periods on both wet and dry surfaces. *Acinetobacter* may also colonize or live in a patient without causing infection or symptoms, especially in tracheostomy sites and open wounds (Nwadike et al. 2014; Isler et al. 2018). The mechanisms underlying antimicrobial resistance in MDR-AB are complex, such as β-lactamase production, efflux pumps, decreased membrane permeability, and altered antibiotic target sites (Vrancianu et al. 2020). The control of MDR-AB has become a significant challenge in clinical practice (Asif et al. 2018).

According to the Hospital Infection Outbreak Control guideline (WS/T524-2016; The Ministry of Public Health 2009), there were no outbreaks in our hospital-based on this criterion. After intervention by the clinicians, only two cases were diagnosed with a NI, and it was not an outbreak within the hospital. The other three cases were regarded as colonization. It demonstrated that the system was used effectively to collect and analyze the clinical information of infected patients, help ICD confirm the diagnosis, actively treat the patients, and implement control measures (Du et al.2014), such as antibiotic use instructions, analyzing the distribution of the bacteria within the patient, and contemplating bed adjustment. As demonstrated, data on the nosocomial transmission of drug-resistant bacteria can be retrieved accurately and rapidly with a real-time system, and variations in bacterial susceptibility to antibiotics can be determined (Chen et al. 2018). Compared with the original manual report, which generally requires confirmation of the infection and sending a report form to the Hospital Management Department, the system report can issue an early warning in real-time within 24 h and confirmation in the system (Huang et al. 2010). These data are compared with NI control targets established by health authorities to strengthen the actions of the ICD for preventing and controlling MDR bacterial infections. The system automatically extracts data and calculates the detection and infec-

tion rates and antimicrobial drug use in each hospital department every day (Leclère et al. 2017).

The RT-NISS was used to monitor infections in real-time. At the same time, the ICD promptly extracted clinical and epidemiologic information using the RT-NISS and instituted targeted measures to prevent infections and outbreaks (Zingg et al. 2015). The ICD systematically monitors the on-site status of clinical departments to avoid physician misconduct and initiates infection prevention and control measures, including epidemiologic investigations, patient isolation, environmental sanitation sampling, training, and measures to prevent and control multi-drug resistant bacteria. Moreover, the ICD should also cooperate with other departments to identify risk factors for spreading infections, control NIs, and promote the rational use of antibiotics (Zingg et al. 2015). The drug susceptibility data of pathogenic bacteria in the hospital, the bedside monitoring results of patients infected with XDR bacteria, and the prevention and control of drug-resistant bacteria spread can be obtained from the ICD monthly (Wieland et al. 2007). Each hospital department's pathogenic bacteria susceptibility data can be released every six months. Data collected daily and monthly by the RT-NISS on the number of NIs, use of antibacterial drugs, number of patients infected with XDR bacteria, drug susceptibility of pathogenic bacteria, and the prevalence and control of NI and NI outbreaks of drug-resistant bacteria can be shared between hospitals.

Furthermore, epidemiologic surveys and environmental sanitation sampling and identification should be carried out (Zingg et al. 2015). In our study, 55.5% of the environmental samples were contaminated, and MDR-AB was detected in five samples; however, no new infections were detected in the following seven days after the hospital infection management workers began to intervene in the investigation. This finding confirms that RT-NISS and the ICD can cooperatively monitor and prevent NIs in the hospital to some degree.

The research limitations of this study were as follows. First, the system generated false alarms; thus, an effective and reproducible framework is needed to evaluate and compare these algorithms. The computer screening algorithm did not include medical records; thus, the terminology application may not be uniform. Second, polymerase chain reaction tests of the samples were not completed due to the lack of hardware equipment in the hospital, and the classification of bacteria was achieved from the microbiology laboratory. Bacterial resistance is generally only identified using the MIC method in routine clinical work due to the costs involved. The antibiotic susceptibility test method based on the MIC values can guide the treatment and control of infections macroscopically. However, without genotyping or phenotyping tests, this is not an acceptable approach for accurately judging whether there is an infection outbreak cluster. Also, PCR detection from environmental swabs was not performed due to the cost, which might affect the apparent correlation between AB strains isolated from patients and the environment. Finally, no automatic alarm appeared when the specimens were limited, and the early warning standard was not reached.

Conclusions

In summary, the RT-NISS integrated with the clinical diagnoses made by physicians enhances the timeliness and effectiveness of NI control and surveillance. The universal significance should be researched and explored by multiple hospitals.

Data availability

The data that support the findings of this study are available on request from the corresponding author. The data are not publicly available due to the privacy of research participants.

Acknowledgment

The authors would like to thank the colleagues in the neurosurgery ICU for their assistance during the investigation.

Author contributions

CB initiated and supervised the study. YZ and MN designed the study design. All authors participated in the clinical study and data collection. XF and TL conducted the analysis. YZ, YS, RD have written the manuscript. XH and CB have made critical revisions on the manuscript. All authors have read and approved the manuscript before submission.

Funding

This study was supported by Wuhu City Soft Science Project (Grant No. 2020kx1-4).

Conflict of interest

The authors do not report any financial or personal connections with other persons or organizations, which might negatively affect the contents of this publication and/or claim authorship rights to this publication

Literature

Andrews JM. Determination of minimum inhibitory concentrations. J Antimicrob Chemother. 2001 Jul;48(Suppl 1):5–16. https://doi.org/10.1093/jac/48.suppl_1.5

Arzilli G, Scardina G, Casigliani V, Petri D, Porretta A, Moi M, Lucenteforte E, Rello J, Lopalco P, Baggiani A, et al. Screening for antimicrobial-resistant Gram-negative bacteria in hospitalised patients, and risk of progression from colonisation to infection: Systematic review. J Infect. 2022 Feb;84(2):119–130. https://doi.org/10.1016/j.jinf.2021.11.007

Asif M, Alvi IA, Rehman SU. Insight into *Acinetobacter baumannii*: pathogenesis, global resistance, mechanisms of resistance, treatment

options, and alternative modalities. Infect Drug Resist. 2018 Aug 21; 11:1249–1260. https://doi.org/10.2147/IDR.S166750

Basri R, Zueter AR, Mohamed Z, Alam MK, Norsa'adah B, Hasan SA, Hasan H, Ahmad F. Burden of bacterial meningitis: a retrospective review on laboratory parameters and factors associated with death in meningitis, Kelantan Malaysia. Nagoya J Med Sci. 2015 Feb;77(1–2):59–68.

Chen Y, Ai L, Guo P, Huang H, Wu Z, Liang X, Liao K. Molecular characterization of multidrug resistant strains of *Acinetobacter baumannii* isolated from pediatric intensive care unit in a Chinese tertiary hospital. BMC Infect Dis. 2018 Dec 4;18(1):614. https://doi.org/10.1186/s12879-018-3511-0

CLSI. Procedures for the handling and processing of blood specimens for common laboratory tests; Approved guideline fourth edition. CLSI document GP44-A4. Wayne (USA): Clinical and Laboratory Standards Institute; 2010.

Correa AAF, Fortaleza CMCB. Incidence and predictors of health care-associated infections among patients colonized with carbapenem-resistant *Enterobacteriaceae*. Am J Infect Control. 2019 Feb; 47(2):213–216. https://doi.org/10.1016/j.ajic.2018.08.007

Du M, Xing Y, Suo J, Liu B, Jia N, Huo R, Chen C, Liu Y. Real-time automatic hospital-wide surveillance of nosocomial infections and outbreaks in a large Chinese tertiary hospital. BMC Med Inform Decis Mak. 2014 Jan 29;14:9. https://doi.org/10.1186/1472-6947-14-9

Fitzpatrick MA, Suda KJ, Poggensee L, Vivo A, Wirth M, Wilson G, Evans M, Evans CT. Epidemiology and clinical outcomes associated with extensively drug-resistant (XDR) *Acinetobacter* in US Veterans' Affairs (VA) medical centers. Infect Control Hosp Epidemiol. 2021 Mar;42(3):305–310. https://doi.org/10.1017/ice.2020.450

Howard A, O'Donoghue M, Feeney A, Sleator RD. *Acinetobacter baumannii*: an emerging opportunistic pathogen. Virulence. 2012 May 1;3(3):243–250. https://doi.org/10.4161/viru.19700

Huang SS, Yokoe DS, Stelling J, Placzek H, Kulldorff M, Kleinman K, O'Brien TF, Calderwood MS, Vostok J, Dunn J, et al. Automated detection of infectious disease outbreaks in hospitals: A retrospective cohort study. PLoS Med. 2010 Feb 23;7(2):e1000238. https://doi.org/10.1371/journal.pmed.1000238

Isler B, Doi Y, Bonomo RA, Paterson DL. New treatment options against carbapenem-resistant *Acinetobacter baumannii* infections. Antimicrob Agents Chemother. 2018 Dec 21;63(1):e01110-18. https://doi.org/10.1128/AAC.01110-18

Jiang M, Chen X, Liu S, Zhang Z, Li N, Dong C, Zhang L, Wu H, Zhao S. Epidemiological analysis of multidrug-resistant *Acinetobacter baumannii* isolates in a tertiary hospital over a 12-year period in China. Front Public Health. 2021 Aug 12;9:707435. https://doi.org/10.3389/fpubh.2021.707435

Kollef KE, Schramm GE, Wills AR, Reichley RM, Micek ST, Kollef MH. Predictors of 30-day mortality and hospital costs in patients with ventilator-associated pneumonia attributed to potentially antibiotic-resistant Gram-negative bacteria. Chest. 2008 Aug; 134(2):281–287. https://doi.org/10.1378/chest.08-1116

Kramer A, Schwebke I, Kampf G. How long do nosocomial pathogens persist on inanimate surfaces? A systematic review. BMC Infect Dis. 2006 Aug 16;6:130 https://doi.org/10.1186/1471-2334-6-130

Landelle C, Legrand P, Lesprit P, Cizeau F, Ducellier D, Gouot C, Bréhaut P, Soing-Altrach S, Girou E, Brun-Buisson C. Protracted outbreak of multidrug-resistant *Acinetobacter baumannii* after intercontinental transfer of colonized patients. Infect Control Hosp Epidemiol. 2013 Feb;34(2):119–124. https://doi.org/10.1086/669093

Leclère B, Buckeridge DL, Boëlle PY, Astagneau P, Lepelletier D. Automated detection of hospital outbreaks: A systematic review of methods. PLoS One. 2017 Apr 25;12(4):e0176438. https://doi.org/10.1371/journal.pone.0176438

Li YJ, Pan CZ, Fang CQ, Zhao ZX, Chen HL, Guo PH, Zhao ZW. Pneumonia caused by extensive drug-resistant *Acinetobacter baumannii* among hospitalized patients: genetic relationships, risk factors and mortality. BMC Infect Dis. 2017 May 30;17(1):371. https://doi.org/10.1186/s12879-017-2471-0

Ma MY, Xu J, Yu N, Huang GM. [Analysis of drug resistance of *Acinetobacter baumannii* and its related factors in ICU] (in Chinese). Zhonghua Wei Zhong Bing Ji Jiu Yi Xue. 2013 Nov;25(11):686–689. https://doi.org/10.3760/cma.j.issn.2095-4352.2013.11.012

Nasr P. Genetics, epidemiology, and clinical manifestations of multidrug-resistant *Acinetobacter baumannii*. J Hosp Infect. 2020 Jan; 104(1):4–11. https://doi.org/10.1016/j.jhin.2019.09.021

Nwadike VU, Ojide CK, Kalu EI. Multidrug resistant *Acinetobacter* infection and their antimicrobial susceptibility pattern in a Nigerian tertiary hospital ICU. Afr J Infect Dis. 2014;8(1):14–18. https://doi.org/10.4314/ajid.v8i1.4

Repizo GD, Viale AM, Borges V, Cameranesi MM, Taib N, Espariz M, Brochier-Armanet C, Gomes JP, Salcedo SP. The environmental *Acinetobacter baumannii* isolate DSM30011 reveals clues into the preantibiotic era genome diversity, virulence potential, and niche range of a predominant nosocomial pathogen. Genome Biol Evol. 2017 Sep 1;9(9):2292–2307. https://doi.org/10.1093/gbe/evx162

Sebeny PJ, Riddle MS, Petersen K. *Acinetobacter baumannii* skin and soft-tissue infection associated with war trauma. Clin Infect Dis. 2008 Aug 15;47(4):444–449. https://doi.org/10.1086/590568

Strich JR, Palmore TN. Preventing transmission of multidrug-resistant pathogens in the intensive care unit. Infect Dis Clin North Am. 2017 Sep;31(3):535–550. https://doi.org/10.1016/j.idc.2017.05.010

The Ministry of Public Health. The management standard of report and disposal nosocomial infected outbreak. Gazette Min Health PR China 2009;9:37–39.

Turton JF, Kaufmann ME, Gill MJ, Pike R, Scott PT, Fishbain J, Craft D, Deye G, Riddell S, Lindler LE, et al. Comparison of *Acinetobacter baumannii* isolates from the United Kingdom and the United States that were associated with repatriated casualties of the Iraq conflict. J Clin Microbiol. 2006 Jul;44(7):2630–2634. https://doi.org/10.1128/JCM.00547-06

Vrancianu CO, Gheorghe I, Czobor IB, Chifiriuc MC. Antibiotic resistance profiles, molecular mechanisms and innovative treatment strategies of *Acinetobacter baumannii*. Microorganisms. 2020 Jun 21; 8(6):935. https://doi.org/10.3390/microorganisms8060935

Wieland SC, Brownstein JS, Berger B, Mandl KD. Automated real time constant-specificity surveillance for disease outbreaks. BMC Med Inform Decis Mak. 2007 Jun 13;7:15. https://doi.org/10.1186/1472-6947-7-15

Wilks M, Wilson A, Warwick S, Price E, Kennedy D, Ely A, Millar MR. Control of an outbreak of multidrug-resistant *Acinetobacter baumannii-calcoaceticus* colonization and infection in an intensive care unit (ICU) without closing the ICU or placing patients in isolation. Infect Control Hosp Epidemiol. 2006 Jul;27(7):654–658. https://doi.org/10.1086/507011

Zingg W, Holmes A, Dettenkofer M, Goetting T, Secci F, Clack L, Allegranzi B, Magiorakos AP, Pittet D; Systematic review and evidence-based guidance on organization of hospital infection control programmes (SIGHT) study group. Hospital organisation, management, and structure for prevention of health-care-associated infection: A systematic review and expert consensus. Lancet Infect Dis. 2015 Feb;15(2):212–224. https://doi.org/10.1016/S1473-3099(14)70854-0

ORIGINAL PAPER

Polish Journal of Microbiology
2022, Vol. 71, No 1, 115–121
https://doi.org/10.33073/pjm-2022-014

Expression Level of the *mip*, *pmp18D*, and *ompA* Genes in *Chlamydia abortus* Isolated from Aborted Ewes

EMAN DHAHIR ARIF[1*], NAHLA MOHAMMAD SAEED[1*], SHWAN KAMAL RACHID[2], HIEWA OTHMAN DYARY[3] and PESHNYAR M.A. RASHID[4, 5]

[1] Department of Microbiology, College of Veterinary Medicine, University of Sulaimani, Sulaymaniyah, Iraq
[2] Charmo University, Sulaymaniyah, Iraq
[3] Department of Basic Sciences, College of Veterinary Medicine, University of Sulaimani, Sulaymaniyah, Iraq
[4] Kurdistan Institution for Strategic Studies and Scientific Research, Sulaymaniyah, Iraq
[5] Molecular Diagnostic Laboratory, Directorate of Veterinary Services in Sulaymaniyah, Sulaymaniyah, Iraq

Submitted 4 November 2021, accepted 20 February 2022, published online 22 March 2022

Abstract

In this manuscript, we report the proteins macrophage infectivity potentiator (*mip*, CAB080), major outer membrane protein (*momp*, CAB048), and polymorphic outer membrane protein (*pmp18D*, CAB776) that are expressed in different times of pregnancy in mice infected with *Chlamydia abortus*. Enzootic abortion of ewes (EAE) by *C. abortus*, an obligate intracellular pathogen, is a critical zoonotic disease-causing significant economic loss to livestock farming globally. This study was carried out for the detection and characterization of macrophage infectivity potentiator (*mip*, CAB080), major outer membrane protein (*momp*, CAB048), and polymorphic outer membrane protein (*pmp18D*, CAB776) using RT-qPCR. These proteins are believed to be expressed as virulence factors in *C. abortus* isolated from aborted ewes. BALB/c mice (pregnant and nonpregnant) were used as an animal model to be injected intraperitoneally with *C. abortus* culture in Vero cells since the endometrial lymphoid tissues of these animals resembles that of ewes. Also, the short duration of pregnancy in mice makes them a suitable animal model for obstetric studies. Tissue samples were taken from the mice after 10, 15, and 20 days of pregnancy to compare the expression of the genes *mip, pmp18D*, and *ompA*. Transcription level was quantified using RT-qPCR, the GAPDH transcription quantification, as a normalization signal. Abortion occurred in pregnant mice, and apparent differences between the transcriptional levels of the *mip, pmp18D*, and *ompA* genes in the samples taken during different time intervals of pregnancy were not observed ($p > 0.05$). The result indicated that the three bacterial genes, *mip*, *pmp18D*, and *ompA*, play a role as virulence factors in abortion and are differentially expressed in pregnant and nonpregnant animals. Inactivation of the genes is suggested to confirm the hypothesis.

K e y w o r d s: *Chlamydia abortus*, RT-qPCR, macrophage infectivity potentiator (*mip*), polymorphic membrane protein (*pmp*), major outer membrane protein (*momp*)

Introduction

Enzootic abortion of ewes (EAE) induced by *Chlamydia abortus* is a significant cause of reproductive failures in most sheep-producing countries (Borel et al. 2018). The disease in sheep is characterized by abortion in the later stages of pregnancy, after three months of gestation, when *Chlamydiae* begin to invade placentomes. The infection causes a diffuse inflammatory response, thrombotic vasculitis, and tissue necrosis. The birth of a vital lamb may occur, but these lambs usually cannot survive for more than two days (Spičic et al. 2015). Mice have been widely used and considered helpful animal models for *C. abortus* infections and evaluating new vaccine candidates to reduce economic losses from chlamydial infections (Kerr et al. 2005; Caro et al. 2009). Abortion in experimentally infected mice occurs in the final stages of pregnancy (about day 20), whether *C. abortus* is inoculated on day seven or day 11 (Rodolakis et al. 1998).

* Corresponding authors: E.D. Arif, Department of Microbiology, College of Veterinary Medicine, University of Sulaimani, Sulaymaniyah, Iraq; **e-mail: eman.arif@univsul.edu.iq**
N.M. Saeed, Department of Microbiology, College of Veterinary Medicine, University of Sulaimani, Sulaymaniyah, Iraq; **e-mail: nahla.saeed@univsul.edu.iq**

Chlamydia species are obligate intracellular microorganisms that occur in two distinct forms during their lifecycle, switching between an extracellular infectious phase and an intracellular replicative (noninfectious) phase (McClure et al. 2017). Elementary bodies (EBs) are environmentally stable and can infect epithelial cells. Reticulate bodies (RBs) cannot infect cells but are active metabolically and can replicate (Brunham and Rey-Ladino 2005).

Chlamydiae possess a cell wall and are bordered by an outer membrane (OM) and a cytoplasmatic inner membrane (IM) (Elwell et al. 2016). The EB outer membrane contains phospholipids, lipids, lipooligosaccharides (LOS), and proteins, while the cell wall contains a small amount of peptidoglycan (Singh et al. 2020). A part of the *Chlamydia* cell wall is insoluble in sarkosyl, and this fraction is known as the *Chlamydia* outer membrane complex (COMC). This complex mainly consists of the polymorphic membrane proteins (*pmps*), major outer membrane protein (*momp*), and two cysteine-rich proteins (CRP): EnvA or OmcA and EnvB or OmcB (Stephens and Lammel 2001). *Momp* is a cysteine-rich protein of about 41.9 kDa (Longbottom et al. 2019) that covers more than half of the EB outer membrane and almost all RB (Hatch and McClarty 1998). *Pmps* are only present in Chlamydiales and were first detected at the surface of *C. abortus* S26/3 (Longbottom et al. 1996). *Pmps* are ordinarily responsible for virulence and immune response avoidance (Tan et al. 2006). Different studies have shown that the macrophage infectivity potentiator (*mip*) is a solid immunoreactive protein (Forsbach-Birk et al. 2013; Hagemann et al. 2016).

Diagnosis of EAE can be made with DNA- or protein-based assays (Essig and Longbottom 2015). Lately, conventional and real-time PCRs have mainly been used to detect *C. abortus* in clinical samples. PCR methods are based on amplifying the chlamydial OMP genes *ompA*, *omp1*, *omp2*, the polymorphic membrane gene *pmp*, genes encoding 16S rRNA and helicase, and the 16S-23S rRNA intergenic interval (Berri et al. 2009). Speedy and dependable diagnostic assays are essential to rapid disease control.

The expression and role of the *mip*, *pmp18D*, and *ompA* genes of *C. abortus* in abortion in ewes have not been adequately elucidated. Hence, this work aimed to identify and purify *C. abortus* from ovine abortion samples and characterize three proteins expressed as virulence factors in *C. abortus* isolated from aborted ewes using RT-qPCR. The studied genes were the macrophage infectivity potentiator (*mip*, CAB080), major outer membrane protein (*momp*, CAB048), and polymorphic outer membrane protein (*pmp*, CAB776). The genes' expression level was also compared in experimentally infected pregnant and nonpregnant mice with *C. abortus*.

Experimental

Materials and Methods

Bacterial culture in Vero cell line. *C. abortus*, isolated from an aborted bovine fetus in Sulaimani province, north Iraq (Arif et al. 2020), was used in this study. Vero cells were also provided as a gift by the Cell Culture Unit at the College of Medicine/Babylon University, Iraq.

Monolayers of Vero cells were grown in 25 ml tissue culture flasks at 2×10^6 cells/ml. Confluent monolayers (70–80%) were achieved 24 hours after incubation at 37°C with 5% CO_2 with Dulbecco's Modified Eagle medium (DMEM) supplemented with 10% fetal bovine serum (Labiran 2014). About 25 µl of a frozen stored suspension of an aborted ewe's placental tissue was thawed in SPG (0.25 M sucrose, 10 mM sodium phosphate, and 5 mM L-glutamic acid) and added to Vero cell cultures. Tissue culture flasks were incubated for one hour at 37°C in a saturated humidity environment and 5% CO_2. After incubation, DMEM, supplemented with 10% fetal bovine serum and gentamicin (20 µg/ml), was added, and the tissue culture flasks were incubated again at 37°C for 48–72 hours. After 48 hours, *Chlamydia* inclusions were large enough to be visualized under an inverted microscope (Campos-Hernández et al. 2014).

Vero cells were harvested two days after infection with *C. abortus* by high-speed centrifugation ($30{,}000 \times g$) for 45 minutes. *Chlamydiae* were released from the intracellular vacuoles by ultra-sonication and centrifuged again at low speed ($500 \times g$ for 10 minutes) to separate the bacteria from cell debris (Labiran 2014).

C. abortus cells were stained with Giemsa solution and observed under an inverted microscope at 400× magnification. The EBs of *Chlamydia* appeared as small cocci occurring singly and in clusters in the infected cells' cytoplasm (Arif et al. 2020).

Experimental infection of mice. Thirty-six female and six male albino mice of *Mus musculus* species, BALB/c strain, were used in the study. The mice, 6–8 weeks old, between 25 and 30 grams, were obtained from the Research Center at the College of Veterinary Medicine/University of Sulaimani. All mice-involving procedures were executed humanely according to the Guide for the Care and Use of Laboratory Animals, and the Ethics Committee at the College of Veterinary Medicine, University of Sulaimani, approved the experimental protocol (Approval number AUP-20/9). The 36 female mice were divided into two equal groups; Group 1 of pregnant mice (clinical case) and Group 2 of nonpregnant mice (control). The mice were injected intraperitoneally with 0.2 ml of the supernatant collected from the isolation of *C. abortus*

in Vero cells (kept at –70°C). The solution contained 1,000 inclusion-forming units (IFU) of *C. abortus* in 0.9% saline solution, following a previously described method (Livingstone et al. 2009). Injection of *C. abortus* was conducted after one week of pregnancy in Group 1.

Animal euthanasia and sample collection. The duration of pregnancy was divided into three stages. The first stage was on the 10th day of pregnancy, while stages two and three were after 15 and 20 days. In each stage, six mice were euthanized from each group by intraperitoneal injection of a mixture of xylazine (16 mg/kg) and ketamine (100 mg/kg), followed by cervical dislocation (Schoell et al. 2009).

Following the mice's euthanasia, the external surface was cleaned and disinfected with 70% ethanol, and the abdomen was opened using aseptic procedures. Fragments were resected from the liver, spleen, lung, kidney, placenta, and fetus. The organ fragments were ground and pooled together. The samples were subjected to RNA extraction using a tissue RNA extraction kit, RT05O (Gene aid, Taiwan). The procedure was conducted following instructions provided by the manufacturer.

RNA quantification and RT-qPCR program. RNA measurement was performed using a Nanodrop, ND-8000 (8-sample spectrophotometer, USA). RNA sample absorbance was measured at 230 nm, 260 nm, and 280 nm.

The primer for the *mip* gene was previously designed by Forsbach-Birk et al. (2013), the primers of *pmp18D* and *ompA* genes were designed by Wheelhouse et al. (2009) (Table I), while the *GAPDH* primer was designed for this study. Profiling was executed using a real-time PCR-based array and *GAPDH* (glyceraldehyde-3-phosphate dehydrogenase) transcript as a normalization signal. The AddRT-qPCR SYBR kit (Add Bio, Korea), a single tube real-time one-stepRT-qPCR, was used in this study. Furthermore, q-PCR was undertaken in an IQ5 Multicolor Real-time PCR system (BIO-RAD, USA).

Optimization of PCR reactions, data analysis, and mRNA expression. Each reaction was run in a final volume of 20 µl containing 500 ng of the RNA, 1 µl (10 pmol) of each primer, and 10 µl SYBR Green PCR Mastermix (Add Bio/Korea). The amplification profile was 50°C for 20 minutes. Then, at 95°C for 10 minutes, denaturation was followed by 40 cycles of 95°C for 30 seconds and 60°C for 30 seconds.

Data analysis and mRNA expression. The RT-qPCR data obtained from the above reaction were analyzed using the comparative CT (2-ΔCT) method, a convenient way to analyze gene expression's relative changes from real-time quantitative PCR experiments. The Ct values for each gene were first obtained through the RT-qPCR machine used in this study. These values were then imported into a Microsoft Excel file for further calculation and analysis.

The expression levels of mRNAs were normalized to *GAPDH*. mRNA expression was quantified as ΔCt values for both pregnant and nonpregnant separately, where Ct = threshold cycle and ΔCt = Ct target gene – average Ct of *GAPDH*. After comparing it with the pooled sample, all mRNAs' expression levels were measured in standard tissue samples. The ΔΔCt values, which are expressed as ΔCt target gene – ΔCt of the pooled sample, were used to quantify mRNA expression of the *pmp18D, ompA*, and *mip* genes in infected pregnant mice compared to infected nonpregnant mice. The equation 2-ΔΔCt was used to calculate the fold change of the gene.

Results

Isolation in cell culture. *C. abortus* organisms were successfully cultivated into Vero cells monolayer. Giemsa staining showed the *Chlamydial* inclusions in the cytoplasm of Vero cells after 48 hours of inoculation. The DNA was detectable from the infective Vero cells.

mRNA expression. RT-qPCR data were obtained using the ΔΔ Ct method (fold change mean), normalizing to the reference *GAPDH*. The effect of different time intervals of pregnancy (10 days, 15 days, and 20 days) was assessed by the relative expression of the *mip*,

Table I
Sequences of the forward and reverse primers of four genes used in Real-time PCR.

Target gene	Primer sequence (5′ to 3′)	Size (bp)
GAPDH	Forward: GGGGTCCCAGCTTAGGTTCA Reverse: ACGGCCAAATCCGTTCACA	95
mip	Forward: AAGAAAACCTCTCCCTAGCC Reverse: CTGAAGGTTTCCCTGATATTG	139
ompA	Forward: GCGGCATTCAACCTCGTT Reverse: CCTTGAGTGATGCCTACATTGG	85
pmp18D	Forward: TCCACTGGGATGATCACCAATA Reverse: GCATAGAAAGCGTATCGAGAATCAC	81

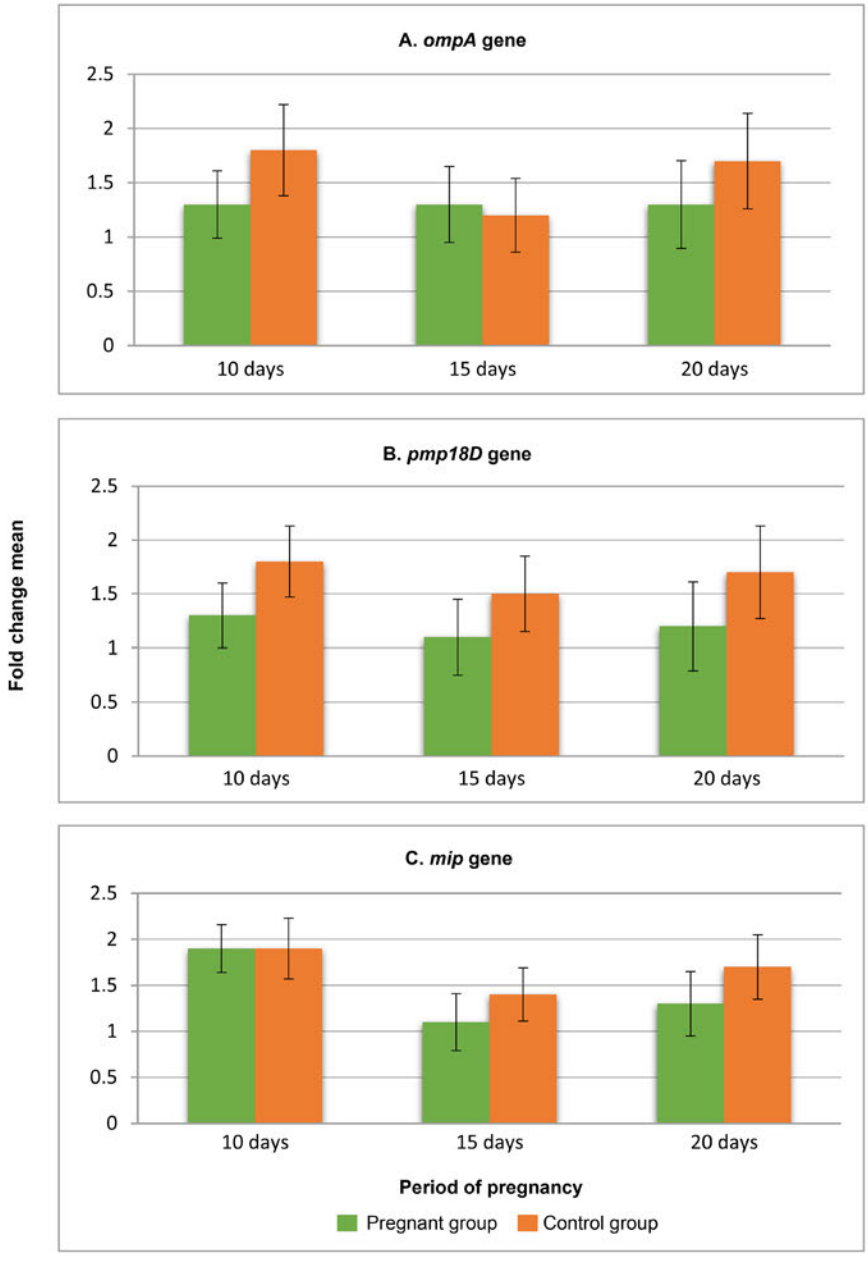

Fig.1. mRNA expression levels of the *ompA, pmp18D*, and *mip* genes as fold change in pregnant and nonpregnant mice tissues at different pregnancy times by RT-qPCR. Data are presented as means of values for six mice (columns) ± SEM (error bars).

pmp18D, and *ompA* gene transcripts in murine tissues as a fold change mean using the RT-qPCR analysis with normalizing to the reference *GAPDH*. Abortion occurred only after 20 days of pregnancy, and Fig. 1A–1C indicate apparent differences between the transcriptional levels of the *mip, pmp18D*, and *ompA* gene among different time intervals of pregnancy. The RT-qPCR analysis revealed that the mRNA level of *mip* increased in both the pregnant and nonpregnant groups by 1.9-fold change on day 10 (Fig. 1A, Table II), and there was no statistically significant difference ($p = 0.593$).

Moreover, the RT-qPCR analysis also revealed an increase in *pmp18D* mRNA expression level by 1.2 times in the pregnant group on day 20. Compared with the nonpregnant group, which increased on the tenth day by 2.2 folds, the difference was insignificant statistically (Fig. 1B, Table II).

The *ompA* mRNA level increased in the pregnant group by 1.3-fold on day 15. However, compared with

Table II
Wilcoxon signed-rank test analysis of the *mip, pmp18D*, and *ompA* genes expression between the pregnant groups in comparison to the nonpregnant groups at each time interval of pregnancy.

Group	Gene type	Period of pregnancy (days)	*p*-values
Pregnant group – nonpregnant	*mip*	10	0.593
		15	0.655
		20	0.655
Pregnant group – nonpregnant	*pmp18D*	10	0.109
		15	0.593
		20	0.593
Pregnant group – nonpregnant	*ompA*	10	0.285
		15	1.000
		20	0.655

its expression in the nonpregnant group, the difference was insignificant ($p = 0.285$) (Fig. 1C, Table II).

According to the statistical analyses, there was no statistically significant difference (p-values > 0.05) in the fold change means of these three genes at each sample time point by using Wilcoxon signed-rank test, as shown in Table II. These results imply that different time intervals do not affect the expression of each *mip, pmp18D*, and *ompA* in the pregnant group compared to the nonpregnant.

Discussion

Chlamydia isolation from aborted tissues is the standard for definitive diagnosis. Nevertheless, bacterial isolation requires collecting samples in optimal conditions; the samples must be fresh, with little or no contamination, and contain a suitable amount of live and viable microorganisms (Li et al. 2015). *Chlamydia* cultivation in cell culture is considered the gold standard. However, this lengthy technique is only applicable to certain cultivable strains. Besides, many strains are challenging to grow, and not all labs have the required facilities to grow the microorganism. The odds for diagnosing *Chlamydia* have considerably increased since the introduction of DNA-based techniques. For example, PCR allows direct identification from clinical samples and species differentiation (Hailat et al. 2018; Saeed et al. 2019).

In this study, the culturing of *C. abortus* was followed by Giemsa staining, and the DNA of *Chlamydia* could be detected from the infected Vero cells. The sample was diagnosed as positive for *C. abortus* after the microscopic examination of Giemsa-stained smears. This outcome implies that *C. abortus* growth may be related to the number of bacteria in the inoculum or their developmental cycle. Like contamination, storage circumstances, and tissue homogenization, other factors may affect *C. abortus* elementary bodies' viability and cause slow growth and appearance in culture (Zhang et al. 2015).

The current study investigated and quantified the expressions of *mip*, *pmp18D*, and *ompA* in *C. abortus* using RT-qPCR. *C. abortus* naturally infects ewes, but mice can be infected via parenteral administration, such as the intraperitoneal or intravenous routes (Kerr et al. 2005).

This method has not been adopted in the Kurdistan and Iraq so far. Combining three gene transcriptomes by RT-qPCR detects virulence factors that might show a substantial role in the pathogenesis of *C. abortus*. Besides, this method may increase the chances of better identifying the abortion mechanisms in sheep caused by *Chlamydia* and help diagnose disease in the future.

Chlamydia species express a wide range of virulence factors. Some of these factors are presumed to be involved in processes associated with the regulation of host adaptation. Our results revealed that *mip* mRNA expression increased in both the pregnant and nonpregnant groups at the same gestation period (1st stage, 10th day) without any significant difference between the two groups (p-values > 0.05). The results also showed no measurable increase in mRNA *pmp18D* expression in the pregnant group at the third stage of gestation (20th day) compared to its nonpregnant group expression. Furthermore, a significant difference between the two groups was not detected (p-values > 0.05). The results showed that the mRNA level of *ompA* expression increases in the pregnant group at the second stage of gestation (15th day) compared to its nonpregnant group expression. Still, the difference between the two groups was not statistically significant.

Chlamydial pathogens have evolved sophisticated mechanisms to elude lytic damage in the host cell (Fields and Hackstadt 2002). As a survival method and equivocation of elimination, chlamydial virulence-associated factors are integrated into the inclusion

membrane (Rockey et al. 2002) or secreted into the host cell cytoplasm (Valdivia 2008), which can modulate the host immune reaction.

This difference in the expression of these genes at different time intervals of pregnancy in mice might be due to various causes, for example, technical reasons, sample size, and criteria for evaluating the result. In addition to the bacteria's virulence characteristics, the host-mediated immune response's quality and intensity could be responsible for the host specificity of individual species and strains of *Chlamydia* (Braukmann et al. 2012).

It cannot be concluded that the mouse model results are similar to sheep since there are substantial differences in the type of placenta and local immune response. However, it is well known that lymphoid cells in sheep endometrial tissues are morphologically and functionally analogous to pregnant mouse uterus' granulate material gland cells (Chavan et al. 2016). Our results showed that the different time intervals of pregnancy do not affect the expression of *mip*, *pmp18D*, and *ompA* in pregnant mice. Inactivation of the genes is suggested to confirm the hypothesis.

ORCID
Nahla Mohammad Saeed https://orcid.org/0000-0003-1187-0688

Author contributions

E.A., N.S., and S.R. conceived and designed the experiments; E.A. and H.D. drafted and revised the manuscript; E.A. and P.R. performed the experiments and analyzed the data.

Conflict of interest

The authors do not report any financial or personal connections with other persons or organizations, which might negatively affect the contents of this publication and/or claim authorship rights to this publication.

Literature

Arif ED, Saeed NM, Rachid SK. Isolation and identification of *Chlamydia abortus* from aborted ewes in Sulaimani province, Northern Iraq. Pol J Microbiol. 2020 Mar 25;69(1):65–71. https://doi.org/10.33073/pjm-2020-009

Berri M, Rekiki A, Boumedine K, Rodolakis A. Simultaneous differential detection of *Chlamydophila abortus*, *Chlamydophila pecorum* and *Coxiella burnetii* from aborted ruminant's clinical samples using multiplex PCR. BMC Microbiol. 2009;9(1):130. https://doi.org/10.1186/1471-2180-9-130

Borel N, Polkinghorne A, Pospischil A. A review on chlamydial diseases in animals: still a challenge for pathologists? Vet Pathol. 2018 May;55(3):374–390. https://doi.org/10.1177/0300985817751218

Braukmann M, Sachse K, Jacobsen ID, Westermann M, Menge C, Saluz HP, Berndt A. Distinct intensity of host-pathogen interactions in *Chlamydia psittaci*- and *Chlamydia abortus*-infected chicken embryos. Infect Immun. 2012 Sep;80(9):2976–2988. https://doi.org/10.1128/IAI.00437-12

Brunham RC, Rey-Ladino J. Immunology of *Chlamydia* infection: implications for a *Chlamydia trachomatis* vaccine. Nat Rev Immunol. 2005 Feb;5(2):149–161. https://doi.org/10.1038/nri1551

Campos-Hernández E, Vázquez-Chagoyán JC, Salem AZM, Saltijeral-Oaxaca JA, Escalante-Ochoa C, López-Heydeck SM, de Oca-Jiménez RM. Prevalence and molecular identification of *Chlamydia abortus* in commercial dairy goat farms in a hot region in Mexico. Trop Anim Health Prod. 2014 Aug;46(6):919–924. https://doi.org/10.1007/s11250-014-0585-6

Caro MR, Buendía AJ, Del Rio L, Ortega N, Gallego MC, Cuello F, Navarro JA, Sanchez J, Salinas J. *Chlamydophila abortus* infection in the mouse: A useful model of the ovine disease. Vet Microbiol. 2009 Mar;135(1–2):103–111. https://doi.org/10.1016/j.vetmic.2008.09.029

Chavan AR, Bhullar BAS, Wagner GP. What was the ancestral function of decidual stromal cells? A model for the evolution of eutherian pregnancy. Placenta. 2016 Apr;40:40–51. https://doi.org/10.1016/j.placenta.2016.02.012

Chun T, Spitznagel JK, Shou H, Hsia R, Bavoil PM. The polymorphic membrane protein gene family of the *Chlamydiaceae*. In: Bavoil PM, Wyrick PB, editors. *Chlamydia*: genomics and pathogenesis. Wymondham (UK): Horizon Bioscience; 2006. p. 195–218.

Elwell C, Mirrashidi K, Engel J. *Chlamydia* cell biology and pathogenesis. Nat Rev Microbiol. 2016 Jun;14(6):385–400. https://doi.org/10.1038/nrmicro.2016.30

Essig A, Longbottom D. *Chlamydia abortus*: new aspects of infectious abortion in sheep and potential risk for pregnant women. Curr Clin Microbiol Rep. 2015 Mar;2(1):22–34. https://doi.org/10.1007/s40588-015-0014-2

Fields KA, Hackstadt T. The chlamydial inclusion: escape from the endocytic pathway. Annu Rev Cell Dev Biol. 2002 Nov;18(1):221–245. https://doi.org/10.1146/annurev.cellbio.18.012502.105845

Forsbach-Birk V, Foddis C, Simnacher U, Wilkat M, Longbottom D, Walder G, Benesch C, Ganter M, Sachse K, Essig A. Profiling antibody responses to infections by *Chlamydia abortus* enables identification of potential virulence factors and candidates for serodiagnosis. PLoS One. 2013 Nov 15;8(11):e80310. https://doi.org/10.1371/journal.pone.0080310

Hagemann JB, Simnacher U, Longbottom D, Livingstone M, Maile J, Soutschek E, Walder G, Boden K, Sachse K, Essig A. Analysis of humoral immune responses to surface and virulence-associated *Chlamydia abortus* proteins in ovine and human abortions by use of a newly developed line immunoassay. J Clin Microbiol. 2016 Jul;54(7):1883–1890. https://doi.org/10.1128/JCM.00351-16

Hailat N, Khlouf S, Ababneh M, Brown C. Pathological, immunohistochemical and molecular diagnosis of abortions in small ruminants in Jordan with reference to *Chlamydia abortus* and *Brucella melitensis*. Pak Vet J. 2018 Mar 01;38(01):109–112. https://doi.org/10.29261/pakvetj/2018.022

Hatch GM, McClarty G. Cardiolipin remodeling in eukaryotic cells infected with *Chlamydia trachomatis* is linked to elevated mitochondrial metabolism. Biochem Biophys Res Commun. 1998 Feb; 243(2): 356–360. https://doi.org/10.1006/bbrc.1998.8101

Kerr K, Entrican G, McKeever D, Longbottom D. Immunopathology of *Chlamydophila abortus* infection in sheep and mice. Res Vet Sci. 2005 Feb;78(1):1–7. https://doi.org/10.1016/j.rvsc.2004.08.004

Labiran C. Molecular epidemiology of *Chlamydia trachomatis*: valuation, implementation and development of high resolution genotyping [PhD Thesis]. Southampton (UK): University of Southampton, Faculty of Medicine, Division of Clinical and Experimental Science; 2014.

Li Z, Cao X, Fu B, Chao Y, Cai J, Zhou J. Identification and characterization of *Chlamydia abortus* isolates from yaks in Qinghai, China. Biomed Res Int. 2015;2015:658519. https://doi.org/10.1155/2015/658519

Livingstone M, Wheelhouse N, Maley SW, Longbottom D. Molecular detection of *Chlamydophila abortus* in post-abortion sheep at oestrus and subsequent lambing. Vet Microbiol. 2009 Mar; 135(1–2):134–141. https://doi.org/10.1016/j.vetmic.2008.09.033

Longbottom D, Livingstone M, Aitchison KD, Imrie L, Manson E, Wheelhouse N, Inglis NF. Proteomic characterisation of the *Chlamydia abortus* outer membrane complex (COMC) using combined rapid monolithic column liquid chromatography and fast MS/MS scanning. PLoS One. 2019 Oct 24;14(10):e0224070. https://doi.org/10.1371/journal.pone.0224070

Longbottom D, Russell M, Jones GE, Lainson FA, Herring AJ. Identification of a multigene family coding for the 90 kDa proteins of the ovine abortion subtype of *Chlamydia psittaci*. FEMS Microbiol Lett. 1996 Sep;142(2–3):277–281. https://doi.org/10.1111/j.1574-6968.1996.tb08443.x

McClure EE, Chávez ASO, Shaw DK, Carlyon JA, Ganta RR, Noh SM, Wood DO, Bavoil PM, Brayton KA, Martinez JJ, et al. Engineering of obligate intracellular bacteria: progress, challenges and paradigms. Nat Rev Microbiol. 2017 Sep;15(9):544–558. https://doi.org/10.1038/nrmicro.2017.59

Rockey DD, Scidmore MA, Bannantine JP, Brown WJ. Proteins in the chlamydial inclusion membrane. Microbes Infect. 2002 Mar; 4(3):333–340. https://doi.org/10.1016/S1286-4579(02)01546-0

Rodolakis A, Salinas J, Papp J. Recent advances on ovine chlamydial abortion. Vet Res. 1998 May–Aug;29(3–4):275–288.

Saeed NM, Talib SM, Dyary HO. Molecular detection of outer membrane protein 2 gene in isolated brucella from sheep and goats in Sharazor/Kurdistan region of Iraq. Pak Vet J. 2019 Jul 01;39(03): 383–388. https://doi.org/10.29261/pakvetj/2019.043

Schoell AR, Heyde BR, Weir DE, Chiang PC, Hu Y, Tung DK. Euthanasia method for mice in rapid time-course pulmonary pharmacokinetic studies. J Am Assoc Lab Anim Sci. 2009 Sep;48(5): 506–511.

Singh R, Liechti G, Slade JA, Maurelli AT. *Chlamydia trachomatis* oligopeptide transporter performs dual functions of oligopeptide transport and peptidoglycan recycling. Infect Immun. 2020 Apr 20; 88(5):e00086–e20. https://doi.org/10.1128/IAI.00086-20

Spičic S, Račić Ivana, Andrijanić M, Duvnjak S, Zdelar-Tuk M, Stepanić M, Cvetnić Z. Emerging cases of chlamydial abortion in sheep and goats in Croatia and Bosnia and Herzegovina. Berl Munch Tierarztl Wochenschr. 2015 May-Jun;128(5–6):183–187.

Stephens RS, Lammel CJ. *Chlamydia* outer membrane protein discovery using genomics. Curr Opin Microbiol. 2001 Feb;4(1):16–20. https://doi.org/10.1016/S1369-5274(00)00158-2

Valdivia RH. *Chlamydia* effector proteins and new insights into chlamydial cellular microbiology. Curr Opin Microbiol. 2008 Feb; 11(1):53–59. https://doi.org/10.1016/j.mib.2008.01.003

Wheelhouse N, Aitchison K, Spalding L, Livingstone M, Longbottom D. Transcriptional analysis of *in vitro* expression patterns of *Chlamydophila abortus* polymorphic outer membrane proteins during the chlamydial developmental cycle. Vet Res. 2009 Sep;40(5):47. https://doi.org/10.1051/vetres/2009030

Zhang Q, Huang Y, Gong S, Yang Z, Sun X, Schenken R, Zhong G. *In vivo* and *ex vivo* imaging reveals a long-lasting chlamydial infection in the mouse gastrointestinal tract following genital tract inoculation. Infect Immun. 2015 Sep;83(9):3568–3577. https://doi.org/10.1128/IAI.00673-15

SHORT COMMUNICATION

Polish Journal of Microbiology
2022, Vol. 71, No 1, 123–129
https://doi.org/10.33073/pjm-2022-004

Helicobacter pylori and Epstein-Barr Virus Co-Infection in Polish Patients with Gastric Cancer – A Pilot Study

MAGDALENA DZIKOWIEC[1]*, PRZEMYSŁAW LIK[2], JUSTYNA KISZAŁKIEWICZ[1], ALEKSANDRA KUCZYŃSKA[3], MAREK MORDALSKI[4], DARIUSZ NEJC[2], JANUSZ PIEKARSKI[2], EWA BRZEZIAŃSKA-LASOTA[1] and DOROTA PASTUSZAK-LEWANDOSKA[3]

[1] Department of Biomedicine and Genetics, Chair of Biology and Medical Microbiology, Medical University of Lodz, Lodz, Poland
[2] 2nd Oncological Surgery Ward – Oncologic Surgery Clinic, Provincial Multispeciality Center of Oncology and Traumatology named after M. Kopernik in Lodz, Lodz, Poland
[3] Department of Microbiology and Laboratory Medical Immunology, Chair of Biology and Medical Microbiology, Medical University of Lodz, Lodz, Poland
[4] Central Clinical Hospital of the Medical University of Lodz, Lodz, Poland

Submitted 30 October 2021, accepted 3 January 2022, published online 27 February 2022

Abstract

The infectious agents may be the etiological factor of up to 15–20% of cancers. In stomach cancer, attention is paid to *Helicobacter pylori* and Epstein-Barr virus, both of which cause gastritis and can lead to tumor development. In co-infection, the inflammatory process is much more intense. We assessed the seroprevalence towards *H. pylori* and EBV in 32 patients with diagnosed gastric cancer. *H. pylori* antibodies were found in 69% patients, and anti-EBV – in all of them. The study confirmed that co-infection of *H. pylori* and EBV seems to be important in etiopathology of gastric cancer.

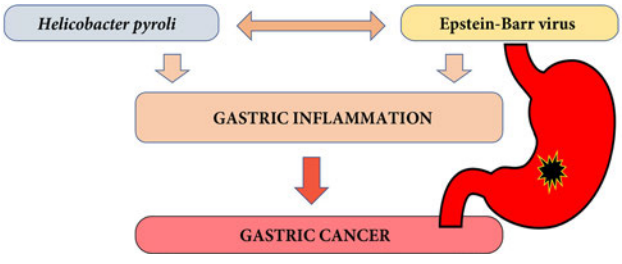

K e y w o r d s: co-infection, EBV, gastric cancer, *Helicobacter pylori* prevalence, infection agents in cancer

There has been tremendous progress in science and medicine in recent years, but despite this, cancer is the second leading cause of death after cardiovascular disease and is undeniably one of the most critical public health challenges. Neoplastic cells are characterized by reduced growth control, invasiveness to the tissues in which they occur, and the ability to spread. More and more often, attention is paid to the contribution to neoplasms formation by broadly understood infectious agents (Fol and Jachowicz 2016; Masrour-Roudsari and Ebrahimpour 2017; Palrasu et al. 2021). It is estimated that they could cause up to 20% of cancers. Infectious agents can promote tumor development by affecting cell growth, destabilizing the host's immune system, or leading to changes in cells resulting from long-term infection. The neoplastic process can be a consequence of infections caused by certain viruses (most often), bacteria, or even parasites (Fol and Jachowicz 2016). According to the World Health Organization, in 2020, about 10 million people were diagnosed with new cases of cancer, and stomach cancer was in the sixth place (1.09 million), while in terms of the number of deaths, it was in the fourth place (769 thousand), after lung, colon, and liver cancer (WHO 2021). Stomach cancer incidences and mortality vary greatly depending on environmental factors such as diet, alcohol consumption, smoking, cancer stage at diagnosis, and genetic burden. *Helicobacter pylori* and the Epstein-Barr virus

* Corresponding author: M. Dzikowiec, Department of Biomedicine and Genetics, Chair of Biology and Medical Microbiology, Medical University of Lodz, Lodz, Poland; **e-mail:magdalena.dzikowiec@umed.lodz.pl**

are mentioned as significant risk factors for developing gastric cancer (Fasciana et al. 2019a; Machlowska et al. 2020; Sexton et al. 2020; Palrasu et al. 2021).

H. pylori was first isolated from the stomach in 1983, and already in 1994, the International Agency for Research on Cancer (IARC) classified *H. pylori* as a class 1 carcinogen (Santacroce et al. 2008; Fasciana et al. 2019b; Palrasu et al. 2021). In most cases, the infection is asymptomatic, but 1–2% of people develop stomach cancer. It has been shown that these bacteria are a strong risk factor for stomach cancer; infection can lead to chronic inflammation, followed by intestinal metaplasia, dysplasia, and gastric cancer (Correa 1992; Santacroce et al. 2008). It is estimated that in 2015 there were approximately 4.4 billion individuals with *H. pylori* infection worldwide. A substantial variation in *H. pylori* occurrence of bacteria depends on the region of the world and the country. The prevalence is very high in most developing countries and is mainly related to socioeconomic status and hygiene levels. The highest prevalence is in Africa, South America, and West Asia; the lowest in Oceania, Western Europe, and North America. In Europe, the lowest prevalence was recorded in Switzerland (18.9%), and the highest in Portugal, 86.4%; in Poland, it is about 66.6% (Hooi et al. 2017).

The Epstein-Barr virus (EBV) is ubiquitous globally, affecting over 90% of people, and is associated with certain cancers such as post-transplant lymphoproliferative diseases, nasopharyngeal cancer, Hodgkin's lymphoma, and gastric cancer (Shinozaki-Ushiku et al. 2015; Smatti et al. 2018). According to the molecular classification of gastric cancer, Epstein-Barr virus-associated gastric carcinoma (EBVaGC) is a distinct subtype in terms of oncogenesis and molecular features and accounts for approximately 10% of cases (Cancer Genome Atlas Research Network 2014; Shinozaki-Ushiku et al. 2015; Yang et al. 2020). EBV has long been linked to some undifferentiated gastric carcinoma, thus indicating that focal EBV infection occurs before oncogenic transformation (Shibata et al. 1991). Interestingly, EBV-positive carcinomas have a better prognosis and a lower percentage of lymph node metastases than EBV-negative carcinomas, as demonstrated by clinical-pathological studies (Kobayashi et al. 2019).

More and more attention is paid to research on the coexistence of *H. pylori* and EBV in gastric diseases and cancer (Morales-Sanchez and Fuentes-Panana 2017; Polakovicova et al. 2018; Dávila-Collado et al. 2020; Rihane et al. 2020). Although less is known on EBV participation in chronic gastric inflammation, many studies recognize both pathogens as etiological agents of chronic gastritis, and in the case of co-infections, the inflammatory process is significantly increased (Cárdenas-Mondragón et al. 2015; Morales-Sanchez and Fuentes-Panana 2017).

The research performed by Santacroce et al. (2000) has indicated a significant relationship between *H. pylori*-positivity and the presence of mast cells in gastritis. It has been shown that neutrophils, eosinophils, mast cells, and dendritic cells can directly infiltrate the gastric epithelium during *H. pylori* infection (Ieni et al. 2016). That is a way these innate immune cells occupy strategic positions and make it easy to initiate chronic active inflammation. Virulent strains of *H. pylori* stop the correct phagosome maturation process in macrophages and dendritic cells and generate large autophagosomes, in which the bacteria can multiply, weakening the host's immune defense. Eventually, apoptosis or functional depletion of macrophages and dendritic cells can be observed in chronic *H. pylori* infection (Ieni et al. 2016). Also, MALT lymphomas, the most frequent lymphoid neoplasms of the digestive tract, are strongly associated with *H. pylori* infection (Santacroce et al. 2008; Violeta Filip et al. 2018). The pathogenesis of primary gastric lymphoma may also be related to other risk factors, including the EBV virus. Interestingly, *H. pylori* and EBV infections alter the expression of the host miRNA, which modulates the host's inflammatory immune response, favoring the survival of bacteria in the gastric mucosa and inhibiting apoptosis in EBV-positive cells (Morales-Sanchez and Fuentes-Panana 2017; Polakovicova et al. 2018).

The aim of the research was to determine the prevalence of *H. pylori* and EBV and their possible co-infections in patients with gastric cancer.

The admission criterion for the research study was the diagnosis of gastric cancer in an adult patient with no history of other neoplasms. After complete gastrectomy, blood serum was obtained from 32 patients diagnosed with gastric cancer (adenocarcinoma). Patients were treated in 2018–2020 at the 2nd Oncological Surgery Ward – Oncologic Surgery Clinic, Provincial Multispeciality Center of Oncology and Traumatology named after M. Kopernik in Lodz and the Central Clinical Hospital of the Medical University of Lodz. The patient group consisted of 20 men and 15 women, aged 36–93 years (mean age 68). The study was approved by the Bioethics Committee at the Medical University of Lodz (No. RNN/206/19/KE). The reference material was serum obtained from people without neoplastic diseases.

In patients with adenocarcinoma, after complete gastrectomy, the primary tumor size and its' invasion into adjacent tissues (T), the state of regional lymph nodes (N), and the presence or absence of distant metastases (M) were analyzed histopathologically (TNM classification) (Rosen and Sapra 2021).

Detection of anti-cagA antibodies against *H. pylori* was performed using ELISA kits (EIA Helicobacter MONO IgM, EIA Helicobacter MONO IgG, EIA

Table I
The number of tumor specimens (n) classified according to TNM classification and AJCC staging.

	TNM classification								
	T1	T2	T3	T4	N0	N1	N2	N3	M0
n	7	3	18	4	11	5	7	9	32
AJCC staging									
	stage I (localized cancer)		stage II (locally advanced cancer, early stages)				stage III (locally advanced cancer, late stages)		
n	8		9				15		

Helicobacter MONO IgA, TestLine Clinical Diagnostics s.r.o.). In the case of EBV, the presence of antibodies against viral capsid, early and nuclear antigens were analyzed, for which the indirect immunofluorescence method (IIFT) was used. The IIFT method is considered the gold standard in EBV diagnostics (IIFT BIOCHIP EBV, Euroimmun).

Statistical analysis was performed using Statistica StatSoft Inc. The significance of differences between the control and study groups was assessed using the Kruskal-Wallis test, with the significance level $p < 0.05$. Correlations of the presence of antibodies to *H. pylori* infection with demographic factors (age, sex) and the degree of tumor development (TNM classification, AJCC staging) were determined using the Spearman Rank Correlation, with the significance level $p < 0.05$.

The results of histopathological analysis are collected in Table I.

In search for *H. pylori*, IgM, IgG, and IgA antibodies were assessed to obtain the most reliable results, excluding false-negative results. The prevalence of infection among patients was 69%. IgG antibodies were detected in nine patients only, IgG and IgA antibodies were present in 12 others, and one patient had only IgA antibodies against *H. pylori*. The obtained results indicated the past infection, as no IgM antibodies were detected in any of the patients, which would point to a recent infection. Antibody assays in the control group showed the presence of infection in 42% of subjects – in one case, the presence of IgM was detected, which indicated a recent infection. In the remaining cases, the infection occurred in the past; in seven persons, IgG and IgA antibodies were present, in five – only IgG antibodies, and in one case, only IgA antibodies were detected.

Statistical analysis showed a positive correlation (Spearman rank correlation, $p < 0.05$) between a tumor stage and the presence of IgG against *H. pylori* (Fig. 1), and between the size of the primary tumor and the presence of IgG against *H. pylori* (Fig. 2). There was no statistically significant difference between the patients' age and the cancer stage and between the patients' age and the prevalence of antibodies to *H. pylori*.

Serological analysis of anti-EBV antibodies included IgM and IgG antibodies to capsid antigens (CA), early antigens (EA), and nuclear antigens (EBNA). The avidity of IgG antibodies was also assayed. A positive

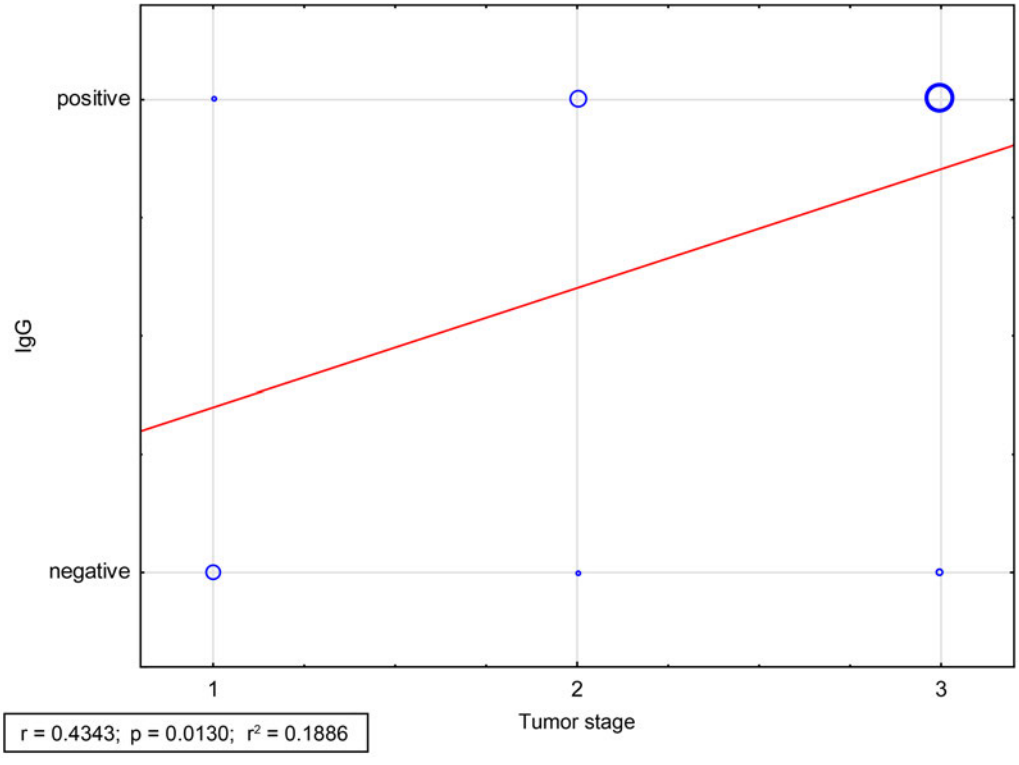

Fig. 1. The correlation between tumor stage and the presence of IgG against *H. pylori*.

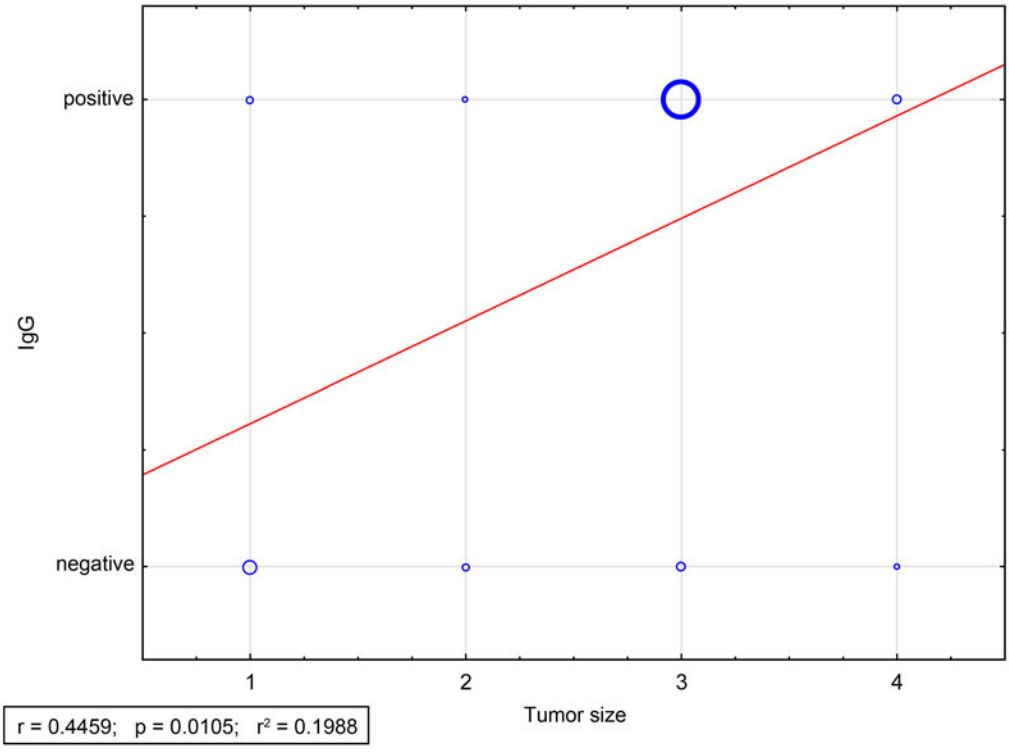

Fig. 2. The correlation between tumor size (TNM classification) and the presence of IgG against *H. pylori*.

anti-CA (IgM) results are the classic marker of fresh infection. IgG anti-CA antibodies remain at the same level throughout life. About 6–8 weeks after the infection, antibodies against nuclear antigens (anti-EBNA) are produced, and their presence indicates a past EBV infection. It is helpful to test the avidity, i.e., the binding strength of specific IgG antibodies to the antigen. Thanks to the avidity test, it can be determined whether the positive reaction of IgG antibodies results from a recent or past infection. At first, the immune system responds to infection by producing antibodies in the IgG class with low antigen-binding power (low avidity). As the infection progresses, the avidity of IgG antibodies increases. The late-stage or past infection is suspected if high avidity antibodies are detected. The study on the avidity of anti-CA antibodies in the IgG class in the diagnostics of EBV infections allows for interpretation of the problematic and questionable results. Based on the simultaneous detection of the presence of several specific antibodies, and the assessment of their avidity, it can be estimated whether the antibodies present in the patient's serum are the result of an active infection or the evidence of a past infection. None of the patients had IgM anti-CA antibodies, which would indicate a new infection, but all had high avidity anti-CA IgG antibodies, eight patients had anti-EA IgG antibodies, and five patients did not have anti-EBNA antibodies.

Gastric cancer is one of the most common neoplasms, and since the symptoms of the disease appear at an advanced stage, it is diagnosed very late. It develops due to genetic and environmental factors, such as eating habits, alcohol drinking, cigarette smoking, and excessive body weight. Stomach cancer usually has a poor long-term prognosis; only the five-year survival rate in Japan is relatively good, reaching 90%. In Europe, this value ranges from 10% to 30%. Therefore, it is very essential to understand the etiology and the ability to early diagnose of gastric cancer (Sitarz et al. 2018; Machlowska et al. 2020). Stomach cancer rates increase with age and reach a plateau between 55 and 80. On average, gastric cancer incidence rates are 2 to 3 times higher in men than in women (Machlowska et al. 2020; Thrift and El-Serag 2020). Also, in our study group, the majority of patients were men (20 men versus 12 women), and the age of the patients in most cases ranged from 60 to 80 years.

More and more often, infectious agents are mentioned to trigger cancer development. In the case of gastric cancer, *H. pylori* is regarded as the leading environmental risk factor with proven pathogenicity; however, the contribution of EBV in its development is not fully understood (Cárdenas-Mondragón et al. 2015; Singh and Jha 2017; de Souza et al. 2018; Castaneda et al. 2019; de Martel et al. 2020; Sexton et al. 2020). It has been estimated that approximately 2.2 million cases of infection-related cancers were diagnosed worldwide in 2018, corresponding to an infection-related age-standardized incidence rate (ASIR) of 25.0 cases per 100,000 persons yearly. *H. pylori* appeared in the first place as a cancer-related infectious agent. ASIR

attributed to infection was the highest in eastern Asia – 37.9 cases per 100,000 persons per year, and lowest in northern Europe – 13.6 cases per 100,000 persons per year (de Martel et al. 2020).

To the best of our knowledge, this is the first project about the coexistence of *H. pylori* and EBV in the development of gastric cancer in the Polish population. Both pathogens are involved in the development of inflammation, which may be a consequence of changes in the gastric mucosa that may lead to the development of the neoplastic process (Dávila-Collado et al. 2020; Rihane et al. 2020). The incidence of gastric cancer varies widely geographically. Over 50% of new cases occur in developing countries. Likewise, the prevalence of *H. pylori* is the highest in the developing world, and the infection is widespread in East Asia, strongly associated with the development of gastric cancer (Hooi et al. 2017). In our study, antibodies against *H. pylori* were detected in 69% of patients with gastric cancer, a much higher prevalence than the control group (42%). The obtained results have also confirmed a correlation between *H. pylori* infection and the degree of tumor stage and the correlation between *H. pylori* infection and tumor size, indicating the role of the pathogen in the progression of gastric cancer.

In Poland, little research has been conducted on the epidemiology of *H. pylori*. Multicenter studies on the presence of *H. pylori* in children and adults (6 months-89 years of age) in Poland occurred in 2002–2003. The presence of antibodies was detected in over 58% of the subjects studied: 32% in children and 84.2% in adults. In adults, a statistically significant correlation was found between *H. pylori* seropositivity and the occurrence of gastrointestinal symptoms. In histopathological specimens, inflammation predominated in children, and atrophic gastritis and intestinal metaplasia were common in adults (Iwanczak et al. 2014). An earlier study, performed in 2008, showed a lower infection rate in pediatric patients of approx. 16% (Biernat et al. 2016). However, the later study used the 13C-urea breath test (UBT) for current *H. pylori* infection showed a positive result for 23.6% of cases (Szaflarska-Popławska and Soroczyńska-Wrzyszcz 2019), indicating an increasing trend. In our study, the incidence of *H. pylori* in the entire group (patients and controls) was 55.5%, similar to the results reported in later studies carried out in Poland, although our group was relatively small.

Relatively recently, attention was paid to the role of EBV as an etiological factor in the development of gastric cancer. The presence of viral DNA in cancer cells was confirmed by molecular methods in 1990. It has even been suggested that focal EBV infection occurs before oncogenic transformation (Shibata et al. 1991).

The incidence of EBV infection in gastric cancer ranges from 2 to 20%, the global average is about 10% (Shinozaki-Ushiku et al. 2015). Researches carried out in various regions of the world has shown that the incidence of gastric cancer associated with EBV is different, and in Europe, it is 13.9%, in America – 12.5%, and in Asia – 7.5% (Camargo et al. 2014). The differentiation in the occurrence of EBVaGC can also be observed, depending on individual countries, e.g., it ranges from 4% in China to 17.9% in Germany, while in Poland, it is about 12.5% (Czopek et al. 2003; Sitarz et al. 2018). In our study, based on serological results, the presence of EBV antibodies in the serum of all gastric cancer patients was demonstrated.

Inflammation of the gastric mucosa is much more severe in *H. pylori* and EBV co-infection than infection with a single pathogen (Cárdenas-Mondragón et al. 2015; Polakovicova et al. 2018; Castaneda et al. 2019). Cardenas-Mondragón et al. (2015) analyzed antibodies against EBV and *H. pylori* in 525 patients with gastric diseases from Mexico and Paraguay. They found that 94.7% of patients had positive antibodies to EBV and 87.7% to *H. pylori*, with a similar incidence in both countries. A relationship has been demonstrated between the coexistence of EBV and *H. pylori* and pre-neoplastic lesions and intestinal gastric carcinoma. Castaneda et al. (2019) studied patients with gastric cancer in Peru, where the incidence of *H. pylori* was 60.8%, EBV – 14.1%, co-infection was found in 7.8% of cases.

Studies on the coexistence of EBV and *H. pylori* have also been conducted in pediatric patients with severe gastritis. Based on the study of antibodies in children with chronic abdominal pain, it has been shown that a single infection is associated with mild inflammation, while co-infection of both pathogens significantly worsens gastric inflammatory state. Even in *H. pylori* $CagA^+$ strain infection, inflammation was not as strong as in co-infections (Cárdenas-Mondragón et al. 2013).

In a study conducted by de Souza et al. (2018), the co-infections with *H. pylori* $CagA^+$ and EBV were correlated with the most advanced stages of cancer. Although only 20% of tumors were positive for EBV, infection with this virus was associated with distant metastases.

Gastric cancer is one of the most common cancers globally, with a very high mortality rate. Due to the lack of characteristic symptoms, it is usually diagnosed late. Therefore, early and effective diagnosis is critical, and the search for non-invasive markers will allow for early cancer detection and effective treatment. In this respect, it is crucial to understand tumor biology, i.e., the mechanisms underlying the neoplastic process. Although many factors contribute to the development of cancer, both genetic and environmental, the increasingly important role is assigned to infectious factors, primarily *H. pylori* and EBV. Both pathogens cause inflammation within the gastric mucosa, and in the case of their co-infection, it is much more intense. The

results of our study show a high prevalence of *H. pylori* and EBV in patients with gastric cancer and the correlation of infection with its progression.

The seroprevalence of *H. pylori* was positively correlated with both tumor size and tumor stage, according to TNM classification and AJCC staging, respectively. The co-presence of anti-EBV antibodies (anti-CA IgG) and IgG against *H. pylori* was confirmed in 69% of patients. This result suggests that co-infection of *H. pylori* and EBV, both harmful biotic agents, could be linked with the advanced stages of gastric cancer and its progression.

The number of patients included in the study is not large. The material was collected from 2018 to 2020. At the time of the announcement of the SARS-CoV2 pandemic, the access to treatment of diseases other than COVID-19 was limited. Hence, the difficulties in obtaining biological material from cancer patients. That is why we describe the study as a pilot study – to share the results obtained so far. We are still collecting material from patients and will continue our research, extending it to other factors related to gastric carcinogenesis.

ORCID
Magdalena Dzikowiec https://orcid.org/0000-0002-4044-6424

Conflict of interest

The authors do not report any financial or personal connections with other persons or organizations, which might negatively affect the contents of this publication and/or claim authorship rights to this publication.

Literature

Biernat MM, Iwańczak B, Bińkowska A, Grabińska J, Gościniak G. The prevalence of *Helicobacter pylori* infection in symptomatic children: a 13-year observational study in the Lower Silesian region. Adv Clin Exp Med. 2016 Mar-Apr;25(2):303–308. https://doi.org/10.17219/acem/44372

Camargo MC, Kim WH, Chiaravalli AM, Kim KM, Corvalan AH, Matsuo K, Yu J, Sung JJY, Herrera-Goepfert R, Meneses-Gonzalez F, et al. Improved survival of gastric cancer with tumour Epstein-Barr virus positivity: an international pooled analysis. Gut. 2014 Feb; 63(2):236–243. https://doi.org/10.1136/gutjnl-2013-304531

Cancer Genome Atlas Research Network. Comprehensive molecular characterization of gastric adenocarcinoma. Nature. 2014 Sep 11; 513(7517):202–209. https://doi.org/10.1038/nature13480

Cárdenas-Mondragón MG, Carreón-Talavera R, Camorlinga-Ponce M, Gomez-Delgado A, Torres J, Fuentes-Pananá EM. Epstein Barr virus and *Helicobacter pylori* co-infection are positively associated with severe gastritis in pediatric patients. PLoS One. 2013 Apr 24;8(4):e62850. https://doi.org/10.1371/journal.pone.0062850

Cárdenas-Mondragón MG, Torres J, Flores-Luna L, Camorlinga-Ponce M, Carreón-Talavera R, Gomez-Delgado A, Kasamatsu E, Fuentes-Pananá EM. Case-control study of Epstein-Barr virus and *Helicobacter pylori* serology in Latin American patients with gastric disease. Br J Cancer. 2015 Jun 9;112(12):1866–1873. https://doi.org/10.1038/bjc.2015.175

Castaneda CA, Castillo M, Chavez I, Barreda F, Suarez N, Nieves J, Bernabe LA, Valdivia D, Ruiz E, Dias-Neto E, et al. Prevalence of *Helicobacter pylori* infection, its virulent genotypes, and Epstein-Barr virus in Peruvian patients with chronic gastritis and gastric cancer. J Glob Oncol. 2019 Sep;5:1–9. https://doi.org/10.1200/JGO.19.00122

Correa P. Human gastric carcinogenesis: a multistep and multifactorial process – First American Cancer Society Award Lecture on Cancer Epidemiology and Prevention. Cancer Res. 1992 Dec 15;52(24): 6735–6740.

Czopek JP, Stojak M, Sinczak A, Popiela P, Kulig J, Rudzki Z, Stachura J. EBV-positive gastric carcinomas in Poland. Pol J Pathol. 2003;54(2):123–128.

Dávila-Collado R, Jarquín-Durán O, Dong LT, Espinoza JL. Epstein-Barr virus and *Helicobacter pylori* co-infection in non-malignant gastroduodenal disorders. Pathogens. 2020 Feb 6;9(2):104. https://doi.org/10.3390/pathogens9020104

de Martel C, Georges D, Bray F, Ferlay J, Clifford G. Global burden of cancer attributable to infections in 2018: a worldwide incidence analysis. Lancet Glob Health. 2020 Feb;8(2):e180–90. https://doi.org/10.1016/S2214-109X(19)30488-7

de Souza CRT, Almeida MCA, Khayat AS, da Silva EL, Soares PC, Chaves LC, Burbano RMR. Association between *Helicobacter pylori*, Epstein-Barr virus, human papillomavirus and gastric adenocarcinomas. World J Gastroenterol. 2018 Nov 21;24(43):4928–4938. https://doi.org/10.3748/wjg.v24.i43.4928

Fasciana T, Di Carlo P, Jouini A, Di Giulio M. *Helicobacter pylori*: infection and new perspective for the treatment. Can J Infect Dis Med Microbiol. 2019a Jul 29;2019:9431369. https://doi.org/10.1155/2019/9431369

Fasciana T, Serra N, Capra G, Mascarella C, Gagliardi C, Di Carlo P, Cannella S, Simonte MR, Lipari D, Sciortino M, et al. *Helicobacter pylori* and Epstein-Barr virus infection in gastric diseases: correlation with IL-10 and IL1RN polymorphism. J Oncol. 2019b Dec 6; 2019:1785132. https://doi.org/10.1155/2019/1785132

Fol M, Jachowicz E. [Infectious agents in carcinogenesis] (in Polish). Med Og Nauk Zdr. 2016;22(1):7–14. https://doi.org/10.5604/20834543.1198717

Hooi JKY, Lai WY, Ng WK, Suen MMY, Underwood FE, Tanyingoh D, Malfertheiner P, Graham DY, Wong VWS, Wu JCY, et al. Global prevalence of *Helicobacter pylori* infection: Systematic review and meta-analysis. Gastroenterology. 2017 Aug;153(2): 420–429. https://doi.org/10.1053/j.gastro.2017.04.022

Ieni A, Barresi V, Rigoli L, Fedele F, Tuccari G, Caruso RA. Morphological and cellular features of innate immune reaction in *Helicobacter pylori* gastritis: a brief review. Int J Mol Sci. 2016 Jan 15;17(1):109. https://doi.org/10.3390/ijms17010109

Iwanczak B, Laszewicz W, Iwanczak F, Dzierzanowska-Fangrat K, Rozynek M, Dzierzanowska D, Gosciniak G, Dlugosz J; Task force of the Polish Society of Gastroenterology. Genotypic and clinical differences of seropositive *Helicobacter pylori* children and adults in the Polish population. J Physiol Pharmacol. 2014 Dec;65(6):801–807.

Kobayashi Y, Kunogi T, Tanabe H, Murakami Y, Iwama T, Sasaki T, Takahashi K, Ando K, Nomura Y, Ueno N, et al. Gastric submucosa-invasive carcinoma associated with Epstein-Barr virus and endoscopic submucosal dissection: A case report. Gastrointest Oncol. 2019 Oct 15;11(10):925–932. https://doi.org/10.4251/wjgo.v11.i10.925

Machlowska J, Baj J, Sitarz M, Maciejewski R, Sitarz R. Gastric cancer: epidemiology, risk factors, classification, genomic characteristics and treatment strategies. Int J Mol Sci. 2020 Jun 4;21(11):4012. https://doi.org/10.3390/ijms21114012

Masrour-Roudsari J, Ebrahimpour S. Causal role of infectious agents in cancer: An overview. Caspian J Intern Med. 2017 Summer; 8(3):153–158. https://doi.org/10.22088/cjim.8.3.153

Morales-Sanchez A, Fuentes-Panana EM. Epstein-Barr virus-associated gastric cancer and potential mechanisms of oncogenesis. Curr Cancer Drug Targets. 2017;17(6):534–554. https://doi.org/10.2174/1568009616666160926124923

Palrasu M, Zaika E, El-Rifai W, Que J, Zaika AI. Role of bacterial and viral pathogens in gastric carcinogenesis. Cancers (Basel). 2021 Apr 14;13(8):1878. https://doi.org/10.3390/cancers13081878

Polakovicova I, Jerez S, Wichmann IA, Sandoval-Bórquez A, Carrasco-Véliz N, Corvalán AH. Role of microRNAs and exosomes in *Helicobacter pylori* and Epstein-Barr virus associated gastric cancers. Front Microbiol. 2018 Apr 5;9:636. https://doi.org/10.3389/fmicb.2018.00636

Rihane FE, Hassou N, Nadifi S, Ennaji MM. Chapter 25 – Status of *Helicobacter pylori* coinfection with Epstein-Barr virus in gastric cancer. In: Ennaji MM, editor. Emerging and reemerging viral pathogens. Cambridge (USA): Academic Press; 2020. p. 571–585. https://doi.org/10.1016/B978-0-12-819400-3.00025-9

Rosen RD, Sapra A. TNM Classification [Internet, updated 2021 Feb 23]. Treasure Island (USA): StatPearls Publishing; 2021 [cited 2021 Sep 30]. Available from https://www.ncbi.nlm.nih.gov/books/NBK553187/

Santacroce L, Bufo P, Latorre V, Losacco T. [Role of mast cells in the physiopathology of gastric lesions caused by *Helicobacter pylori*] (in Italian). Chir Ital. 2000 Sep-Oct;52(5):527–531.

Santacroce L, Cagiano R, Del Prete R, Bottalico L, Sabatini R, Carlaio RG, Prejbeanu R, Vermesan H, Dragulescu SI, Vermesan D, et al. *Helicobacter pylori* infection and gastric MALTomas: an up-to-date and therapy highlight. Clin Ter. 2008 Nov-Dec;159(6):457–462.

Sexton RE, Al Hallak MN, Diab M, Azmi AS. Gastric cancer: a comprehensive review of current and future treatment strategies. Cancer Metastasis Rev. 2020 Dec;39(4):1179–1203. https://doi.org/10.1007/s10555-020-09925-3

Shibata D, Tokunaga M, Uemura Y, Sato E, Tanaka S, Weiss LM. Association of Epstein-Barr virus with undifferentiated gastric carcinomas with intense lymphoid infiltration. Lymphoepithelioma-like carcinoma. Am J Pathol. 1991 Sep;139(3):469–474.

Shinozaki-Ushiku A, Kunita A, Fukuyama M. Update on Epstein-Barr virus and gastric cancer (Review). Int J Oncol. 2015 Apr;46(4): 1421–1434. https://doi.org/10.3892/ijo.2015.2856

Singh S, Jha HC. Status of Epstein-Barr virus coinfection with *Helicobacter pylori* in gastric cancer. J Oncol. 2017;2017:3456264. https://doi.org/10.1155/2017/3456264

Sitarz R, Skierucha M, Mielko J, Offerhaus GJA, Maciejewski R, Polkowski WP. Gastric cancer: epidemiology, prevention, classification, and treatment. Cancer Manag Res. 2018 Feb 7;10:239–248. https://doi.org/10.2147/CMAR.S149619

Smatti MK, Al-Sadeq DW, Ali NH, Pintus G, Abou-Saleh H, Nasrallah GK. Epstein-Barr virus epidemiology, serology, and genetic variability of LMP-1 oncogene among healthy population: An update. Front Oncol. 2018 Jun 13;8:211. https://doi.org/10.3389/fonc.2018.00211

Szaflarska-Popławska A, Soroczyńska-Wrzyszcz A. Prevalence of *Helicobacter pylori* infection among junior high school students in Grudziadz, Poland. Helicobacter. 2019 Feb;24(1):e12552. https://doi.org/10.1111/hel.12552

Thrift AP, El-Serag HB. Burden of gastric cancer. Clin Gastroenterol Hepatol. 2020 Mar;18(3):534–542. https://doi.org/10.1016/j.cgh.2019.07.045

Violeta Filip P, Cuciureanu D, Sorina Diaconu L, Maria Vladareanu A, Silvia Pop C. MALT lymphoma: epidemiology, clinical diagnosis and treatment. J Med Life. 2018 Jul-Sep;11(3):187–193. https://doi.org/10.25122/jml-2018-0035

WHO. Cancer [Internet]. Geneva (Switzerland): World Health Organization; 2021 [cited 2021 Sep 30]. Available from https://www.who.int/news-room/fact-shwhoeets/detail/cancer

Yang J, Liu Z, Zeng B, Hu G, Gan R. Epstein-Barr virus-associated gastric cancer: A distinct subtype. Cancer Lett. 2020 Dec 28; 495: 191–199. https://doi.org/10.1016/j.canlet.2020.09.019

Polish Journal of Microbiology
2022, Vol. 71, No 1, 131–138

INFORMACJE Z POLSKIEGO TOWARZYSTWA MIKROBIOLOGÓW

Od ostatniej informacji o działalności Zarządu Głównego Polskiego Towarzystwa Mikrobiologów, zamieszczonej w zeszytach nr 4 z 2021 r. kwartalników *Advancements of Microbiology – Postępy Mikrobiologii* i *Polish Journal of Microbiology*, ZG PTM zajmował się następującymi sprawami:

I. W dniu 10.01.2022 r. w wersji on-line odbyła się konferencja „VI Mazowieckie Spotkanie Mikrobiologów i Epidemiologów organizowana przez Wiceprezes PTM, Konsultanta Wojewódzkiego w dziedzinie Mikrobiologia Lekarska Panią prof. dr hab. Ewę Augustynowicz-Kopeć.

II. Europejskie Towarzystwo Mikrobiologii Klinicznej i Chorób Zakaźnych (ESCMID) podjęło decyzję o wprowadzeniu od stycznia 2022 r. opłaty dla stowarzyszonych towarzystw (Affiliated Society), a takim jest PTM, w zależności od liczby członków. W związku z faktem, że na koniec 2021 w PTM było 880 członków, składka wynosi 250 Euro (≥ 100 and < 1000 members). Do tej pory towarzystwa mikrobiologiczne liczące poniżej 1000 członków nie płaciły żadnej składki.

III. Opłaciliśmy składkę roczną w wysokości 275 USD za członkostwo PTM w Publishers International Linking Association, Inc Dba CROSSREF, organizacji nadającej numery Doi dla artykułów w *Polish Journal of Microbiology*.

IV. Uruchomiono stronę internetową Kongresu IUMS. https://iums2022.com/, który będzie odbywać się w formie hybrydowej w Rotterdamie, Holandia w dniach 19–22 lipca 2022 r. Opłaty rejestracyjne są zróżnicowane https://iums2022.com/register/. Abstrakty prac można nadsyłać do 6 kwietnia 2022 r. Późne abstrakty można nadsyłać w okresie 2–18 maja 2022 r.

V. Pierwsze spotkanie naukowe Sekcji Mikrobiologii Środowiskowej PTM odbyło się on-line dnia 20 stycznia 2022 r. Wykład pt. „Metaboliczna różnorodność cyjanobakterii bałtyckich – środowiskowe znaczenie i biotechnologiczny potencjał" wygłosiła Pani prof. Hanna Mazur-Marzec z Zakładu Biotechnologii Morskiej Instytutu Oceanografii, Uniwersytetu Gdańskiego.

VI. Oddział PTM w Krakowie zaprosił 27 stycznia 2022 r. na posiedzenie naukowo-szkoleniowe on-line z wykładem pt.: „Nanotechnologia w praktyce mikrobiologicznej – oddziaływanie bakterii z powierzchniami ciał stałych", który wygłosił dr Wojciech Pajerski Absolwent Środowiskowych Studiów Doktoranckich „Interdyscyplinarność dla medycyny innowacyjnej" InterDokMed.

VII. W dniu 28.01.2022 r. odbyło się on-line e-Sympozjum pt. „COVID-19 – Raport z oblężonego świata" współorganizowane przez Oddziały Terenowe PTM w Warszawie i Szczecinie. Przedstawiono 4 wykłady:
   a) „Zwierzęta w transmisji wirusa SARS-CoV-2" – dr hab. inż. Paweł Nawrotek, prof. ZUT; Katedra Mikrobiologii i Biotechnologii, Wydział Biotechnologii i Hodowli Zwierząt, Centrum Dydaktyczno-Badawcze Nanotechnologii Zachodniopomorski Uniwersytet Technologiczny w Szczecinie,
   b) „Ko-infekcje w przebiegu COVID-19" – dr n. med. Joanna Jursa-Kulesza; Samodzielna Pracownia Mikrobiologii Lekarskiej, Katedra Mikrobiologii, Immunologii i Medycyny Laboratoryjnej Pomorski Uniwersytet Medyczny w Szczecinie,
   c) „Szczepienia przeciwko COVID-19 przed piątą falą pandemii – fakty i mity" – dr hab. n. med. Ernest Kuchar; Klinika Pediatrii z Oddziałem Obserwacyjnym, Warszawski Uniwersytet Medyczny,
   d) „Postępowanie z chorym na COVID-19" – dr n. med. Jacek Nasiłowski; Tymczasowy Szpital Narodowy, CSK MSWiA, Katedra i Klinika Chorób Wewnętrznych, Pneumonologii i Alergologii, WUM.

VIII. Oddział PTM w Krakowie w dniu 24.02.2022 r. zorganizował posiedzenie naukowo-szkoleniowe on-line z wykładem pt.: „Środki dezynfekujące w wytwórni farmaceutycznej z punktu widzenia laboratorium mikrobiologicznego", który wygłosiła mgr Katarzyna Bucała-Śladowska Z-ca Kierownika Centrum ds. Mikrobiologii Farmaceutycznej, Kierownik Zapewnienia Jakości Osoba Wykwalifikowana z Centrum Badań Mikrobiologicznych i Autoszczepionek imienia dr Jana Bobra.

IX. Opłaciliśmy składkę roczną za członkostwo PTM w International Union of Microbiological Societies (IUMS) w wysokości 1144 USD = 880 członków PTM × 1,3 USD oraz składkę roczną za uczestnictwo PTM w Federation of European Microbiological Societies w wysokości 1232 Euro = 880 członków PTM × 1,4 Euro. Szkoda, że niewielu członków PTM występuje do FEMS o finansowanie staży zagranicznych i wyjazdów na konferencje (https://fems-microbiology.org/ zakładka GRANTS).

X. W dniu 31.01.2022 r. informacja o PTM i składzie Zarządu Głównego została wprowadzona do Centralnego Rejestru Beneficjentów Rzeczywistych.

XI. Prezydium Zarządu Głównego Polskiego Towarzystwa Mikrobiologów działając zdalnie, w dniu 31.01.2022 r. podjęło następujące uchwały: **Uchwałę nr 1–22** w sprawie wynagrodzenia członków redakcji Advances in Microbiology – *Postepy Mikrobiologii* w 2022 r.; **Uchwałę nr 2-2022** w sprawie wynagrodzenia członków redakcji *Polish Journal of Microbiology* w 2022 r.; **Uchwałę nr 3-2022** w sprawie wynagrodzenia sekretarki ZG PTM do 31.10.2022 r.; **Uchwałę nr 4-2022** w sprawie wynagrodzenia księgowej PTM do 31.12.2022 r.; **Uchwałę nr 5-2022** w sprawie organizacji kolejnej edycji **Nagrody Naukowej PTM im. Prof. Edmunda Mikulaszka**, która będzie przyznana w roku 2022, za artykuły opublikowane w latach 2020–2021 oraz w sprawie przedłużenia kadencji pracy na 2022 r. Komisji Konkursowej powołanej Uchwałą nr 20-2018. Zasady przyznawania nagrody są określone w **Regulaminie Nagrody Naukowej PTM im. Prof. Edmunda Mikulaszka** znajdującym się na stronie PTM (https://www.microbiology.pl/nagrody/nagroda-im-prof-edmunda-mikulaszka/)
Nagroda w 2022 roku dotyczy prac opublikowanych w latach 2020–2021.
Termin składania wniosków: 15.03.2022 r.
Ogłoszenie wyników konkursu: 30.04.2022 r.
Uchwałą nr 6-2022 jednomyślnie postanowiono przyjąć 4 osoby w poczet członków zwyczajnych PTM.

XII. Prezydium Zarządu Głównego PTM przyjęło **Uchwalę nr 7-2022** w sprawie objęcia patronatem honorowym IV Ogólnopolskiej Konferencji „IMPLANTY 2022: Inżynieria, medycyna i nauka – w pogoni za implantem doskonałym", w trakcie której będą omawiane również aspekty mikrobiologiczne. Konferencja organizowana będzie w dniach 27–28.05.2022 r. przez Politechnikę Gdańską, Wydział Inżynierii Mechanicznej i Okrętownictwa w Gdańsku; e-mail: konferencja-implanty.wm@pg.edu.pl.

XIII. W dniu 24.01.2022 r. odbyło się spotkanie członków Komitetu Organizacyjnego Zjazdu PTM. Przyjęto ostateczny układ 18 sesji naukowych, w tym jednej sponsorowanej przez firmy, oraz ustalono osoby, które byłyby odpowiedzialne za organizację tych sesji. Zwrócono się do wybranych osób, aby potwierdziły chęć organizacji wskazanych sesji.

XIV. Nieoczekiwanie skomplikowały się sprawy organizacji Zjazdu PTM. W dniu 27.01.2022 r. otrzymaliśmy informację: „W związku z podjęciem przez Zarząd Sangate Sancak Spółka Komandytowa decyzji o rozpoczęciu realizacji nowej inwestycji w miejscu obecnie działającego hotelu Sangate Hotel Airport informujemy, iż działalność w hotelowo – konferencyjna w Sangate Hotel Airport z dniem 30.04.2022 zostaje zakończona. Wszelkie wykraczające poza wskazany termin rezerwacje zostaną anulowane."

XV. W dniu 22.02.2022 r. odbyło się kolejne spotkanie członków Komitetu Organizacyjnego Zjazdu PTM. Omawiano organizację 18 sesji naukowych, ustalono, że Zjazd odbędzie się w Arche Hotel Krakowska w Warszawie, Aleja Krakowska 237. Ponadto ustalono, że ze względów epidemicznych i lokalowych, w Zjeździe w sposób bezpośredni może uczestniczyć tylko 500 osób w tym delegaci na Walne Zgromadzenie Delegatów PTM. Możliwa jest również prezentacja e-plakatów przez e-uczestników Zjazdu.

XVI. **XXIX Ogólnopolski Zjazd PTM 15–17 września 2022 r. w Warszawie**.
Bardzo dużo pracy zostało włożone w ustalenie konfiguracji strony internetowej XXIX Ogólnopolskiego Zjazdu PTM: www.zjazdptm2022.pl oraz sytemu rejestracji na Zjazd.
Strona Zjazdu została uruchomiona od 15.03.2022 r. Wszystkich członków PTM i osoby zainteresowane mikrobiologią zachęcamy do zapoznania się ze stroną, zarejestrowanie się i zgłaszania streszczeń na Zjazd, jak również pobrania plakatu Zjazdu i rozpropagowania wydarzenia.

XVII. Intensywnie poszukujemy sponsorów i wystawców na nasz Zjazd. Niestety zainteresowanie firm jest niewielkie. Spodziewamy się większego zaangażowania w tym obszarze członków i Przewodniczących Oddziałów Terenowych PTM, którzy są współorganizatorami Zjazdu.

XVIII. PTM podpisało z firmą De Gruyter Poland Sp. z o.o., działającą pod nazwą „Sciendo" aneksy dotyczące przedłużenia do 31.12.2022 r. umów na usługi wydawnicze Open Acccess Publishing Agreement pomiędzy Exeley Inc. i PTM, a dotyczących czasopism AM-PM i PJM, z uwzględnieniem przeniesienia praw i obowiązków Exeley na Sciendo.

XIX. Zdecydowano, że doroczne zebranie członków Zarządu Głównego i zaproszonych gości odbędzie się w dniu 28.03.2022 r. on-line. Przygotowano i rozesłano materiały na to spotkanie.

XX. Władze Warszawskiego Uniwersytetu Medycznego, który nieodpłatnie udostępnia PTM pomieszczenia na Biuro PTM w 2022 r. podniósł opłaty eksploatacyjne z 100 zł za pomieszczenie (7,7 m^2) w 2021 r. do 78,50 zł netto za 1 m^2 pomieszczenia w 2022 r. Ustalono, że PTM będzie płaciło miesięcznie za 2 m^2 pomieszczenia 193,11 zł brutto.

XXI. **W dniu 24.02.2022 r. rozpoczęła się agresja Rosji wobec Ukrainy**.

Prezydium ZG PTM zaapelowało do FEMS, IUMS i ESCMID nie tylko o solidarność z Ukrainą, w tym z członkami Society of Microbiologists of Ukraine, wyrażoną przez towarzystwa mikrobiologiczne zrzeszone w FEMS/IUMS/ESCMID, ale i o podjęcie sankcji w stosunku do towarzystw mikrobiologicznych krajów agresorów. Zawnioskowaliśmy do FEMS/ IUMS/ESCMID o zawieszenie towarzystw mikrobiologicznych z Rosji i z Białorusi w prawach członka FEMS/IUMS/ ESCMID oraz pozbawienie ich przywilejów przysługujących członkom federacji FEMS/ IUMS oraz ESCMID do czasu zakończenia wojny. Zaproponowaliśmy również blokadę artykułów wydawanych przez czasopisma FEMS/IUMS nadsyłanych przez autorów z afiliacją Rosji i Białorusi do czasu zakończenia wojny, **Uchwała nr 8-2022** z **02.03.2022 r. w załączeniu**.

Tego samego dnia PTM poparło Apel Prezesa Naczelnej Rady Lekarskiej Pana prof. dr hab. Andrzeja Matyja dotyczący zawieszenia współpracy z instytucjami rosyjskimi.

W odpowiedzi na Uchwalę nr 8-2022 szybko zareagowała Pani prof. Hilary Lappin-Scott Prezydent FEMS (**list w załączeniu**).

Prezydium ZG PTM jednogłośnie podjęło również **Uchwałę nr 9-2022**, o następującej treści:

„W związku z napaścią Rosji na suwerenny kraj – Ukrainę i prowadzeniu przez nią krwawej i niszczycielskiej wojny, której ofiarami jest ludność cywilna, a także w związku z udostępnianiem przez Białoruś swojego terytorium do ataków zbrojnych wojsk Rosyjskich na Ukrainę, Prezydium ZG PTM podejmuje decyzję w sprawie blokady artykułów wydawanych przez czasopisma PTM: *Polish Journal of Microbiology* (PJM) oraz *Advancements of Microbiology – Postępy Mikrobiologii* (AM-PM), nadsyłanych przez autorów z afiliacją Rosji i Białorusi do czasu zakończenia wojny. Blokada dotyczy manuskryptów już będących w trakcie procesu wydawniczego jaki i tych które dopiero zostaną nadesłane do redakcji czasopism."

W dniu 09.03.2022 r. odbyło się spotkanie Prezydent FEMS i 2 członków zarządu FEMS z prof. Elżbietą A. Trafny i prof. S. Tyskim reprezentującymi PTM, na temat stanowiska FEMS i PTM w sprawie wojny na Ukrainie. Uzgodniono, że FEMS podejmie działania wskazane w piśmie PTM, a także rozważy pomoc finansową dla naukowców ukraińskich uciekających przed wojną. Nasza Uchwała nr 8-2022 została przez biuro FEMS rozesłana do wszystkich zrzeszonych towarzystw mikrobiologicznych z informacją o zwołaniu Nadzwyczajnego Zebrania Delegatów – FEMS Council w sprawie podjęcia decyzji o zawieszeniu 4 towarzystw w FEMS. Zebranie FEMS Council odbędzie się dopiero 07.04.2022 r.

Warszawa, 16.03.2022 r.

SEKRETARZ
Polskiego Towarzystwa Mikrobiologów
dr hab. n. farm. Agnieszka E. Laudy

PREZES
Polskiego Towarzystwa Mikrobiologów
prof. dr hab. Stefan Tyski

Uchwała 8-2022 z dnia 02 marca 2022 r.
Prezydium Polskiego Towarzystwa Mikrobiologów, przyjęta jednomyślnie, adresowana do Federation of European Microbiological Societies (FEMS) i International Union of Microbiological Societies (IUMS).

W związku z trwającą wojną na Ukrainie, Polskie Towarzystwo Mikrobiologów **potępia i piętnuje postępowanie Rosji**, która napadła na suwerenny kraj – Ukrainę, zabijając obywateli tego kraju i niszcząc jego infrastrukturę. PTM **potępia także postępowanie Białorusi**, która udostępniła swoje terytorium do ataków zbrojnych wojsk rosyjskich na Ukrainę i sprzyja działaniom wojennym Rosji.

Polskie Towarzystwo Mikrobiologów liczące prawie 900 członków i działające od 1927 roku było współzałożycielem FEMS i IUMS, a na przestrzeni 95 lat doznawało wielu wstrząsów. Polska, która poniosła ogromne straty w czasie II wojny światowej i jest sąsiadem Ukrainy doskonale rozumie w jakiej sytuacji znaleźli się obywatele Ukrainy i wspiera ich na wiele możliwych sposobów. Skala barbarzyństwa najeźdźców jest ogromna i przerażająca, dlatego uważamy, że musimy zająć wyraźne stanowisko. Na każdym możliwym polu należy wyrazić swój sprzeciw wobec działań wojennych Rosji skierowanych nie tylko wobec Ukrainy, ale całej zachodniej kultury i przeciw wartościom jakie wyznajemy jako ludzie cywilizowani. Tylko widoczny sprzeciw, także wyrażony na polu naukowym, pozwoli dostrzec obywatelom Rosji i Białorusi, poddanych manipulacjom i propagandzie państwa, brak akceptacji i sprzeciw Europy wobec barbarzyństw dokonywanych w stosunku do niewinnych ludzi.

Polskie Towarzystwo Mikrobiologów apeluje nie tylko o solidarność z Ukrainą, w tym z członkami Society of Microbiologists of Ukraine, wyrażoną przez towarzystwa mikrobiologiczne zrzeszone w FEMS/IUMS, ale i o podjęcie kroków sankcyjnych w stosunku do towarzystw mikrobiologicznych krajów agresorów:

- Interregional Russian Microbiological Society,
- Interregional Association for Clinical Microbiology and Antimicrobial Chemotherapy,
- All-Russian Public Organization "National Academy of Mycology",
- Belarussian Non-governmental Association of Microbiologists.

Wnioskujemy do FEMS/IUMS o zawieszenie powyższych czterech towarzystw mikrobiologicznych w prawach członka FEMS/IUMS i pozbawienie ich przywilejów przysługujących członkom FEMS/IUMS do czasu zakończenia wojny. Proponujemy również blokadę artykułów wydawanych przez czasopisma FEMS/IUMS nadsyłanych przez autorów z afiliacją Rosji i Białorusi do czasu zakończenia wojny.

Takie działania podjęte przez FEMS/IUMS będą jawnym znakiem aktywnego sprzeciwu europejskiej/światowej nauki wobec zbrodniczego ataku na Ukrainę i podstawowe prawa wolności każdego człowieka. Być może będzie to pierwszy odebrany czytelny znak dla rzeszy mikrobiologów rosyjskich i białoruskich, że Europa/Świat mówi **STOP WOJNIE**.

Należy zdawać sobie sprawę, że działania zbrojne podejmowane przez Rosję i Białoruś nie mają wpływu na prowadzoną działalność naukową w tych krajach. Natomiast mają bezpośredni wpływ na zawieszenie badań naukowych na Ukrainie. Teraźniejszość Ukrainy to okrutna wojna, mężczyźni – naukowcy są zmobilizowani i z bronią w ręku walczą o niepodległość kraju, kobiety – naukowcy chowają się z dziećmi po schronach, a budynki instytutów i uczelni oraz aparatura badawcza są niszczone. Jakie projekty badawcze mogą być realizowane, jakie publikacje mogą powstawać, w takich warunkach?

Mamy dzisiaj obowiązek stanąć po stronie wolności jednostki, jak i po stronie prawa do niepodległości państwa położonego w centrum Europy.

SEKRETARZ
Polskiego Towarzystwa Mikrobiologów
dr hab. n. farm. Agnieszka E. Laudy

PREZES
Polskiego Towarzystwa Mikrobiologów
prof. dr hab. Stefan Tyski

Polskie Towarzystwo Mikrobiologów
Zarząd Główny
ul. Banacha 1 b, 02-097 Warszawa
NIP 521-11-21-855

https://www.microbiology.pl/ e-mail: ptm.zmf@wum.edu.pl

FEMS Business Office, Delftechpark 37a, 2628 XJ Delft, The Netherlands
T: +31 (0) 15 302 0050 E: fems@fems-microbiology.org W: fems-microbiology.org

Federation of European Microbiological Societies

Prof. Stefan Tyski
Polish Society of Microbiologists
National Medicines Institute
Chełmska 00-725
Warsaw
Poland

RE: FEMS response to the invasion of Ukraine

4 March 2021

Dear Stefan,

Thank you for your letter on the resolution adopted unanimously by the Polish Society of Microbiologists requesting FEMS show solidarity with Ukraine by suspending the FEMS membership of microbiological societies from Russia and Belarus and introduce a boycott of authors with affiliations of those countries submitting to FEMS journals. I will reply to each proposal separately to provide as full a response as possible to what we are doing right now and how we plan to proceed.

The Federation is appalled by the invasion of Ukraine and gives its full support to the people of Ukraine and all those impacted by this senseless and illegal aggression by the Russian Government. To that end we have written expressing our support to the Society of Microbiologists of Ukraine and have issued a public statement calling on the Russian Government to end the invasion immediately. We are also preparing a range of financial support for microbiologists in Ukraine and are appealing to our Member Societies and their members to host Ukrainian researchers, for which FEMS will also provide support.

The FEMS *Articles of Association*, which govern the way the organization can act, make clear that suspension of FEMS membership can only be approved by our Member Societies. To that end the Board of Directors has decided to convene an 'extraordinary meeting' of the FEMS Council to vote on the proposed suspensions. This invitation will be issued to all Member Societies shortly, with the vote being held within the timescales laid out in the *Articles*.

The introduction of any restriction on manuscripts from authors with Russian or Belarussian affiliation in FEMS journals must be made in collaboration with our publisher Oxford University Press and, with the involvement of the Editors-in-Chief of each journal who have autonomy over what is published in their journals. Consequently, a decision on this will take a little longer to achieve.

FEMS is working with the Society of Microbiologists of Ukraine and, Prof Sibirny, the FEMS Director of Education & Public Outreach, to understand how best to support Ukrainian microbiologists who have had

FEMS Business Office, Delftechpark 37a, 2628 XJ Delft, The Netherlands
T: +31 (0) 15 302 0050 E: fems@fems-microbiology.org W: fems-microbiology.org

Federation of European Microbiological Societies

their lives, work and, studies destroyed. To that end (and to be communicated shortly to all Member Societies) FEMS will:

1. Explore what practical resources and funding can be provided to support Ukrainian microbiologists continue or begin placements at institutions outside of the country
2. Contact our Member Societies to outline what this support will look like and to encourage societies to contact institutions who could potentially host Ukrainian colleagues.

Finally, I hope we can speak about this issue, to better understand the perspective and priorities of the Polish Society. FEMS Managing Director, Matthew Harvey, and I are very keen to arrange a meeting via Zoom with you as soon as possible and will share our availability next week. Please just let us know what times suit you and we can provide the Zoom links for the call.

I hope this letter provides both an explanation of the steps that FEMS is taking and the reasoning behind these. Please be assured that we are all working on these matters with the highest priority and will look to what support we can provide at speed both now and in the future. I look forward to hearing your comments and if you would be available to discuss these matters further with us.

Warm regards

Hilary Lappin-Scott

Hilary Lappin-Scott OBE
FEMS President


XXIX OGÓLNOPOLSKI ZJAZD
POLSKIEGO TOWARZYSTWA
MIKROBIOLOGÓW
15-17 WRZEŚNIA 2022,
WARSZAWA
PTM
POLSKIE TOWARZYSTWO MIKROBIOLOGÓW
XXIX OGÓLNOPOLSKI ZJAZD
POLSKIEGO TOWARZYSTWA
MIKROBIOLOGÓW
15-17 WRZEŚNIA 2022,
WARSZAWA
Miejsce Zjazdu:
Arche Hotel Krakowska
Warszawa, Aleja Krakowska 237
Główny Organizator Zjazdu:
Polskie Towarzystwo Mikrobiologów
ul. Stefana Banacha 1b, 02-097 Warszawa
ptm.zmf@wum.edu.pl, www.microbiology.pl

CZŁONKOWIE WSPIERAJĄCY PTM

Członek Wspierający PTM – Srebrny
od 12.09.2017 r.

Firma Ecolab Sp. z o.o. zapewnia: najlepszą ochronę środowiska pracy przed patogenami powodującymi zakażenia podczas leczenia pacjentów, bezpieczeństwo i wygodę personelu, funkcjonalność posiadanego sprzętu i urządzeń. Firma jest partnerem dla przemysłów farmaceutycznego, biotechnologicznego i kosmetycznego.

Członek Wspierający PTM – Zwyczajny
od 12.09.2017 r.

Merck Sp. z o.o. jest częścią międzynarodowej grupy Merck KGaA z siedzibą w Darmstadt, Niemcy i dostarcza na rynek polski od roku 1992 wysokiej jakości produkty farmaceutyczne i chemiczne, w tym podłoża mikrobiologiczne